
***Core-Shell Macromolecules with Dendritic
Polyphenylene Core and Polymer Shells***

Dissertation zur Erlangung des Grades
„Doktor der Naturwissenschaften“
am Fachbereich Chemie, Pharmazie und Geowissenschaften
der Johannes Gutenberg-Universität in Mainz

vorgelegt von

Vladimir M. Atanasov
geb. in Blagoevgrad, Bulgarien

Mainz 2004

Dekan:

1. Berichterstatter:

2. Berichterstatter:

Datum der mündlichen Prüfung: 04. 01. 2006

Die vorliegende Arbeit wurde in der Zeit von August 2000 bis September 2003 am Max-Planck-Institut für Polymerforschung in Mainz unter Anleitung von Herrn Prof. K. Müllen durchgeführt.

I would like to thank my thesis advisors Prof. Dr. K. Müllen and Dr. M. Klapper for giving me the possibility to work on this challenging and fascinating research project in an excellent research environment. His constant search for perfection, as well as the enlightening and fruitful discussions we have had, were a constant source of inspiration and motivation.

List of used abbreviations

ACPA	4,4'-Azo-bis(4-cyanopentanoic acid)
ACPC	4,4'-Azo-bis(4-cyanopentanoyl chloride)
AIBN	2,2'-Azo-bis(isobutyronitrile)
δ	Chemical shift [ppm]
ν	Wave number [cm^{-1}]
BP	Benzylpotassium
BPB	2-Bromopropionyl bromide
CMC	Critical micelles concentration
CP	Cumylpotassium
d	Doublet
DCM	Dichloromethane
DLS	Dynamic light scattering
DMF	N,N-Dimethylformamide
DMSO	Dimethylsulfoxide
DPE	1,1-Diphenylethylene
DPHLi	1,1-Diphenylhexyllithium
DPMP	Diphenylmethylpotassium
EO	Ethylene oxide
FD	Field Desorption
G1, G2, G3	First, second and third generation dendrimers
GPC	Gel permeation chromatography
HPLC	High performance liquid chromatography
IR	Infrared

J	Coupling constant [Hz]
MALDI-TOF	Matrix-assisted laser desorption/ionization-time of flight
MeOH	Methanol
MF	Magnetic field
M_n	Number average molecular weight
MS	Mass spectroscopy
MW	Molecular weight
M_w	Weight average molecular weight
MWD	Molecular weight distribution
<i>n</i> -BuLi	<i>n</i> -Butyllithium
NMR	Nuclear magnetic resonance
PAA	Polyacrylic acid
PAMAM	Polyamidoamine dendrimers
PBA	Polybutylacrylate
PDI	Polydispersity index
PEO	Polyethylene oxide
Ph	Phenyl
PI	Polyisoprene
PMMA	Polymethylmetacrylate
PPD	Polyphenylene dendrimer
PPE	Poly(2,6-dimethyl-1,4-phenylene ether)
ppm	Parts per million
PSLi	Polystyryllithium
PS-OH	hydroxy end-functionalized polystyrene

PSt*	Polystyryl radical
R_h	Hydrodynamic radius
RT	Room temperature
s	Singlet
<i>s</i> -BuLi	<i>sec</i> -Butyllithium
<i>sec</i> -BuCl	<i>sec</i> -Butylchlorid
T	Temperature [K]
t	Triplet
<i>t</i> -BuOK	Potassium <i>tert</i> -butoxide
<i>t</i> -BuP ₄	1- <i>tert</i> .-Butyl-4,4,4-tris-(dimethylamino)-2,2-bis-[tris-(dimethylamino)-phosphoranylidenamino]-2 Λ^5 ,4 Λ^5 -catenadi-(phosphazen)
TEA	Triethylaluminum
TGA	Thermal Gravimetric Analysis
THF	Tetrahydrofuran
TOA	Trioctylaluminum
UV	Ultra violet

TABLE OF CONTENTS:

Chapter I. Introduction	1
I.1. Dendrimers – history and architecture	1
I.2 Dendrimer hybrids	4
I.3. Multiple polymer-dendrimer hybrids	5
I.3.1 Grafting-from approach	5
I.3.2 Grafting-onto approach	6
I.3.3 Polymer redistribution reaction	8
I.4. Dendrimers and denrimer-polymer hybrids bearing chromophores	9
I.5. Dendrimer-polymer hybrids based on polyphenylene dendrimers	10
I.6. Polyphenylene dendrimers used in the present study	12
References	15
Chapter II. Objectives of the Current Work	20
Motivation	20
Aim of the present study	21
Chapter III. Anionic Polymerization – a Tool for Preparation of Dendrimer-Polymer Hybrids.	23
III.1. Anionic versus radical polymerization.	23
III.2. Anionic polymerization	24

III.2.1. Monomers	25
III.2.2. Initiators	25
III.2.3. Kinetics of anionic polymerization	28
II.2.3.1. Initiation reaction	28
II.2.3.2. Propagation reaction	29
References	30
Chapter IV. Core-Shell Macromolecules with Dendritic Polyphenylene Core and Poly(ethylene oxide) Shell	34
IV.1. Introduction	34
IV.2. Polyethylene oxide – arms for preparation of dendrimer-polymer hybrids.	34
IV.2.1. Introduction	34
IV.2.2. Synthesis and characterization of polyethylene oxide	35
IV.3. Synthesis of chloromethyl functionalized polyphenylene dendrimer TdG ₂ (CH ₂ Cl) ₋₁₂	37
IV.4. Synthesis of core-shell possessing polyphenylene dendrimer core and PEO shell – “grafting-onto” approach.	39
IV.5. Synthesis of core-mono-shell macromolecules using “grafting-from” method.	47
IV.5.1. Grafting of EO from 1,4-dihydroxymethyl benzene – model reaction.	48
IV.5.2. Synthesis of core-shell possessing polyphenylene dendrimer core and PEO shell – “grafting-from” approach.	49

Summary and conclusions	52
References	54
Chapter V. Core-Shell Macromolecules with a Perylenediimide Containing Polyphenylene Dendrimer for the Core and Polyethylene Oxide for the Shell	
V.1. Synthesis of core-shell macromolecules containing perylenediimide	57
V.2. Dynamic light scattering	62
V.3. Fluorescent correlation spectroscopy (FCS) studies	63
V.4. Preparation of supra-molecular architecture by self-assembly of block copolymers onto core-shell macromolecules.	69
Summary and conclusions	73
References	74
Chapter VI. Core-double-Shell Macromolecules Based on Polyphenylene Dendrimers.	
VI.1. Introduction	75
VI.2. Preparation of block copolymer arms	76
VI.2.1 Poly(styrene-block-ethylene oxide)	78
VI.2.1.1 Introduction	78
VI.2.1.2 Synthesis and characterization of hydroxyl end-functionalized polystyrene.	79
VI.2.1.3 Synthesis of poly(styrene-block-ethylene oxide)	83
VI.2.2 Poly(isoprene-block-ethylene oxide)	87

VI.2.2.1 Introduction	87
VI.2.2.2 Synthesis and characterization of hydroxyl end-functionalized polyisoprene.	89
VI.2.2.3 Synthesis of poly(isoprene-block-ethylene oxide) (PI-b-PEO)	92
VI.3. Poly(styrene-block-ethylene oxide) and poly(isoprene-block-ethylene oxide) copolymers grafting-onto polyphenylene dendrimers.	94
VI.3.1. Surface polarity of thin layers – mutable structure to media polarity.	102
VI.4. Synthesis of core-double-shell macromolecules by drafting-from method.	105
VI.4.1 Synthesis of poly(styrene-b-ethylene oxide-b-styrene) – model reaction for preparation of core-double-shell macromolecules by grafting-from strategy.	105
VI.4.2 Synthesis of core-shell ATRP macroinitiators.	109
VI.4.2 Synthesis of core-double-shell macromolecules. ATRP of styrene initiated from core-shell macroinitiator.	113
Summary and conclusions	115
References	117
Chapter VII. Applications of core-shell systems	119
VII.1 Core-Shell Systems - applications as metallocene supports in heterogeneous olefin polymerization	119
VII.1.1 Introduction	119
VII.1.2 Applications of the core-shell systems as carriers for metallocene based catalysts and their use as model compounds for heterogeneous olefin polymerization.	121
VII.1.2.1 Polymerization of ethene.	121

VII.1.2.2 Copolymerization of ethene with 1-hexene.	125
VII.2. Core-shell macromolecules bearing a chromophore at the focal point - applications as metallocene supports in heterogeneous olefin polymerization. Fragmentation study.	127
VII.3. Application of core-shell macromolecules bearing chromophore as drug delivery assays targeting the Blood Brain Barrier	129
Summary and Conclusions	131
References	133
Chapter VIII. New Approaches in the Synthesis of Block Copolymers	134
VIII.1. Polymerization in a magnetic field. Theoretical background.	134
VIII.2. Effect of high magnetic field upon the decomposition reaction of a radical macroinitiator	135
VIII.2.1. Introduction	135
VIII.2.2. Radical macroinitiators. Introduction	136
VIII.2.3. Synthesis and characterization of 4,4'-azobis(4- cyanopentanoyl) polystyrene radical macroinitiator.	138
VIII.2.4. Synthesis of diblock copolymers utilizing polymerization in a magnetic field.	140
VIII.3. Diblock copolymers bearing 3-(1-phenyl-vinyl)-perylene (dye) between the blocks	150
VIII.3.1. Introduction	150
VIII.3.2. Synthesis of poly(styrene-dye-ethylene oxide) and poly(isoprene-dye-ethylene oxide).	151
Conclusions	154

References	156
Chapter IX. Summary and Conclusions	158
Chapter X. Experimental Part	165
X.1. Analytical instruments:	165
X.2. High vacuum techniques	168
X.2.1. High-vacuum line	168
X.3. Glassware	169
X.4. Simple high vacuum procedures	169
X.4.1. Degassing	169
X.4.2. Distillation	170
X.4.3. Short path distillation	170
X.5. Purification of reagents	170
X.5.1. Solvents	170
X.5.2. Monomers	171
X.5.3. Terminating agents.	172
X.5.4. Coupling agents.	172
X.6. Preparation of initiators.	172
X.6.1. Synthesis of monofunctional initiators	172
X.6.2. Preparation of bifunctional initiators	176

X.6.3. Analysis of the initiators	177
X.7. Polymerization Procedures	178
X.7.1. Synthesis of homopolymers	178
X.7.2. Synthesis of diblock copolymers	182
X.7.3. Synthesis of macroinitiators for radical polymerization.	187
X.7.4. Synthesis of diblock copolymers bearing 3-(1-phenyl-vinyl)- perylene (dye) molecule between the blocks	189
X.7.5. Synthesis of triblock copolymers	191
X.8. Synthesis of core-mono-shell macromolecules	193
X.8.1. PEO grafting-onto TdG ₂ (CH ₂ Cl) ₋₁₂ .	193
X.8.2. PEO grafting-from TdG ₂ (CH ₂ OH) ₁₆	195
X.8.2.1. Polymerization of EO on 1,4-dihydroxymethyl benzene (model reaction)	195
X.8.2.2. PEO grafting-from TdG ₂ (CH ₂ OH) ₁₆	196
X.9. Preparation of core-shell macromolecules bearing covalently bonded chromophore molecule	198
X.10. Preparation of core-double-shell macromolecules by “grafting-onto” method	201
X.11. Preparation of core-double-shell macromolecules by “grafting-from” method	204
Acknowledgements	
Curriculum Vitae	

Chapter I. Introduction

I.1. Dendrimers – history and architecture

Organic chemistry was born in 1828 with Wohler's announcement of the synthesis of urea. During its youth, organic chemists have learned how atoms can be linked with one another to form molecules, and how the covalent bonds those hold atoms together in molecules can be manipulated to produce new molecular compounds. Later they began to appreciate and even to predict what the consequences of some of these connectivities could be, and they worked out how to measure the properties of their molecular creations. Organic chemists are constantly reaching out in new directions to satisfy their curiosities. As a result, a considerable leap into the unknown was made almost 25 years ago when dendrimers burst on to the scientific scene. These molecules, which have beautiful and compelling structures that are reminiscent of fractals and coral, are a reminder of just how much there is yet to discover in the chemical universe. For many years, the potential of dendrimers to do something useful lay elusively out of the chemist's reach. Research was driven largely by speculation and curiosity. Now, as we are in the 21st century, applications for dendrimers are beginning to become a reality as we learn how to exploit the unique properties that make them such exotic and exciting macromolecules.

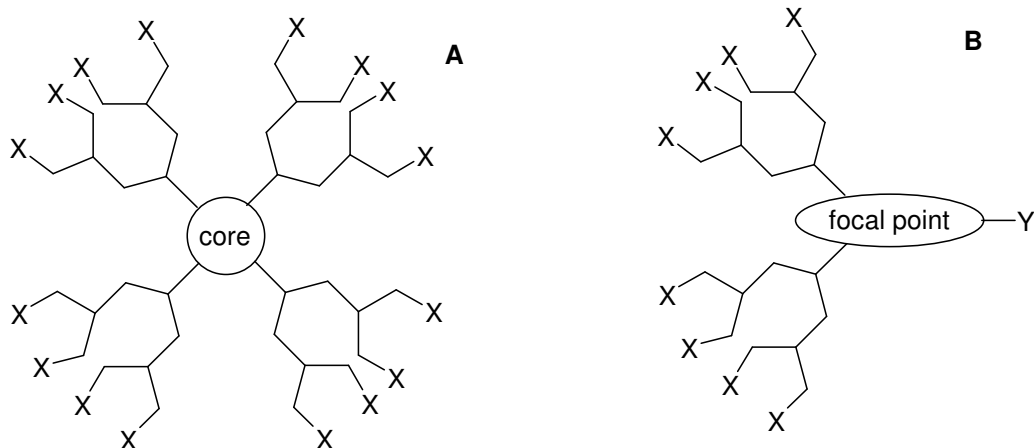
Toward the end of the 1970's a great deal of interest was starting to be generated in the new areas of host-guest[1,2] and supramolecular[3-6] chemistry. In the quest for large, substrate-selective ligands, several research groups became interested in the synthesis of "octopus"[7] and "tentacle"[8] molecular compounds - some of these compounds were found to act as selective hosts or catalysts despite their highly flexible structures. Other researchers were concentrating their efforts on the synthesis of crown ethers, cryptands and other molecular receptors. It was in the pursuit of this kind of research beyond the molecular domain that led to the first attempted dendrimer synthesis by Voegtle and co-workers.[9] A "cascade" synthesis concerning exhaustive Michael-type addition of acrylonitrile to an amine e.g. benzylamine produced bisnitrile, was described.

The study of highly branched macromolecules had also been addressed by polymer chemists, and it was from this arena that the first breakthroughs towards the

synthesis of highly branched, monodisperse polymers were made. The polymerization of a monomer of the AB₂ type had been suggested decades earlier by Flory,[10] and much theoretical work on the possible outcome of this type of reaction had been carried out.[11,12] This suggested that unusual architectures might be formed. Denkwalter *et al.*[13] employed the techniques of peptide chemistry to synthesize highly branched polylysine derivatives, which incorporate chiral centers in each branching unit, where the branches are also of unequal lengths. Tomalia's group devised a synthetic route whereby a "stepwise polymerization" could be performed, giving highly branched polymers with extremely low polydispersities.[14-18] These polyamidoamine (PAMAM) series were called "starburst dendrimers" (the term "starburst" is a trademark of the Dow Chemical Company), after star-branched polymers and the Greek word *dendru* for a tree. The term "dendrimer" is now used almost universally to describe highly branched, monodisperse macromolecular compounds.

The unusual nature of dendrimers lies not only in their shape. Their structures have eccentricities that stem from their interesting architectures as well. Dendrimers are molecules with regularly placed branched repeat units. Each dendrimer has a core or focal point. The core is the central unit of a symmetrical dendrimer and is the center of symmetry for the entire molecule. The core has its characteristic branching functionality, i.e. the number of chemical bonds by which it is connected to the rest of the molecule (Figure 1A). The focal point in an asymmetrical dendrimer plays a similar role to the core. It has a chemical functional group not found elsewhere in the dendrimer (Figure 1B). Attached to the core or focal point is a first layer of branched repeat units or monomers. This layer is alternatively considered to be the zeroed or first generation of the dendrimer. Each successive generation is placed onto the previous generation.

Figure 1. Schematic representation of the different parts of a dendrimer; stands for the repeat branching unit (monomer); X are terminal functional groups; Y is the functional group of the focal point: **A** core with generation two homologues; **B** focal point with generation two dendrimer.



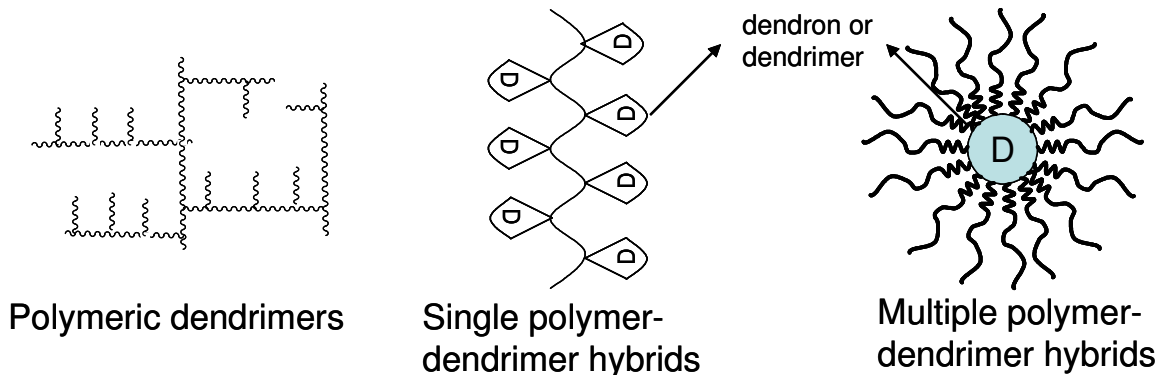
Each generation usually, but not necessarily, contains the same branched repeat units. The process of growth is extendable to several more generations. Because of the multifunctionality of each repeat unit, the number of segments in each generation grows exponentially. The functional groups of the outermost generation are called peripheral or terminal groups. The description of dendrimers as outlined suggests that there is a fixed special arrangement in dendrimers whereby the core or focal group forms the center, successive generations radiate outwardly and end-groups of the outermost generation form an outer surface. This is only partly true. A dendrimer is indeed a framework of chemical bonds and bond angles between atoms that has little variance; however, the torsion angles about the σ -bonds allow for a wide range of conformations and numerous dynamic transitions between them. Therefore, the core is not necessarily the physical center of the dendrimer nor are the end groups necessarily permanently located at the periphery of the dendrimer. The steady branching pattern of the dendrimer architecture is paralleled by the exponential increase of the molecular mass with each successively added generation. Dendrimers with more than a few generations have molecular weights that resemble those of step-growth polymers (104–105 kDalton). For that reason and for the presence of an identifiable (branched) repeat unit, higher generation dendrimers are considered polymeric molecules. The increasing branch density with generation also has striking effects on the structures of dendrimers. At higher generations, the steric crowding of

the branches at the surface of dendritic molecules causes them to adopt a globular conformation.[19,20]

I.2. Dendrimer Hybrids

Dendrimers may be used as building blocks for the construction of even larger assemblies. Many research groups interested in the chemistry of dendrimers approach the subject from the viewpoint of a polymer chemist. This background has provided the inspiration of the synthesis of various copolymer architectures (Figure 2), including polymeric dendrimers (hyperbranched polymers)[21], single polymer-dendrimer hybrids [22 -25] (comb-burst) [26, 27] and multiple polymer-dendrimer hybrids – core-shell (star) [28].

Figure 2. Dendrimer-polymer hybrids



The objects of the present study are multiple polymer-dendrimer hybrids as a model compounds for preparation and investigation of well-define core-shell structures.

I.3. Multiple Polymer-Dendrimer Hybrids

Dendrimers with their multiple terminal functional groups are ideally suited for the construction of star-shaped polymers and highly organized dendrimer-core and polymer-shell supramolecular structures. Indeed, the terminal functional groups can serve either as initiators for polymerization (“grafting-from” method) or as termination functional groups (“grafting-onto” method). They can also be used as redistribution centers in equilibrium polymerizations.

I.3.1 “Grafting-from” approach

The “grafting-from” method (core first) in which the polymer chains are grown from an active multifunctional dendrimeric initiator, was applied for the first time by *Frèchet et al.* using ring opening polymerization of ϵ -caprolactone initiated from benzyl dendritic polyethers for preparation of polymers possessing hybrid linear-globular architecture.[29] Considerable development of this method was achieved by *Hedrick et al.*, who reported success in preparation of dendrimer-like star block copolymers utilizing both anionic and atom transfer radical polymerization of ϵ -caprolactone, methyl methacrylate and ethylene oxide.[30] The “grafting-from” method was recently extended to the synthesis of star-shaped core-shell macromolecules based on hyperbranched polyglycerols,[31] poly(trimethylene imine) dendrimers[32] and poly(amidoamine) dendrimers.[33]

The “grafting-from” method has been successful for ring opening polymerizations. For example, ϵ -caprolactone polymerization is initiated from poly(propylene imine) dendrimers with $n = 2-16$ terminal amine groups. To be successful this method requires stable dendrimers and preferably little or no reversibility leading to depolymerization and ring formation. The polymerization in bulk at 230°C of ϵ -caprolactam with poly(ethylene imine) dendrimers is also described.[34] The properties of the resulting semicrystalline six-arm star polymers are in all aspects similar to those of the linear nylon-6 except for a 40% lower melt viscosity[35] which is of significant industrial importance.

The “grafting-from” has not been a successful method in anionic polymerization because the required low molecular weight multifunctional organometallic initiators are almost always insoluble. This is also expected to be the case when dendrimers are modified. In cationic polymerizations, however, the dormant species is less polar and more soluble. For example, the hexabenzyl bromide

has been used in the polymerization of 2-methyl-2-oxazoline [36] and it can be envisioned that larger dendritic initiators based on phosphorus can also be used [37].

I.3.2 “Grafting-onto” approach

Within this approach, anionic polymerization was found to be uniquely suited for the preparation of star and core-shell structures. At least for a few monomers under well-defined conditions narrow MWD chains having stable and reactive end-groups are available for reaction with multifunctional dendrimers. It is required, that the dendrimers are essentially of a hydrocarbon nature except for the electrophilic functional groups. In the original disclosure of the formation of 18-arm star polyisoprenes the required octadecachlorocarbosilane coupling agent was prepared by an embryonic recursive method which foreshadowed the divergent dendrimer synthesis.[38] This octadecachlorocarbosilane compound is equivalent to a generation 1.5 dendrimer. The “grafting-onto” process consists of the nucleophilic displacement of Cl with the carbanionic end groups of living polymer chains. No side reactions have been observed when this reaction is performed at room temperature in a hydrocarbon medium; although an excess of living polymer and relatively long reaction times are required.[39,40] This “grafting-onto” route has been extended to the preparation of star polymers with 32-, [40] 64-, and 128-arm star polybutadienes[39] which are built onto carbosilane dendrimers of generations 2.5, 3.5, and 4.5, respectively.[41] It is worth noting that no steric limitations are observed when poly(butadienyllithium) is used. Steric limitations are a problem with poly(isoprenyllithium) and poly(styryllithium). The same coupling agents have been used to prepare star block copolymers in which each arm of the star consists of a diblock copolymer of styrene (30%) and butadiene (70%).[42]

Furthermore, the “grafting-onto” reaction can be controlled to some extent. For example, substitution of the first half of the Si-Cl bonds with one polymer chain is known to be kinetically favored. The remaining Si-Cl is then substituted with another polymer. These polymers are called fuzzy because the two polybutadienes have different molecular weights, thereby presumably, creating a more diffuse surface.[42] In the second application, a miktoarm star polymer with eight polystyrene and eight polyisoprene arms has been synthesized.[43] Although the arms of such multiblock

copolymers are forced to intermingle extensively, the polymers spontaneously form micro-separated two-phase systems.

Recently, PEO has been grafted onto PAMAM dendrimers by means of *N*-succinimidyl propionic acid spacers.[44] When $n=16$ and 32 , experimental and expected functionalization agree satisfactorily. For $n= 64, 128,$ and 256 , progressively lower functionalization is observed. It is not clear whether this result is due to imperfections of the PAMAM dendrimer used or to steric limitations on the extent of the substitution reaction. The star polymers are different from the previously described model star polymers obtained by anionic polymerization because the arm MW has a most probable MWD. Interestingly, it was observed that the hydrodynamic volume of the star polymers as measured by SEC does not vary much with increasing functionality from $f=4$ to $f=64$,[45] although measured $[\eta]$ and calculated MW suggest an important increase in R_{η} . [46] The hydrodynamic volume measured by dynamic light scattering is clearly an increasing function of the functionality of the stars at constant arm length, as well as under conditions of increasing arm length and constant dendrimer functionality. This apparent difference may be due to different averages probed by the two methods. The SEC maximum is close to a weight average while the dynamic light scattering measures a *z*-average value of the hydrodynamic volume.

In resume both methods succeed in preparation of dendrimer-polymer hybrids with some limitations concerning the particular feature of the method. For example, the “grafting-onto” method suffers from the fact that polymers (especially for high molecular weight polymers) are relatively large molecules that once attached to any surface occupy significant space and thus shield the vicinity surface. Often dendrimers possess highly dense functionality on their surface and the “grafting-onto” method is not sufficient for polymers having relatively bulky end-functionality as polystyryllithium and polyisoprenoyllithium.[42,44] The “grafting-from” method solves this problem by utilizing the dendrimer functionality as initiator centers for monomer polymerization. However, the initiator center in terms of ionic polymerization (as the most usable method) means ions. Now imagine a dendrimer with a highly dense ionic functionality on its surface – a relatively big molecule with highly charged surface. Such particles are soluble and stable exclusively and only in relatively polar solvents [47,48] such as water and alcohols (all protic solvents). Thus,

in the more common solvents for ionic polymerization those particles are either insoluble (hexane and toluene) or partially soluble (THF and DMSO).[49]

The disadvantages of both methods reported above often result in incomplete surface coverage and an increase of polydispersities of the obtained dendrimer-polymer hybrids. Some particular procedures manage, however, to suppress and even eliminate these undesirable effects. For example Roovers *et al.* [50,51] have used less concentrated solutions and more polar solvents for polymerization of ethylene oxide by the “grafting-from” method. Hadjichristidis *et al.* have used carbosilane dendrimers possessing spare functionality on their surface and extremely active polystyryllithium to ensure completeness of the “grafting-onto” reaction[39,40].

Vasilenko *et al.* reported another way to achieve star shaped polymers based on carbosilane dendrimers.[52,53] They used polyolithium derivatives of carbosilane dendrimers as initiators for the anionic polymerization of different monomers such as styrene, hexamethylcyclotrisiloxane, and ethylene oxide. The polyolithium derivatives were obtained by hydrosilylation of allyl terminated dendrimers with the sterically demanding bidecylmethylsilane. This led to the reaction of only one half of the end groups leaving allyl groups unreacted in the interior of the dendrimer. The reaction of these allyl groups with sec-butyllithium yielded the desired polyolithium derivative of the carbosilane dendrimer. Due to the location of the lithium atoms in the inner space of the dendrimer, a main problem of polyolithium compounds, the high tendency of aggregation, was solved.

I.3.3 Polymer redistribution reaction

The polymer redistribution reaction with functionalized dendrimers has been investigated by Van Aert *et al.* for the case of the transesterification of poly(2,6-dimethyl-1,4-phenylene ether) (PPE) by means of phenols attached to dendrimers.[39] The number average molecular weight of the arms is controlled by the ratio of moles of PE units to the moles of added phenol. Phenols have been attached to poly(propylene imine) dendrimers by means of *tert*-butyloxycarbonyl tyrosine. The redistribution rate is slow, but it can be increased by adding a CuCl/4-dimethylaminopyridine catalyst. Oxygen-free conditions are required during the redistribution in order to avoid oxidative polymerization and oxidative side reactions. Transamidation has been performed with poly(propylene imine) dendrimer and

poly(ϵ -caprolactone). The linear chain is fragmented, and a mixture of star and linear polymers are formed.[34] The average MW of the arms is equal to the MW of the linear fragments.

I.4. Dendrimers and dendrimer-polymer hybrids bearing chromophores.

Dendrimers containing a dye in the core,[54-57] in the periphery[58-61], or as a host-guest complex[62-71] have been intensively studied during the last decade. They were applied as labeled delivery of genes and oligonucleotides to a cell,[61] as nanoreservoirs for dye containing solutions, in inkjet printing and related techniques.[67] The most facile way to obtain dye labeled dendrimers is based on the ability of dendrimers to extract dyes from water solution by host-guest interactions. The forces inducing this phenomenon can be either the non-specific insertion of guests into the more or less porous inside of the dendrimer skeleton or the complexation to complementary binding sites in the dendrimer. The influence on these interactions of generation,[64,65,68,69] pH and ion strength[66] has been established for poly(propyleneimine) and poly(amidoamine) dendrimers. A promising feature of the fluorophore containing dendrimers is inter- or intramolecular energy transfer observed in the presence of both electron (photon) donor and acceptor molecule. The process of “light harvesting” is based on photon absorption by the chromophores coupled to the dendrimer periphery, and transferred to the central laser dye which emits its own fluorescence.[58] In the most prominent case, chromophore molecules are chemically bounded to the dendrimer, which fulfills the requirement for a defined space between both quenching molecules.

Particular interest has been raised for dendrimer-polymer hybrids in terms of core-shell structures.[51] In the core-shell macromolecules based on dendrimers the organic polymer shell determines the external chemical properties of such materials and their interaction with the environment. Their physical properties are governed by both size and shape of the dendritic core and the surrounding organic layer. Very few authors have reported the synthesis of dendrimer-polymer hybrids containing chromophore molecules.[72,73] The luminescent labeled structures were obtained by host-guest interaction between chromophore and dendritic core-shell macromolecules. Thus, studying their solution structures and their ability to solubilize organic

compounds in water, the hydrophile/lipophile balance can be varied systematically for nanoscopic transport agents and for catalysts.

I.5. Dendrimer-Polymer Hybrids Based on Polyphenylene Dendrimers

Most of the dendrimer-polymer hybrids examined up to now possessed a soft or semirigid dendritic part, while polymers with different morphologies and behaviors were utilized for building a huge variety of macromolecular structures. Architectures based on rigid, stiff dendrimers are the main scope in the present study.

It has been proven that rigid dendrimers based on polyphenylenes have stiff branches and the back folding in solutions is impossible [74] as is the case of flexible dendrimers [75]. Additionally, contrary to dendrimers containing flexible repeat units (*e.g.* PAMAM) rigid polyphenylene dendrimers proved to contain large stable inner voids of a distinct size between their dendritic branches due to the shape persistence [76]. The authors found that the size of the inner cavities increases with the size respectively generation of the polyphenylene dendrimer. Due to these voids, polyphenylene dendrimers are potentially attractive with respect to the selective incorporation of guest molecules. Further, due to their very dense intramolecular packing, these monodisperse polyaromatic dendrimers are of interest with respect to the design of nanostructures with invariant shape.[77] Besides their significantly enhanced thermal and chemical stability, their postulated rigidity as compared to aliphatic dendrimer systems provides the basis for their potential application, *e.g.*, as a support for catalysts[78], dyes[79], or biological active substances in human diagnosis.[80,81]

Polyphenylene dendrimers, due to the outstanding shape-persistence, allow the attachment of functional groups in well-defined positions on the dendrimers surface [82] and are the best candidates to be used as a stiff core in a star shaped dendritic-core polymer-shell hybrids.

First examples of core-shell particles base on polyphenylene dendrimers consist of a core of twisted, interlocked benzene rings and an external shell of dodecyl chains.[83] Three kinds of second generation dendrimers with tetrahedral or a disk-like shape with 16- and 12-fold alkyl chains on the periphery were described to spontaneously form a stable, almost pinhole free monolayer on a graphite surface. The

lateral organization of alkyl-substituted polyphenylene dendrimers on the basal plane of graphite has been investigated using atomic force microscopy. Two-dimensional crystals with parallel rows of 6 nm spacing and complex two-dimensional arrangements have been observed. The structures have been found to depend on the structure of the dendrimer, on the solvent, and on the concentration. The work was extended to four new dendrimers which differ in number, position and length of alkyl chains in order to study their influence on the structures formed.[84] All observed structures were divided into three types that can coexist on one sample: (1) granular regions, where individual dendrimers could be identified in a glasslike phase, (2) diffuse, homogeneous regions and (3) nanorod regions consisting of parallel rows of 5.1-5.9 nm spacing. Dendrimers differ in alkyl chains length have shown the same spacing between nanorods due to parallel orientation (to the direction of the nanorods) of the alkyl chains.

The second direction attracting considerable interest in terms of biological active substances is the use of dendrimers combining multifunctionality as well as bioactivity and water solubility as a high potential sensitive probes for investigations in a biological environment down to the single molecule level. Thus, the synthesis of a polyphenylene dendrimer carrying three perylenemonoimide dyes and one biotin group has been demonstrated [80]. Due to the hydrophobic polyphenylene scaffold, the dendrimer as well as dyes are insoluble in water thus preventing investigations in aqueous media. The use of an appropriate detergent (*Tween 20*) has resulted in the formation of well-defined supramolecular dendrimer-detergent complexes being soluble in aqueous media. The complexes have exhibited a high stability in the presence of blood serum proteins. The specific binding of the dendrimer-detergent complexes carrying a single biotin group to the protein streptavidin has been demonstrated using a magnetic bead assay. Another very promising core-shell system based on polyphenylene dendrimers functionalized with up to 16 lysine residues or substituted with short peptide sequences composed of 5 lysine or glutamic acid repeats and a C- or N-terminal cysteine residue have been prepared as model compounds for DNA complexation and condensation and investigation their potential as building blocks for the electrostatic layer-by-layer self-assembly of ultrathin nanostructured supramolecular films [81]. In the same direction extremely important experiments have proved that specifically functionalized polyphenylene dendrimers can cross the blood brain barrier (the main obstacle for the administration of drugs

acting in the central nervous system) [85]. The system used, had a first generation dendrimer as a core decorated with both cholesterol and pentyllysine moieties as a shell, which makes the compound conceptually analogous to lipoproteins. The cholesterol residues were believed to facilitate the transport across the cell membrane and the polypeptide chains have ensured the water solubility of the compound. The way to develop the new generation drug carriers, particularly applicable to drugs acting in the central nervous system has been found.

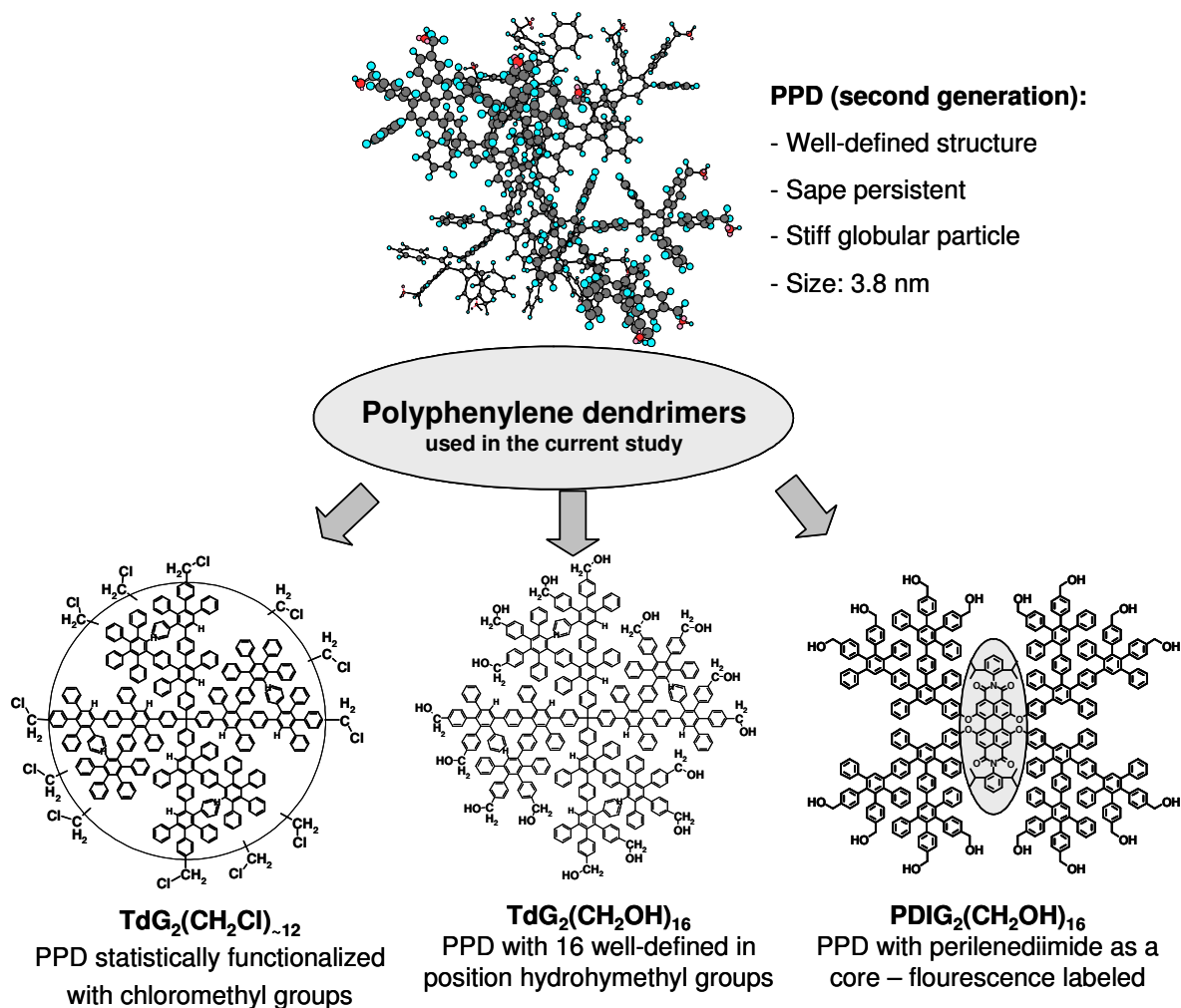
I.6. Polyphenylene Dendrimers Used in the Present Study.

In general, core-shell structures are interesting because of their stiff core and flexible shell. The most prominent case of latex particles, consisting of a styrene and butylacrylate, achieved by a two-step emulsion polymerization wherein the polystyrene core was synthesized first and then surrounded with a very flexible polybutylacrylate shell by addition of the acrylate.[86] However, such particles have a size of 200-500 nm.[87,88] To decrease the size and to get more defined structures dendrimer based core-shell systems are ideal candidates. Polyphenylene dendrimers used as the core in the present study, have typically a diameter of 3-10 nm[89] which depends on the type of shell the diameter of such nano-particles are predicted to be in range of 5-30 nm, which is at least one magnitude order smaller than the particles prepared by emulsion polymerization. Even if they cannot be prepared in large amounts they can serve as model compounds for studying the properties and applications of the larger and broader distributed latex particles. As examples should be mentioned the investigation of film formation of dispersions or fragmentation processes of polymeric supports for metallocenes applied in olefin polymerizations. As most utilized dendrimers are very flexible (*e.g.* PAMAM, aromatic/aliphatic polyethers/polyesters and poly(carbosilane)s) and therefore not suitable for synthesizing models for stiff-core flexible-shell latex particles. The polyphenylene dendrimers are ideal molecules to create hard cores due to their shape-persistence. As one is able to decorate them with hydrophilic flexible chains such as PEO chains on the surface, model compounds for latex particles are thus available.

To achieve this demanding challenge we developed two different strategies based on a second-generation polyphenylene dendrimer with tetrahedral core (**TdG₂**) which is functionalized with PEO and PEO containing block copolymer chains both

by a “grafting-onto” and “grafting-from” methods. It is predicted that by attaching these chains access to amphiphilic stiff-core-flexible-shell nano-particles will arise. Within the “grafting onto” approach chloromethylated dendrimers $\text{TdG}_2(\text{CH}_2\text{Cl})_{-12}$ ~8 were used (see Figure I.1). Those dendrimers were obtained (by Dr. Veselin Sinigerski) by a simpler synthetic scheme than others (chloromethylation of nonfunctionalized dendrimer) that promote their use as a test system for preparation of core-shell macromolecules. Thus, in spite of the fact that test dendrimers had a well-define structure, but a statistical number of functional groups, the obtained core-shell molecules possessed narrow molecular weight distribution and adjustable nanoscale size (see section IV.4 for further discussion).

Figure I.1 Polyphenylene dendrimers.



The second-generation hexadeca-hydroxymethyl functionalized polyphenylene dendrimer with tetrahedral core (**TdG₂(CH₂OH)₁₆**) was prepared by Dr. Veselin Sinigerski [82] (see Figure I.1) served as a multifunctional initiator for the polymerization of ethylene oxide, was utilized within the “grafting-from” approach. In contrast to the first dendrimer used, **TdG₂(CH₂OH)₁₆** possesses both a well-defined structure, number and position of the functional groups, which enable the preparation of core-shell molecules with a definite structure and morphology. A similar dendrimer with a hydroxymethyl functionality, but fluorescently labeled by the use of perylenediimide as a core surrounded by the dendrons (**PDIG₂(CH₂OH)₁₆**) was prepared by Dr. Roland Bauer. It was utilized for a more detailed investigation of the size and size distribution in terms of hydrodynamic radius. The fluorescent labeled dendrimer introduces the possibility for utilizing powerful methods like fluorescence correlation spectroscopy (FCS), and further potential use of surface plasmon fluorescence spectroscopy (SPFS) or even more modern like fluorescence recovery after photobleaching (FRAP), in order to investigate the behavior and properties of the core-shell particles in both – liquid and solid phase. Mostly, these methods are applied to determine the size of the molecules either as monolayers on a substrate or by determination of their diffusion coefficient in a solution. Fluorescently labeled dendrimer and the core-shell molecules well-defined in size can be therefore used as standards for these techniques.

References

1. Cram, D. J.; Cram, J. M., *Science*, **1974**, 183, 803.
2. Pedersen, C. J., *Angew. Chem. Int. Ed. Engl.*, **1988**, 27, 1021.
3. Lehn, J.-M., *Act. Chem. Res.*, **1978**, 11, 49.
4. Lehn, J.-M., *Pure Appl. Chem.*, **1978**, 50, 871.
5. Lehn, J.-M., *Science*, **1985**, 227, 849.
6. Lehn, J.-M., *Angew. Chem. Int. Ed. Engl.*, **1988**, 27, 89.
7. Vogtle, F.; Weber, E., *Angew. Chem. Int. Ed. Engl.*, **1974**, 13, 814.
8. Murakami, Y.; Nakano, A.; Akiyoshi, K.; Fukuya, K., *J. Chem. Soc. Perkin Trans I*, **1974**, 2800.
9. Buhleier, E.; Wehner, W.; Vogtle, F., *Synthesis*, **1978**, 155.
10. Flory, P. J., *J. Am. Chem. Soc.*, **1952**, 74, 2718.
11. Maciejewski, M., *J. Macromol. Sci.-Chem.*, **1982**, A17, 689.
12. Burchard, W.; Kajiwara, K.; Nerger, D., *J. Polym. Sci., Phys. Edn*, **1982**, 20, 157.
13. Denkwalter, R. G.; Kolc, J.; Lukasavage, W. J., *US Patent No. 4 289 872*, **1981**; assigned to Allied Corp.
14. Tomalia, D. A.; Baker, H.; Dewald, J.; Hall, M.; Kallos, G.; Martin, S.; Roeck, J.; Ryder, J.; Smith, P., *Polym. J.*, **1985**, 17, 117.
15. Tomalia, D. A.; Baker, H.; Dewald, J.; Hall, M.; Kallos, G.; Martin, S.; Roeck, J.; Ryder, J.; Smith, P., *Macromolecules*, **1986**, 19, 2466.
16. Tomalia, D. A.; Hall, M.; Hedstrand, D., *J. Am. Chem. Soc.*, **1987**, 109, 1601.
17. Tomalia, D. A.; Berry, V.; Hall, M.; Hedstrand, D. M., *Macromolecules*, **1987**, 20, 1164.
18. Tomalia, D. A.; Dewald, J. R., *US Patent No. 4 587 329*, **1986**; assigned to Dow Chemical Co.
19. Kim, Y. H.; Webster, O. W., *J. Am. Chem. Soc.*, **1990**, 112, 4592.
20. Jannerfeldt, G.; Boogh, L.; Manson, J. A. E., *J. Polym Sci Part A: Polym Chem* **1999**, 37, 206.
21. Voit, B. *J. Polym.Sci. Part A: Polym. Chem.* **2000**, 38, 2505.
22. Gitsov I, Fréchet JMJ *J Am Chem Soc* **1996**, 118, 3785.

-
23. Matyjaszewski K, Shigemoto T, Fréchet JMJ, Leduc M *Macromolecules* **1996**, 29, 4167.
 24. Chapman TM, Hillyer GL, Mahan EJ, Shaffer KA *J Am Chem Soc* **1994**, 116, 11,195.
 25. van Hest JCM, Delnoye DAP, Baars MWPL, van Genderen MHP, Meier EW *Science* **1995**, 268, 1592.
 26. Schlüter, A.D., Claussen, W., Amoulong-Kirstein, E. Karakaya, B., *Proc. Am. Chem. Soc., Div. Polym. Mater.:Sci. Eng.* **1995**, 73, 226
 27. Yin, R., Swanson, D.R., Tomalia, D.A., *Proc. Am. Chem. Soc., Div. Polym. Mater.:Sci. Eng.* **1995**, 73, 277.
 28. Gitsov, I., Frechet, J.M.J., *Proc. Am. Chem. Soc., Div. Polym. Mater.:Sci. Eng.* **1995**, 73, 129.
 29. Gitsov, I.; Ivanova, P.; Fréchet, J. M. *J. Macromol. Rapid Commun.* **1994**, 15, 387.
 30. Hedrick, J. L.; Trollsås, M.; Hawker, C. J.; Athoff, B.; Claesson, H.; Heise, A.; Miller, R. D.; Mecerreyes, D.; Jérôme, R.; Dubois, Ph. *Macromolecules* **1998**, 31, 8691.
 31. Haag, R.; Stumbe, J.-F.; Sunder, A.; Frey, H.; Hebel, A. *Macromolecules* **2000**, 33, 8158.
 32. Aoi, K.; Hatanaka, T.; Tsutsumiuchi, K.; Okada, M.; Imae, T. *Macromol. Rapid Commun.* **1999**, 20, 378.
 33. Balogh, L.; de Leuse-Jallouli, A.; Dvornic, P.; Kunugi, Y.; Blumstein, A.; Tomalia, D. A. *Macromolecules* **1999**, 32, 1036.
 34. Warakomski, J., *Chem Mat*, **1992**, 4,1000.
 35. Risch, B.G.; Wilkes, G.L.; Warakomski, J.M.; *Polymer*, **1993**, 34, 2330.
 36. Chang JY, Ji HJ, Han MJ, Rhee SB, Cheong S, Yoon M *Macromolecules*, **1994**, 27, 1376.
 37. Slany M, Bardaji M, Caminade A-M, Chaudret B, Majoral JP, *Inorg Chem* **1997**, 36, 1939.
 38. Fetters, L.J.; Hadjichristidis, N., *Macromolecules*, **1980**, 13, 191.
 39. Bauer, B.J.; Fetters, L.J.; Graessley, W.W.; Hadjichristidis, N.; Quack, G.E., *Macromolecules*, **1989**, 22, 2337.

40. Zhou, L.L.; Hadjichristidis, N.; Toporowski, P.M.; Roovers, J., *Rubber Chem Techn*, **1992**, 65, 303.
41. Zhou, L.L.; Roovers, J., *Macromolecules*, **1993**, 26, 963.
42. Roovers, J.; *Macromolecules*; **1994**, 27, 5359.
43. Avgeropoulos, A.; Poulos, Y.; Hadjichristidis, N.; Roovers, J., *Macromolecules*, **1996**, 29, 6076.
44. Yen, D.R.; Merrill, E.W., *Polymer Preprints* **1997**, 38, 531.
45. van Aert, H.A.M.; Burkard, M.E.M.; Jansen, J.F.G.A.; van Genderen, M.H.P.; Meijer, E.W.; Oevering, H.; Buning, G.H.W., *Macromolecules*, **1995**, 28, 7967.
46. van Aert, H.A.M.; van Genderen, M.H.P.; Meijer, E.W., *Polym Bull*, **1996**, 37, 273.
47. Comanita, B.; Noren, B.; Roovers, J. *Macromolecules* **1999**, 32, 1069.
48. Souza, N. C.; Zucolotto, V.; Silva, J. R.; Santos, F. R.; Santos Jr., D. S.; Balogh, D. T. Oliveira Jr., O. N.; Giacometti, J. A. *Journal of Colloid and Interface Science* **2005**, 285, 544–550.
49. Quirk, R. P.; Tsai, Y. *Macromolecules* **1998**, 31, 8016.
50. Roovers, J.; Zhou, L.-L.; Toporowski, P. M.; van der Zwan, M.; Iatrou, H.; Hadjichristidis, N. *Macromolecules* **1993**, 26, 4324.
51. Roovers, J. Comanita, B. *Adv. Polym. Sci.* **1999**, 142, 179.
52. Vasilenko, N.G.; Getmanova, E.V.; Myakushev, V.D.; Rebrov, E.A.; Moeller M.; Muzafarov A.M. *Polym Sci Ser A* **1997** 39, 977.
53. Vasilenko N.G., Rebrov E.A., Muzafarov A.M., Sheiko S.S., Moeller M. *Polym Prepr (Am Chem Soc Div Polym Chem)* **1998**, 39, 479.
54. Yokoyama, S.; Otomo, A.; Nakahama, T.; Mashiko, S., *Thin Solid Films*, **2001**, 393, 124.
55. Yokoyama, S.; Nakahama, T.; Otomo, A.; Mashiko, S., *Colloids and Surfaces A: Physicochemical and Engineering Aspects*, **2002**, 198-200, 433.
56. Takaguchi, Y.; Saito, K.; Suzuki, S.; Hamada, K.; Ohta, K.; Motoyoshiya, J.; Aoyama H., *Bull. Chem. Soc. Jpn.*, **2002**, 75, 1347.
57. Cardona, C. M.; Jannach, S. H.; Huang, H.; Itojima, Y.; Leblanc, R. M.; Gawley, R. E.; Baker, G. A.; Brauns, E. B., *Helvetica Chimica Acta*, **2002**, 85, 3532.

-
58. Froehling, P., *Dyes and Pigments*, **2001**, 48, 187.
 59. Hackbarth, S.; Horneffer, V.; Wiehe, A.; Hillenkamp, F.; Röder, B., *Chemical Physics*, **2001**, 269, 339.
 60. Ahmed, S. M.; Budd, P. M.; McKeown, N. B.; Evans, K. P.; Beaumont, G. L.; Donaldson, C.; Brennan, C. M., *Polymer*, **2001**, 42, 889.
 61. Yoo, H.; Juliano, R. L., *Nucleic Acids Research*, **2000**, 28, 4225.
 62. Köhn, F.; Hofkens, J.; Wiesler, U.-M.; Cotlet, M.; van der Auweraer, M.; Muellen, K.; De Schryver, F. C., *Chem. Eur. J.*, **2001**, 7, 4126.
 63. Azzellini, G. C., *An. Acad. Bras. Ci.*, **2000**, 72, 33.
 64. Balzani, V.; Ceroni, P.; Gastermann, S.; Gorka, M.; Kauffmann, C.; Vögtle, F., *Tetrahedron*, **2000**, 58, 629.
 65. Richter-Egger, D. L.; Tesfai, A.; Tucker, S. A., *Analytical Chemistry*, **2001**, 73, 5743.
 66. Chen, S.; Yu, Q.; Li, L.; Boozer, C. L.; Homola, J.; Yee, S. S.; Jiang, S., *J. Am. Chem Soc.*, **2002**, 124, 3395.
 67. Khopade, A. J.; Caruso, F., *American Chemical Society*, **2002**, 2, 415.
 68. Karukstis, K. K.; Perelman, L. A.; Wong, W. K., *Langmuir*, **2000**, 18, 10363.
 69. Watkins, D. M.; Sayed-Sweet, Y.; Klimash, J. W.; Turro, N. J.; Tomalia, D. A., *Langmuir*, **1997**, 13, 3136.
 70. Yokoyama, S.; Otomo, A.; Mashiko, S., *Applied Physics Letters*, **2002**, 80, 7.
 71. Oertel, U.; Appeihans, D.; Friedel, P.; Jehnichen, D.; Komber, H.; Pilch, B.; Hänel, B.; Voit, B., *Langmuir*, **2002**, 18, 105.
 72. Schenning, A. P. H. J.; Peeters, E.; Meijer, E. W., *J. Am. Chem. Soc.*, **2000**, 122, 4489.
 73. Pan, Y.; Ford, W. T., *Macromolecules*, **2000**, 33, 3731.
 74. Wind, M.; Wiesler, U.M.; Saalwaechter, K.; Muellen, K.; Spiess, H.W., **2001**, *Adv. Mater.* 13, 752.
 75. Boris, D.; Rubinstein, M., **1996**. *Macromolecules* 29, 7251.
 76. Marek, T. Suvegh, K. Vértes, A. Ernst, A. Bauer, R. Weil, T. Wiesler, U. Klapper, M. Muellen, K. *Radiation Physics and Chemistry* **2003**, 67, 325.
 77. Perec, V. Ahn, C. Ungar, G. Yeardley, D. Moeller, M. Sheiko, S. *Nature* **1998**, 319, 161.

-
78. Atanassov, V. Jang, Y.-J. Nenov, N. Bauer, R. Sinigersky, V. Klapper, M. Muellen, K. *in preparation*
 79. Liu, D. De Feyter, S. Cotlet, M. Stefan, A. Wiesler, U.-M. Herrmann, A. Grebel-Koehler, D. Qu, J. Muellen, K. De Schryver F. C. *Macromolecules* **2003**, *36*, 5918.
 80. Minard-Basquin, C. Weil, T. Hohner, A.. Raeder, J. O Muellen, K. *J. Am. Chem. Soc.* **2003**, *125*, 5832.
 81. Herrmann, A. Mihov, G. Vandermeulen, G. W. M. Klok H.-A. Muellen, K. *Tetrahedron* **2003**, *59*, 3925.
 82. Wiesler, U.-M.; Weil, T.; Müllen, K., *Topics in Current Chemistry, Vol. 212, Dendrimers III Design, Dimension, Function* F. Vögtle (Vol. ed.), **2000**
„Nanosized Polyphenylene Dendrimers“.
 83. Loi, S. Wiesler, U.-M. Butt, H.-J. Muellen, K. *Macromolecules* **2001**, *34*, 3661.
 84. Loi, S. Butt, H.-J., Hampel, C. Bauer, R. Wiesler, U.-M. Muellen, K. *Langmuir* **2002**, *18*, 2398.
 85. Mihov, G. *PhD Dissertation*, University of Mainz, **2004**.
 86. Distler, D. „*Wässrige Polymerdispersionen – Synthese, Eigenschaften, Anwendungen*“ WILEY-VCH Verlag GmbH, D-69469 Weinheim, **1999**.
 87. Kann, C. Y.; Liu, D. S.; Kong, X. Z.; Zhu, X. L. *J. Appl. Poly. Sci.*, **2001**, *82*, 3194.
 88. André, A.; Henry, F. *Colloid Polym. Sci.*, **1998**, *276*, 1061.
 89. Wiesler, U.-M. *Ph.D. Thesis*, Johannes Gutenberg University – Mainz, Germany **2000**.

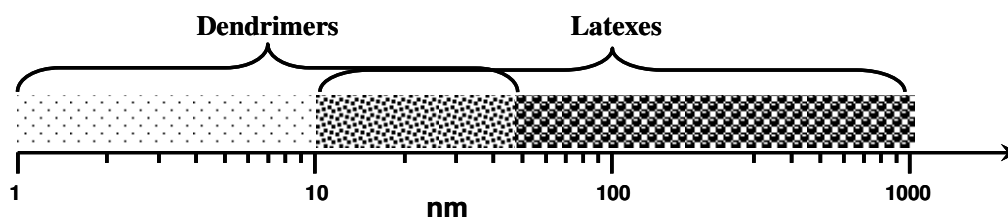
Chapter II. Objectives of the current work

Motivation

Core-shell macromolecular structures have become of great interest in materials science because they gave an opportunity to combine a large variety of chemical and physical properties in the single molecule, by combination of different (in terms of chemistry and physics) cores and shells. The interest in such complex structures was provoked by their potential applications in the coating and painting industry (latexes), as supports for catalysts in polymer industry, or as nano-containers and transporters for genes or drug delivery. The synthesis of core-shell molecules possessing new chemical and physical properties, for all these applications, is an important task nowadays.

In order to obtain core-shell structures several strategies have been developed for synthetic chemistry but two of them have been the most progress: (i) emulsion polymerization, copolymerization and emulsion polymerization using di- or tricopolymers as emulsifiers; (ii) synthesis of dendrimers, hyperbranched structures or dendrimer-polymer hybrids. The first method (i) is well-developed and has been applied in industry for preparation of large variety of coating and paintings. The core-shell molecules obtained by this method (named “latexes”) possess in general a hydrophobic core (PS, P(M)MA or polyolefins) and a hydrophilic shell (polyacrylates). Since emulsion polymerization techniques were used for the synthesis, their structure and functionalities were not well-defined leading to rather broad size distribution. The need for more defined (in terms of structure, functionalities and size) core-shell particles led to the idea of using dendrimers or dendrimer-polymer hybrids (ii), which are being intensively developed nowadays. Dendrimers combine excellent physical characteristics (well-defined structures, functionalities and size distribution) with the possibility for full control over their design and size. All of which makes them the best candidates for preparation of well-defined core-shell molecules. Since the size of the particles is one of the most important physical characteristics to be controlled, it should be noted that a main advantage of dendrimers is the ability of dendrimers of different generations and so the control of the size of the obtained particles.

Figure II. 1 Size range of the core-shell particles based on dendrimers and latexes.



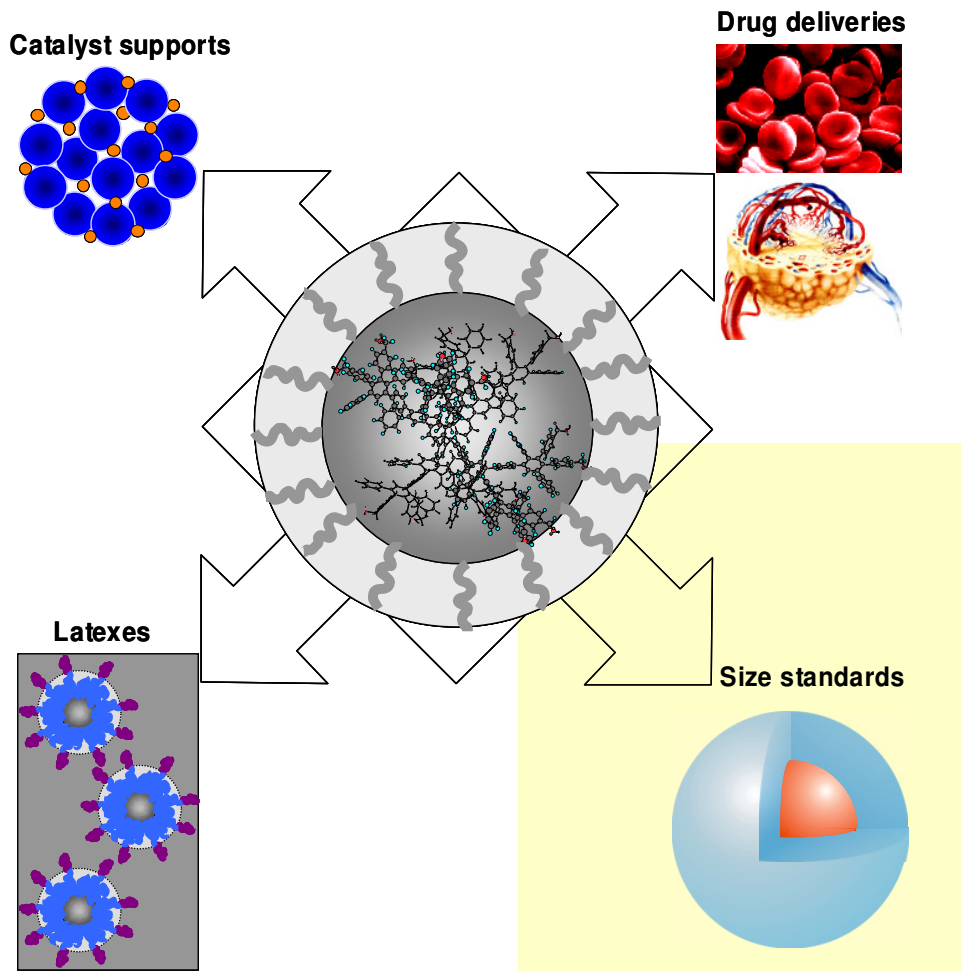
Since latexes can cover most of the range from 10 nm to 1 μm , dendrimers needed to fill the gap in the sizes up to 1 nm. Even if dendrimers are more difficult to be obtained than latexes, they can serve as ideal model compounds for stiff-core flexible-shell latex particles as part in various applications ranging from film formation of dispersions, through fragmentation processes of polymeric supports for metallocenes applied in olefin polymerizations to drug delivery in biological or biomimetical systems (Figure II.2).

Aim of the present study

Core-shell molecules based on dendrimer-polymer hybrids have already been developed utilizing various dendrimers as the core: (poly(amidoamine), poly(propylene imine), poly(trimethylene imine), poly(benzylic ethers), hyper branched polyglycerols and carbosilane dendrimers). While most of the examined core-shell structures possess “soft” or “semirigid” dendrimers cores, their rigid analogues were still elusive. Recently, the synthesis of stiff polyphenylene dendrimers was developed in our group. Significant development of the different methods for functionalization of polyphenylene dendrimers not only statistically but also in a well-defined way with a broad variety of functional groups has been achieved in the recent years. In the present study the aim was to obtain and investigate core-shell structures based on this unique type of dendrimers using two approaches for the formation of flexible-shell and stiff-core particles: (i) a “grafting-onto” reaction of polymer chains to properly functionalized polyphenylene dendrimer; and (ii) a “grafting-from” reaction using polyphenylene dendrimers functional groups as initiators for polymerization.

The choice of the polymer forming the shell was determined by the applications mentioned above and the thus required properties of the target core-shell molecules. Thus, the polymer shell should display hydrophilicity (amphiphilicity is in the great importance for many physical and chemical applications) as well as nucleophilicity (requirement for supports of the metallocene catalysts in olefin polymerization) and bio-compatibility (for bio-applications) (Figure II.2). A polymer covering all the above-mentioned requirements is poly(ethylene oxide) and its block copolymers.

Figure II.2. Applications of PPD-polymer hybrids.



Chapter III

ANIONIC POLYMERIZATION – A TOOL FOR PREPARATION OF DENDRIMER-POLYMER HYBRIDS.

III.1. Anionic versus radical polymerization.

Anionic polymerization is a well-established and widely applicable technique for the preparation of polymer and polymer related structures[1]. In spite of its strong restriction to water and oxygen free conditions, the method is a unique one in case mono-disperse polymer and polymer containing architectures are required. Therefore this technique was successfully applied to the preparation of the polymeric shell in dendrimer-polymer core-shell hybrids [2].

Ionic and techniques as controlled radical with main variants - Atom-Transfer Radical Polymerization (ATRP) and Reversible Addition-Fragmentation chain Transfer (RAFT) as well as Ring Opening Polymerizations (ROP) were tested for preparation of dendrimer-polymer hybrids during the period of about 20 years. This covered a wide range of dendrimers and polymers combined in supramolecular architectures such as the core-shell[3]. In every particular case, depending on the aim of the researchers, an appropriate technique was utilized. For example, the polymerization of N-isopropylacrylamide (NIPAAm) on a dithiobenzoate-terminated dendrimer was performed by the use of RAFT polymerization technique. This produced a temperature-sensitive systems able to decrease their hydrodynamic volume by a temperature above lower critical solution temperature (LCST) and thus applicable as a nano-material for drug release [4]. RAFT polymerization was used in cases of polybutylacrylate (PBA) [5] and polystyrene (PS) [5,6] modified dithiobenzoate terminal dendrimers. The shielding effect of their arms was found to experience a higher probability of irreversible termination. This occurred by the help of the coupling of the polymer-arm radical and forming a dead linear polymer as a draw-back of the method[6]. ATRP and its combination with ring opening polymerization have been applied for the preparation of dendrimer-core possessing mono- or multiple-polymeric shell architectures[7]. Unfortunately, due to side reactions (termination, chain transfer etc.) often these methods result in multimodal molecular distributed products [8,9] with relatively high PDI (down to 1.2) [10-12].

Additionally, the products always contain contaminants as Cu and Cu salts (used as initiator complex in ATRP), which colorized the product and often causes difficulty for any optical investigations on the material. The major problem of the controlled radical polymerization is that obtained polymer-arms possess relatively high PDI, which was shown after the arms have been cleaved from the dendritic core [5,9,11]. In all the cases decreasing the PDI of the core-shell macromolecules compare to this of the polymeric arms due to additional averaging of the molecular distribution of the arms included in the macrostructure. Therefore, the addition of even single polymeric chain obtained by radical polymerization provides a significant increase in the polydispersities of the entire system [13]. In order to reduce the influence of side reactions within the radical polymerization and keep the monomolecularity of the dendrimer to dendrimer-polymer hybrids, scientists have used ionic or combination of ionic and radical polymerizations [14].

Both anionic and cationic polymerizations have succeeded in preparation of almost monodispersed dendrimer based architectures [2]. The uses of these techniques have produced materials possessing PDI, which rarely exceed 1.1 and often are below 1.05 [15]. Thus, the need of this chapter was suggested by the author because the anionic polymerization technique is predominant used in the current study. Most of polymers and copolymers were synthesized by this technique and were further used as anion-living polymers by the formation of the shell on the dendrimer surface. Therefore, the short review over this polymerization technique is required and helps the reader to specify the entire topic.

III.2. Anionic polymerization

Anionic polymerization is a powerful tool for the synthesis of a variety of materials with well-defined molecular characteristics. However, specially designed apparatus and appropriate high-vacuum techniques are needed in order to exclude from the reaction environment all contaminants that may react with the anionic centers. In order to obtain polymers with predictable molecular weights and narrow MWD it is required to have a homogeneous reaction throughout initiation and propagation, to have an initiation rate higher than the rate of propagation and to exclude all possible terminating impurities from the system.

III.2.1. Monomers

The monomers that are susceptible to anionic polymerization are those that can form stable carbanionic species under polymerization conditions. The most studied monomers are styrenes, dienes, and also hetero-cycles that can react with nucleophiles leading to ring opening.[16,17] The double bond must have substituents that can stabilize the negative charge by charge withdrawing thus making the anions stable to possible nucleophilic attack by other species. Consequently, strong electrophilic groups or relatively acidic proton donating groups, such as amino-, carboxyl-, hydroxyl, or acetylene functional groups will interfere with anionic polymerization and thus must be excluded from the monomer unit or be protected as a suitable derivative. In contrast aromatic rings, double bonds, carbonyl, ester, cyano, sulfone groups, etc., stabilize the negative charge and promote the anionic polymerization. The existence of polar substituents, such as carbonyl, cyano, or nitro groups leads to a complex situation, because they may react with the initiator or with the propagating anionic species. The living polymerization of monomers bearing such polar substituents is possible only under very specific conditions (e.g., low polymerization temperature, use of bulky initiators, selected counterion, etc.). Monomers that have been successfully polymerized under anionic polymerization conditions are styrene and styrene derivatives (α -methyl styrene, *p*-methyl styrene, *t*-butyl styrene, etc.),[18-22] dienes (isoprene, butadiene, etc.)[23-27], (meth)acrylates (at low temperatures, using bulky initiators to avoid side reactions with the carbonyl group),[28-32] vinyl pyridines[33-35] (at low temperatures, due to the reactivity of the pyridine ring), cyclic siloxanes,[36] epoxides,[37] and lactones.[38,39]

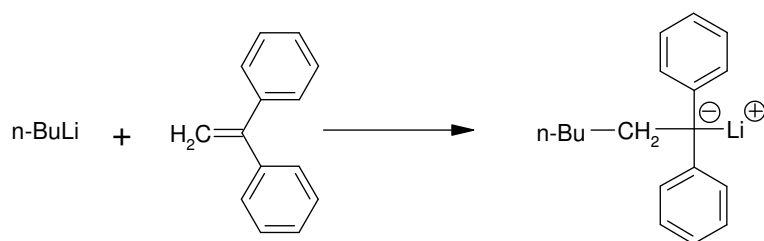
III.2.2. Initiators

The most versatile and useful anionic initiators are alkyllithium compounds, since many of them are commercially available, and others can be rather easily prepared by the reaction of the corresponding alkyl chloride with Li metal. They are soluble in a variety of solvents, including hydrocarbons and most importantly they are efficient initiators for anionic polymerization. The unique characteristic of the organolithium compounds, among the other organometallic compounds with alkali metals, is that the C-Li bond exhibits properties of both covalent and ionic bonds.[40,41] This is a consequence of the fact that lithium, compared to the other

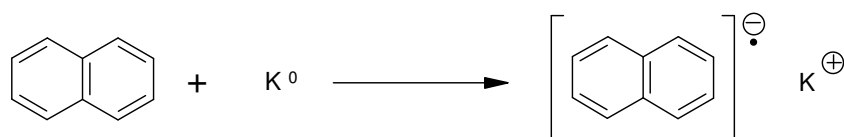
alkali metals has the smallest radius, the highest electronegativity and the highest ionization potential.[42] In addition rather low energy unoccupied *p*-orbitals are available for bonding. The covalent character of the C-Li bond along with the strong aggregation of the ionic pairs[43-45] is responsible for the higher solubility of the organolithium compounds in hydrocarbon solvents, compared to the solubility of the anions with other alkali metals as a counter ion. However, it was found that in the solid state and in solution these compounds form aggregates. The structure of the organic moiety greatly influences the degree of aggregation. Unhindered alkyllithium compounds form hexameric aggregates in hydrocarbon solvents, but when the alkyl group has a branching point at the α - or β -carbon then the aggregates are tetrameric. The degree of association is also influenced by the nature of the solvent, the solution concentration and temperature. In general, the degree of association is decreased by decreasing concentration, by using a strongly solvating solvent (*e.g.* aromatic solvents), by increasing the temperature and by using an organic group capable to delocalize electrons. [46-51] It was shown that the reactivity of the alkyllithium initiators is directly connected with their degree of association: the lower the degree of association the higher the reactivity of the initiator.[52,53] This is evident by the data, concerning the relative reactivities of various alkyllithium initiators versus the degree of association (given in parenthesis) for styrene and diene polymerizations, given below:[54]



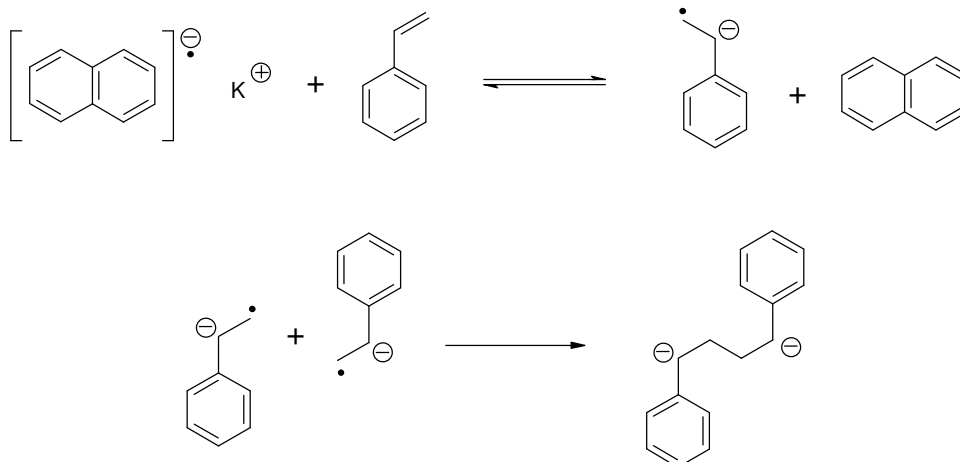
Alkyllithium initiators are usually preferred for the polymerization of styrene and dienes, but are too reactive for the polymerization of methacrylates, because they attack the carbonyl group. For this reason less reactive initiators[28-32] have been used successfully, for example, diphenylhexyllithium (DPHLi), prepared by the reaction of *n*-BuLi with 1,1-diphenylethylene, DPE:



Another class of initiators are the radical anions formed by the reaction of alkali metals with aromatic hydrocarbons in polar solvents.[55] The most common case is the reaction of naphthalene with K^0 or Na^0 metal in THF:



These radical anions react with monomers by reversible electron transfer to form the corresponding monomer radical anions. The example with styrene is given below:



According to the scheme, radical anions lead to initiators possessing two living anions, useful for the synthesis of triblock copolymers, cyclic polymers, telechelics, and more complex structures as H-, super H- and P-shaped polymers. Similar difunctional initiators can be prepared by the reaction of alkali metals with such as α -methylstyrene. Tetrameric dianions are the main product from the reaction of α -methylstyrene with sodium metal[56] and dimeric dianions from the corresponding reaction with Na/K alloy.[57] One of the most effective bifunctional initiators, soluble in hydrocarbon media, is the one formed by the addition reaction of *sec*-BuLi with 1,3-bis(1-phenyl-ethenyl)benzene.[58-61]

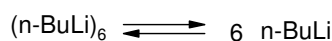
III.2.3. Kinetics of Anionic Polymerization

III.2.3.1. Initiation Reaction

The initiation kinetics of styrene and dienes using alkyllithium initiators in hydrocarbon solvents are the best-studied examples in anionic polymerization. The classic work of Worsfold and Bywater[50] concerning the initiation reaction of styrene polymerization with *n*-BuLi in benzene led to the following relationship:

$$R_i \propto [n\text{-BuLi}]^{1/6} [\text{St}]$$

The fractional kinetic order of the initiation rate on the total initiator concentration implies that the active species for the polymerization are a small fraction of dissociated initiator molecules, produced by the following equilibrium:



Similar kinetic order dependencies have been observed in other systems in aromatic solvents. However, this conclusion was based on theoretical results and experimental measurements of the energy of activation of the initiation reaction, which appears to be too low to include also the energy of the complete dissociation of the aggregates.[62-64] Consequently it seems more likely that an incomplete or stepwise dissociation exists leading to aggregates with lower degrees of association.[65] These intermediate aggregates are not totally inactive towards the polymerization of the monomer. The situation is much more complex in aliphatic solvents, since the inverse correspondence between the reaction order and the degree of alkyllithium aggregation is not always observed.[66] Consequently it seems that the polymerization starts exclusively from the initiator aggregates. A further complication arises from the appearance of cross-associated structures between the organolithium compounds and growing living polymer chains having benzylic or allyliclithium end-groups.[67-69] Generally, initiation is faster in aromatic than in aliphatic solvents and is accelerated by the addition of Lewis bases, because they facilitate the dissociation of the alkyllithium aggregates.

III.2.3.2. Propagation Reaction

The propagation kinetics for styrene polymerization with lithium as the counterion has been studied in both aromatic and aliphatic solvents yielding the same equation,[70,71] shown below:

$$R_p \propto [\text{PStLi}]^{1/2} [\text{St}]$$

where $[\text{PStLi}]$ and $[\text{St}]$ are the living polymer and the monomer concentrations, respectively. In analogy with the initiation kinetics the one-half kinetic order dependence on the living polymer concentration is due to the association of the living polymer chains into dimers in the hydrocarbon solvents. These dimers are not reactive for monomer addition and consequently a dissociation step to unassociated living chains is required. A more complex situation was observed for the propagation kinetics of dienes. In the polymerization of both isoprene and butadiene a first order dependence on the monomer concentration and fractional order dependencies on the concentration of the living chain ends were observed. The fractional order dependence ranges from one-half to one-fourth or even one-sixth.[72-76] Considering the dissociation model, as previously mentioned, the degree of association of the active chain ends has to be defined. However, contradictory results have been reported in the literature. It can be concluded that the degree of association of the polydienyllithium chains is at least two depending on several parameters, such as the molecular weight of the chain, the temperature, and the nature of the solvent. Tetrameric, hexameric, and even larger structures[77] have been also reported. These results are not always compatible with the observed propagation rates and thus the exact mechanism cannot be unambiguously described.

References

- 1 Hong, K. Uhrig, D. Mays J. W. *Current Opinion in Solid State and Materials Science* **1999**, 4, 531.
- 2 Hadjichristidis, N. Pitsikalis, M. Pispas, S. Iatrou, H. *Chem. Rev.* **2001**, 101, 3747.
- 3 Roovers, J. Comanita, B. *Advances in Polymer Science*, **1999**, 142, 180.
- 4 You, Y.-Z. Hong, Ch.-Y. Pau, C.-Y. Wang, P.-H. *Adv. Mater.* **2004**, 16, 1953.
- 5 Hao, X. Nilsson, C. Jesberger, M. Stenzel, M. H. Malstroem, E. Davis, T. P. Stmark, E. Barner-Kowollik, C. *J. Polym. Sci.: Part A: Polym. Chem.*, **2004**, 42, 5877.
- 6 Darcos, V. Dure´ault, A. Taton, D. Gnanou, Y. Marchand, P. Caminade, A.-M. Majoral, J.-P. Destarac, M. Leising, F. *Chem. Commun.*, **2004**, 2110.
- 7 Hedrick, J. L. Trollsås, M. Hawker, C. J. Atthoff, B. Claesson, H. Heise, A. Miller R. D. *Macromolecules* **1998**, 31, 8691.
- 8 Pyun, J. Tang, C. Kowalewski, T. Fre´chet, J.M.J. Hawker, C.J. *Macromolecules* **2005**, 38, 2674.
- 9 Zhao, Y. Shuai, X. Chen, C. Xi, F. *Macromolecules* **2004**, 37, 8854.
- 10 Shuai, X. Chen, C. Xi, F. *Chem. Mater.* **2003**, 15, 2836.
- 11 Zhao, Y. Zhang, J.-M. Jiang, J., Chen, C. Xi, F. *J. Poly. Sci: Part A: Polym. Chem.*, **2002**, 40, 3360.
- 12 Hovestad, N.J. van Koten, G. Bon, S.A.F. Haddleton, D.M. *Macromolecules* **2000**, 33, 4048.
- 13 Emrick, T. Hayes, W. Fre´chet J.M.J. *J. Poly. Sci: Part A: Polym. Chem* **1999**, 37, 3748.
- 14 Hou, S. Chaikof, E.L. Taton, D. Gnanou, Y. *Macromolecules* **2003**, 36, 3874.
- 15 Matsuo, A. Watanabe, T. Hirao, A. *Macromolecules* **2004**, 37, 6283.
- 16 Riess, G.; Hurtrez, G. *Encyclopedia of Polymer Science and Engineering*, 2nd ed.; Kroschwitz, J. I., Ed.; Wiley: New York, **1985**; Vol. 2, p 324.
- 17 Jerome, R.; Fayt, R.; Ouhadi, T. *Prog Polym Sci* **1984**, 10, 87.
- 18 Mays, J. W.; Hadjichristidis, N. *Polym Bull* **1989**, 22, 471.
- 19 Conlon, D. A.; Crivello, J. V.; Lee, J. L.; O' Brien, M. J. *Macromolecules* **1989**, 22, 509.

- 20 Konigsberg, I.; Jagur-Grodzinski, J. *J Polym Sci Polym Chem Ed* **1983**, 21, 2535.
- 21 Okay, O.; Funke, W. *Macromolecules* **1990**, 23, 2623.
- 22 Fetters, L.J.; Morton, M. *Macromolecules* **1969**, 2, 453.
- 23 Elgert, K.-F.; Ritter, W. *Makromol Chem* **1976**, 177, 2021.
- 24 Zhongde, X.; Mays, J. W.; Xuexin, N.; Hadjichristidis, N.; Schilling, F. C.; Bair, H. E.; Pearson, D. S.; Fetters, L. J. *Macromolecules* **1985**, 18, 2560.
- 25 Blondin, D.; Regis, J.; Prud'homme, J. *Macromolecules* **1974**, 7, 187.
- 26 Suzuki, T.; Tsuji, Y.; Tagekami, Y.; Harwood, H. J. *Macromolecules* **1979**, 12, 234.
- 27 Zhong, X. F.; Francois, B. *Makromol Chem* **1990**, 191, 2743.
- 28 Hatada, K.; Kitayama, T.; Ute, K. *Prog Polym Sci* **1988**, 13, 189.
- 29 Yuki, H.; Hatada, K. *Adv Polym Sci* **1979**, 31, 1.
- 30 Allen, R. D.; Long, T. E.; McGrath, J. E. *Polym Bull* **1986**, 15, 127.
- 31 Varshney, S. K.; Jacobs, C.; Hautekeer, J. P.; Bayard, P.; Jerome, R.; Fayt, R.; Teyssie, P. *Macromolecules* **1991**, 24, 4997.
- 32 Ozaki, H.; Hirao, A.; Nakahama, S. *Macromolecules* **1992**, 25, 1391.
- 33 Luxton, A. R.; Quig, A.; Delxaux, M.-J.; Fetters, L. J. *Polymer* **1978**, 19, 1320.
- 34 Muller, M.; Lenz, R. W. *Makromol Chem* **1989**, 190, 1153.
- 35 Soum, A. H.; Tien, C.-F.; Hogen-Esch, T. A.; D'Accorso, N. B.; Fontanille, M. *Makromol Chem Rapid Commun* **1983**, 4, 243.
- 36 Fisch, D.; Khan, I. M.; Smid, J. *Makromol Chem Macromol Symp* **1990**, 32, 241.
- 37 Inoue, S.; Aida, T. G. *Encyclopedia of Polymer Science and Engineering*, Suppl Vol.; Kroschwitz, J. I., Ed.; Wiley: New York, **1990**; p 412.
- 38 Kricheldorf, H. R.; Berl, M.; Scharnagl, N. *Macromolecules* **1988**, 21, 286.
- 39 Dubois, P.; Jerome, R.; Teyssie, P. *Makromol Chem Macromol Symp* **1991**, 42/43, 103.
- 40 Lambert, C.; von Rague Schleyer, P. *Angew Chem Int Ed Engl* **1994**, 33, 1129.
- 41 Schade, C.; von Rague Schleyer, P. *Adv Organomet Chem* **1987**, 27, 169.
- 42 Rundle, R. E. *J Phys Chem* **1957**, 61, 45.
- 43 Brown, T. L. *Adv Organomet Chem* **1965**, 3, 365.

- 44 Brown, T. L. *Pure Appl Chem* **1970**, 23, 447.
- 45 Dietrich, H. *J. Organomet Chem* **1981**, 205, 291.
- 46 Brown, T. L.; Dickerhoff, D. W.; Baffus, D. A. *J Am Chem Soc* **1962**, 84, 1371.
- 47 Lewis, H. L.; Brown, T. L. *J Am Chem Soc* **1970**, 92, 4664.
- 48 Margerison, D.; Pont, J. D. *Trans Faraday Soc* **1971**, 67, 353.
- 49 Fraenkel, G.; Beckenbaugh, W. E.; Yang, P. P. *J Am Chem Soc* **1976**, 98, 6878.
- 50 Bywater, S.; Worsfold, D.J. *J Organomet Chem* **1967**, 10, 1.
- 51 Weiner, M.; Vogel, C.; West, R. *Inorg Chem* **1962**, 1, 654.
- 52 Hsieh, H. L. *J Polym Sci A-3* **1965**, 153, 163.
- 53 Selman, C. M.; Hsieh, H. L. *Polym Lett* **1971**, 9, 219.
- 54 Hsieh, H. L.; Glaze, W. H. *Rubber Chem Technol* **1970**, 43, 22.
- 55 Szwarc, M. *Adv Polym Sci* **1983**, 49, 1.
- 56 Richards, D. H.; Williams, R. L. *J Polym Sci* **1973**, 11, 89.
- 57 Lee, C. L.; Smid, J.; Szwarc, M. *J Phys Chem* **1962**, 66, 904.
- 58 Tung, L. H.; Lo, T. Y.-S. *Macromolecules* **1994**, 27, 2219.
- 59 Bredeweg, C. J.; Gatzke, A. L.; Lo, T. Y.-S.; Tung, L. H. *Macromolecules* **1994**, 27, 2225.
- 60 Lo, T. Y.-S.; Otterbacher, E. W.; Gatzke, A. L.; Tung, L. H. *Macromolecules* **1994**, 27, 2233.
- 61 Lo, T. Y.-S.; Otterbacher, E. W.; Pews, R. G.; Tung, L. H. *Macromolecules* **1994**, 27, 2241.
- 62 Clark, T.; Schleyer, P. V.; Pople, J. A. *J Chem Soc Chem Commun* 1978, 137.
- 63 Baird, N. C.; Barr, R. F.; Datta, R. K. *J Organomet Chem* **1973**, 59, 65.
- 64 Van Beylen, M.; Bywater, S.; Smets, G.; Szwarc, M.; Worsfold, D. *J. Adv Polym Sci* **1988**, 86, 87.
- 65 Graham, G.; Richtsmeier, S.; Dixon, D. A. *J Am Chem Soc* **1980**, 102, 5759.
- 66 Guyot, A.; Vialle, J. *J Polym Sci Part B* **1968**, 6, 403.
- 67 Roovers, J. E. L.; Bywater, S. *Macromolecules* **1968**, 1, 328.
- 68 Schue, F.; Bywater, S. *Macromolecules* **1969**, 2, 458.
- 69 Morton, M.; Pett, R. A.; Fetters, L. J. *Macromolecules* **1970**, 3, 333.
- 70 Cubbon, R. C. B.; Margerison, D. *Proc Roy Soc* **1962**, 268A, 260.

- 71 Johnson, A. F.; Worsfold, D. J. *J Polym Sci Part A-3*, **1965**, 449.
- 72 Morton, M.; Bostick, E. E.; Livigni, R. A.; Fetters, L. J. *J Polym Sci Part A* **1963**, 1, 1735.
- 73 Francois, B.; Sinn, V.; Parrod, J. *J Polym Sci Part C* **1963**, 4, 375.
- 74 Guyot, A.; Vialle, J. *J Macromol Sci Chem* **1970**, A4, 107.
- 75 Worsfold, D. J.; Bywater, S. *Can J Chem* **1964**, 42, 2884.
- 76 Alvarino, J. M.; Bello, A.; Guzman, G. M. *Eur Polym J* **1972**, 8, 53.
- 77 Fetters, L. J.; Balsara, N. P.; Huang, J. S.; Jeon, H. S.; Almdal, K.; Lin, M. Y. *Macromolecules* **1995**, 28, 4996.

Chapter IV

CORE-SHELL MACROMOLECULES WITH DENDRITIC POLYPHENYLENE CORE AND POLYETHYLENE OXIDE SHELL

IV.1. Introduction

There has been a growing interest in the design and the synthesis of macromolecules with high level of organization, forming core-shell nano-structures with ever-increasing degrees of complexity and to control over their composition and structures. In many cases, the design, construction and desired properties of these materials are inspired by biological systems and their applications in biological or biomedical fields are promising.[1-5] This is especially true for polyethylene oxide (PEO) containing particles.[6] PEO is a hydrophilic, soft polymer showed to have non-toxicity and biocompatibility, known to prevent the nonspecific adsorption by means of intermolecular interactions and biological systems (*e.g.* proteins),[7-9] and interact only minimally with both hydrophilic and hydrophobic surfaces (*e.g.* polyphenylene dendrimer surface).[10] All of the properties of PEO attract a considerable interest over the PEO, which have been used in a wide variety of applications ranging from hydrophilic coatings[11] to thickeners and emulsifiers.[12-14] All mentioned above support the use of PEO as shell in preparation of dendrimer-polymer core-shell hybrids. PEO is mainly prepared by an anionic polymerization technique, which fulfill the criteria for narrow molecular distribution as discussed in the previous section - III.1. The preparation of PEO arms by anionic polymerization is given below.

IV.2. Polyethylene oxide–arms for preparation of dendrimer-polymer hybrids.

IV.2.1. Introduction

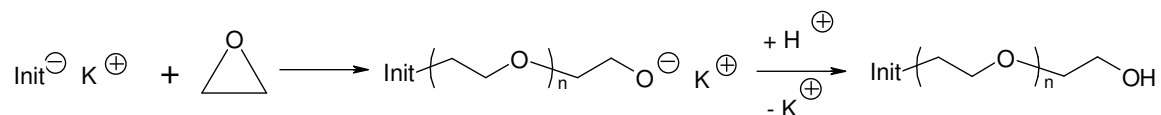
The anionic polymerization of ethylene oxide (EO) has been intensively studied using several alkali metal counterions, for example, Na⁺, K⁺, and Cs⁺. [15-20] For lithium counterions, only initiation but no propagation has been observed under conventional reaction conditions.[21,22] This effect was attributed to the strong aggregation of lithium alkoxides resulting from the comparatively high charge density of the lithium cation. In general, the strength of aggregates decreases with the decreasing of charge density (increasing size) of the counterion, *i.e.* in the order Li⁺, Na⁺, K⁺, Rb⁺, and Cs⁺. Recently Esswein *et al.* showed that in the presence of a strong Lewis base, for example the phosphazene base, polymerization of ethylene oxide with Li⁺ counterions can be achieved.[23,24] In this case, the phosphazene

base forms a strong complex with Li^+ resulting in a break up of the strong lithium alkoxide aggregates, and thus making the polymerization of ethylene oxide possible. Furthermore, because of the strongly basic character of the phosphazene base $t\text{-BuP}_4$ even alcohols can be used as initiators. Anionic polymerization of ethylene oxide in the presence of Li^+ counterions is of particular interest for the synthesis of polyethylene oxide or PEO-containing block copolymers by sequential anionic polymerization.[23,25-29] Since most of the applicable monomers are commonly polymerized using organolithium initiators, the use of base has the advantage that the block copolymer can be prepared without an exchange of the cation.

IV.2.2. Synthesis and characterization of polyethylene oxide.

Synthesis of polyethylene oxide was performed using different initiators in order to understand their influence over polymerization process and find the most appropriate one for the purpose needed. A classical anionic synthetic scheme was used involving four different types of initiators.

Scheme IV.1. Synthesis of polyethylene oxide



Initially, cumylpotassium, an appropriate initiator for polymerization of vinyl or allyl containing monomers, was used for polymerization of ethylene oxide in THF at 40°C (see 4.1 in Table IV.1). The obtained polymer showed a relatively high molecular weight with a M_n slightly different from the theoretical expectations, and high polydispersity which could be attributed to the fact that the initiator possesses relatively high activity (compared to alkoxides) combined with the strong association effect of THF. [30]

The use of potassium alkoxides as initiators solves the problem with initiators associations. Potassium benzoate was prepared by titration of hydroxyl group of benzyl alcohol with potassium naphthalide. The polymer obtained with this initiator again showed a relatively high PDI, which is possibly due to the fact that naphthalene potassium can also initiate polymerization of ethylene oxide, leading to polymers with lower molecular weight and broader polydispersity (see 4.2 in Table IV.1).

Table IV.1. Type of initiator and molecular weights of polyethylene oxides.

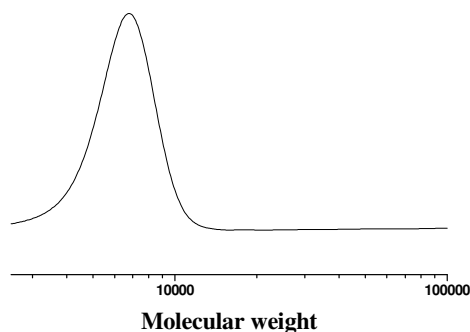
No	Type of initiator	Theoret.* M_n	GPC		¹ H-NMR M_n
			M_n	PDI	
4.1	CP	100 000	74 000	1.21	35 400
4.2	BOK	10 000	4 000	1.23	6 600
4.3	BuOK	15 000	13 700	1.09	14 000
4.4	BuOK	10 000	7 300	1.06	9 000
4.5	BuOK	670	1 700	1.23	1 300
4.6	BuOK	670	1 100	1.18	1 900
4.7	BuOK	670	650	1.11	980
4.8	BuOK	670	340	1.33	440

* M_n = g EO/mol initiator;

CP-cumylpotassium, BOK-benzoxypotassium, BuOK-potassium-*tert*-butoxide.

In order to avoid any post reaction impurities that could initiate the polymerization of ethylene oxide, commercially available potassium *tert*-butoxide was used. The obtained product showed excellent characteristics – molecular weight near to expectations and PDI below 1.1 (see **4.3** and **4.4** in Table IV.1 and Figure IV.1). The need of low molecular weight polymers was accompanied by increase of the PDI from 1.11 to 1.33 for **4.7**, and **4.8** respectively.

Figure IV.1. GPC (Water – eluent, polyethylene oxide – standard) of **4.4**.



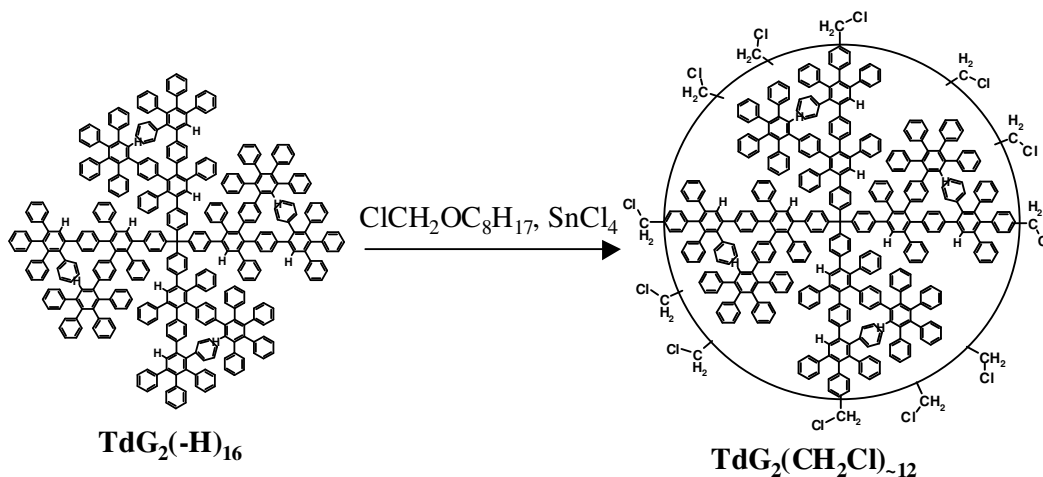
Thus, one can conclude that in each particular case the optimal conditions and a proper initiator for preparation of well-defined PEOs possessing desired molecular weight and low polydispersity were found. Products **4.3**, **4.4** and **4.8** were further applied as PEO-arms in the preparation of dendrimer-polymer hybrids by “grafting-onto” approach (see section IV.4)

IV.3. Synthesis of chloromethyl functionalized polyphenylene dendrimer $\text{TdG}_2(\text{CH}_2\text{Cl})_{\sim 12}$.

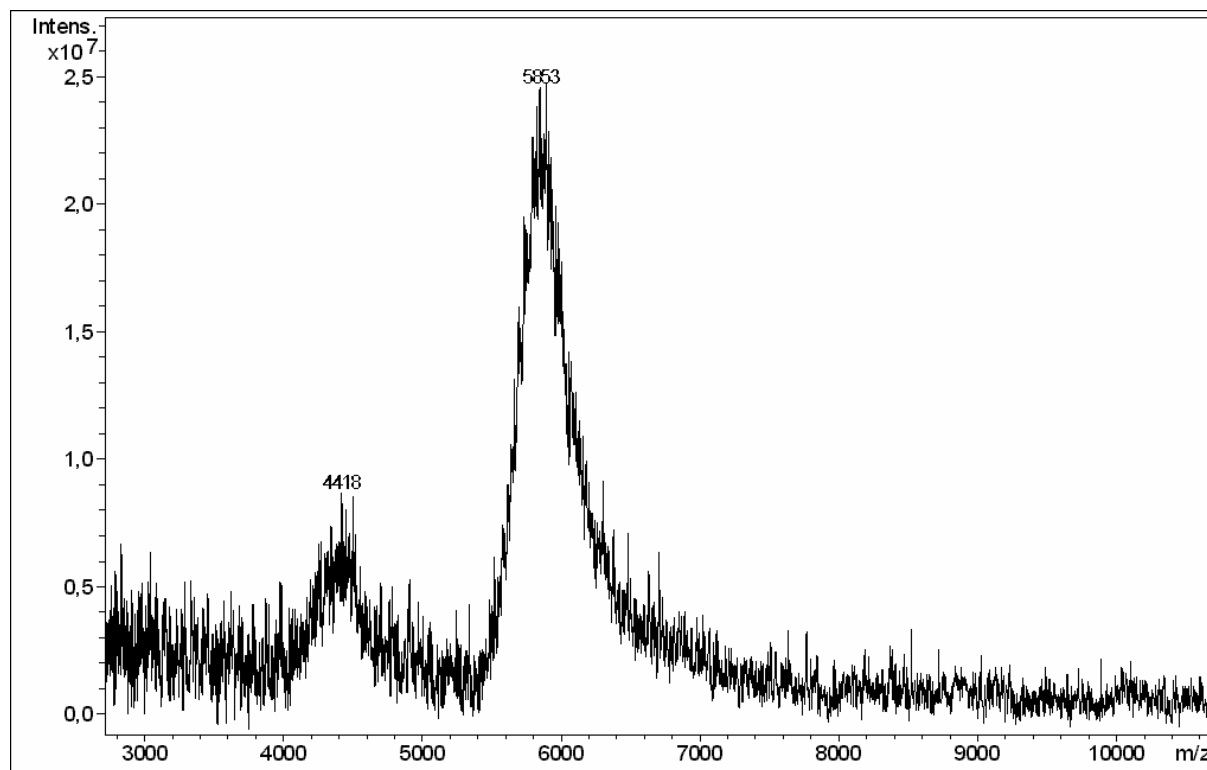
In order to synthesize core-shell nano-particles with a defined structure, the availability of suitable core molecules possessing the desired functional groups is essential. Furthermore, reactions that can be applied only by these functional groups have to be utilized. The reaction conditions in anionic living polymerization exclude any contaminants and thus leads to lower polydispersity of the obtained polymers and regioselectivity of the end-coupling reaction.

For the grafting of living PEO chains onto functionalized polyphenylene dendrimers, Dr. Veselin Sinigersky (AK Müllen) investigated the chloromethylation reaction of non-functionalized dendrimer ($\text{TdG}_2(-\text{H})_{16}$) by using 80 equivalents of chloromethyloctylether in the presence of SnCl_4 . A statistically chloromethylated TdG_2 containing an average of 12 chloromethyl groups $\text{TdG}_2(\text{CH}_2\text{Cl})_{\sim 12}$ was obtained (see Scheme IV.2). The number of CH_2Cl groups was determined by MALDI-ToF mass-spectrometry and $^1\text{H-NMR}$ spectroscopy.

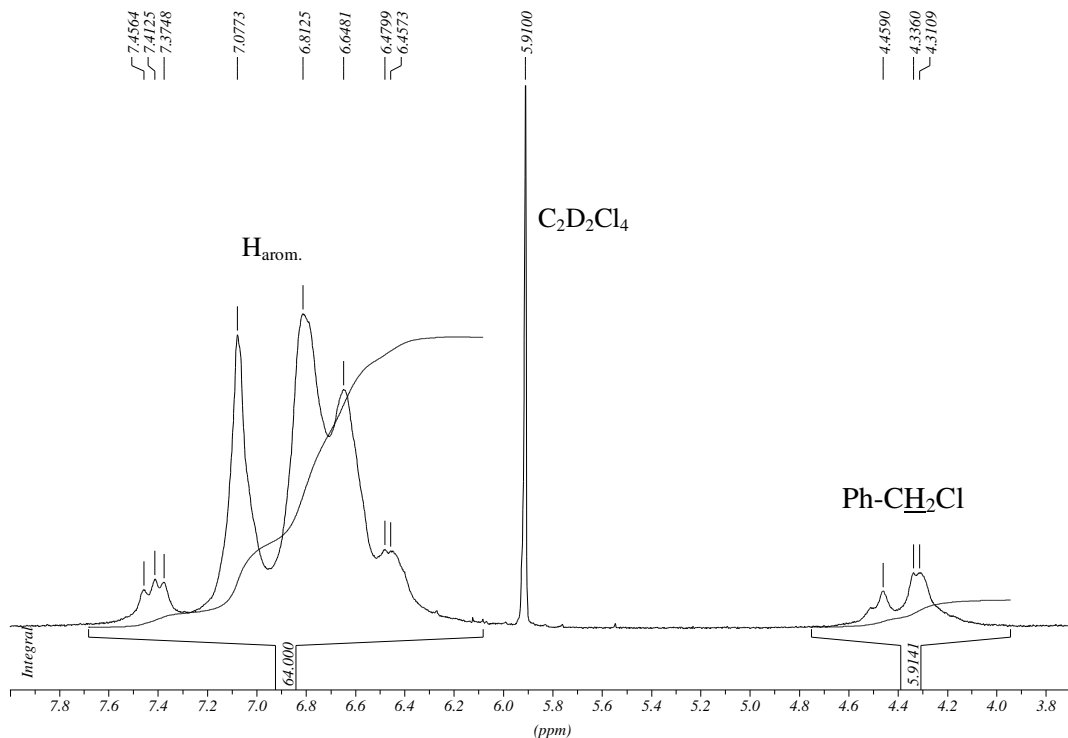
Scheme IV.2. Chloromethylation of $\text{TdG}_2(-\text{H})_{16}$.



In the MALDI-ToF mass-spectra of $\text{TdG}_2(\text{CH}_2\text{Cl})_{\sim 12}$ (see Figure IV.2) two broad peaks were observed, the main peak corresponds to chloromethylated products with molecular weights ranging from 5300 to 5760 Dalton, indicating 8-17 chloromethyl groups. A second peak at 4000-4300 Dalton corresponds to 3/4 of the molecular weight of the $\text{TdG}_2(\text{CH}_2\text{Cl})_{\sim 12}$, due to the cleavage of one branch from the dendrimer during the mass-spectrometric measurement. This phenomenon has previously been observed and discussed in the literature.[31]

Figure IV. 2 MALDI-TOF mass spectrum (matrix-dithranol, DCM, Ag⁺) of **TdG₂(CH₂Cl)₋₁₂**

The average number of chloromethyl groups can also be calculated from their ¹H-NMR spectra (see Figure IV.2) using the relative intensity of the aromatic protons at 7.6 - 6.2 ppm and the chloromethyl protons at 4.7 - 4.0 ppm indicate the presence of 12 CH₂Cl-groups, which is in a good agreement with the MALDI-ToF data. The broad signal at 4.7 - 4.0 ppm results from the different isomeric CH₂Cl groups on the dendrimer due to the statistical chloromethylation reaction, which causes variously ortho-, meta- and para-substitution on the different aromatic rings.

Figure IV. 2 ^1H -NMR spectrum (500 MHz, $\text{C}_2\text{D}_2\text{Cl}_4$, RT) of $\text{TdG}_2(\text{CH}_2\text{Cl})_{-12}$.

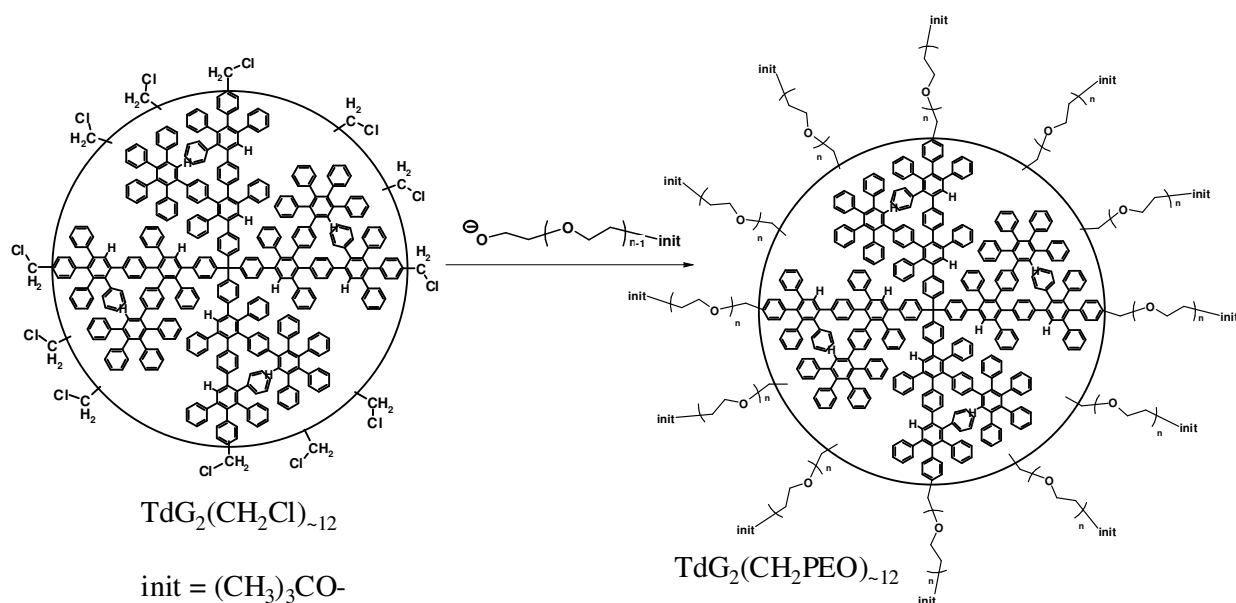
IV.4. Synthesis of core-shell possessing polyphenylene dendrimer core and PEO shell – “grafting-onto” approach.

The use of a dendrimer possessing a well-defined structure combined with a statistical distribution of its functional groups seems paradoxical at first sight (dendrimer well-defined in structure and functionalities is recommended for the synthesis of well-define core-shell molecules (see section IV.5)). However, statistically functionalized polyphenylene dendrimers can be easily obtained (by the functionalization of a non-functional dendrimer (see scheme IV.2) in a single step reaction), while the preparation of a dendrimer with define functionalities requires an additional synthesis of functional cyclopentadienone. The control over the number of functional groups is poorer in the case of statistically functionalized dendrimers, but the number of functionality is broader (140 available para-position for statistical functionalization and 4-32 for well-define one). This allows one to find the relations between the number of dendrimer functional groups and the conversion of the “grafting-onto” reaction and thus adjust the density and the related thickness of the polymeric shell. The advantage of the statistical functionalization is the ease of introducing a different number and

types of functional groups using the same non-functionalized dendrimer. This makes the method attractive from synthetic point of view. It is useful for preparation of core-shell molecules with different polymer densities in the shell and its influence over the particle properties. Finally, the molecular weight distribution of the core-shell molecules is related to the statistical distribution of the dendrimer functional groups (increase of functional distribution is accompanied by increase of molecular weight distribution of core-shell molecules) and additionally is limited due to sterical hindrance of already attached chains that shield the remaining functionalities of the dendrimer (see below). Therefore, when obtained by the “grafting-onto” method, core-shell macromolecules possess a relatively narrower molecular weight distribution than those obtained by “grafting-from” method, where 16 fold hydroxymethylated well-defined polyphenylenen dendrimer was used (see section IV.5).

The preparation of core-*mono*-shell macromolecules by the “grafting-onto” method utilized a chloromethylated dendrimer involved in a two-step synthesis. First, ethylene oxide was polymerized by living anionic polymerization to give PEO with well-defined chain lengths. In a second step, these living PEO chains were grafted-onto the surface of $\text{TdG}_2(\text{CH}_2\text{Cl})_{-12}$ by a nucleophilic substitution reaction (Williamson reaction) between the living anionic ends of the PEO chains and the chloromethyl groups of the dendrimer (see Scheme IV.3).

Scheme IV.3. PEO grafting onto the surface of $\text{TdG}_2(\text{CH}_2\text{Cl})_{-12}$.



A 10-fold molar excess of PEO chains to each chloromethyl group was used. The crude product was purified from unreacted single PEO chains using a Stirred Ultrafiltration Cell equipped with a polyethersulfone membrane. After purification the GPC elugrams (see Figure IV.3) showed monodisperse products with a low polydispersity index.

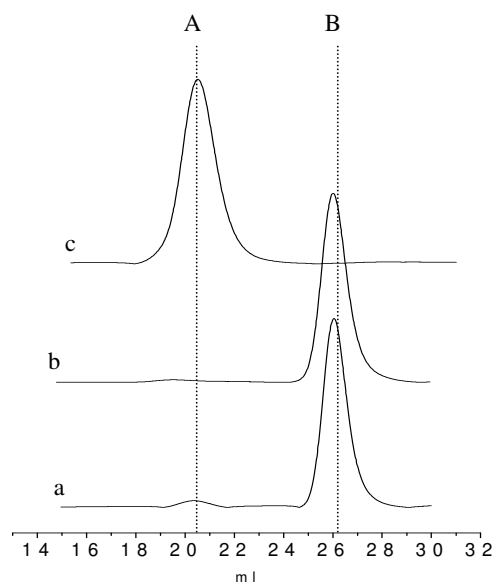


Figure IV.3. Purification of the product (see **4.9** in Table IV.2) by ultrafiltration - GPC elugrams (standard: PEO, eluent: DMF):

a) Crude mixture before purification; b) Single PEO chains removed by ultrafiltration; c) Core-shell particles after purification from the single PEO chains. A) Appearance of the core-*mono*-shell particles. B) Appearance of the single PEO chains (**4.8**).

The molecular weight of a single PEO chain was calculated theoretically and from the $^1\text{H-NMR}$ spectra by comparing the relative signal intensities of the *tert*-butyl (from the initiator of the EO polymerization) and the PEO protons (see Table IV.2). The GPC data were obtained from aliquots taken from the reaction mixture before addition of the $\text{TdG}_2(\text{CH}_2\text{Cl})_{-12}$. A relatively high polydispersity index was obtained for low molecular weight PEO (Table IV.2, **4.9**), and nearly monodisperse PEO was obtained for a higher molecular weight (Table IV.2, **4.10** and **4.11**). This due to the well known fact that equal difference in the molecular weights between the polymeric chains of two polymers with lower and higher molecular weight leads to higher and lower PDI respectively. The differences in the molecular weights, in terms of anionic polymerization, occurred from the difference in the induction period of every particular system. Often, longer induction period due to associations of the initiator molecules or reaction of the initiator with contaminants.

Table IV.2. Molecular weight of the single PEO chains and the obtained core-*mono*-shell nanoparticles by $^1\text{H-NMR}$ spectroscopy (250 MHz, RT, CD_2Cl_2) and GPC (standard: PEO, eluent: DMF), number of PEO arms per dendrimer molecule and hydrodynamic radius (R_h) by Dynamic Light Scattering (DLS) in THF.

No	PEO arms			Core-shell nanoparticles					
	$^1\text{H-NMR}$ M_n	GPC		$^1\text{H-NMR}$		UV M_n	GPC		DLS R_h [nm]
		M_n	PDI	M_n	NA *		M_n	PDI	
4.9	440	340	1.33	10 500	11.4	10 100	9 400	1.69	4.0
4.10	9 000	7 300	1.06	91 500	9.6	84 400	110 000	1.08	10.4
4.11	14 000	13 700	1.09	130 000	8.9	134 000	200 000	1.34	12.0

* NA – number of PEO arms calculated using M_n obtained by $^1\text{H-NMR}$ spectroscopy

The molecular weights of the core-shell nanoparticles prepared by the “grafting-onto” process were determined by GPC and $^1\text{H-NMR}$ spectroscopy (see Table IV.2). M_n was calculated from the relative signal intensities of the protons of the dendrimer scaffold and of the PEO chains.

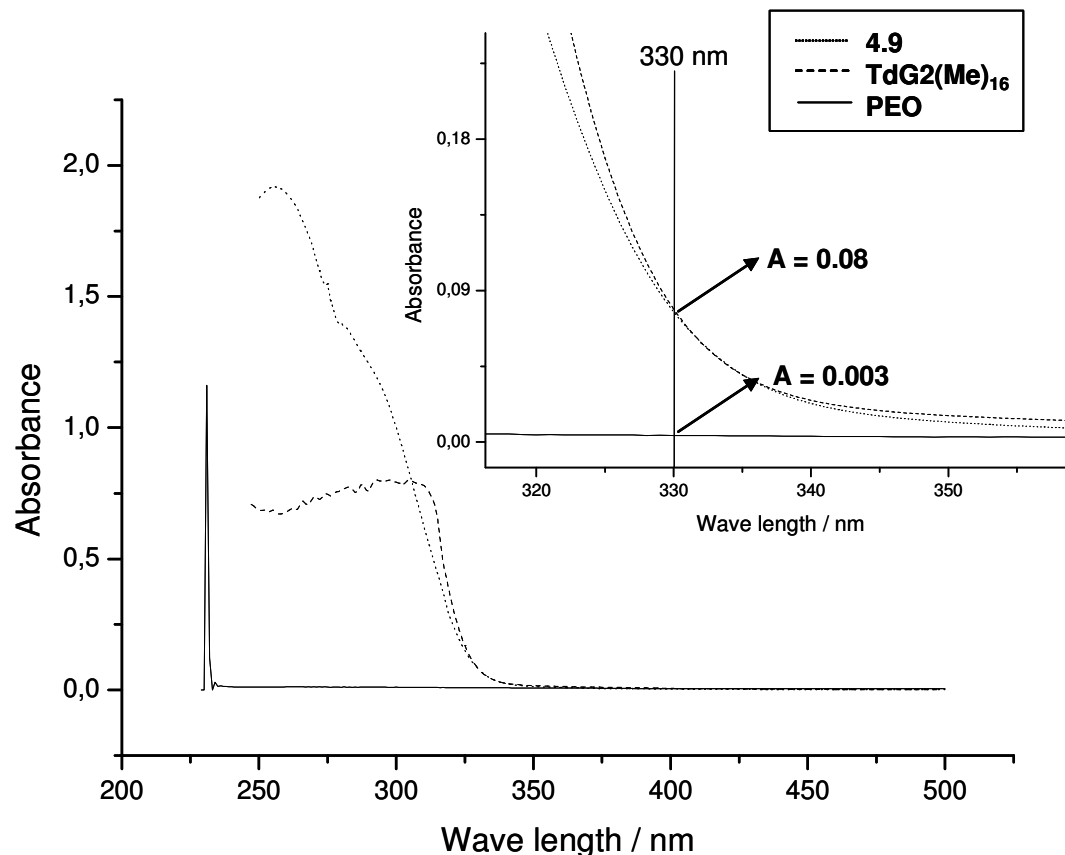
However, determination of molecular weight by UV spectroscopy is possible only if the extinction coefficient of the obtained core-shell structures is known at certain wavelength. In order to obtain the extinction coefficient, UV absorption spectrum of the second-generation polyphenylene dendrimer with tetrahedral core possessing 16 methyl groups on its surface (**TdG2(Me)₁₆**) was measured. Then the extinction coefficient of **TdG2(Me)₁₆** was evaluated for the wavelength $\lambda=330$ nm (it was found to be $13\,600\text{ L mol}^{-1}\text{ cm}^{-1}$) and applied this value as the extinction coefficient of the core-shell macromolecules in the Lambert-Beer law ($A_\lambda = c \cdot \varepsilon_\lambda \cdot l$, where A_λ is absorption; c is concentration of the core-shell molecules in THF; ε_λ is extinction coefficient and l is pathlength of the light trough the sample). There are three main considerations that justify this procedure (see Figure IV.4):

1. PEO has negligible absorption at 330 nm ($A = 0.003$) in the UV-spectrum and cannot influence the absorbance of core-shell molecules at that wavelength.
2. While λ_{max} is different for the core-shell molecules ($\lambda_{\text{max}} = 255\text{nm}$) and **TdG2(Me)₁₆** ($\lambda_{\text{max}} = 293\text{nm}$), in the interval 325-345nm the UV-spectra for both substances are nearly the same (the shape, slope and position are

identical), which suggests that absorbance in that interval is provoked only by dendritic core.

3. Polyphenylene dendrimers are rigid and shape persistent, while PEO is relatively soft and cannot induce any conformational changes in the core and thus will not influence the absorbance of the dendrimer itself.

Figure IV.4 UV spectra of PEO, **TdG2(Me)₁₆** and **4.9** in chloroform.



Thus, measuring the UV-absorption of the solutions of core-shell molecules with a certain volume the calculation of the amounts of the substance in mol was performed (both **TdG2(Me)₁₆**, PEO and calculated molar concentrations of core-shell solutions were in the range $5\text{-}8\text{E-}6 \text{ mol L}^{-1}$ which fulfill the requirement for substances possessing extinction coefficient over 10 000 to be measured in the solution with $M \leq 1\text{E-}5 \text{ mol L}^{-1}$). Since the weights of substances used for preparation of the solutions were known, the molecular weights were evaluated (see Table IV.2)

The M_n values obtained from UV spectroscopy are consistent with the results from $^1\text{H-NMR}$ spectroscopy (see Table IV.2). Since $^1\text{H-NMR}$ spectroscopy does not use any standards or approximations, the results by this method were considered as the most precise.

Using the molecular weights of the core-*mono*-shell nanoparticles and the single PEO chains, the average number of the PEO-arms attached to the dendrimer core was determined (see Table IV.2). $^1\text{H-NMR}$ spectroscopy revealed that with increasing PEO chain-length the degree of PEO functionalization decreases. Only in the case of the very short PEO chains (440 Dalton, **4.9**) a nearly complete conversion was observed. In the other cases, the conversion was limited, due to steric hindrances caused by the already attached longer polymer chains, which shielded the reactive sites on the dendrimer surface.[32] This concept is supported by the results of earlier work describing the grafting reaction of polystyrene and polyisoprene monoanions on a polyetherketone chain. It has been shown that upon increasing the number of reactive sites, the conversion in the grafting reaction becomes limited by steric factors. Additionally, influence over the effect has the way of functionalizing the dendrimer. It should be remind that chloromethylation of nonfunctionalized dendrimer resulted in variously ortho-, meta-, and the para-substitution on the different aromatic rings, which (due to numerous dynamic conformations) can be both on the periphery and inside the dendrimer globe. Thus, functionalities hindered inside the dendrimer are supposed to be hardly reachable and rarely get into the reaction.

One important characteristic of the core-*mono*-shell systems is the size of the particles, usually defined as the hydrodynamic radius (R_h) in a particular solvent. The R_h values in every particular case were found using Dynamic Light Scattering (DLS). In the DLS method, the time fluctuations of the intensity of the scattering light, $I_s(t)$, are analyzed. These fluctuations are caused by Brownian motion (rotational and translational) of the particles that cause perpetual variation of the concentration with the resulting change of the pattern of scattered light. The time course of the detection signal can be analyzed either by a spectrum analyzer or by a correlator. Here only the second case is considered since this was the method chosen for experiments performed. Correlators compute the autocorrelation function of the intensity of the light, I_s , defined as:

$$g^{(2)}(q, \tau) \equiv \frac{1}{\langle I_s \rangle_t^2} \lim_{T \rightarrow \infty} \frac{1}{2T} \int_{-T}^T I_s(t) I_s(t + \tau) dt = \langle I_s(t) I_s(t + \tau) \rangle / I_s(t)_t^2 \quad (\text{IV.1})$$

It can be shown that

$$g^{(2)}(q, \tau) = \int_{-\infty}^{+\infty} \left[\delta(\omega) + \frac{2q^2 D / \pi}{\omega^2 + (2q^2 D)^2} \right] \cos(\omega \tau) d\omega = 1 + \exp(-2q^2 D \tau) \quad (\text{IV.2})$$

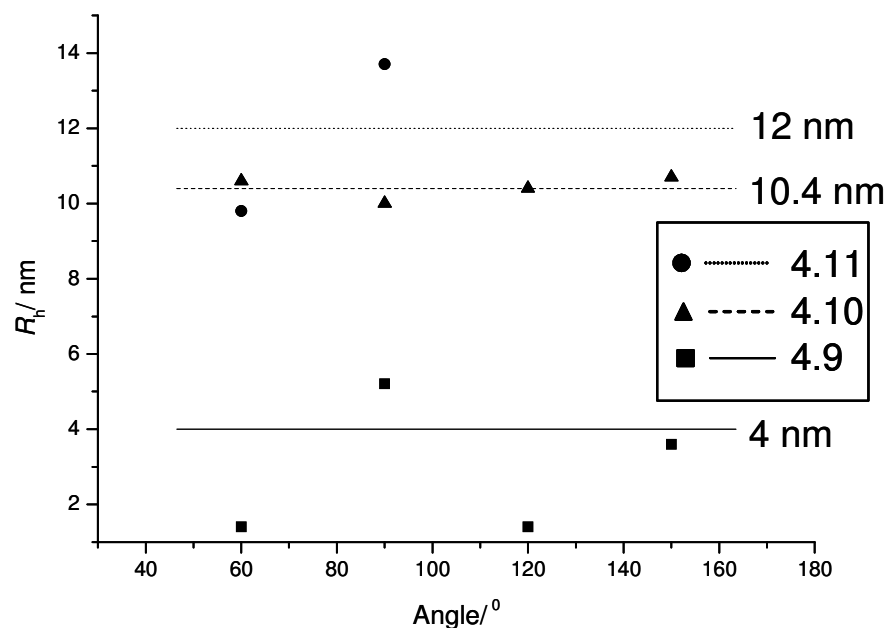
In the equation IV.2 $q = 4\pi n/\lambda_0 \sin(\theta/2)$ is the magnitude of the scattering vector, n is the refractive index of the medium, λ_0 is the wavelength of the scattered light (laser) and θ is the angle at which the detection is done, $\delta(\omega)$ is the delta function, and D is the diffusion coefficient of the scattering species. Equation IV.2 together with the Einstein relation (eq. IV.3) provides the calculation of the hydrodynamic radius, R_h , from the scattered light:

$$R_h = \frac{k_B T}{6\pi\eta D} \quad (\text{IV.3})$$

In the equation above, $k_B T$ is the thermal energy and η is the viscosity of the medium. It should be mentioned that the equation IV.3 is derived considering the scattering object as a perfect sphere. The spherical shape of PPD has already been proven and been studied elsewhere [33]. PEO is a relatively soft polymer [34] which is assumed to have a statistically globular shape in good solvents (*e.g.* water, chloroform, THF) with stretched conformation depending on both the solvating strength of the solvent and environmental space. In this particular case, environmental space should be considered as the polymers close to the dendrimer surface are space limited, and so possessed a more stretched conformation than those at the periphery. Thus, both the dendrimeric core and the polymer shell should contribute to the spherical shape of the entire molecule and the equation IV.3 can be applied for determination the R_h of those systems.

The R_h s of the prepared core-*mono*-shell nanoparticles were found to increase from 4 to 12 nm (see Table IV.2 and Figure IV.5) with the extension length of the PEO chains grafted onto the dendrimer surface (by comparison, the R_h of **TdG**₂ was reported to be 3 nm).[35,36]

Figure IV.5. Hydrodynamic radius of the core-shell systems **4.9**, **4.10** and **4.11** prepared by “grafting-onto” method obtained by DLS in THF.



It should be pointed out that the second process was observed in all cases, corresponding to particles with R_h up to 120 nm. This process had much higher intensity signal (see section IV.5.2 for a more detailed discussion) and disturbed the single particle R_h determination. The presence of a second process is mostly due to aggregates. The aggregation behavior of the obtained core-*mono*-shell systems is provoked either by high affinity of the PPD (valid mostly for product **4.9**, where the shell is shorter) or more reasonably intermolecular entanglement of the polymer shells (by **4.11**, where polymer arms are longer). Therefore, in the cases **4.9** and **4.11** the R_h measurements significantly deviate from the average value. In the case **4.10** the core is covered by the PEO chains much longer (M_n of the single chain is 7 300, see Table IV.2) than those of **4.9** (M_n of the single chain is 340). The larger the shell, the better the separation of the cores is. Additionally, the PEO shell of **4.10** is half as large as in **4.11**. This can explain the decrease of the amount aggregates (shorter polymer chains - less probability for intermolecular entanglements). The absence of aggregates of course allowed more precise determination of the R_h of **4.10** (see Figure IV.5)

IV.5. Synthesis of core-*mono*-shell macromolecules using “grafting-from” method.

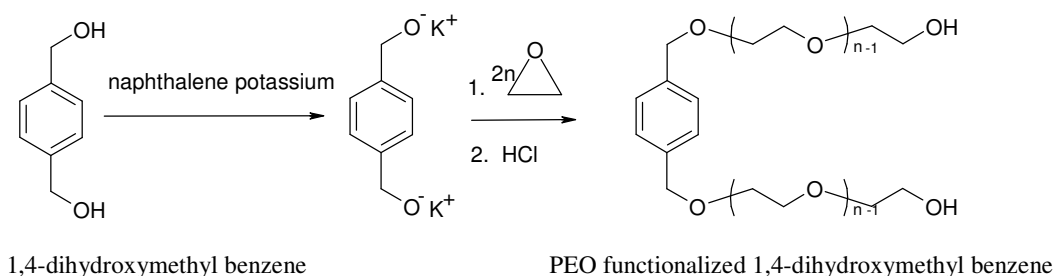
In a second approach core-*mono*-shell systems were synthesized by a “grafting-from” procedure. Advantage of the “grafting-from” procedure is that the number of attached chains is defined by the number of initiator sites (dendrimer functionality) on the dendrimer surface. Thus, the molecular weight distribution of the prepared core-shell particles depending only on those of the polymer chains attached to the dendrimer. The truthfulness of these statements have been already supported by the results of earlier work concerning anionic polymerizations using multifunctional macroinitiators.[37,38] Additionally, in the case of EO polymerization with multifunctional initiators, Gnanou *et. al.* [37] demonstrated that the polymerization starts from each functional group even in the case that only 30% of hydroxyl groups were deprotonated due to the fact that rate of polymerization ($R_p = k_p[O^-][M]$) was found to be much lower than the rate of the proton exchange between protonated and deprotonated OH groups ($R_{exch} > R_p$, $R_{exch} = k_{exch}[O^-][OH]$).

However, the most discussed problem of the multi-anionic initiators is their poor solubility of common solvents for anionic polymerization (*e.g.* tetrahydrofurane, hexane, dioxane, dimethylsulfoxide and toluene) due to the fact that multi-anions provide high polarity of the initiator fragment. Therefore, they possess a high tendency towards aggregation, which result in an increasing polydispersity of the molecules obtained by those initiators. Additionally, in this particular case, the chain length and distribution of the attached polymer can not be determined as there is no possibility to cleave them from the dendritic core.

IV.5.1. Grafting of EO from 1,4-dihydroxymethyl benzene – model reaction.

In order to check the feasibility of the reaction chosen, model experiments for polymerization of EO on 1,4-dihydroxymethyl benzene were performed (see Scheme IV.4).

Scheme IV.4. Polymerization of EO on 1,4-dihydroxymethyl benzene.



The products were characterized by $^1\text{H-NMR}$ spectroscopy and GPC. The molecular weights, theoretically calculated and determined from the $^1\text{H-NMR}$ spectroscopy and GPC, are presented in Table IV.3.

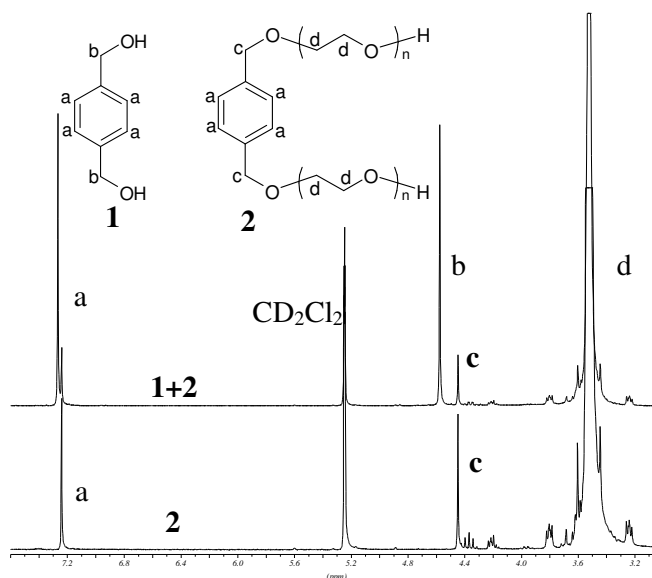
Table IV.3. Molecular weights of the products prepared by polymerization of EO from 1,4-dihydroxymethyl benzene.

Exp. No	Theoret.* M_n	$^1\text{H-NMR}$ M_n	GPC	
			M_n	PDI
4.12	1 000	1 200	1 100	1.13
4.13	6 000	6 200	4 800	1.27
4.14	20 000	18 700	19 000	1.07

*grams(EO)/moles(Initiator)

The $^1\text{H-NMR}$ spectra (see Figure IV.6) indicate that the peak corresponded to methylene protons (“b” protons) of 1,4-dihydroxymethyl benzene (substance **1**) is shifted considerably from the peak of the methylene protons between benzene rings and PEO (“c” protons) in the PEO functionalized 1,4-dihydroxymethyl benzene (substance **2** – **4.12**). Moreover, there are no peak corresponded to “b” protons in the spectrum of substance **2**, which suggests no residual -OH groups left in the system, and thus polymerization of EO proceeds from all available hydroxymethyl groups.

Figure IV.6. $^1\text{H-NMR}$ spectra (250MHz in CD_2Cl_2) of 1,4-dihydroxymethyl benzene and PEO functionalized one (**4.12**).

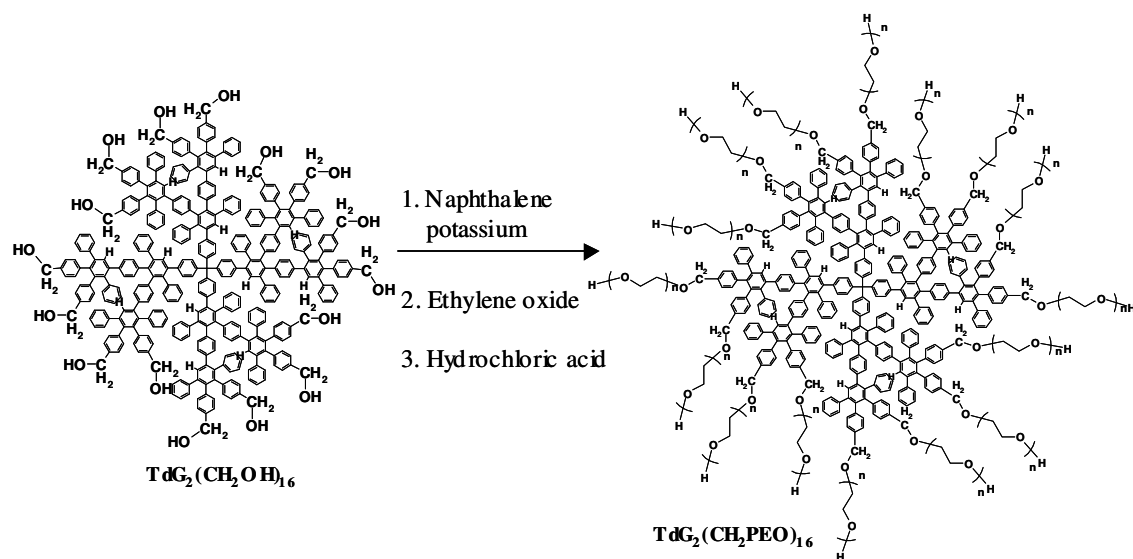


IV.5.2. Synthesis of core-shell possessing polyphenylene dendrimer core and PEO shell – “grafting-from” approach.

Having obtained successful results in the model experiments, a second-generation polyphenylene dendrimer with 16 hydroxymethyl groups on its surface $\text{TdG}_2(\text{CH}_2\text{OH})_{16}$ was used,[39] in order to prepare well-defined core-shell nano-particles comprising a stiff polyphenylene core and flexible PEO shell by polymerization of EO from the dendrimer surface.

The dendrimer $\text{TdG}_2(\text{CH}_2\text{OH})_{16}$ was prepared by Dr. Veselin Sinigerski from the group of Prof. Müllen. For the synthesis of the dendrimer acetyl protected 2,4-cyclopentadien-1-one, 3,4-bis[4-(hydroxymethyl)phenyl]-2,5-diphenyl-(9CI) was used in order to introduce exactly 16 functional groups on the dendrimer surface. More over, all functionalities are at para-positions in the phenyl rings, which minimize the influence of the torsions angle around σ -bonds. All those verify the functional groups are not sterically hindered or shielded by dendrons.

Thus initially, the dendrimer $\text{TdG}_2(\text{CH}_2\text{OH})_{16}$ was converted to a macromolecular initiator $\text{TdG}_2(\text{CH}_2\text{O}^-)_{16}$ by deprotonation with naphthalene potassium (see Scheme IV.5).[40]

Scheme IV.5. Polyethylene oxide “grafting-from” the surface of $\text{TdG}_2(\text{CH}_2\text{OH})_{16}$.

The obtained core-*mono*-shell molecules were characterized by $^1\text{H-NMR}$ -, $^{13}\text{C-NMR}$ -, UV-spectroscopy, GPC, DSC and DLS. Molecular weights (see Table IV.4), calculated from $^1\text{H-NMR}$ spectra, were much higher than the M_n values obtained by GPC. Such “underestimation” of the molecular weights determined by GPC has already been reported for calixarene star polymers[41] and poly(methylmethacrylate) star polymers[42] and is attributed to the difference in shape between the stars and the linear PEO standards used in the GPC measurements. Monomodal distributions were observed in all cases. UV spectroscopy measurements, approximation and calculations were performed in the same way as for the products obtained by the “grafting-onto” method (see section IV.4).

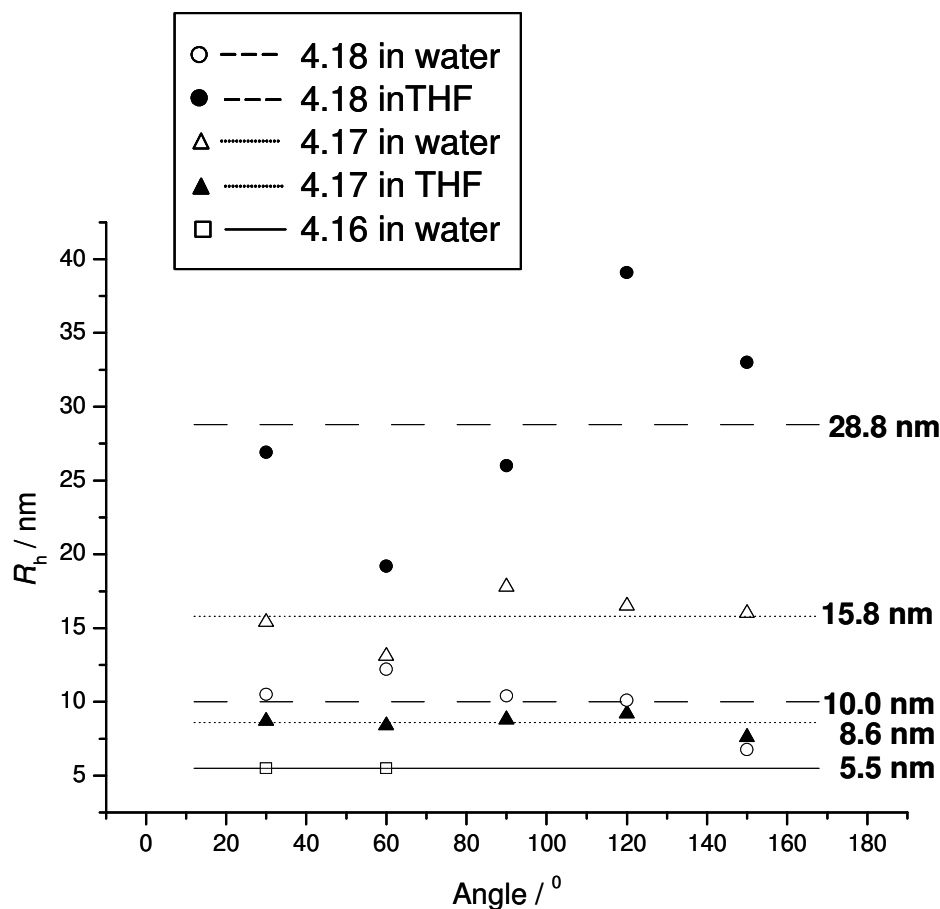
Table IV.4. Molecular weights of the core-*mono*-shell particles prepared by grafting of EO from $\text{TdG}_2(\text{CH}_2\text{OH})_{16}$ ($^1\text{H-NMR}$ - 250 MHz, CD_2Cl_2 , RT; GPC – standard: PEO, eluent: DMF; DLS in THF and water).

Exp No	$^1\text{H-NMR}$ M_n	UV M_n	GPC		DLS, R_h nm	
			M_n	PDI	THF	Water
4.15	8 700	6 700	4 100	2.17	Aggregates	Aggregates
4.16	50 200	65 800	17 000	1.24	-*	5.5
4.17	353 000	254 000	75 700	1.34	8.6	15.8
4.18	1 040 000	956 000	120 000	1.58	28.8	10.0

* out of the range of the instrument

In order to measure R_h of the prepared core-shell nano-particles, DLS measurements in THF and water were performed (see Table IV.4 and Figure IV.7). The results showed that an increase in size accompanies the increase in molecular weight, as well as the increase in the PEO chain length, with the exception of **4.18** in water where the R_h was smaller than the R_h of **4.17**. It should be pointed out that the R_h s in water are approximately twice as large as those in THF. This fact can be explained by a more stretched conformation of PEO in water than in THF [43]. The R_h of 2.3 nm (**4.16** in THF) is definitely wrong, because the R_h of the dendrimer itself was reported to be 3 nm [31,36]. This error can be attributed to the lower limit measurement of the machine being 5 nm.

Figure IV.7 R_h obtained by DLS of the core-shell systems prepared by “grafting-from” method.



Additionally, it should be mentioned that in all cases, the second process corresponding to particles with R_h up to 200 nm has been observed. These approximately 10 times bigger particles are an indication of aggregates being present in the system. The amphiphilic nature of the particles induces such aggregation behavior. Due to the shorter PEO

chains the separation of the hydrophobic cores is decreased which facilitates aggregation.[44] In the case of longer polymer chains (*e.g.* **4.18**) this effect should not be dominant, however the aggregates (especially in THF) were observed. The appearance of aggregates in this case can be attributed to the tendency of PEO to make associates in THF itself.[43] The associates present can be attributed to the polarity of the solvent (THF has dielectric constant $\epsilon = 7.5$) which may be not sufficiently enough to dissolve the entire molecule. Thus, intermolecular interactions between the less solvated parts of the molecules result in micro-associates.[45] The fact that associates were less prominent in water solutions ($\epsilon = 80$), supports the assumptions made above. The appearance of associates in water was rarely observed and probably due either to amphiphilicity of the molecules or to intermolecular entanglement of PEO arms. It should be pointed out that even a very small number of larger aggregates results in a much more intense signal.[46]

In order to quantitatively characterize the presence of the aggregates, GPC measurements should be more reliable.[43] However, as they fail to reveal aggregates it can be assumed that they are present only in a negligible amount.

Summary and conclusions

“Grafting-onto” and “grafting-from” methods were used for the synthesis of core-shell nanoparticles. In the “grafting-onto” process a statistically functionalized dendrimer GPC and light scattering confirm that the resulting core-shell nanoparticles exhibit low polydispersities. The “grafting-onto” method allows better characterization of the products obtained - number and length of the PEO-arms was determined. The drawback of this method is a shielding effect of already connected polymer chains limiting the number of attachable arms. The “grafting-from” method avoids this limitation allowing the growth of the chains from all initiating sites on the dendrimer. However, the products obtained by this method could not be fully characterized since the length of a single polymer chain attached to the dendrimer cannot be determined.

The hydrodynamic radii of all core-shell nano-particles were proved by Dynamic Light Scattering. A strong influence of the lengths of the PEO chains on the hydrodynamic radius was investigated. Increasing the length of the PEO arms, and hence M_n of the core-shell system increases the R_h of the particles. The amphiphilic nature of the macromolecules

produces aggregation in all DLS measurements, which disturb the single particle measurements and so precluded Static Light Scattering measurements.

These new stiff-core flexible-shell nanoparticles are more than one magnitude smaller than comparable core-shell latex particles. The suggestion is that such particles will serve as model compounds for all applications of organic nanoparticles where size of the particle plays an important role for the properties. Thus, they were investigated as supports for metallocenes catalyzing the olefin polymerization. It is expected that the obtained results can improve the understanding of the role of the established organic supports[47] in the heterogenized olefin polymerization. In earlier experiments a drastic influence of the supports size on the polymerization behavior was observed as indicated by an increase in the activity and productivity of the catalysts (see Chapter VII).

Comparing polyphenylene dendrimers to other dendritic structures it should be emphasized that polyphenylene dendrimers are rigid and shape persistent. The functionalities are locally fixed on the surface of the dendrimer and cannot disappear in the core by conformational movements. The globular structure cannot be changed by a solvent or by swelling. As a major advantage it can be considered that due to the stiffness of the core all changes of size, conformation or surface polarity can be exclusively attributed to the shell. Furthermore, they are due to the absence of amide bonds or ester linkage extremely hydrophobic, which maximizes the differences in polarity between the core and a hydrophilic shell. This should facilitate the systematic investigation of solvent effects on the conformation but also of the incorporation of different compounds as drugs or dyes into the core-shell architecture (see Chapters VI and VII).

References

1. Comanita, B.; Noren, B.; Roovers, J. *Macromolecules* **1999**, *32*, 1069.
2. Langer, R. *Nature* **1998**, *392*, 5.
3. Kataoka, K. *Controlled Drug Delivery: the Next Generation*; Park, K. E., Ed.; American Chemistry Society: Washington, DC, **1997**; Chapter 4.
4. Peracchia, M. T.; Gref, R.; Minamitake, Y.; Domb, A.; Lotan, N.; Langer, R. *J. Controlled Release* **1997**, *6*, 223.
5. Herrmann, A. Mihov, G. Vandermeulen, G. W. M. Klok H.-A. Müllen, K. *Tetrahedron* **2003**, *59*, 3925.
6. Zhang, L.; Eisenberg, A. *Science* **1995**, *268*, 1728.
7. K. L. Prime, G. M. Whitsides, *Science* **1991**, *252*, 1164.
8. Lee, J. H., Lee, H. B. Andrade, J. D. *Progress in Polymer Science* **1995**, *20*, 1043.
9. Du, H., Chandaroy, P. and Hui, S. W. *Biochimica et Biophysica Acta* **1997**, *1326*, 236.
10. Ariga, K., Shin, J. S. and Kunitake, T. *Journal of Colloid and Interface Science* **1995**, *170*, 440.
11. Chen, W.-L.; Shull, K. R. *Macromolecules* **1999**, *32*, 6298.
12. Hourdet, D.; L'allouret, F.; Audebert, R. *Polymer* **1997**, *38*, 2535.
13. Hourdet, D.; L'allouret, F.; Durand, A.; Lafuma, F.; Audebert, R.; Cotton, J.-P. *Macromolecules* **1998**, *31*, 5323.
14. Bromberg, L. In *Handbook of Surfaces and Interfaces of Materials*; Nalwa, H. S., Ed.; Academic Press: New York, 2001; Vol. 4, Chapter 7.
15. Sigwalt, P.; Boileau, S. *J. Polym. Sci., Polym. Symp.* **1978**, *62*, 51.
16. Kazanskii, K.S.; Solovyanov, A.A.; Entelis, S.G. *Eur. Polym. J.* **1971**, *7*, 1421.
17. Boileau, S. in: "Comprehensive Polymer Science", G. Allen, Ed., Pergamon, Oxford **1989**, *3*, 467.
18. Reuter, H.; Horig, S.; Ulbricht, J. *Eur. Polym. J.* **1989**, *25*, 1113.
19. Solovyanov, A.A.; Kazanskii, K.S. *Polym. Sci. USSR (Engl. Transl.)* **1972**, *A14*, 1186.
20. Penczek, S.; Duda, A. *Makromol. Chem., Macromol. Symp.* **1993**, *67*, 15.
21. Hsieh, H. L.; Quirk, R. P. *Anionic polymerization: principles and practical applications*, New York: Marcel Dekker, 1996.
22. Wesdemiotis, C.; Arnould, M.A.; Lee, Y.; Quirk, R.P. *Polym. Prepr. (Am. Chem. Soc., Div. Polym. Chem.)* **2000**, *41*, 629.
23. Eßwein, B.; Moeller, M. *Angew. Chem.* **1996**, *108*, 703.
24. Eßwein, B.; Molenberg, A.; Moeller, M. *Macromol. Symp.* **1996**, *107*, 331.

25. Forster, S.; Kraemer, E. *Macromolecules* **1999**, *32*, 2783.
26. Floudas, G.; Vazaiou, B.; Schipper, F.; Ulrich, R.; Wiesner, U.; Iatrou, H.; Hadjichristidis, N. *Macromolecules* **2001**, *34*, 2947.
27. Schmalz, H.; Boeker, A.; Lange, R.; Abetz, V. *Polym. Mater. Sci. Eng.* **2001**, *85*, 478.
28. Zhu, L.; Cheng, S.Z.D.; Calhoun, B.H.; Ge, Q.; Quirk, R.P.; Thomas, E.L.; Hsiao, B.S.; Yeh, F.; Lotz, B. *Polymer* **2001**, *42*, 5829.
29. Schmalz, H.; Knoll, A.; Mueller, A.J.; Abetz, V. *Macromolecules* **2002**, *35*, 10004.
30. J. Matecki, M. Dutkiewicz, *Journal of Solution Chemistry*, **1998**, *28*, 1999.
31. Morgenroth, F. *Ph.D. Thesis*, Johannes Gutenberg University – Mainz, Germany.
32. Klapper, M.; Wehrmeister, T.; Müllen, K. *Macromolecules* **1996**, *29*, 5805.
33. S. Rosenfeldt, N. Dingenouts, D. Poetschke, M. Ballauff, A.J. Berresheim, K. Muellen, P. Lindner, K. Saalwaechter *Journal of Luminescence* **2005**, *111*, 225.
34. L.-Z. Liu, Q. Wan, T. Liu, B. S. Hsiao, B. Chu *Langmuir* **2002**, *18*, 10402.
35. Wiesler, U.-M. *Ph.D. Thesis*, Johannes Gutenberg University – Mainz, Germany **2000**.
36. Marek, T.; Suvegh, K.; Vertes, A.; Ernst, A.; Bauer, R.; Weil, T.; Wiesler, U.-M.; Klapper, M.; Muellen K. *Radiation Physics & Chemistry*. **2003**, *67*, 325.
37. Angot, S.; Taton, D.; Gnanou, Y. *Macromolecules* **2000**, *33*, 5418.
38. Taton, D.; Cloutet, E.; Gnanou, Y. *Macromol. Chem. Phys.*, **1998**, *199*, 2501.
39. Wiesler, U.-M.; Weil, T.; Müllen, K. *Topics in Current Chemistry*, Vol. 212, *Dendrimers III Design, Dimension, Function* F. Vögtle (Vol. ed.), „Nanosized Polyphenylene Dendrimers“ **2000**, 1.
40. Gitsov, I.; Ivanova, P.; Fréchet, J. M. J. *Macromol. Rapid Commun.* **1994**, *15*, 387.
41. Angot, S.; Murthy, K. S.; Taton, D.; Gnanou, Y. *Macromolecules* **1998**, *31*, 7218.
42. Heise, A.; Nguyen, C.; Malek, R.; Hedrick, J.L.; Frank, C.W.; Miller, R.D. *Macromolecules* **2000**, *33*, 2346.
43. T. Song, S. Dai, K. C. Tam, S. Y. Lee, S. H. Goh *Langmuir* **2003**, *19*, 4798.
44. C. Kohl, T. Weil, J. Qu, K. Muellen, *Chem. Eur. J.* **2004**, *10*, 5297.
45. P. Pang, P. Englezos, *Colloids and Surfaces A : Physicochem. Eng. Aspects* **2002**, *204*, 23.
46. B. J. Berne; R. Pecora, *Dynamic light scattering with applications to chemistry, biology, and physics* New York, Wiley, **1976**.
47. Koch, M.; Falcou, A.; Nenov, N.; Klapper, M.; Müllen K. *Macromol. Rapid Commun.* **2001**, *22*, 1455.

Chapter V

CORE-SHELL MACROMOLECULES WITH A PERYLENEDIIMIDE CONTAINING POLYPHENYLENE DENDRIMER FOR THE CORE AND POLYETHYLENE OXIDE FOR THE SHELL

In the present Chapter a “grafting-from” approach was applied in order to prepare core-shell structures based on polyphenylene dendrimer with a chemically attached perylenediimide molecule at the focal point (**PDIG₂(CH₂OH)₁₆**),[1] possessing 16 PEO outer chains. By thus, combining an amphiphilicity with nano-scale and fluorescence efficiency, it is suggested that such particles will serve as model compounds for applications of fluorescence labeled organic nanoparticles wherein the size of the particle plays an important role in determining the properties. Therefore, they are currently being investigated as supports of metallocenes catalyst in olefin polymerization. It is expected that the results obtained will improve the understanding of the role of the already established organic supports in the heterogeneous olefin polymerization. In the first experiments a drastic influence of the size of the supports on the activity and productivity of the catalysts was observed (see Chapter VII).[2]

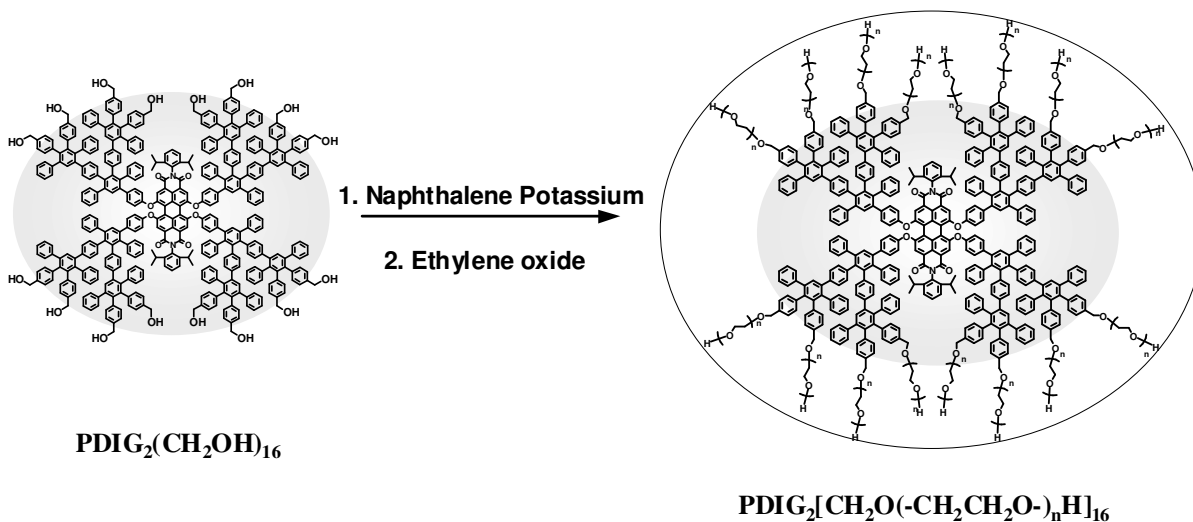
V.1. Synthesis of Core-Shell Macromolecules Containing Perylenediimide.

As it was already discussed in the Chapter IV, for the synthesis of core-shell molecules with a defined structure, the availability of suitable core molecules possessing the desired number of functional groups is essential. Therefore, a polyphenylene dendrimer with a chemically bonded perylenediimide molecule in a focal point possessing 16 hydroxymethyl groups on its surface (synthesized by Roland Bauer from Prof. Müllens group)[1] was used as a multifunctional macroinitiator in anionic polymerization of ethylene oxide, which gives access to core-shell systems synthesized by a “grafting-from” procedure. The use of the “grafting-onto” method is unacceptable due to the presence of amide groups of the perylenediimide core (see Scheme V.1), that can simultaneously react (even they are partially shielded from the dendrimer) with the living anionic end of the polymers. This undesired reaction will not only change the structure of the core-shell molecules (where shell supposed to be at the periphery), but will have a strong influence over the photoactive properties of the perylenediimide. In order to prevent any damages of the perylenediimide core, the “grafting-

from” method was selected as one performed in milder conditions - mild base like naphthalene potassium (see Scheme V.1) and low temperatures (0°C) ensured the preservation of the perylenediimide core. It is supposed that the growing PEO chains do not interact with the perylenediimide core by both intramolecular (the growth of polymer from the dendrimer surface outwards is entropy favorable) and intermolecular means (there is considerable shielding effect of both dendrimer surrounded by polymer shell and Coulomb-Coulomb repulsion between anionically charged living polymer ends).

Considering all above and keeping in mind the advantages and the disadvantages of the “grafting-from” method discussed in the Chapter IV (the number of attached chains is defined by the number of initiator sites on the dendrimer; the polymerization has started from all hydroxyl functional group; the chain lengths of the attached PEO molecules cannot be determined as there is no possibility of cleaving them from the core) it was suggested that all 16 hydroxymethyl groups on the dendrimer can act as efficient initiators in the polymerization of ethylene oxide (see Scheme V.1) [3,4] for preparation of the well-define core-shell molecules with a dye in a focal point by “grafting-from” method.

Scheme V.1. Polymerization of ethylene oxide (EO) using the sixteen-fold deprotonated dendrimer as the initiator.



The starting dendrimer **PDIG₂(CH₂OH)₁₆** was converted to a multifunctional macroinitiator **PDIG₂(CH₂O⁻)₁₆** by deprotonation with naphthalene potassium.[5] Three polymerizations were performed, varying the molar ratios of EO to hydroxymethyl groups of **PDIG₂(CH₂OH)₁₆** thus producing core-shell macromolecules with different lengths of the polymer arms, corresponding to different thickness of the polymer shell. The molecular

weights of the obtained core-shell structures were determined by GPC, UV and $^1\text{H-NMR}$ spectroscopy (Table V.1).

Table V.1. Molecular weights of the core-shell macromolecules prepared by polymerization of EO from $\text{PDIG}_2(\text{CH}_2\text{OH})_{16}$.

Experiment No	GPC		UV Spectroscopy M_n	$^1\text{H-NMR}$ Spectroscopy M_n
	M_n	PDI		
5.1	33 000	1.57	74 000	100 000
5.2	74 000	1.67	178 000	130 000
5.3	160 000	1.97	670 000	530 000

Although GPC is a very common method for determination of M_n and PDI, this method cannot give exact M_n for these systems, because of the linear polymers (PEO in this case) used as standards. The shape of the core-shell macromolecules in solution is globular and in addition the molecule is amphiphilic, so that the hydrodynamic volume for a given M_n will differ (see Table V.1). The polydispersity index is relatively high, which could be explained by the poor solubility of the multianionic initiator $\text{PDIG}_2(\text{CH}_2\text{O})_{16}$ in the reaction medium (THF).

Concerning molecular weight determination, another very convenient and fast method is UV spectroscopy. Similarly to the method described in Chapter IV - if the extinction coefficient is known for a given sample, by measuring an absorbance, one can calculate the molar concentration, followed by the number of moles in a solution of a known volume. Since the weight of the substance measured is known, calculation of the molecular weight of the substance is then possible. In order to obtain the extinction coefficient of the prepared core-shell macromolecules, the UV absorbance of the $\text{PDIG}_2(\text{CH}_2\text{OH})_{16}$ was measured and at 572 nm (λ_{max}), calculated the extinction coefficient and this value ($\epsilon(\text{PDIG}_2(\text{CH}_2\text{OH})_{16}) = 33\,300 \text{ L mol}^{-1} \text{ cm}^{-1}$) was applied as the extinction coefficient of the obtained core-shell macromolecules. This approximation is reasonable, because PEO does not have any absorbance at 572 nm in UV spectrum. Moreover, PPD are rigid and shape persistent so the PEO shell cannot influence the UV absorbance of the dendritic core (see Figure V.1 and Chapter IV).

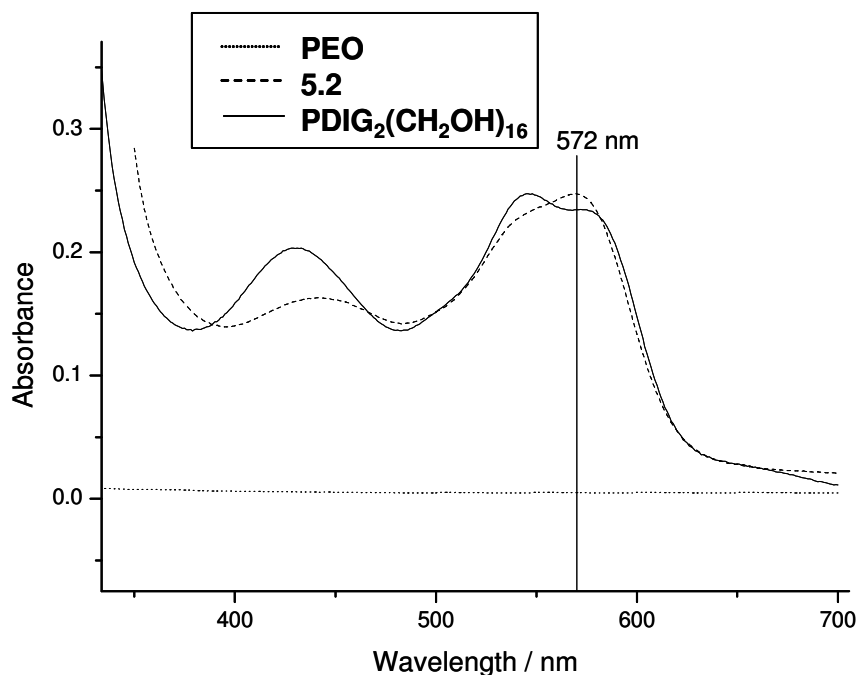
Figure V.1 UV spectra of PEO, PDIG₂(CH₂OH)₁₆ and 7.2 in chloroform.

Table V.1 presents the molecular weight calculated from UV spectroscopy, which are consistent with the molecular weight calculated from ¹H-NMR spectroscopy, indicating that the approximation is reasonable.

Molecular weights were also calculated using ¹H-NMR spectroscopy (see Table V.1). Calculations were based on the integral ratio between the signals of aromatic protons of dendritic core and the signal of the PEO's protons (see Figure V.2). ¹H-NMR spectroscopy does not include any standard or approximations within the molecular weight determination and therefore the method is assumed to give more precise results, than GPC and UV spectroscopy.

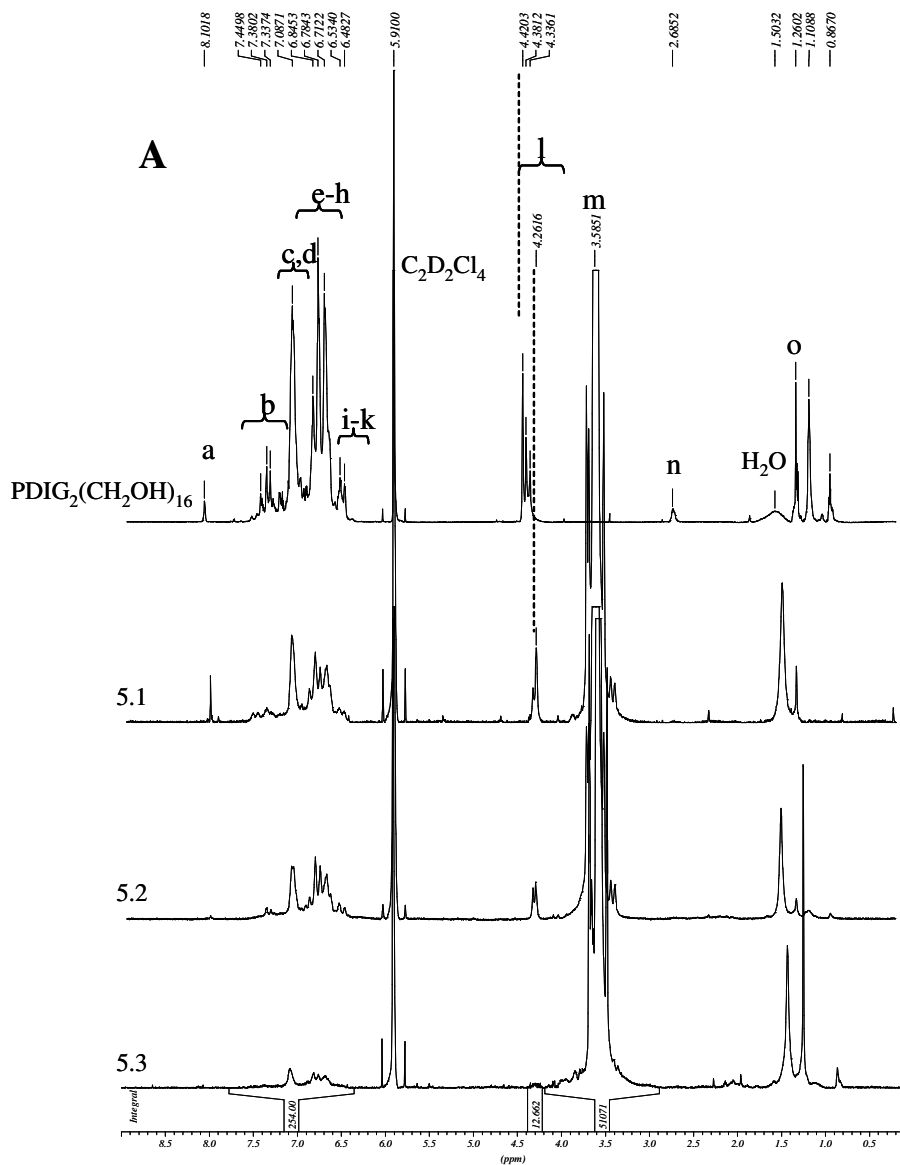
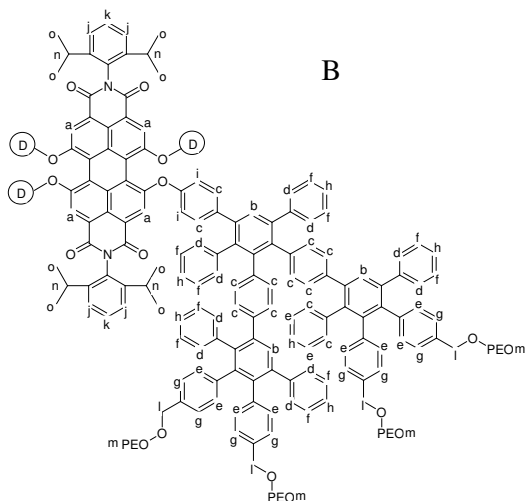


Figure V.2. (A) $^1\text{H-NMR}$ spectra (700MHz, 373K) of $\text{PDIG}_2(\text{CH}_2\text{OH})_{16}$ and of the obtained core-shell macromolecules in $\text{C}_2\text{D}_2\text{Cl}_4$. (B) Numeration of the protons depending on their chemical shifting in the $^1\text{H-NMR}$ spectra.

(D) - dendrons. The complete structure is drawn in Scheme V.1.

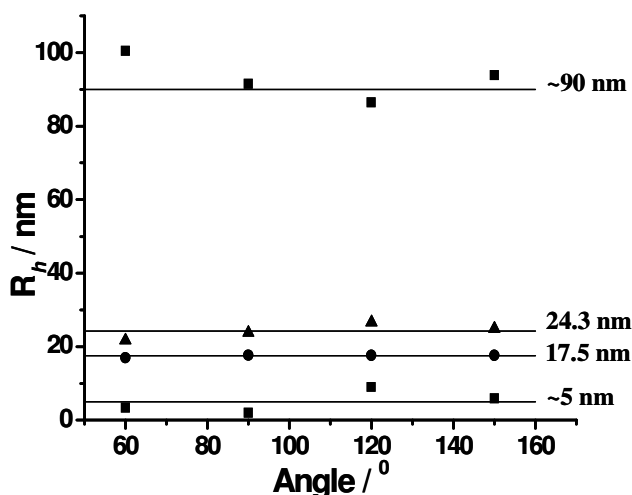


The most important difference between the $^1\text{H-NMR}$ spectra of $\text{PDIG}_2(\text{CH}_2\text{OH})_{16}$ and core-shell macromolecules is the chemical shift of the protons signals (*l*) (see Figure V.2B). In the case of $\text{PDIG}_2(\text{CH}_2\text{OH})_{16}$, these protons signals appear at 4.42, 4.38, 4.34 ppm, whereas in the $^1\text{H-NMR}$ spectra of core-shell macromolecules, these protons signals appear in the range of 4.34-3.26 ppm (see Figure V.2A). This shift of the protons signals (*l*) to higher field due to alteration of the neighbors - hydroxyl in the case of $\text{PDIG}_2(\text{CH}_2\text{OH})_{16}$ and ether in the case of core-shell systems. Aromatic protons (*a*) belonging to the perylene ring appear at 8.10 ppm and are clearly visible in all spectra. The area of the aromatic protons of the dendrimer can be separate to four series of signals – 7.50-7.20 ppm where appeared the protons (*b*), that are in the weakest field (single protons in the pentaphenyl substituted benzene ring); 7.20-6.95 ppm (*c,d*) ortho-protons in mono- or diphenyl substituted benzene ring; 6.95-6.60 ppm (*e-h*) meta- and para-protons in monophenyl substituted benzene ring as well as protons at benzene ring connected to a PEO arm; 6.60-6.45 ppm (*i-k*) PDI aromatic protons and ortho-protons of the benzene rings connected *via* ether bond to PDI. The methine protons (*n*) of the isopropyl groups unfortunately are visible only in the spectrum of $\text{PDIG}_2(\text{CH}_2\text{OH})_{16}$, whereas the methyl protons (*o*) are visible in the spectra of $\text{PDIG}_2(\text{CH}_2\text{OH})_{16}$, **5.1** and **5.2** (see Figure V.2A).

V.2. Dynamic Light Scattering (DLS)

One important characteristic of the core-shell systems is the size of the particles, considered respectively as the R_h in a certain solvent. The R_h s of the prepared core-shell nanoparticles were measured by DLS in water (see Figure V.3).

Figure V.3. DLS of **5.1** (■), **5.2** (●), **5.3** (▲) in water.



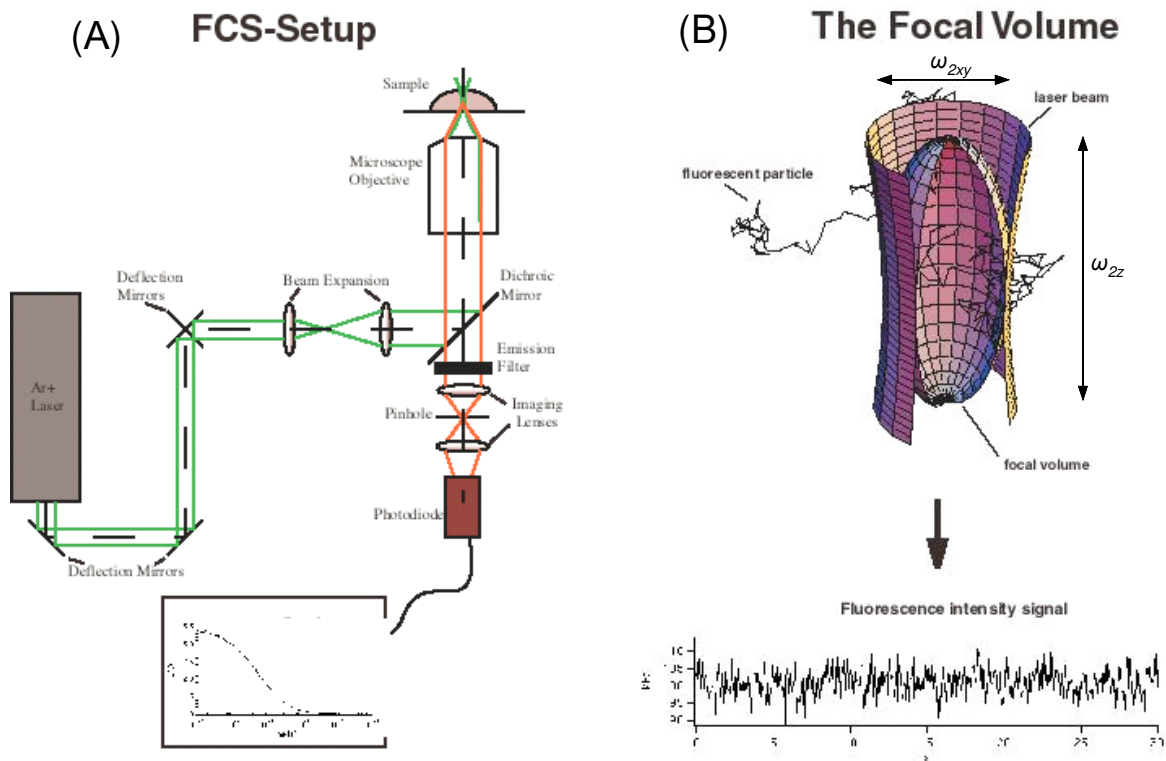
The results showed that an increase in size accompanies the increase in molecular weight, respectively the increase in the PEO chain length. It should be pointed out that in all cases aggregates were observed with R_h between 90 and 150 nm. This could be explained by the amphiphilic nature of the investigated nano-particles, which hydrophobic cores tending to aggregate in polar solvents [6]. In the case of the shortest PEO arms **5.1** this effect is even stronger, because the hydrophobic cores are less separated and stabilized and can easily aggregate in polar media (*e.g.* water). The R_h of the core-shell system **5.1** was found to be around 5 nm, but this value was an average value of very disordered first process, because of the strong influence of the second process indicating aggregates (see more discussion in section IV.5.2). Thus, the error can be attributed to aggregate formation as well as to the lower limit measurement of the machine being 5 nm. For this reason Static Light Scattering measurement is not applicable for obtaining the molecular weight of these compounds.

V.3. Fluorescent Correlation Spectroscopy studies (FCS).

In order to find more precisely the R_h value of the core-shell system **5.1** and to examine the influences of the length of the polymer shell to the R_h of the prepared core-shell structures, Fluorescent Correlation Spectroscopy study was performed for all the core-shell macromolecules (**5.1**, **5.2**, **5.3**), **PDIG₂(CH₂OH)₁₆** and 3,4,9,10-tetraphenoxyperylene diimide (**PDI(OPh)₄**) (see the structure at Figure V.5 and V.6) as a model compound of the dye molecule in the focal point of **PDIG₂(CH₂OH)₁₆**.

A commercial FCS setup was used (see Figure V.4A and experimental part). Basically, FCS monitors the fluorescent fluctuations in a femtoliter excitation volume, which is approximated as a ellipsoid with radii $\omega_{x,y}$ and ω_z (see Figure V.4B). On the diffusion of a fluorescent labeled molecule through the excitation volume, the fluorophore emits photons that are detected by a highly sensitive avalanche photodiode.

Figure V.4 Schematic representation of the FCS-setup and the focal volume.



Fluorescent fluctuations can be caused by Brownian diffusion and flow or chemical reactions. In case the fluorescence fluctuations only result from the diffusion through the excitation volume, the autocorrelation function $G(\tau)$ as a function of variable τ takes the following form:

$$G(\tau) = 1 + (1/N)f(\tau/\tau_d) \quad (1)$$

with

$$f(\tau/\tau_d) = [1/(1 + \tau/\tau_d)][1/(1 + (\omega_{x,y} + \omega_z)^2 \tau/\tau_d)]^{1/2} \quad (2)$$

The autocorrelation function $G(\tau)$ allows the determination of the translation diffusion time (τ_d), which characterizes the average residence time in the excitation volume and the average number of particles in the excitation volume (N). The translation diffusion coefficient (D) can be calculated from τ_d by the following equation:

$$D = \omega_{x,y}^2 / 4\tau_d \quad (3)$$

The relation between D and R_h can be presented by following equation:

$$D = kT/6\pi\eta R_h \quad (4)$$

Where k is the Boltzman constant, T is the temperature (K), and η is the dynamic (absolute) viscosity (cp). According to equation 4, R_h and viscosity depending on the

temperature, that's why temperature was measured during the experiments using thermocouple and corrected viscosity and diffusion coefficient (D_{Ref}) value approximating that R_h of a reference molecule (Rhodamine 6G) is the same at different temperatures. Using D_{Ref} and measuring τ_{Ref} it was able to calculate $\omega_{x,y}$:

$$\omega_{x,y} = 2(D_{Ref} \cdot \tau_{Ref})^{1/2} \quad (5)$$

Applying the calculated $\omega_{x,y}$ value in equations 3 and 4 to calculate R_h of the studied systems (see Table V.2).

Table V.2. Parameters and results from FCS measurements.

Sample	Conc. nmol/L	Temp. ° C	Viscosity cp	Diff.time µs	Diff. Coef.x10 ⁻¹² m ² /s	R_h nm	d_s nm
PDI(OPh)₄	50	22.7	*0.56707	28.1	330	1.16	0
PDIG₂(CH₂OH)₁₆	70	22.6	*0.56789	72.2	128	2.97	2.7
5.1	19	23.3	**0.92910	466.3	21.4	10.9	7.9
5.2	41	23.6	**0.92255	712.1	14.0	16.8	13.8
5.3	29	24.6	**0.90137	1209.3	8.56	28.3	25.3

*methanol solution; **water solution, d_s – shell thickness.

In the cases of **PDI(OPh)₄** and **PDIG₂(CH₂OH)₁₆** methanol was used as solvent, because both substances were slightly soluble in water. In order to correct the diffusion coefficient of referee (D_{Ref}) for methanol as media with different viscosity, the following equation was used:

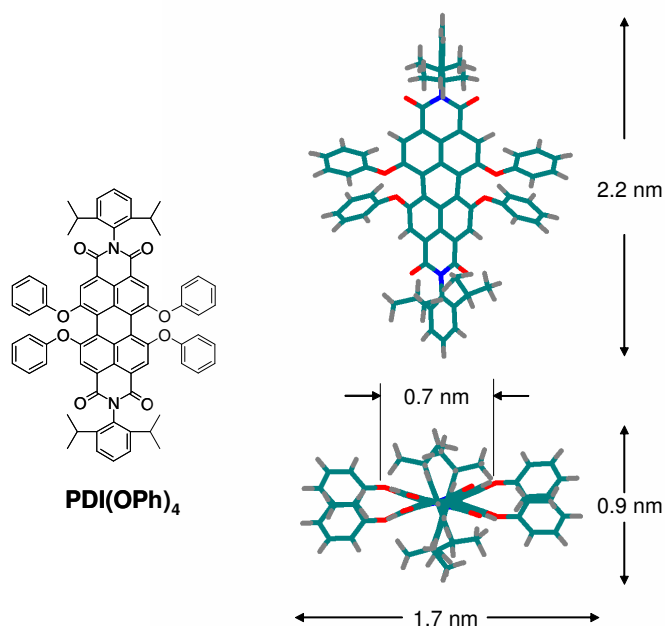
$$D_{Ref}(\text{methanol}) = [\eta_{\text{water}} D_{Ref}(\text{water})] / \eta_{\text{methanol}} \quad (6)$$

Repeating the same procedure (described above) it was able to determine the R_h of the dye **PDI(OPh)₄**, dye-cored dendrimer **PDIG₂(CH₂OH)₁₆** and prepared core-shell macromolecules (see Table V.2).

In order to check the reliability of R_h for **PDI(OPh)₄**, computer simulations were run using MM2 (MM+) force field method, as implemented in HyperChemPro 6(Hypercube Inc.). This simulation concerns the minimization energy of the structures resulting in the most favorable conformational structure. It should be mentioned that iteration calculations were approximated for a molecule conformation in a vacuum with a minimum gradient of 0.005 units. The diameters of the molecule were determined from the optimized three-dimensional structures and are presented in Figure V.5. From the global minimum obtained, a maximal

radius resulted of 1.10 nm, which is in agreement with the experimentally established one - 1.16 nm (see Table V.2). The difference between theoretical and experimental values in this particular case may be due to a solvation effect of the **PDI(OPh)₄**, resulting in an increase of the R_h measured. Such an effect cannot be considered by the theoretical simulation. The force field method minimizes the energy of the structures in vacuum.

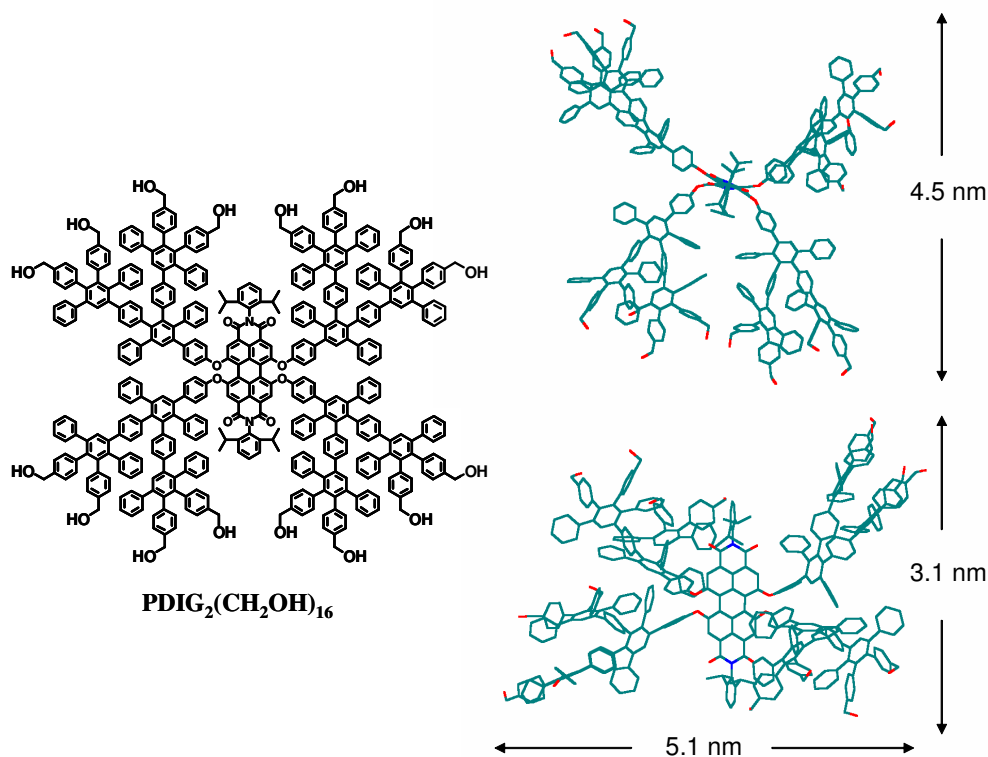
Figure V.5. Molecular simulation of structural conformation of **PDI(OPh)₄** by HyperChemPro 6 software program.



Subsequently, optimization of the polyphenylene dendritic scaffold (**PDIG₂(CH₂OH)₁₆**) was performed by combining four second-generation dendrons with the **PDI(OPh)₄** core molecule and minimizing both systems (see Figure V.6). Due to the fairly flat hypersurface obtained for the second-generation dendritic scaffold, the three-dimensional structure represents one out of several possible local minima. The diameters of up to 5.1 nm of **PDIG₂(CH₂OH)₁₆** can be determined from the optimized three-dimensional structures, which is in good agreement with the values obtained by FCS (5.94 nm). The difference in size between the theoretically optimized structure and the experimental one is greater in the case of **PDI(OPh)₄**. The larger value of R_h for the dendrimer, measured by FCS may due to the solvation effect of the medium, discussed above. In the case of **PDIG₂(CH₂OH)₁₆** the

structure possesses a higher degree of conformational freedom. This allows for a stronger influence of the solvent effect on the conformational changes.

Figure V.6. Molecular simulation of structural conformation of **PDIG₂(CH₂OH)₁₆**.



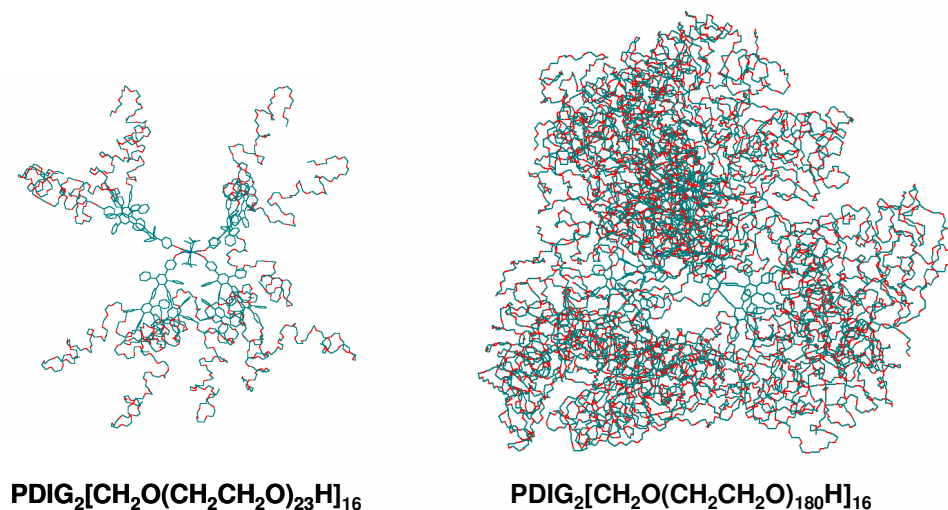
It was already proven by DLS that the R_h of the second-generation PPD with tetrahedral core is 3 nm.[7,8] According to the R_h of **PDIG₂(CH₂OH)₁₆** obtained by FCS (2.97 nm) and taking into account that the theoretical distance between two aryether bonds is 0.7 nm (see Figure V.5), the average thickness of the dendritic shell was calculated to be 2.7 nm. The estimation of the size of the PDI core is in a good agreement with experimental data due to the less pronounced solvation effect in the case of relatively small and defined molecules (see discussion concerning R_h of **PDI(OPh)₄** above). Additionally, the shielding effect of the dendrons decreases the possibility for penetration of solvent molecules to the dendrimer core.

As was expected and proven by DLS and also by FCS, the R_h of investigated dendrimer-polymer hybrids increases with increasing length of the PEO chains, respectively with their molecular weight. The comparison between R_h obtained by FCS measurements and these by DLS are in very good agreement for the product **5.2** (only 0.4 nm difference, see

Figure V.3 and Table V.2), however it is less pronounced for the product **5.3** where the difference is already 4 nm. In the case of **5.1**, the strong influence of aggregates often made the single particle measurements by DLS impossible. However, the R_h of 10.9 nm was found by FCS measurements of system **5.1** in water. The advantage of this method is the ability to use nanomolar solutions, where aggregation is less pronounced. Additionally, the intensity of fluorescent light does not depend on the radius of the examined sample (see relation IV.4 in chapter IV). Thus, even the less populated associates (caused *e.g.* by entanglement of polymer shells, or dendrimer-dendrimer attraction) are present in the system and their influence over the results of FCS measurements will be less notable.

The simulation of the conformations and determination of the molecular dimensions of the core-shell systems having PEO as the shell was impossible. The force field method is applicable and gives a reasonable results only in the cases of relatively small molecules with define structure. However, the method was able to give an impression of the shape of the dendrimer-polymer hybrids (see Figure V.7).

Figure V.7. Molecular simulation of structural conformation of **PDIG₂[CH₂O(CH₂CH₂O)₂₃H]₁₆** and **PDIG₂[CH₂O(CH₂CH₂O)₁₈₀H]₁₆**.



Two examples of core-shell molecules with **PDIG₂(CH₂OH)₁₆** as the core and 16 PEO chains each possessing 23 and 180 repeating units are given. The optimization of the simulation of both systems was performed similarly to that applied for **PDIG₂(CH₂OH)₁₆**. First **PDIG₂(CH₂OH)₁₆** structure was optimized followed by optimization of every single PEO chain. Then the core and all the arms were connected in a macromolecule and the energy

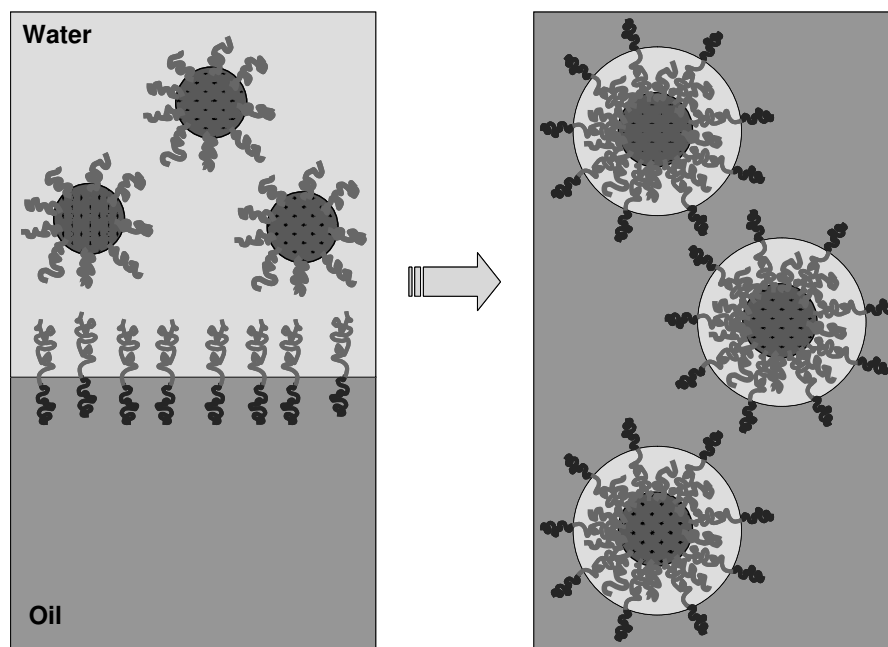
was minimized. Even if the method is not very reliable for such complex structures, it is clearly shown that polymer arms are rather remote in space in the case of **PDIG₂[CH₂O(CH₂CH₂O)₂₃H]₁₆** and allow freely permeation of small molecules (*e.g.* solvent, dye, drug) through the shell to the dendrimer's cavity. However, the loading process is supposed to be limited in case of **PDIG₂[CH₂O(CH₂CH₂O)₁₈₀H]₁₆** due to the shielding effect of the denser polymer shell.

V.4. Preparation of supra-molecular architecture by self-assembly of block copolymers onto core-shell macromolecules.

In order to prepare a core-*double*-shell or more general core-*multi*-shell supra-structures using the “grafting-from” or “grafting-onto” approaches, one should simply replace homopolymer (*e.g.* PEO see Chapter IV) with a di- or multiblock copolymers. However, this is an extremely complicated task in terms of criteria that should fulfill those polymers: *i*) they should not intermolecularly interact to prevent formation of aggregates; *ii*) should possess appropriate anchor groups in order to chemically adsorb on the dendrimer surface; *iii*) should not physically adsorb on the dendrimer surface and thus hinder the chemical interactions. Although, there are polymers that could fulfill the entire requirements, it is still difficult to synthesize multi-blockcopolymers out of these polymers. In order to avoid the complex synthetic work, the idea concerns self-assembly intermolecular interaction between already prepared core-shell macromolecules (see Chapters IV and V) and block copolymers. In this particular case, the self-assembly method consists of an interaction between two polymers (polymer-shell by core-shell molecules and external polymer forming the second shell after interaction) by means of aggregation (polymers tend to aggregate in poor solvents and thus perform a kind of polymer-polymer interaction) or a presence of forces between the polymer chains (*e.g.* Vanderwaals or Coulomb-Coulomb interactions [9] and H-bonds or complex formations [10]).

To exploit the polymer-polymer interactions one could utilize emulsions (in the particular case inverted nano-emulsion), where core-shell particles are finely dispersed to a molecular scale using as emulsifiers amphiphilic diblock copolymers (see Figure V.8)

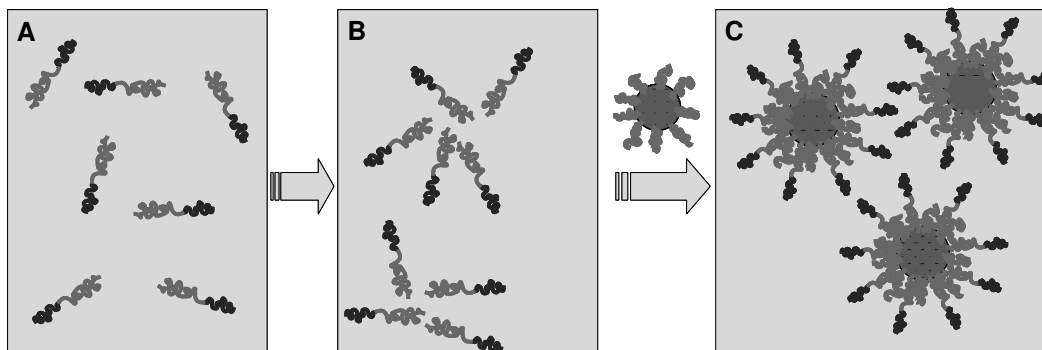
Figure V.8 Schematic representation of inverted nano-emulsion containing core-shell particles.



However, very recent results confirmed the mechanism of flocculation of water drops in emulsions due to the amphiphilic nature of the core-shell hybrid[11]. It was found that amphiphilic block copolymers with dendrimer structures exhibited excellent demulsification performance for crude oil emulsion and became more efficient with more complex molecular structure due to increased penetrability. The physical model of demulsification explained the micromechanism of flocculation and coalescence of water drops in emulsion because of the good adsorption and displacement behaviors of dendrimers.

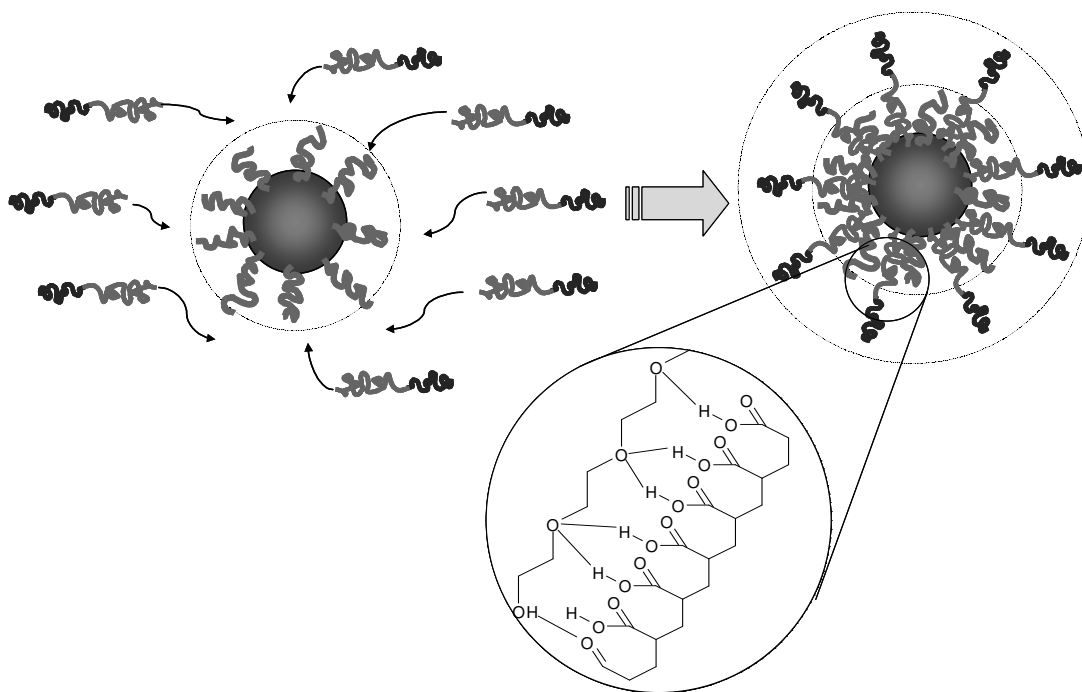
Another strategy that involves polymer-polymer interactions in terms of aggregation is characteristic for every polymer in a certain environmental conditions. This characteristic is known as critical micelle concentration (CMC) and is known for a number of polymers in different solvents and temperatures. CMC is this concentration, for a given polymer in certain media conditions below that, polymers are in a stable solution (polymers chains behave as molecule in an ideal solution) and above that, the polymers collapse in aggregates. Thus, if one manages to reach CMC for a given polymer (*e.g.* PEO) which is a part from amphiphilic diblock copolymer (*e.g.* PS-*b*-PEO), the addition of core-shell particles containing PEO as a shell, will increase the concentration of PEO over the CMC and thus will induce the aggregation of PEO [12](see Figure V.9)

Figure V.9 Preparation of supra-molecular architectures exploiting CMC of polymers: (A) ideal solution, (B) solution with CMC, (C) over CMC - supra-molecular architectures.



The disadvantage of the method is the formation of so called “homo” aggregates – aggregates consisting of only block copolymers or only core-shell molecules. Thus, the formed architectures possess contaminants, which effect the size, size distribution and homogeneties of the system.

The most promising project concerning the preparation of relatively stable supra-molecular structures is based on polymer-polymer interaction by means of forces (Vanderwaals, Coulomb or H-bond formation) between the polymer chains. This method overcomes the problems (based mainly on non-specific interaction) of the methods described above due to the existence of more sufficient forces to control the self-assembly process. While Vanderwaals interaction is relatively weak, the Coulomb-interactions and H-bond formation possess a relatively stronger character. In this particular case, neither block copolymers (or at least most of them) nor core-shell macromolecules are charged and therefore not applicable for Coulomb-interaction. However, it is known that PEO and poly(acrylic acid) (PAA) can undergo an interaction based on H-bond formation between carboxylic groups of PAA and oxygen free electron pairs of PEO [13]. Thus, one was able to use core-shell structures possessing PEO as the shell and PS-*b*-PAA for simultaneous formation of supra-molecular structures *via* H-bond formation between the shell (PEO) and H-donating polymer (PAA) (see Figure V.10)

Figure V.10 Supra-molecular structures *via* H-bond formation

The H-bond formation takes place essentially in pH below 2 where carboxylic groups of PAA are in a protonated form. However at pH 2 intra- and inter-molecular H-bond formations appear between the PAA molecules itself [14]. In order to overcome this problem the concentration of the PAA was kept as low as possible during the experiments. In spite of this, both large aggregates, with size 100-500 nm, and unaffected core-shell molecules were observed in DLS and “particle-sizer” measurements. Additionally, GPC did not improve the presence of any high molecular weights complexes probably due to the fact that the pH in the GPC column is nearly neutral and the complexes based on the H-bond interaction could not stabilize. Therefore, only signals corresponding to molecular weights of PS-*b*-PAA and core-shell molecules were found in GPC.

In order to better examine the complex formation and have a full control over the media conditions, the use of FCS setup was proposed, where the concentrations can reach a nanomolar range and the presence of acidic buffers ($\text{pH} \leq 2$) is not an issue. The requirement for a chromophore-containing probe will be satisfied by using core-shell molecules containing perylenediimide covalently bonded to a dendritic core (see above). Thus, one could use the core-shell structures as a standard and compare the changes (in terms of diffusion coefficient) to the system forming supra-molecular complexes.

Summary and conclusions

A series of new dye containing polyphenylene dendrimers as the core and PEO as the shell macromolecules have been synthesized and characterized. Hydroxyl groups of **PDIG₂(CH₂OH)₁₆** was initially deprotonated and served as initiators for anionic polymerization of EO building the outer shell. The molecular weights of the prepared core-shell macromolecules were determined by GPC, UV- and ¹H-NMR spectroscopy. Since GPC uses standards and UV spectroscopy approximations to obtain molecular weight, ¹H-NMR spectroscopy was denoted to give the most accurate values.

The hydrodynamic radii of the core-shell nano-particles were obtained by DLS. A strong influence of the lengths of the PEO chains on the hydrodynamic radius was established. Increasing the length of the PEO arms, and hence M_n of the core-shell system increases the R_h of the particles. The amphiphilic nature of the macromolecules produces aggregation in all DLS measurements, which prevent the single particle measurements and so precluded Static Light Scattering measurements.

FCS measurements were performed in order to find more accurately R_h of the system **5.1** as well as R_h of the core **PDIG₂(CH₂OH)₁₆** and the dye **PDI(OPh)₄**. Thus, the thickness of each shell was determined (dendritic shell around the dye and PEO shell around the dye containing dendrimer core) and proven, that the increase in length of the PEO arms, (respectively the molecular weight of the prepared core-shell macromolecules) is accompanied by the increases of R_h .

Additionally, FCS was proposed to be useful in case of supra-molecular structure determination. The method is very sensitive and could detect any changes in the diffusion coefficient by formation of the supra-structures, due to either self-assembly or complex formation between the chromophore labeled core-shell system and any amphiphilic spices (PS-*b*-PAA in the particular case). The preparation of such structures is important not only from the scientific point of view, but also as its practical applications (*e.g.* drug deliveries – one could modify the structure in a way to load the different shells and core with a number of substances).

These new stiff-core-flexible-shell nanoparticles can be investigated as model compounds for various materials such as supports for catalysts in olefin polymerization (see Chapter VII), for organic and inorganic impact modifiers but also for elucidating film forming processes (see Chapter VI). Furthermore one can expect that such core-shell structures have a high tendency towards well-controlled self-assembly on surfaces.

References

1. Bauer, R.; Grebel-Koehler, D.;Muellen, K., *in preparation*.
2. V. Atanassov, Y.-J. Jang, N. Nenov, R. Bauer, V. Sinigersky, M. Klapper, K. Muellen, *in preparation*
3. Angot, S.; Taton, D.; Gnanou, Y. *Macromolecules* **2000**, 33, 5418.
4. Taton, D.; Cloutet, E.; Gnanou, Y. *Macromol. Chem. Phys.*, **1998**, 199, 2501.
5. Gitsov, I.; Ivanova, P.; Fréchet, J. M. J. *Macromol. Rapid Commun.* **1994**, 15, 387.
6. C. Kohl, T. Weil, J. Qu, K. Muellen, *Chem. Eur. J.* **2004**, 10, 5297.
7. Wiesler, U.-M. *Ph.D. Thesis*, Johannes Gutenberg University – Mainz, Germany **2000**.
8. Marek, T.; Suvegh, K.; Vertes, A.; Ernst, A.; Bauer, R.; Weil, T.; Wiesler, U.-M.; Klapper, M.; Muellen K. *Radiation Physics & Chemistry.* **2003**, 67, 325.
9. I. F. Hakem, A. Johner, T.A. Vilgis *Europhys. Lett.*, **2000**, 51, 608.
10. Ming Jiang*, Mei Li, Maoliang Xiang, Hui Zhou *Advances in Polymer Science*, **1999**, 146, 121.
11. Z. Zhang, G. Xu ., F. Wang, S. Dong, Y. Chen *Journal of Colloid and Interface Science* **2005**, 282, 1.
12. X. Zushun1, Y. Changfeng, C. Shiyuan, F. Linxian, *Polymer Bulletin* **2000**, 44, 215.
13. Bekturov, E.; Bimendina, L. *Adv Polym Sci* **1981**, 41, 99.
14. V. Baranovsky, S. Shenkov, I. Rashkov, G. Borisov *Eur. Polym. J.* **1992**, 28, 475.

Chapter VI

CORE-DOUBLE-SHELL MACROMOLECULES BASED ON POLYPHENYLENE DENDRIMERS.

VI.1. Introduction

The core-shell architecture features of hybrid inorganic (*e.g.* metals – Au, Pt, Cu, semiconductors – CdS, CdSe, ZnS, or oxides – Fe₂O₃, Al₂O₃, TiO_x, SiO_x etc.) – organic (*e.g.* polymers) nanoscale materials have been described in great detail.[1] An organic polymer shell determines the external chemical properties of such materials and their interaction with the environment, whereas their physical properties are governed by both the size and the shape of the inorganic core and the surrounding organic layer. In many cases, the molecular architecture of these materials is not well-defined with relatively broad distributions of size and molecular weight. This disadvantage is mostly due to a difference in functionalities or inhomogeneities in the surface structure of the inorganic particles that serve as the cores. In order to overcome this problem, hyperbranched[2] and dendrimer[3,4] macromolecules possessing more defined functionalities and structures have been applied.[4,5] As one is able to decorate them with polymer chains on the surface, model compounds for drug deliveries, supports of catalysts and latex particles, where control over the size, structure and functionalities are important features, are thus available.

However, a gap of more complex structure based on well-defined dendrimers (*e.g.* dendrimer(core)-polymer(shell) hybrids) exists and therefore it is the topic in the present work. In the former chapters (chapters IV and V) the core-*mono*-shell systems consist of number of polyphenylene dendrimers as the core and PEO in different length as the shell were present. The lack of core-*multy*-shell dendrimer-polymer hybrids motivates the synthesis and investigation over the properties of such materials. Indeed, only few examples are present in the literature (see section I.3) - preparation of dendrimer-like star block copolymers by both anionic and atom transfer radical polymerization (ATRP) of ϵ -caprolactone, methyl methacrylate and ethylene oxide[6] and preparation of so called “miktoarm” star-polymers based on carbosilane

dendrimers with eight polystyrene and eight polyisoprene arms[7] or diblock copolymers of styrene (30%) and butadiene (70%) as arms.[8]

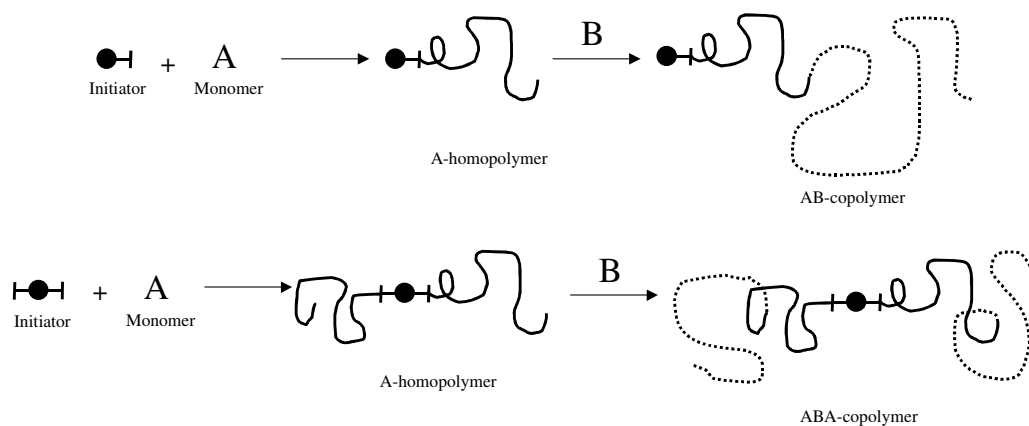
In order to fill the gap and further investigate the properties of dendrimer polymer hybrids based on polyphenylene dendrimers, the synthesis of core-*double*-shell nano-particles utilized second-generation polyphenylene dendrimer with tetrahedral core (**TdG₂**) grafted with PI-*b*-PEO or PS-*b*-PEO, is described in the present chapter. Attaching these chains is predicted to give access to amphiphilic nano-particles possessing a hydrophobic stiff-core surrounded by a hydrophilic inner shell (PEO) and a hydrophobic outer shell (PI or PS). It was proposed that such materials might serve as a drug deliveries allowing selective loading of polar compounds in the hydrophilic PEO-shell or nonpolar - in the dendritic and PI or PS shells. Additionally core-*double*-shell molecules possess amphiphilicity combined with opportunity to rearrange the shells in order to adjust its polarity to the environment. These properties will provoke simultaneous dissolve of the macromolecules in both polar and nonpolar media. In terms of above, it will be of extreme interest to investigate the behavior of these structures in solvents of different polarity. This particular feature is proposed to be advantage for *in vitro* experiments concerning efficient transport of drug loadings through the cell membrane, where both hydrophylicity and lipophilicity are required. Moreover, one may expect that these systems behave like so-called Janus micelles [9], adjusting their surface polarity to the solvent by having in non-polar media the polyisoprene or polystyrene at the surface and in polar media the PEO blocks.

VI.2. Preparation of block copolymer arms

Anionic polymerization was used in the current work as the most studied and effective approach for synthesis of well-defined block copolymers. The main requirement to the copolymers was to be nearly monodisperse, so as to produce an as low as possible polydispersity of the more complex (*e.g.* core-shell) macrostructures based on them. Therefore, a truly living polymerization (chain-type polymerization where the active center only participates in monomer propagation) was applied [10]. After consumption of monomer (A), the active species (*e.g.*, carbanion, organometallic complex) remains “alive” and will continue to propagate upon the addition of monomer (B) (see Scheme VI.1), providing there are no side reactions

(e.g., chain termination or chain transfer) in a “living” polymerization. This is a very strict requirement, and although many polymerization systems are claimed to be living, rigorous evaluation of the above criteria is often lacking.

Scheme VI.1. Di- and triblock copolymer synthesis using living polymerization with sequential addition of monomers.



Since our interest was focused on highly organized macromolecules, diblock copolymers with different chemical and physicochemical behavior will provoke difference in the properties of the desired macrostructures. Thus, amphiphilic copolymers have been chosen as the most appropriate polymers for building up onion like core-*multi*-shell structures.

Preparation of block copolymers anionically is a common task nowadays. However, the polymer obtained by every particular combination of conditions possesses particular characteristics (e.g. microstructure). In the present chapter the author specifies and summarizes in a short overview all the characteristics of the polymers used for further preparation of the core-shell particles.

VI.2.1 Poly(styrene-*block*-ethylene oxide)

VI.2.1.1 Introduction

Block copolymers consisting of two types of incompatible polymer blocks have a variety of industrial and research applications.[11,12] Among them the poly(styrene-*b*-ethylene oxide) (PS-*b*-PEO) block copolymers hold a special place, because polyoxyethylene segments are not only hydrophilic, but also nonionic and crystalline, and can complex monovalent metallic cations. The amphiphilic nature of these copolymers gives rise to special properties in selective solvents, at surfaces as well as in the bulk, owing to microphase separation. They have many uses including polymeric surfactants, electrostatic charge reducers, compatibilizers in polymer blending, phase transfer catalysts or solid polymer electrolytes, etc.

Because of the hydrophilic nature of the PEO block, PS-*b*-PEO copolymers containing > 50% PEO are soluble in water. In aqueous media the copolymers associate to form stable colloidal aggregates or micelles. The colloidal behavior of PS-*b*-PEO copolymers has been widely investigated [13-16], and the most important features of micelle behavior in aqueous solutions due to their ability to solubilize hydrophobic molecules. This properties have been used for determination of critical micelles concentration (CMC) for PS-*b*-PEO block copolymers using pyrene as a fluorescent probe.[17]

In order to study the influence of the chain-length of both blocks in diblock copolymers upon the physicochemical behavior, several methods for preparation of PS-*b*-PEO block copolymers have been developed. *Kahn et al.*[18] used hydroxy-terminated PS which was reactivated with potassium methoxide and used for subsequent polymerization of ethylene oxide. However, the route involving coupling of two homopolymers gives only low yields while introducing yet another moiety at the junction between the two blocks.[14]

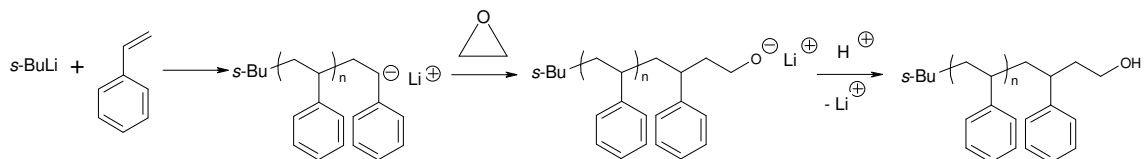
Sequential anionic polymerization *e.g.* the polymerization of ethylene oxide initiated by the PS anion requires the presence of a strongly solvated counterion. Only the potassium cation associated with the propagating chain makes the polymerization of ethylene oxide in solvents of moderate polarity (THF) feasible. The use of sodium requires high pressure and longer polymerization times. Lithium can initiate the polymerization of ethylene oxide in THF but the propagation does not occur.[19] As it

was already discussed in the previous chapter the presence of a strong Lewis base, (*e.g.* phosphazene base) breaks up of the strong lithium alkoxide interaction, and thus making the polymerization of ethylene oxide possible.[20,21] Since most of the applicable monomers are commonly polymerized using organolithium initiators, the use of phosphazene base exclude the cation exchange.

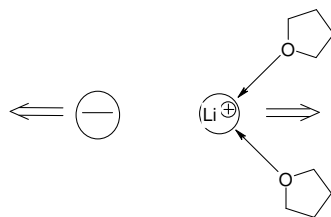
VI.2.1.2 Synthesis and characterization of hydroxyl end-functionalized polystyrene.

A polystyrene block with a hydroxyl end-group was prepared to be use as a macroinitiator for further polymerization of a second monomer (*e.g.* ethylene oxide) in order to obtain diblock copolymers. A classical synthetic method was used with *sec*-buthyllithium as the initiator and ethylene oxide as the end-coupling agent:[22]

Scheme VI.2. Synthesis of hydroxyl end-functionalized polystyrene.



All polymerizations performed in THF (**6.1-6.5**, see Table VI.1) yielded polystyrenes with PDI greater than 1.1. It is known that THF molecules additionally activate anionic centers by solvation of the lithium counterion, pulling it away from the anion:



Accordingly to reduce the PDI a very low temperature ($-100\text{ }^{\circ}\text{C}$) would be required for the polymerization of styrene in THF. Since such temperatures are rather difficult to maintain, the polymerization was instead performed in cyclohexane at $-77\text{ }^{\circ}\text{C}$ (**6.6**, Table VI.1). Aliphatic and cycloaliphatic solvents have been found to be good solvents for organolithium initiators (aggregation effect is weaker) and additionally

lower the rate of the propagation reaction, leading to products with PDIs below 1.1. A major drawback of these solvents was lower solubility (relative to THF) of ethylene oxide added in the next step as end-functionalizing agent. Usually, an excess of ethylene oxide was used in order to guarantee the completeness of the coupling reaction. The excess of ethylene oxide could not provoke its further polymerization, because of the covalent nature of $O^{\delta-}-Li^{\delta+}$ bond, which deactivated the chain-end.

Table VI.1. Molecular weights of hydroxyl end-functionalized polystyrenes.

No	Calculated M_n^*	GPC		1H -NMR
		M_n	PDI	M_n
6.1	5 000	4 000	1.7	4 600
6.2	1 000	3 200	1.30	3 600
6.3	1 000	4 200	1.35	4 800
6.4	1 000	3 800	1.18	4 400
6.5	1 000	3 300	1.23	3 400
6.6	1 000	2 200	1.08	2 200

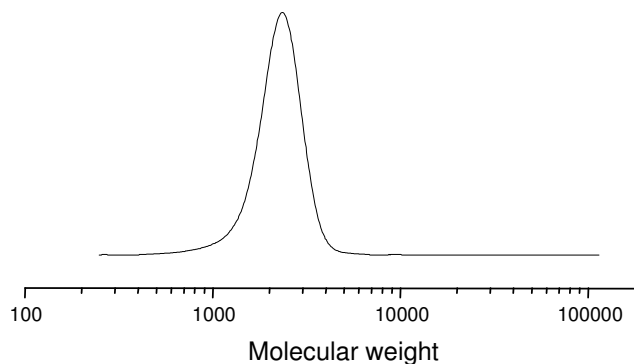
* M_n = g styrene / mol *s*-BuLi

Theoretically, the molecular weight of polystyrene can be calculated stoichiometrically using the following equation:

$$M_n = g_{\text{monomer}} / \text{mol}_{\text{initiator}} \quad (\text{VI. 1})$$

These data often differ from the molecular weight obtained by GPC (see Table VI.1). The reason is mostly a combination of inaccuracies in the amount of initiator or monomer added (errors in volumetric or gravimetric measurements – personal or technical), errors in determination of active-concentration of the initiator solution, and impurities from substances or glassware. All these factors decrease the active-concentration of the initiator or prematurely terminate the growing chains (see **6.1** in Table VI.1). Nevertheless, monomodal molecular weight distribution was achieved in all cases, with a PDI of less than 1.1 in case of **6.6** (see Figure VI.1).

Figure VI. 1 GPC molecular weight diagram (THF – eluent, polystyrene – standard) of **6.6**.

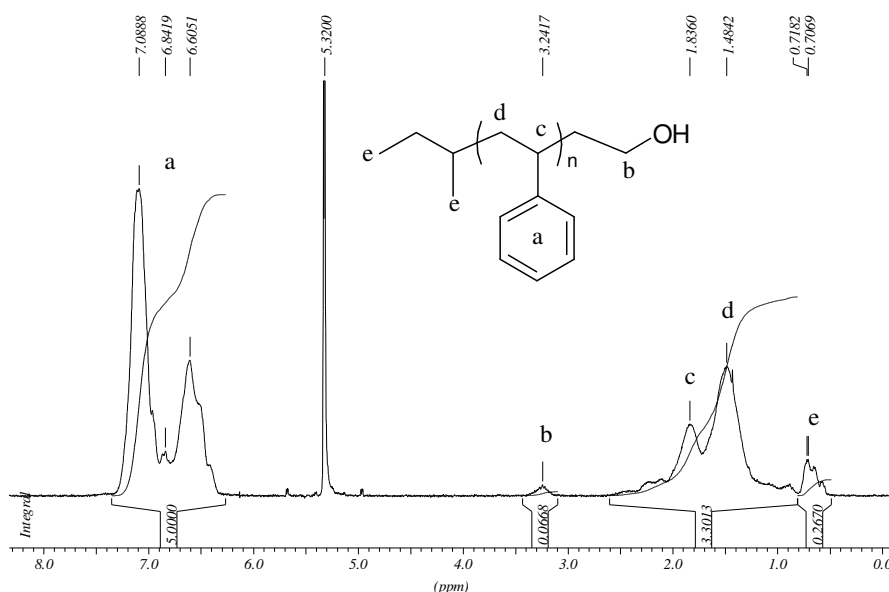


The molecular weight of all products was calculated from the $^1\text{H-NMR}$ spectra using following relation:

$$M_n = (I_a/I_e)M_{St} \quad (\text{VI. 2})$$

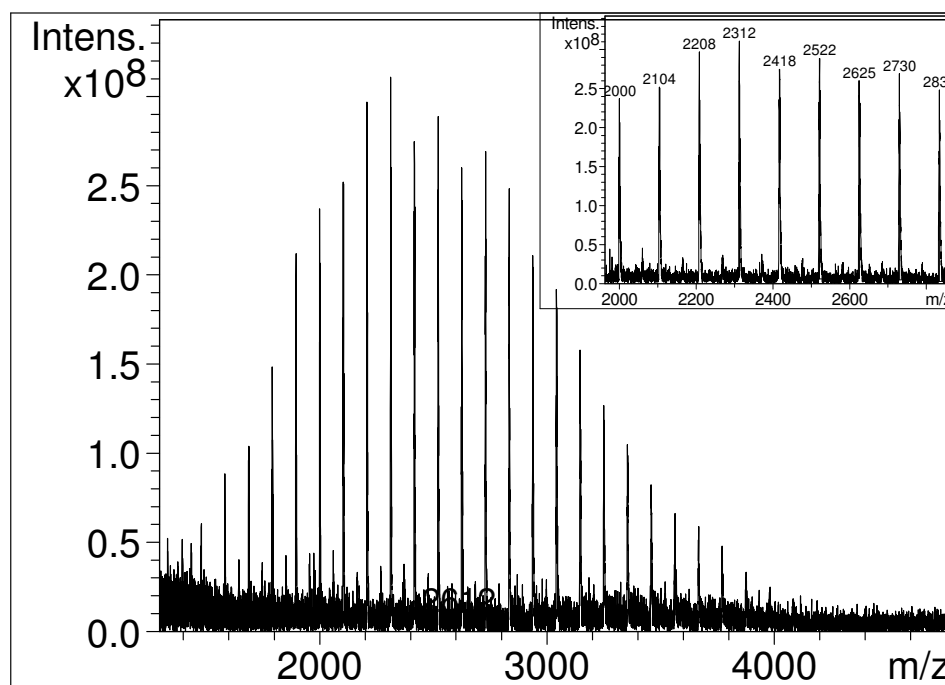
Where I_a and I_e are the integral values for protons **a** and **e** (see Figure VI.2) divided by the number of protons containing each group and M_{St} is the molecular weight of styrene. The values for M_n thus calculated were close but slightly higher than the GPC data (except for **4.6** where the two values correspond exactly), which could be explained by the slightly overlap between the signal of the **e** protons with the signal of the **d** protons (see Figure VI.2), which decreased the integral value (I_e) and increased M_n .

Figure VI. 2 $^1\text{H-NMR}$ spectra (250 MHz, CD_2Cl_2 , RT) of **6.6**.



Finally, the most exact method for molecular weight determination of polymers is matrix-assisted laser desorption/ionization time-of-flight (MALDI-TOF) mass-spectrometry.[23] This method gives homologous series of repetition signals for each population of polymer chains of different molecular weight, and the molecular weight distribution of these populations. Thus, M_n , M_w and PDI can be calculated from the mass-spectrum. This method is often applied for linear homo and copolymers (M_n over 10^5),[24] but is rarely successful for H-, star-shaped or highly organized polymer macrostructures. Herein, the MALDI-TOF mass-spectrum of **6.6** is presented showing homologous series of signals at intervals $m/z = 104 \pm 2$, which correspond to the molecular weight of the styrene monomer unit (104.15)(see Figure VI.3).

Figure VI. 3 MALDI-TOF mass-spectra (matrix-dithranol, THF, Li^+) of **6.6**.

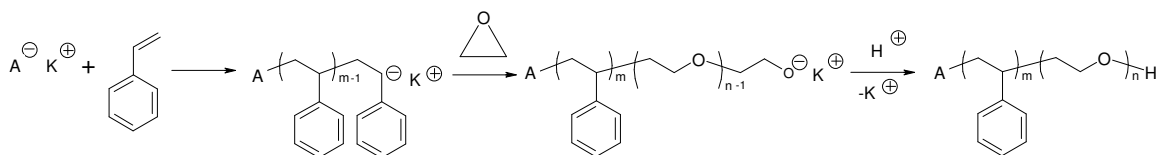


The values found for product **6.6** ($M_n = 2\,400$ and PDI = 1.08) match those obtained by GPC and $^1\text{H-NMR}$ spectroscopy.

VI.2.1.3 Synthesis of poly(styrene-*block*-ethylene oxide) (PS-*b*-PEO)

The general scheme concerning preparation of PS-*b*-PEO block copolymer is given below:

Scheme VI.3. Synthesis of poly(styrene-*block*-ethylene oxide).



The scheme is given for an organopotassium initiator ($A\text{K}^+$), but it is essentially identical for organolithium initiators. The only difference is in preliminary addition of phosphazene base $t\text{-BuP}_4$, which allows PSLi to become efficient initiator for polymerization of ethylene oxide.

Three types of organopotassium initiators have been synthesized (see experimental part) and used – cumylpotassium, diphenylmethylpotassium and benzylpotassium. The use of cumylpotassium resulted copolymers with relatively high both molecular weight and polydispersity (1.05-1.19) (see Table VI.2). PDI of the polystyrene aliquots was found to be much higher than that of the final copolymers, which was explained with the presence of impurities able to terminate propagation reaction, resulting in homopolystyrene with lower molecular weight.

Table VI.2 Type of initiator and molecular weights of obtained diblock copolymers.

No	Type of initiator	GPC				¹ H-NMR	
		M _n PS	PDI	M _n PS- <i>b</i> -PEO	PDI	M _n PS	M _n PS- <i>b</i> -PEO
6.7	CP	58 000	1.28	65 000	1.19	-	5/95 (1x10 ⁶)*
6.8	CP	12 500	1.25	30 800	1.05	-	40/60 (31 000)*
6.9	CP	37 000	2.43	41 000	1.18	39 500	85 000
6.10	CP	25 000	1.56	36 000	1.12	26 000	45 000
6.11	CP	32 000	1.50	36 500	1.07	27 400	35 300
6.12	CP	8 600	1.13	14 700	1.18	9 000	41 000
6.13	CP	4 100	1.53	8 500	1.07	8 000	19 000
6.14	CP	3 000	1.70	6 000	1.11	2 700	6 600
6.15	DPMP	36 600	1.25	45 000	1.06	-	11/89 (330 000)*
6.16	BP	670 000	1.23	790 000	1.21	420 000	1 250 000
6.17	BuLi/BuP4	700 000	1.43	800 000	1.44	-	84/16 (830 000)*
6.18	BuLi/BuP4	2 000	2.37	12 000	1.18	1 500	7 000
6.19	BuLi/BuP4	3 500	1.07	15 000	1.23	4 800	15 300
6.20	PS-OK	2 200	1.08	6 000	1.07	2 200	5 400

* In all this cases molar ratio of styrene/ethylene oxide, calculated from the related integral ratio of the proton signals in ¹H-NMR spectra, was used for calculation M_n of the obtained PS-*b*-PEO, taking M_n of PS from GPC measurements.

CP – cumylpotassium, DPMP – diphenylmethylpotassium, BP – benzylpotassium, BuLi – sec-butylolithium, BuP4 - phosphazene base *t*-BuP₄, PS-OK – hydroxy end-functionalized polystyrene deprotonated by naphthalenepotassium.

Relatively high PDI (1.18-1.19) in the cases **6.7**, **6.10**, and **6.12**, could be attributed to the fact that cumylpotassium might contain small amounts of methoxypotassium (this is a byproduct of cumylpotassium (see experimental part), which can efficiently initiate polymerization of ethylene oxide, resulting in poly(ethylene oxide) as a side product. The copolymer was purified from the low molecular weight polymers by the common fractional technique.

Another contaminant possessing two active anionic ends could be formed by reaction between α -methylstyrene and potassium. This dianion can initiate polymerization of styrene as well as further polymerization of ethylene oxide leading to PEO-*b*-PS-*b*-PEO triblock copolymers. Those polymers with approximately twice-

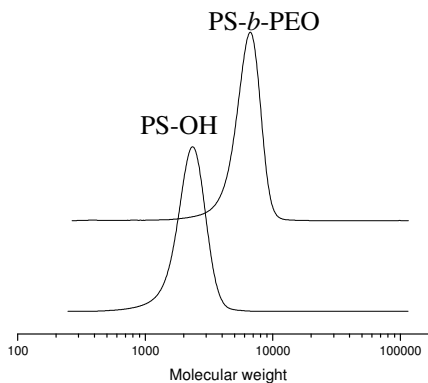
higher molecular weight are the main problem from the purification point of view. The methods applied were fractionation and dialysis.

Diphenylmethylpotassium (DPMP) was obtained by indirect metallation of diphenylmethane with naphthalene potassium. Thus, DPMP might contaminate naphthalene potassium (left after the reaction), which could produce PEO-*b*-PS-*b*-PEO triblock copolymers according to scheme presented at the end of section III.2.2. Similarly to cumylpotassium, benzylpotassium (obtained by reaction between *t*-BuOK and toluene) often contains small amounts of methoxypotassium (see experimental part).

Taking into account all disadvantages of the synthetic initiators, attention was focused on the possibility to use commercially available organolithium initiator (*s*-BuLi is a common initiator for polymerization of styrene in aliphatic solvents) in the presence of strong Lewis base (*e.g.* phosphazene base *t*-BuP₄) could efficiently initiate the polymerization of ethylene oxide. The PS-*b*-PEO block copolymers obtained (**6.17-6.19**) possessed relatively high PDI (see Table V.1), which could be explained by phosphazene base *t*-BuP₄ initiating polymerization of ethylene oxide as well, thus producing poly(ethylene oxide) as a side product.

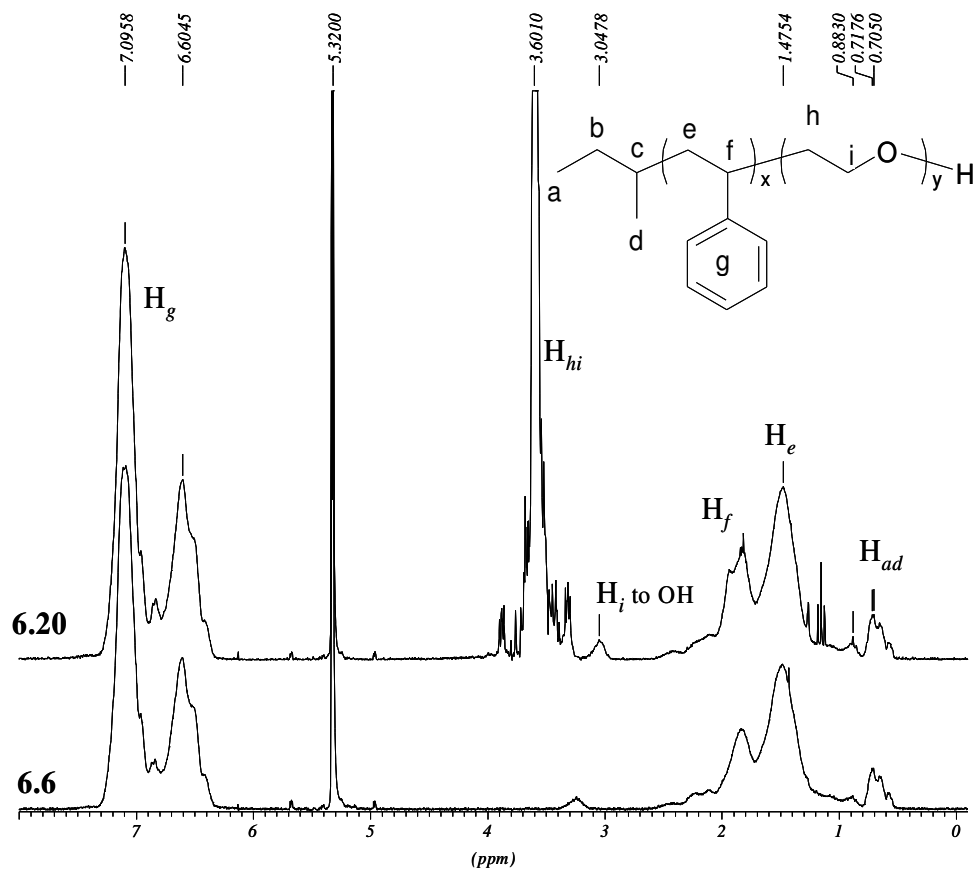
Since all of the initiators discussed above were in fact “one-pot” initiators, a major disadvantage of all of them was a poor control over molecular weight and polydispersity of each of the blocks. The requirement of a better control over both blocks, brought the idea of synthesis and characterization of hydroxyl end-functionalized polystyrene (see **6.6** in section VI.2.1.2), followed by reactivation of the end-functional group (deprotonation of hydroxyl group) and polymerization of ethylene oxide using this polystyryl macroinitiator. The resulting PS-*b*-PEO diblock copolymer possessed PDI 1.07 (confirmed by GPC (see Table VI.2 and Figure VI.4) and MALDI-TOF measurements (Figure VI.6)) and structure of the obtained PS-*b*-PEO block copolymers (confirmed by ¹H- and ¹³C-NMR spectroscopy).

Figure VI.4. GPC (THF – eluent, PS – standard) molecular weights diagrams of PS-OH hydroxyl end-functionalized polystyrene (**6.6**) and PS-*b*-PEO diblock copolymer (**6.20**)



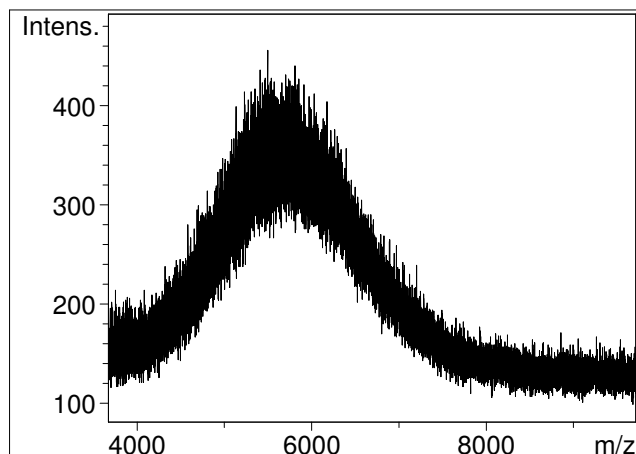
In order to calculate the molecular weights, an indirect method was used, which consisted of initial calculation of molar ratio between styrene and ethylene oxide units using the relative signal intensities in $^1\text{H-NMR}$ spectra (see Figure VI.5). Then taking into account the polystyrene block molecular weight, measured by GPC, a further calculation of the PS-*b*-PEO molecular weight was made. The results (see **6.7**, **6.8**, **6.15**, **6.16** and **6.17** in Table VI.2) indicated a much higher molecular weight of PEO block compared to the GPC data. A possible explanation is aggregation behavior of PEO chains in THF solutions.[25] This explains the fact that in THF PEO has a retention volume much smaller than that of PS of equal molecular weight. Thus, the conclusion is that while GPC is a good method for homopolymers, in case of PEO block copolymers this tool has limited due to the difference in the retention volumes of PS and PEO leading to a calculated MW lower than the real one.

Figure VI.5. $^1\text{H-NMR}$ spectra (500 MHz, CD_2Cl_2 , RT) of **6.6** and **6.20**.



Finally, the molecular weight of **6.20** (see Figure VI.6) was investigated by MALDI-TOF mass-spectrometry.

Figure VI.6. MALDI-TOF mass-spectrum (matrix–dithranol, THF, K^+) of **6.20**.



The method gave a complex of signals with maximum at $m/z = 5\ 817$ with $M_n = 5\ 684$ and $PDI = 1.03$, that support the data obtained from GPC and 1H -NMR analysis. The complexity of the mass-spectrum was due to complexity of the structures (consisting of two different types of monomer units and initiator end-groups) combined with high molecular weight. It is known that with increasing the molecular weight, the signal to noise ratio in MALDI-TOF-MS deteriorates and therefore, spectra of blockcopolymers with a mixed composition are difficult to measure.[26]

VI.2.2 Poly(isoprene-*block*-ethylene oxide)

VI.2.2.1 Introduction

Polyisoprene has a wide range of applications as a thermoplastic elastomeric additive to many commercial synthetic materials for increasing their elasticity, stability and strength. The most studied polyisoprene-containing polymers are di- and triblock copolymer with styrene.[27] Linear and branched poly(styrene-diene-styrene) types of block polymers from Shell[®] and Phillips[®] have achieved commercial importance (commercialization date 1965-68).

The most successful method for synthesis of well defined homo- and end-functionalized polyisoprene was described by *Worsfold*[28] using living anionic polymerization with 3-dimethylaminepropyl-lithium (DMAPLi) as the initiator. This methodology was repeated and further developed by *Hadjichristidis et al.*,[29]who obtained low-molecular weight polyisoprene (M_n 3 500 – 38 000) with a PDI below 1.1 and investigated changes in the microstructures of polyisoprene with molecular weight.

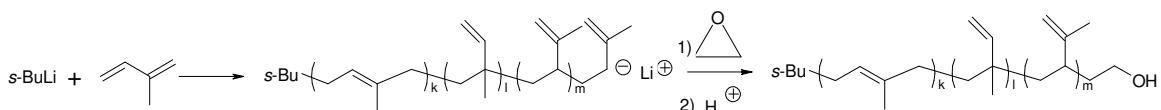
Polymers based on polyisoprene (*e.g.* block copolymers) as poly(butadiene-*b*-ethylene oxide) (PB-*b*-PEO), and poly(isoprene-*b*-ethylene oxide) (PI-*b*-PEO) block copolymers are particularly suitable for experimental investigations of aqueous phase behavior, because they are directly soluble in water even at large hydrophobic block lengths. This is in contrast to PS-*b*-PEO, where the high glass-transition temperature of the PS block mostly prevents direct dissolution in water. The classical anionic synthesis of PI-*b*-PEO block copolymers proceeds in two steps:[30,31] (*i*) the polymerization of the PI block with Li^+ as the counterion and (*ii*) the polymerization of the PEO block with K^+ as counterion. The cross-step involves end-capping with ethylene oxide, purification of the polymer, and reinitiation with organo-potassium compounds such as potassium naphthalide. The reason for this two-step procedure is the tendency of living PEO chain ends to strongly associate with Li^+ , forming ion pairs that terminate the chain propagation. Association is less pronounced for larger alkali metal cations such as K^+ . Crown ethers or cryptands that could encapsulate cations have been found to shift the free-end/cation equilibrium toward the reactive free anions, but no efficient polymerization has been observed.[32]

As it was already mention above, the use of the phosphazene base solved the problem and allowed the synthesis of either poly(isoprene-*b*-ethylene oxide) and poly(butadiene-*b*-ethylene oxide) block copolymer by use of organolithium initiator.[33] However, the major draw back is the appearance of homopoly(ethylene oxide) within even a slight excess of *t*-BuP₄ (relative to BuLi) is used, because *t*-BuP₄ is also an efficient initiator for polymerization of ethylene oxide. On the other hand, insufficiency of *t*-BuP₄ will cost some homopolyisoprene side chains being unable to initiate further polymerization of ethylene oxide.

VI.2.2.2 Synthesis and characterization of hydroxyl end-functionalized polyisoprene.

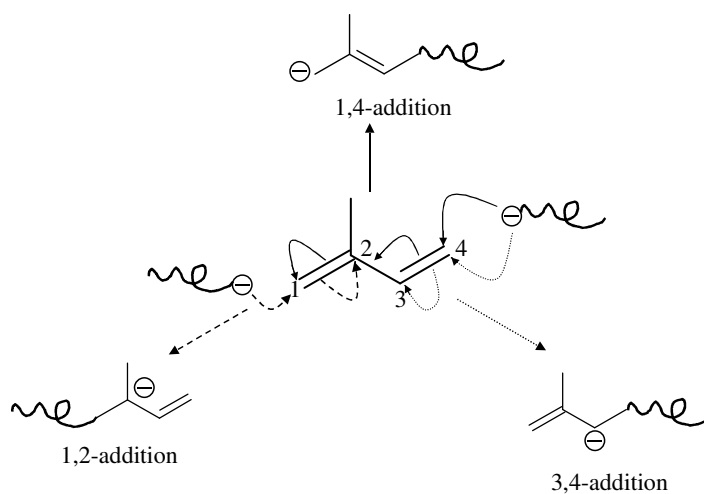
Analogous to the previously discussed polystyrene (see section V.2.1), the synthesis of a polyisoprene with a hydroxyl end-group was developed to produce polyisoprene blocks capable of use as macroinitiators for further polymerization of a second monomer (*e.g.* ethylene oxide) to obtain diblock copolymers:

Scheme VI.4. Synthesis of hydroxyl end-functionalized polyisoprene.



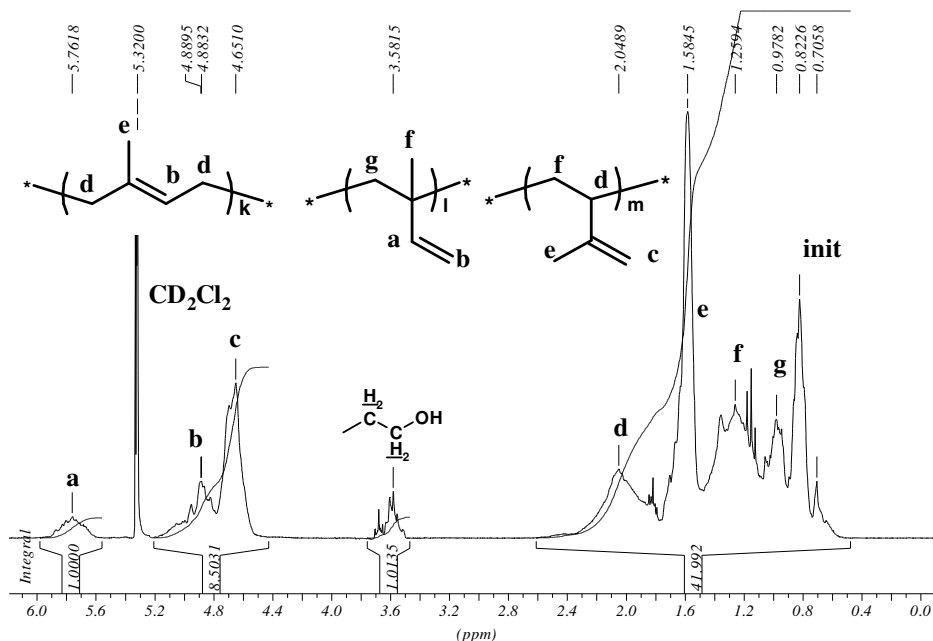
There are four possibilities for addition of isoprene molecule to the active end of the growing polymer chain, leading to four types of polyisoprene microstructure. The first two are a *cis*-1,4- (not drawn in the Scheme VI.4, because it was not found in the obtained polymer) and *trans*-1,4-microstructure (*k*) obtained by a 1,4-nucleophilic addition reaction, generating a double bond between the C2 and C3 atoms of isoprene. 1,2- And 3,4-microstructures (*l* and *m*) were analogous obtained *via* 1,2- and 3,4-nucleophilic addition reactions:

Scheme VI.5. Nucleophilic addition reaction of living anionic chain to isoprene molecule.



The amounts of the different microstructures were determined by $^1\text{H-NMR}$ spectroscopy, comparing the integrals ratio between the signals for protons **a**, **b** and **c**, were found to be 10 : 30 : 60 = 1,4 : 1,2 : 3,4-microstructure (Figure VI.7).

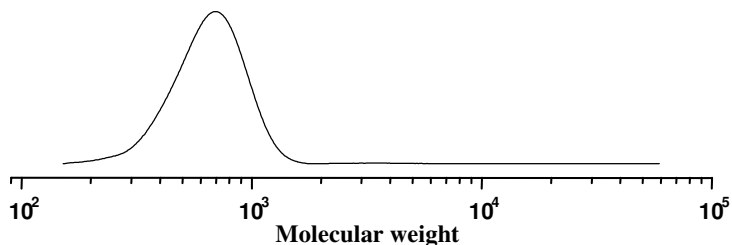
Figure VI.7. $^1\text{H-NMR}$ spectrum (250 MHz, CD_2Cl_2 , RT) of **6.21**.



The calculation concerning the molecular weight based on equation VI.2 was not particularly applicable, because of the overlapping of the protons signals **g** with those of the initiator. The complete end-capping of the polymer chains with ethylene oxide was determined by means of the signal responsible for methylene protons next to the hydroxyl group at 3.58 ppm in the spectrum.

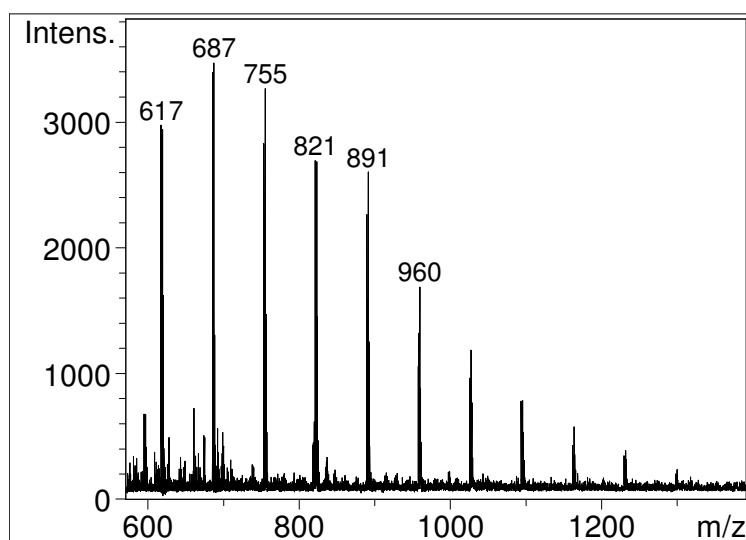
The Molecular weight of prepared polymer was determined by GPC, M_n 700 and PDI 1.11 (see Figure VI.8). This result is rather reasonable having in mind that polydispersity increases with decreasing molecular weight.[34]

Figure VI.8. GPC (THF – eluent, polyisoprene – standard) of **6.21**.



MALDI-TOF data concerning molecular weight (M_n 890 and PDI 1.09) differ from the GPC data of **6.21**. This difference can be explained by the very low molecular weight of the obtained polyisoprene, which signals partially overlap those of the matrix (Figure VI.9).

Figure VI.9. MALDI-TOF MS (matrix-dithranol, THF, Ag^+) of **6.21**. Homologous series of polyisoprene with intervals of $m/z = 68 \pm 2$, corresponding to the molecular weight of the isoprene monomer unit of 68.11.

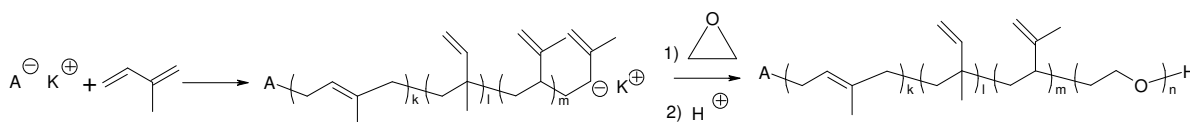


Similarly to homopolymers, block copolymers described in the present chapter were mainly done as polymers building the polymeric shell in the core-shell - dendrimer-polymer hybrids. The requirement to those polymers to be well-defined demands more substantial review over the particular improving the polymer characteristics in terms of anionic polymerization. Additionally, block copolymers were applied in projects (*e.g.* radical polymerization in magnetic field, building of self-assembly supramolecular structure based on hydrogen bond interaction between dendrimer-polymer hybrids and block copolymers and fluorescence labeled polymers) some of them being apart from the main topic of the current work, but exclusively new investigation concerning block copolymers. Thus, the need of copolymers with desire characteristic required the use of anionic polymerization technique.

VI.2.2.3 Synthesis of poly(isoprene-*block*-ethylene oxide) (PI-*b*-PEO)

The synthetic strategies for preparation of PI-*b*-PEO block copolymer are analogous to those used for PS-*b*-PEO. The general scheme for synthesis of PI-*b*-PEO block copolymers is given below:

Scheme VI.6 Synthesis of poly(isoprene-*block*-ethylene oxide)



The main difference between PI-*b*-PEO and PS-*b*-PEO block copolymers is in the ability of the isoprene to form polymers with different microstructures (the mechanisms and appearances of each microstructure were discussed in section VI.2.2.2), which strongly influence the properties of the final polymer. As it was already mentioned, the main control over the appearance of a given microstructure in the polymer chain is the nature of the solvent chosen - nonpolar solvents favor a 1,4-microstructure (k), while polar solvents favor the 1,2- and 3,4-microstructures (l and m). THF was used in all the experiments performed in the present study, and the ratio between the different microstructures was determined by $^1\text{H-NMR}$ spectroscopy, to be in the range of 1,4- : 1,2- : 3,4-microstructure = 10 : 30 : 60, as expected by the previous arguments.

The molecular weights of the produced block copolymers were measured by GPC and found to be in the range of 700 to 34 000 (see Table VI.3.). The polydispersity was rather high (over 1.20 in most cases), due to the factors previously discussed (see the beginning of section VI.2.2.1).

Figure VI.10. GPC (THF – eluent, PI – standard) molecular weights diagrams of PI-OH hydroxyl end-functionalized polyisoprene (6.21) and PI-*b*-PEO diblock copolymer (6.27 see Table VI.3.)

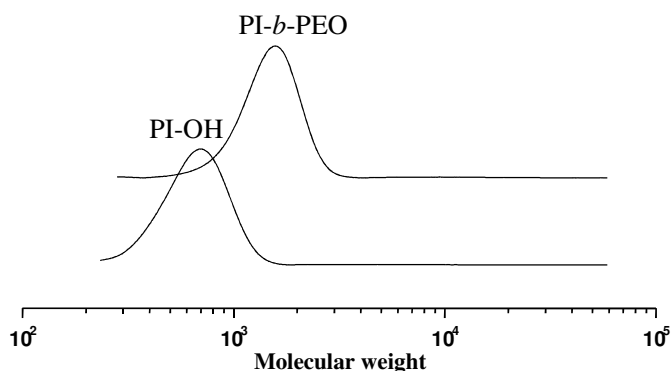


Table VI. 3 Type of initiator and molecular weights of the obtained diblock copolymers.

No	Type of initiator	GPC				¹ H-NMR	
		M _n PI	PDI	M _n PI-b-PEO	PDI	M _n PI	M _n PI-b-PEO
6.22	DPMP	20 000	1.32	23 000	1.22	25 000	30 500
6.23	DPMP	27 000	1.60	34 000	1.32	21 800	30 500
6.24	BuLi/BuP ₄	3 300	1.36	5 000	1.08	-	74/26 (4 500)*
6.25	BuLi/BuP ₄	3 400	1.33	5 200	1.24	-	16/84 (21 300)*
6.26	BuLi/BuP ₄	2 500	1.36	5 700	1.21	-	23/77 (11 000)*
6.27	PI-OK	700	1.11	1 400	1.12	-	-

* In all this cases molar ratio of isoprene/ethylene oxide was calculated the related integral ratio of the proton signals in ¹H-NMR spectra, was used for calculation of M_n of the obtained PI-*b*-PEO, taking M_n of PI from GPC measurements.

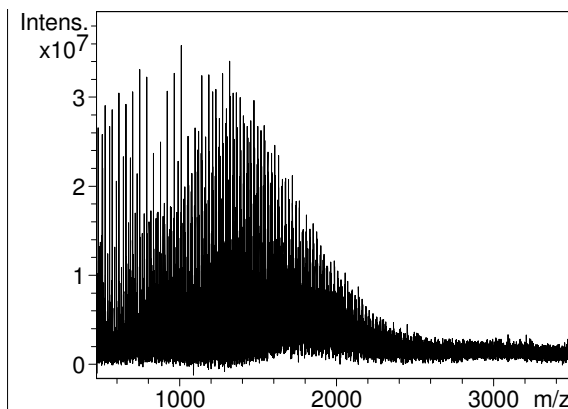
DPMP – diphenylmethylpotassium, BuLi – sec-butyllithium, BuP₄ - phosphazene base *t*-BuP₄, PI-OK – hydroxy end-functionalized polyisoprene deprotonated by naphthalenepotassium.

In the case of DPMP initiated block copolymers (**5.22** and **5.23**), the molecular weights of the styrene block as well as those of the diblock copolymers were calculated from the ¹H-NMR spectra comparing initiator, PI and PEO relative signal integrals. The obtained molecular weights supported those obtained by GPC measurements. (see Table VI.3)

In the case of BuLi/BuP₄ initiated copolymers (**5.24-5.26**), such calculation was limited by the fact that all signals belong to initiator protons were overlapped by the signals of polyisoprene protons. Therefore, molecular weights of the polyisoprene blocks were taken from the GPC of the PI aliquots, and using the ratio between the relative integral signals, the molecular weights of both PEO and PI-*b*-PEO were found.

Finally, the molecular weight of the product **5.27** was proved by MALDI-TOF mass-analysis.

Figure VI.11. MALDI-TOF mass-spectrum (matrix – dithranol, without salt) of **6.27**.



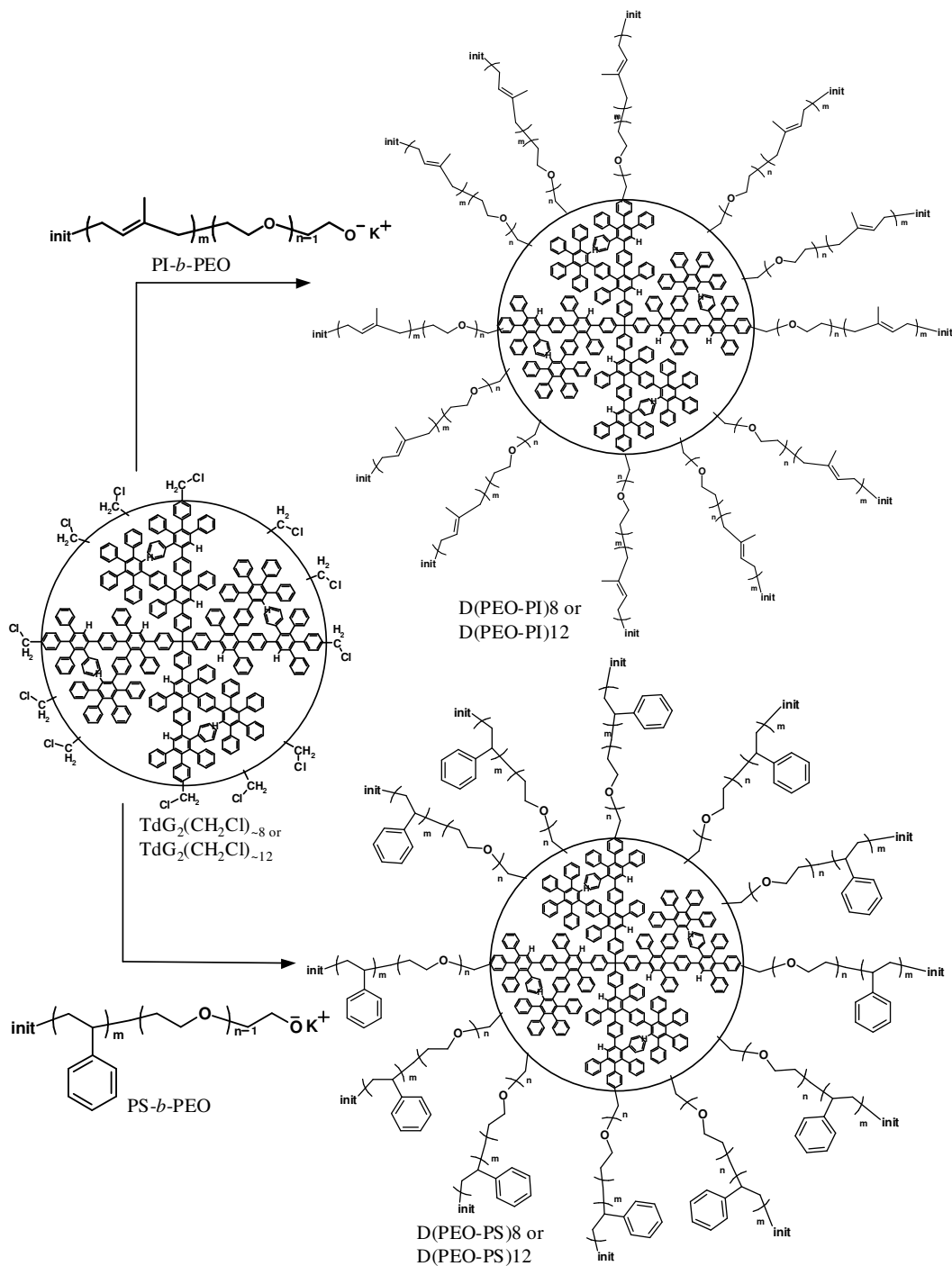
The method gave a composition of signals with maximum at $m/z = 1\ 362$ with M_n 1 395 and PDI 1.15, that completely support the data obtained from GPC and $^1\text{H-NMR}$ analysis (see Table VI.3). Similarly to the case of PS-*b*-PEO, the complexity of the mass-spectrum was due to the complexity of the structure - two different types of monomer units and initiator end-group and closeness of the matrix signals, which disturbs calibration of the spectrum and exactness of the molecular weight determination.

VI.3. Poly(styrene-*block*-ethylene oxide) and Poly(isoprene-*block*-ethylene oxide) Copolymers Grafting-onto Polyphenylene Dendrimers.

Having obtained successful diblock copolymers (see section VI.2), we used second generation polyphenylene dendrimers with average number of 12 ($\text{TdG}_2(\text{CH}_2\text{Cl})_{-12}$) and 8 ($\text{TdG}_2(\text{CH}_2\text{Cl})_{-8}$) chloromethyl groups on their surface, the synthesis of which has been synthesized by Dr. V. Sinigersky and reported elsewhere (see Chapter IV).[35] As it was already discussed in Chapters I and IV, the advantage of this dendrimer, in comparison with one possessing defined number of functional groups, is in the simplicity of its preparation, which requires functionalization of a non-functionalized dendrimer in a one-step reaction. However, the drawback of the “grafting-onto” method, especially for long polymer chains, is sterical hindrance of already attached chains that shielded remaining functionalities of the dendrimer. To minimize this effect relatively short copolymer chains were synthesized (see **6.20** and **6.27** in section VI.2) and their attachments to a TdG_2 with fewer functionalities (*e.g.* $\text{TdG}_2(\text{CH}_2\text{Cl})_{-8}$) investigated.

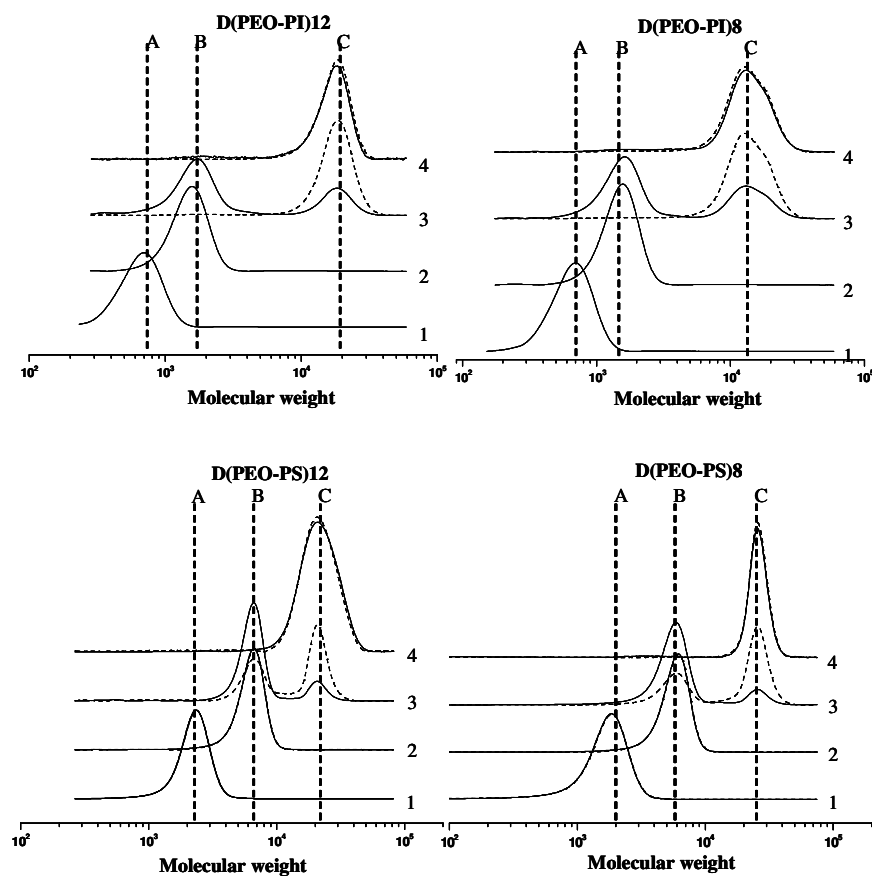
The synthesis of core-double-shell by “grafting-onto” method is essentially the same as in case of core-mono-shell macromolecules (see Scheme IV.3 in section IV.4) differ only in a type of polymer attached (PEO for core-mono-shell and PS-*b*-PEO or PI-*b*-PEO for core-double-shell macromolecules) (see Scheme VI.7).

Scheme VI.7. Synthesis of PI-*b*-PEO and PS-*b*-PEO 8 or 12 fold substituted polyphenylene dendrimer.



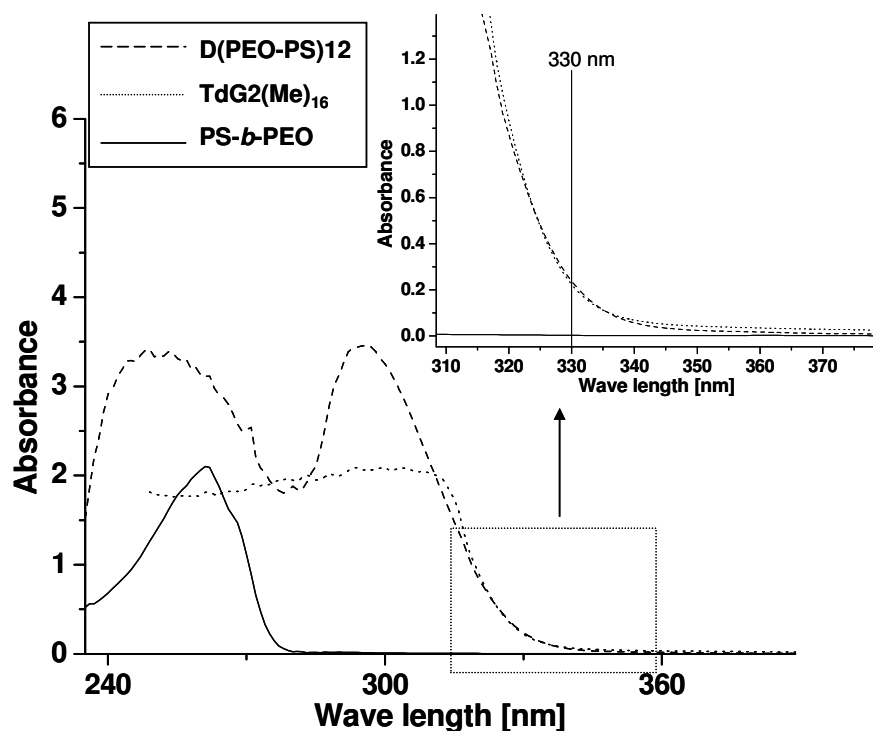
In order to give a better chance to all chloromethyl groups to attend into the nucleophilic substitution reaction (Williamson reaction), a 5-fold molar excess of block copolymer chains in respect to chloromethyl group was used, leading to a large excess of unreacted polymer chains in the crude mixture at the end of the reaction. The crude products (see elugram No 3 in Figure VI.12) were purified from the residual copolymer chains, using preparative GPC. After purification, the GPC elugrams (see elugram No 4 in Figure VI.12) showed monomodal distributed products with a low polydispersity index (1.05-1.13).

Figure VI.12. GPC (PI and PS standards, THF eluent) molecular weights diagram of **D(PEO-PI)12** and **D(PEO-PI)8** (1 - PI-OH; 2 - PI-*b*-PEO; 3 - **D(PEO-PI)12(8)** crude; 4 - **D(PEO-PI)12(8)** purified. A - PI-OH; B - PI-*b*-PEO; C - **D(PEO-PI)12(8)**); and molecular weights diagram of **D(PEO-PS)12** and **D(PEO-PS)8** (1 - PS-OH; 2 - PS-*b*-PEO; 3 - **D(PEO-PS)12(8)** crude; 4 - **D(PEO-PS)12(8)** purified. A - PS-OH; B - PS-*b*-PEO; C - **D(PEO-PS)12(8)**).



Three different methods were applied to determine the molecular weight of the prepared core-double-shell nano-particles – GPC, UV- and $^1\text{H-NMR}$ spectroscopy (see Table VI.4). Although GPC is very common method for determination of M_n and PDI, this method cannot give exact M_n of these materials for the reasons discussed in section IV.4. Another convenient and fast method for determining M_n is UV spectroscopy. The procedure, approximations, standards and calculations used in the present chapter are essentially the same as in section IV.4 (see Figure VI.13)

Figure VI.13 UV spectra of **D(PEO-PS)12**, **TdG2(Me)₁₆** and **PS-*b*-PEO** in chloroform.



Calculations concerning molecular weights using $^1\text{H-NMR}$ spectroscopy were based on relative intensity of the aromatic protons of the dendrimer at $\delta = 7.5\text{-}6.3$ ppm and the PI protons at $\delta = 5.2\text{-}4.5$ ppm in the spectra of **D(PEO-PI)8** and **D(PEO-PI)12**. However, in the case of PS-*b*-PEO substituted dendrimers the signals of the aromatic protons of polystyrene overlap with those of the dendrimer. In these cases

we used the relative intensity of the methylene protons (Dendrimer-CH₂-Cl) and the aromatic protons of the dendrimer in the spectra of **TdG₂(CH₂Cl)₋₈** or **TdG₂(CH₂Cl)₋₁₂** and applied that ratio to the spectra of **D(PEO-PI)₈** and **D(PEO-PS)₁₂** in order to find the integral value of aromatic protons coming from dendrimer and those from polystyrene (see Figure VI.14).

Figure VI.14 ¹H-NMR spectra (500 MHz) of PI-*b*-PEO (A) and PS-*b*-PEO (A'); **TdG₂(CH₂Cl)₋₈** (B and B'); **D(PEO-PI)₈** (C), **D(PEO-PS)₈** (C') in C₂D₂Cl₄.

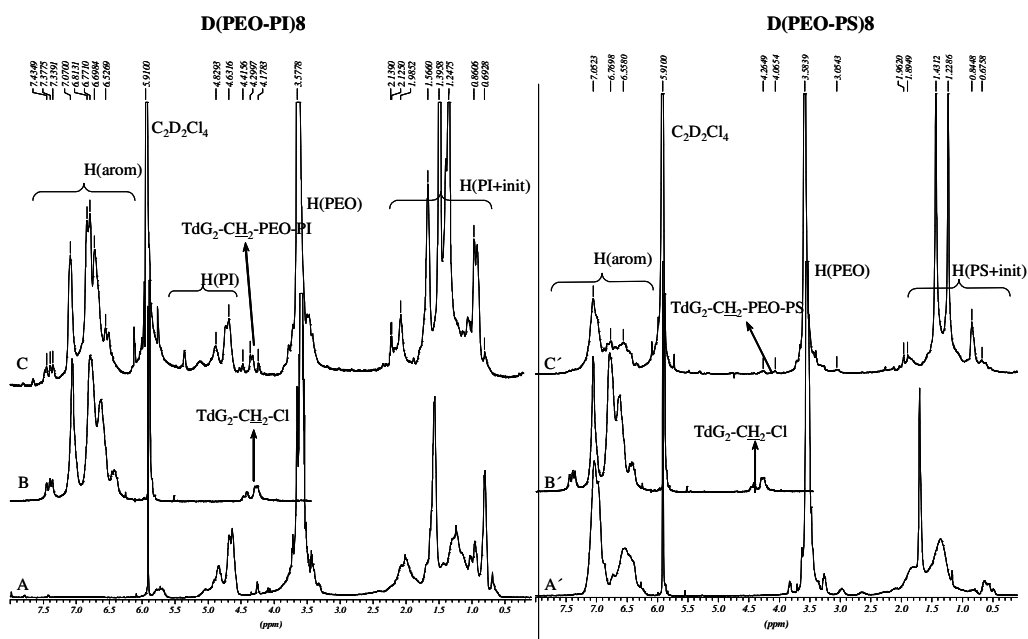


Table VI.4. Number of arms and molecular weight of obtained core-double-shell macromolecules ($^1\text{H-NMR}$: 500 MHz, $\text{C}_2\text{D}_2\text{Cl}_4$, 373K; GPC: PS or PI standards, THF eluent).

Sample	Quantity	GPC*	UV-Spectroscopy	$^1\text{H-NMR}$ Spectroscopy
D(PEO-PI)8	M_n	12 600	21 900	17 100
	Number of arms	5.2	11.8	8.4
D(PEO-PS)8	M_n	28 500	32 200	38 300
	Number of arms	4.1	4.7	5.8
D(PEO-PI)12	M_n	17 100	17 400	19 500
	Number of arms	8.3	8.5	10.0
D(PEO-PS)12	M_n	26 000	40 200	56 000
	Number of arms	3.6	6.1	8.9

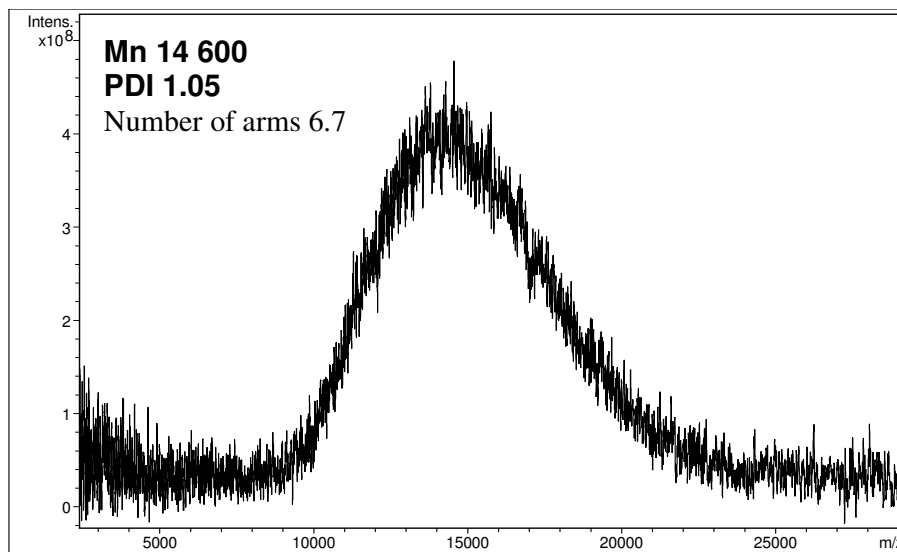
*PDI: **D(PEO-PI)8** 1.13; **D(PEO-PS)8** 1.05; **D(PEO-PI)12** 1.07; **D(PEO-PS)12** 1.05

Complete substitution reaction was observed only for a low density of the functionalities (~ 8) and for shorter block copolymer chains (number of arms 8.4 for **D(PEO-PI)8**). Increasing the number of the average functional groups (~ 12) was accompanied by a decrease the respective number of polymer chains attached to the surface (10 arms only, in case of **D(PEO-PI)12**). The effect is stronger in case of longer copolymer chains - number of arms was 5.8 for **D(PEO-PS)8** and 8.9 for **D(PEO-PS)12**. Obviously, in the case of longer chains and higher density of functionalities a complete conversion cannot be achieved due to steric hindrance. This aspect is supported by the results of Dr. T. Wehrmeister, [36] describing reaction of polymeric anions (*i.e.* multiple anions on a polymeric backbone). It would appear that upon increasing the number of reactive sites on the surface of the core the conversion of the grafting reaction is limited due to steric reasons.

In order to obtain molecular weight of the prepared core-double-shell macromolecules MALDI-ToF mass-spectrometry was also applied. The method succeed in case of the system **D(PEO-PI)8** with the lowest molecular weight (see Figure VI.15). The possible reasons are complexity of the structures, in terms of combination of dendrimer with polymer, combined with higher molecular weight. It is known that with increasing molecular weight, the signal to noise ratio in MALDI-

ToF-MS deteriorates and therefore, spectra of blockcopolymers with a mixed composition are difficult to measure.[37]

Figure VI.15. MALDI-ToF mass-spectrum of **D(PEO-PI)8** (dithranol matrix, Na^+).



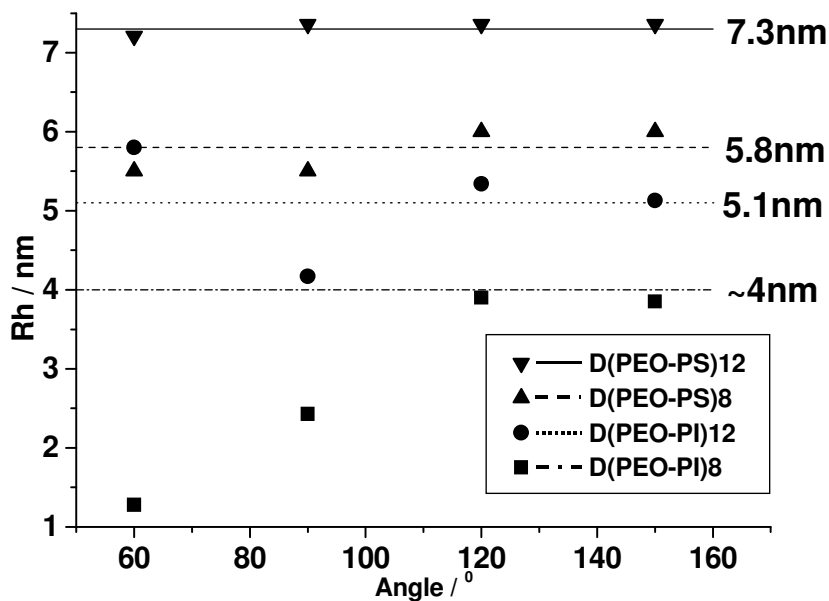
The MALDI-ToF mass-spectrum of **D(PEO-PI)8** indicate a Gaussian molecular weight distribution with extremely low polydispersity index. The distribution in the particular case should be grounded on both distributions of block copolymers and this of dendrimer functionalities. However, the low polydispersity index, obtained either by MALDI-ToF MS or by GPC (see Figure VI.15 and Table VI.4), indicates the presence of self-limiting process. This process is based on the fact that polymers differ in molecular weights are attached to the dendrimer as follow: (i) the number of polymers with molecular weight equal to that of the average molecular weight dominate; (ii) the number of polymers with higher or lower molecular weight attached to the dendrimer surface decrease according to their polymer distribution; (iii) the number of polymers arms which molecular weight equally deviate from the average one is equal. From this three statements one can conclude that Gaussian distribution of polymers (see Figure VI.15) represents the probability of every particular polymer chain to be attached to the dendrimer surface. Since block copolymers used in the present study possess symmetrical Gaussian distribution, the probability to attach chains with molecular weight above and below the average one is equal for polymers with equal deviation. Thus, the total number of monomer units

present in the polymer shell of every core-double-shell system tends to value characteristic for the whole system. The conclusion is that polymer distribution of attached polymers does not play a significant role by the formation of polydispersity index of examined systems.

However, the distribution of dendrimer functionality should affect significantly PDI of the entire system. The fact that this was not observed can be attributed to follow assumptions: (i) as it was already discussed in chapters IV and V, the “grafting-from” method is limiting by the shielding effect of polymers attached to the dendrimer surface over the dendrimer functionalities – this effect becomes self-limiting factor in the case of dendrimer molecules possessing highly dense functionality; (ii) dendrimers with low dense functionality was supposed to possess higher hydrophobicity and thus to become soluble in hexane during the precipitation of the crude product, which is a part of purification procedure (see experimental part), and thus decrease their amounts drastically.

One important characteristic of the core-double-shell systems is the hydrodynamic radius (R_h) in a particular solvent. The R_h of the prepared core-double-shell nanoparticles was measured by Dynamic Light Scattering (DLS) in THF solutions (see Figure VI.16). It is noteworthy that the R_h of the core ($\text{TdG}_2(\text{CH}_2\text{OH})_{16}$) was reported to be 3 nm, [38,39] and this radius increases with both the increasing length of the diblock copolymers and the number of the arms grafted onto the dendrimer surface from 4 to 7.3 nm (Figure VI.16). The relation between the length of the arms and size of the entire particle was already discussed in Chapters IV and V. However, in the present study we were able to establish the relation between the number of attached chains and the size in terms of hydrodynamic radius of the prepared core-double-shell structures. As it was already mentioned above with increase the number of attached chains increases the R_h of the system. This effect should be attributed to the fact that systems having higher number of polymeric chains (**D(PEO-PI)12**, **D(PEO-PS)12**) possess denser packed shell, which result in more stretched conformation of the polymers, compare to those with sparser shell (**D(PEO-PI)8**, **D(PEO-PS)8**).

Figure VI.16. DLS (R_h in THF) of the obtained core-double-shell nanoparticles.



The measurements at low angles (60 and 90⁰), deviated substantially from the linear fit in the cases of **D(PEO-PI)12** and **D(PEO-PI)8**. This error is attributed to the technical limit of the “particle sizer” used (ALV 5000 – Correlator (Malvern instruments) being 5 nm).

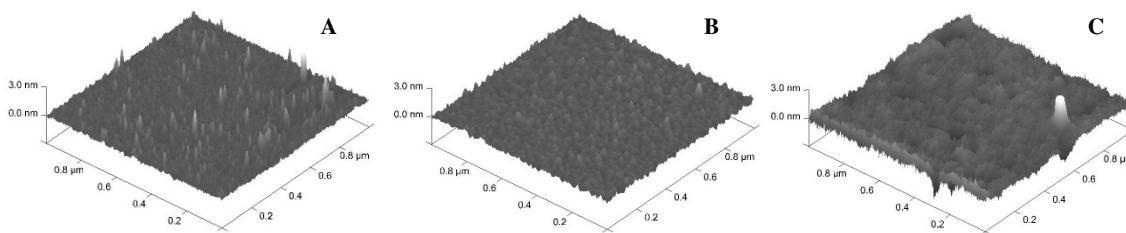
The influence of the solvent polarity over the R_h of those systems failed in the case of water or mixture of THF with water due to the presence of dominant second process, which indicates formation of aggregates. Therefore, alternative method investigating polarity of the systems was utilized.

VI.3.1. Surface polarity of thin layers – mutable structure to media polarity.

As was proposed in the introduction part of the current chapter the systems combining stiff hydrophobic core with relatively flexible amphiphilic shell should give an access to material which adjust its surface polarity to those of the environment with respect to the number of application mention before. Thus, in order to examine those properties a surface polarity of thin films consist of **D(PEO-PS)12** were prepared.

The surface polarity of **D(PEO-PS)12** thin layers was studied by using its solutions in media with different polarities - THF/Water and THF/Hexane. A spin-coating technique was used for preparation of the layers on a silicon oxide surface (silicon-wafers consist of silicon slide covered by native oxide layer, were used as substrates). The thickness of the organic layers was adjusted by varying the concentration of **D(PEO-PS)12** in THF (1.0, 0.1 and 0.01 g/L) by constant velocity of rotation of a spin-coater (3000 rpm). Surface morphologies of **D(PEO-PS)12** layers were examined by AFM shown on Figure VI.17.

Figure VI.17. Surface topographies of **D(PEO-PS)12** layers deposited by spin-coating technique at 3000 rpm on SiO₂ surface from media coating THF with concentration (A) 0.01, (B) 0.1 and (C) 1.0 g/L.



The calculated diameter of the single **D(PEO-PS)12** molecule is roughly 15 nm, which is in a perfect agreement with $R_h = 7.3$ nm found by DLS (see Figure VI.16). The root-mean-square roughness values for the **D(PEO-PS)12** films from 0.01, 0.1, 1.0 g/L solutions are 0.327, 0.198 and 0.180 nm, respectively, indicating that a higher **D(PEO-PS)12** concentration is more favorable for the formation of uniform surface morphologies. Complete coverage of the substrates surface was achieved at 1.0 g/L (Figure VI.17 B) and this concentration was used for preparation of four solutions of **D(PEO-PS)12** in THF with 5 and 1%vol water as well as 5 and 30%vol hexane. The thickness of the layers prepared out of those solutions was determined by ellipsometry (null-type ellipsometer). Contact angle measurements were used for determination polarity of the layers surface. The results are summarized in Table VI.5.

Table VI.5. Solutions ratio, thickness and contact angle of the **D(PEO-PS)12** layers prepared by spin-coating.

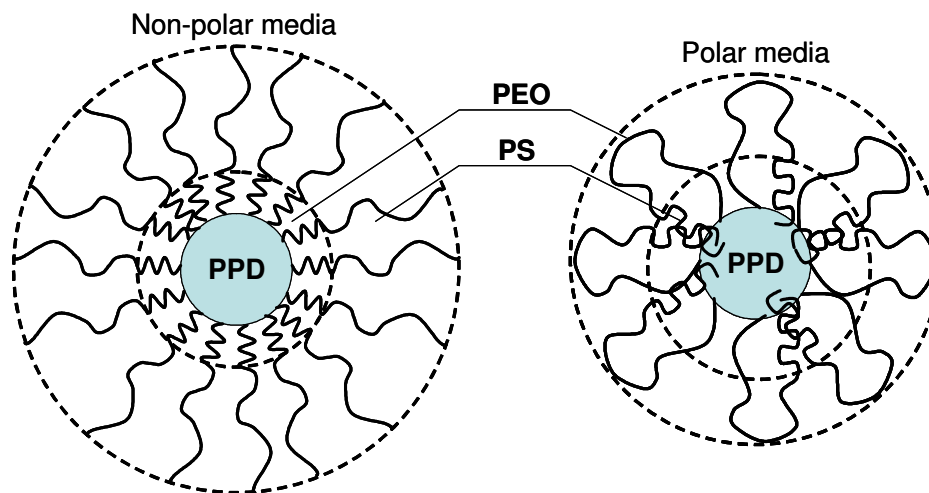
No	Solution	Ratio [v/v%]	Thickness [nm] [*]	Contact angle θ_{water} [grad] ^{**}
1	THF/Water	95/5	38	63.1
2	THF/Water	99/1	36	63.7
3	THF	100	35	64.9
4	THF/Hexane	95/5	36	66.0
5	THF/Hexane	70/30	38	66.9

* Standard deviations less than ± 3 nm

** Standard deviations less than $\pm 1^\circ$

The contact angle measurements indicated that an increase in polarity of the media (Table VI.5. No 1 and 2) is accompanied by a decrease in the contact angle, and *vice versa* (Table VI.5. No 4 and 5). The obtained results confirmed that amphiphilic core-double-shell macromolecules can rearrange their structure depending on the polarity of the surrounding media. Non-polar solvents induce a less polar surface (PS), while polar solvents induce a more polar outer layer (PEO). If we consider the observed effect due to intra-molecular interactions, the structure in polar or non-polar media could be represent as follow:

Figure VI.18 Schematic representation of the conformational shape of the core-double-shell system in polar and non-polar media.



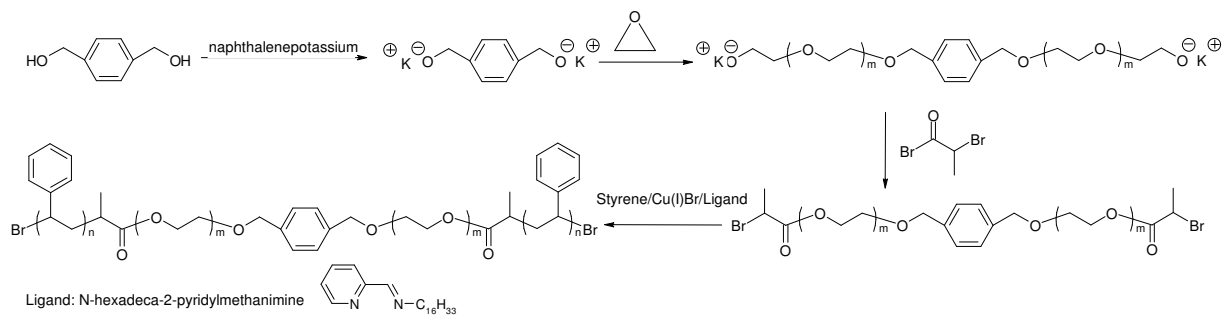
It is expected that in non-polar media, the polystyrene part will be better solvated by the solvent molecules, and therefore, will adopt a more stretched conformation. At the same time, PEO will collapse on the inner shell (Figure VI.18 non-polar media). In polar media PEO is better dissolved and can therefore penetrate the PS shell and moves to the surface. In this case PS chains aggregate and could even cover the cavity of the non-polar dendrimer (Figure VI.18 polar media). In the case of polar media the aggregates formation can be attributed to inter-molecular interaction where either PS or PEO can be involved.[40]

VI.4. Synthesis of core-*double*-shell macromolecules by “grafting-from” method.

VI.4.1 Synthesis of poly(styrene-*b*-ethylene oxide-*b*-styrene) – model reaction for preparation of core-*double*-shell macromolecules by “grafting-from” strategy.

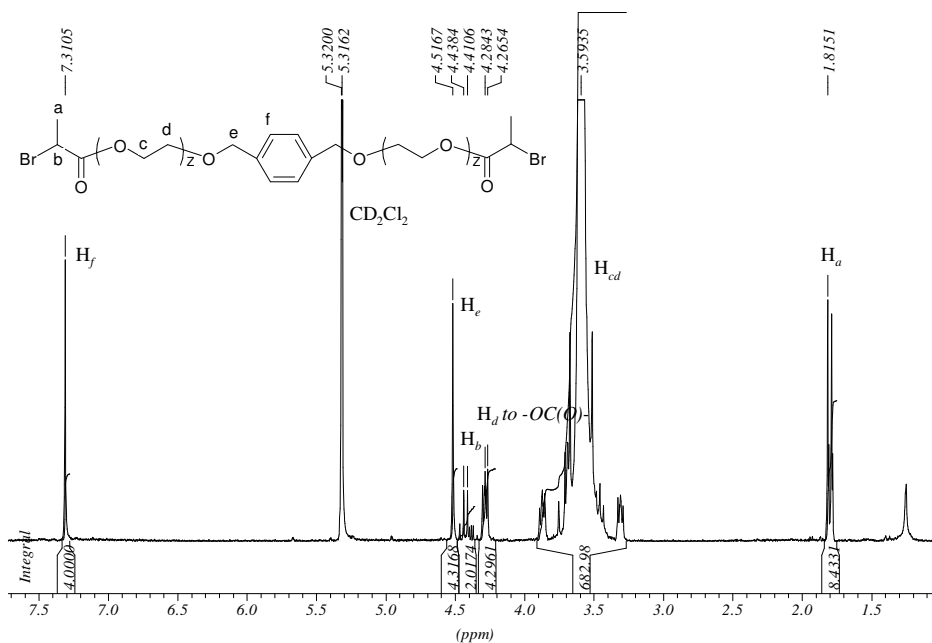
The sequential polymerization of EO followed by styrene required mostly iteration of anionic and radical polymerization, due to the weakness of PEO living anion incapable to initiate styrene polymerization. The need of such strategy was required by the preparation of core-*double*-shell molecules by “grafting-from” method (see next section). The method uses PPD as multifunctional anionic macroinitiator for the polymerization of EO followed by atom transfer radical polymerization (ATRP) of styrene. Thus core-*double*-shell structures possessing rigid hydrophobic core (PPD), covered by soft hydrophilic inner-shell (PEO) and semirigid hydrophobic outer-shell (PS) was available.

In order to check the possibility of the strategy chosen, a model experiments utilizing 1,4-dimethoxyphenylene mimicking the functionality of the $\text{TdG}_2(\text{CH}_2\text{OH})_{16}$, was performed (see Scheme VI.8).

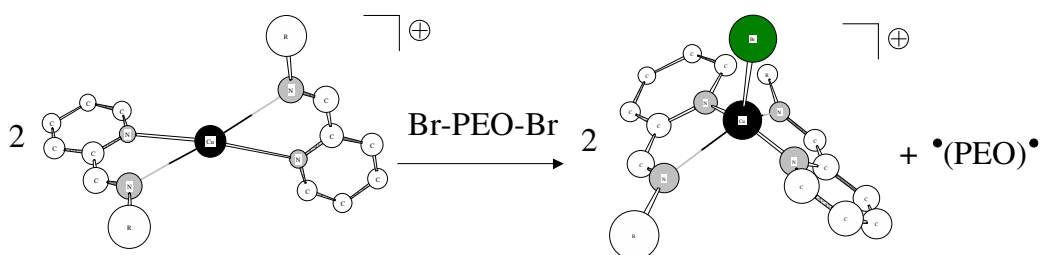
Scheme VI. 8 Synthesis of PS-*b*-PEO-*b*-PS triblock copolymer.

The initial step consisted of polymerization of ethylene oxide using the difunctional initiator 1,4-dimethoxyphenylenepotassium, followed by a termination reaction between the living anionic ends and 2-bromopropionyl bromide[41]. The completeness of termination reaction was determined by $^1\text{H-NMR}$ spectroscopy by comparing the integrals of initiator signals (aromatic protons of 1,4-dimethoxyphenylene at 7.3 ppm) and those of 2-bromopropanoyl end-group (methyl protons at 1.80 ppm, or methene proton at 4.42 ppm) (see Figure VI. 19).

Figure VI. 19 $^1\text{H-NMR}$ spectrum (250 MHz, CD_2Cl_2 , RT) of **6.28**.



The thus obtained and characterized radical macroinitiator (see Table VI.6) in the second step was applied for ATRP of styrene (see scheme VI.8). ATRP is a method possessing all the requirements of radical polymerization (the reaction system should be purified from oxygen and undesired radicals providing or consuming substances), which produces almost monodisperse polymers. This method is well established in the case of styrene polymerization[42,43], where a strong requirement is that the molar ratio of the complex forming compounds must be: initiator / Cu(I)Br / ligand = 1 / 2 / 4. This ratio ensures the formation of a complex, which performs the polymerization:



Initially Cu(I)Br forms a complex with the nitrogen atoms of the ligand (N-hexadeca-2-pyridylmethanimine). In the next step, this complex accepts bromine radical breaking homogeneously the Br-C bond (of the PEO macroinitiator) and creating a macro free radical. When the Cu-ligand complex is in two-fold excess, then radicals which allow ATRP of styrene can be created on both ends of the PEO resulting in a PS-*b*-PEO-*b*-PS triblock copolymer. The macroradical formation reaction is reversible, which ensures relatively low concentrations of the active radicals are present in the system. This keeps the probability for termination reaction (chain-transfer or recombination) as low as possible. Thus, covering all this requirements the triblock copolymers obtained from free polymerization of styrene using PEO ATRP macroinitiator were performed, differing in the molecular weight of styrene blocks, were characterized (GPC and ¹H-NMR spectroscopy) and results are summarized in Table VI.6.

Table VI.6 Molecular weights of PS-*b*-PEO-*b*-PS triblock copolymer and PEO macroinitiator.

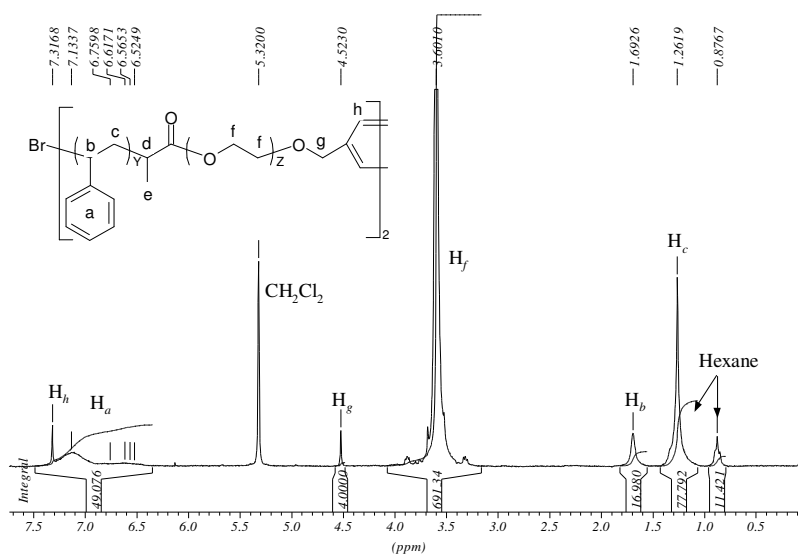
No	GPC		¹ H-NMR
	M _n	PDI	M _n
6.28 *	4 700	1.27	4 000
6.29 **	7 800	1.39	7 900
6.30 **	7 000	1.44	9 250
6.31 **	8 800	1.35	8 950

* PEO macroinitiator

** PS-PEO-PS

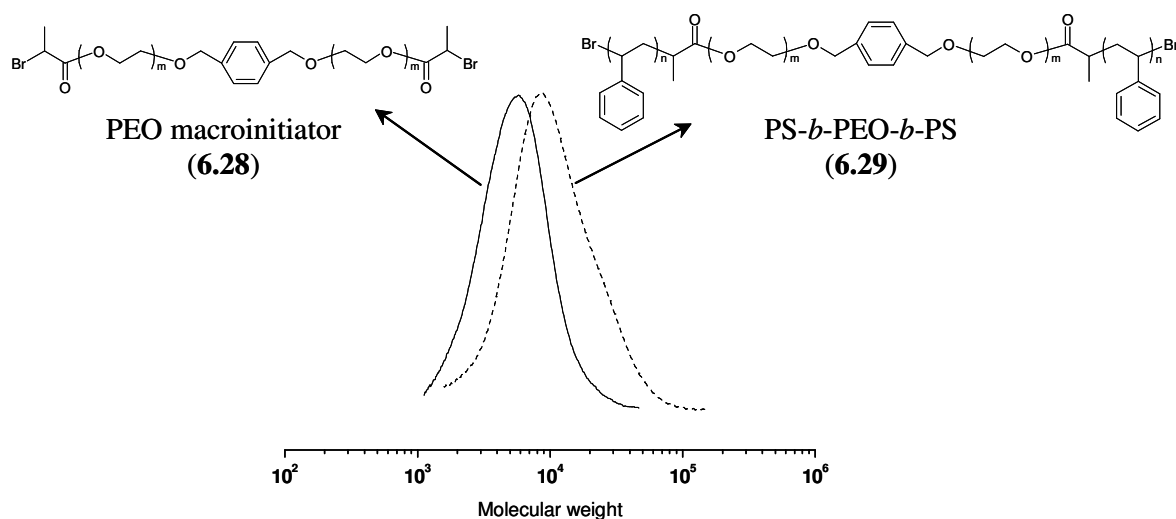
The molecular weights of the copolymers, obtained by both GPC and ¹H-NMR spectroscopy, were found to be in good agreement between each other. Calculation of molecular weight by ¹H-NMR was achieved by comparing relative integrals of the aromatic protons of PS and methylene protons of 1,4-dimethoxyphenylene (H_g, see Figure VI.20) used as initiator in preparation of the PEO macroinitiator.

Figure VI.20 ¹H-NMR spectrum (250 MHz, CD₂Cl₂, RT) of **6.29**.



The PDI, obtained by GPC, was slightly higher than that of the PEO macroinitiator (PDI 1.27), but the curve was still monomodal (see Figure VI.21).

Figure VI.21 GPC (**6.28**: water – eluent, PEO – standard; **6.29**: THF – eluent, PS – standard) molecular weights diagrams of PEO (**6.28**) and PS-*b*-PEO-*b*-PS (**6.29**).



Thus by combining anionic and ATRP methods, PS-*b*-PEO-*b*-PS triblock copolymers possessing defined molecular weight and relatively low PDI were obtained. The drawback of ATRP as a polymerization method is the presence of Cu(II) complexes in the final product. Purification from these substances requires special conditions, which are not applicable in some cases.

VI.4.2 Synthesis of core-shell ATRP macroinitiators.

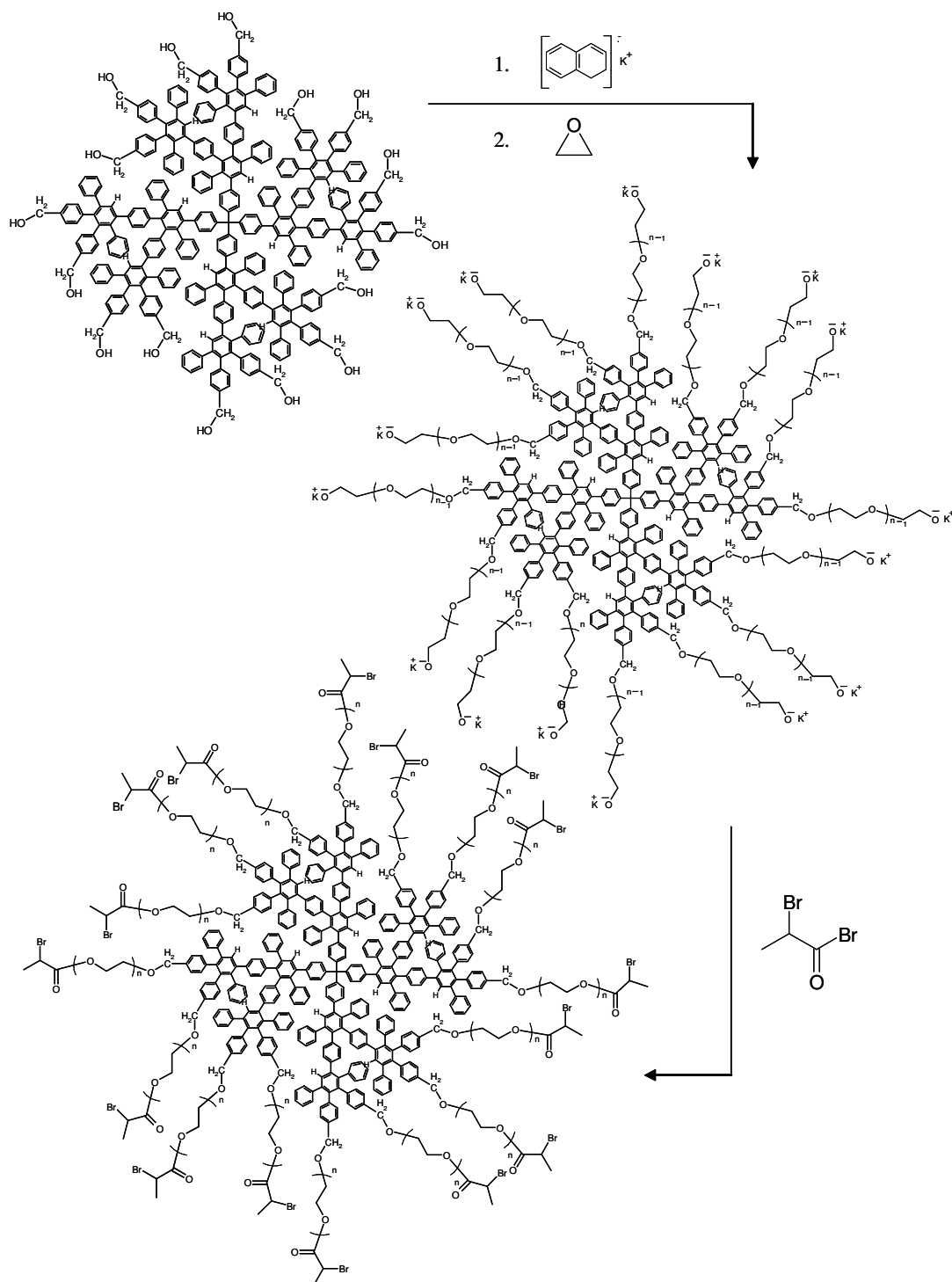
Within the approach aiming to obtain core-double-shell structures, we successfully applied the “grafting-onto” method. Since both “grafting-onto” and “grafting-from” methods succeed by the preparation of core-*mono*-shell structures, one could assume that the “grafting-from” approach can be applied for the synthesis of core-*double*-shell molecules as well. Moreover that “grafting-onto” method suffers from the shielding effect of grafted polymers, resulting in the incomplete conversion of the end terminating reaction. Thus, the “grafting-from” method is the only alternative in case of highly dense functional dendrimers. However, anionic polymerization of EO followed by styrene is limited due to the fact that alcoholates generated on the periphery of the dendrimers. These are relatively weak initiators that are not able to polymerize most of the vinyl monomers (*e.g.* styrene, isoprene, (meth)acrylates). Thus, the method is restricted to the monomers other than EO or propylene oxide and

the combination of monomers becomes very limited. In order to overcome this problem, a combination between anionic and radical polymerizations was required.

As it was already shown, subsequent polymerization of EO followed by styrene succeeds after functional end-capping of a living anionic end of PEO with 2-bromopropionyl bromide. The resulting end-bromofunctionalized poly(ethylene oxide) has been further used as an ATRP macroinitiator for polymerization of styrene in the presence of Cu(I)Br and complex forming ligand N-hexadeca-2-pyridylmethanimine. Moreover, this method was successfully applied to 1,4-dimethoxyphenylenepotassium, which is a difunctional anionic initiator mimicking the structure and functionalities of the dendrimer periphery and thus serves as a model compound for the application of the polymerization to the polyphenylene dendrimers possessing hydroxymethyl functional groups.

The reaction scheme is similar to that of the core-*mono*-shell macromolecules. At first EO was polymerized by a macromolecular initiator $\mathbf{TdG}_2(\mathbf{CH}_2\mathbf{O}^-)_{16}$ (see Scheme IV.5 in the section IV.5.2), followed by end-capping reaction between living anionic ends of the PEOs and 2-bromopropionyl bromide (see Scheme VI.9)

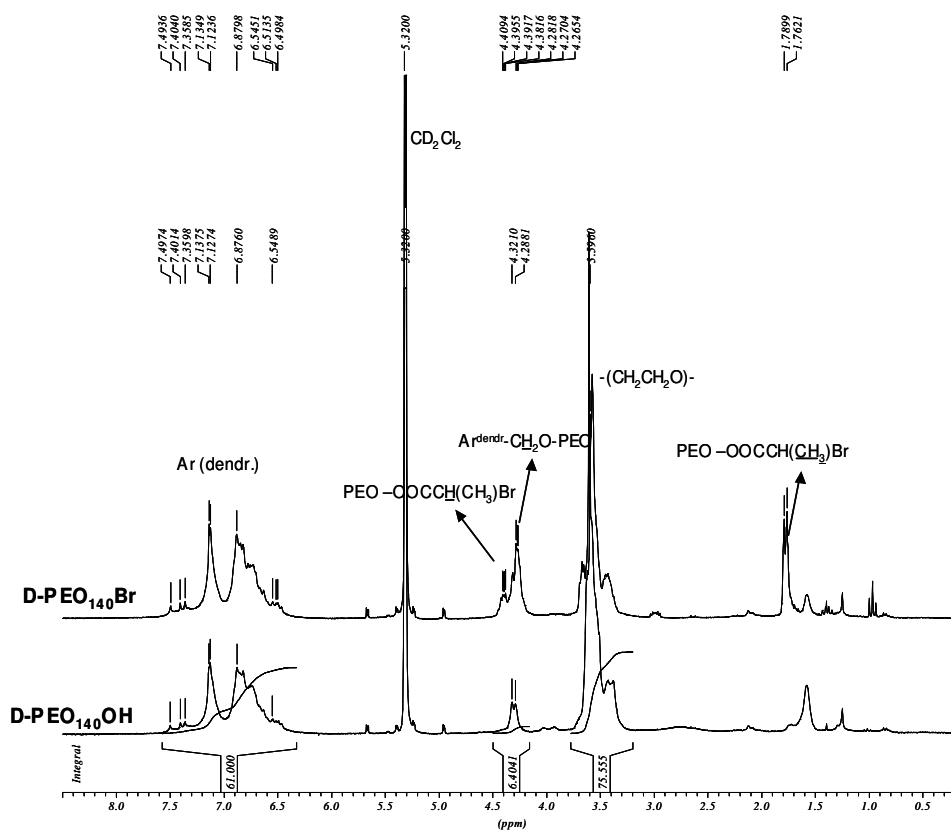
Scheme VI.9 Synthesis of core-shell ATRP macroinitiator.



The crude products were purified by sequential precipitation in hexane, cold acetone and cold methanol in order to remove the excess of 2-bromopropionyl bromide. The absence of traces of 2-bromopropionyl bromide is required for the next

step of the reaction (ATRP of styrene), where this substance can efficiently initiate polymerization of styrene and thus produce a homopolystyrene. Furthermore, the presence of 2-bromopropionyl bromide will hinder the determination of the completeness of the end-capping reaction by $^1\text{H-NMR}$ spectroscopy (see Figure VI.22)

Figure VI.22 $^1\text{H-NMR}$ spectra of **D-PEO₁₄₀OH** and **D-PEO₁₄₀Br**



The presence of the 2-bromopropionyl ester end-group was proven by the multiplet signal at 4.39ppm ($-\text{CH}(\text{CH}_3)\text{Br}$) and doublet at 1.77ppm ($-\text{CH}(\text{CH}_3)\text{Br}$) in the $^1\text{H-NMR}$ spectrum of **D-PEO₁₄₀Br** (“PEO₁₄₀” indicate $M_w(\text{PEO-arm})=140$). Unfortunately, both methine and methyl proton signals are partially overlapped with the signals of dendrimer and water respectively, and calculations concerning the degree of the bromo-functionalization failed.

However, molecular weights of **D-PEO₁₄₀Br** and **D-PEO₁₃₀₀Br** were determined by both $^1\text{H-NMR}$, comparing relative integrals of aromatic (belongs to dendrimer) and PEO protons and GPC (see Table VI.7). In the case of **D-PEO₁₄₀Br**

the values obtained by both methods are in a good agreement. However, in the case of **D-PEO₁₃₀₀Br** the molecular weight, calculated from the corresponding ¹H-NMR spectrum, was double in size than the one found by GPC. The difference (discussed already in section VI.4.1) due to the shape of the obtained core-shell molecules (globular), whereas the linear PEO standards were used for the calibration of the measurements.

Table VI.7 Molecular weights obtained by ¹H-NMR and GPC.

Exp No	¹ H-NMR	GPC	
	M _n	M _n	PDI
D-PEO₁₄₀Br	7 600	7 100	2.0
D-PEO₁₃₀₀Br	26 200	11 600	1.8

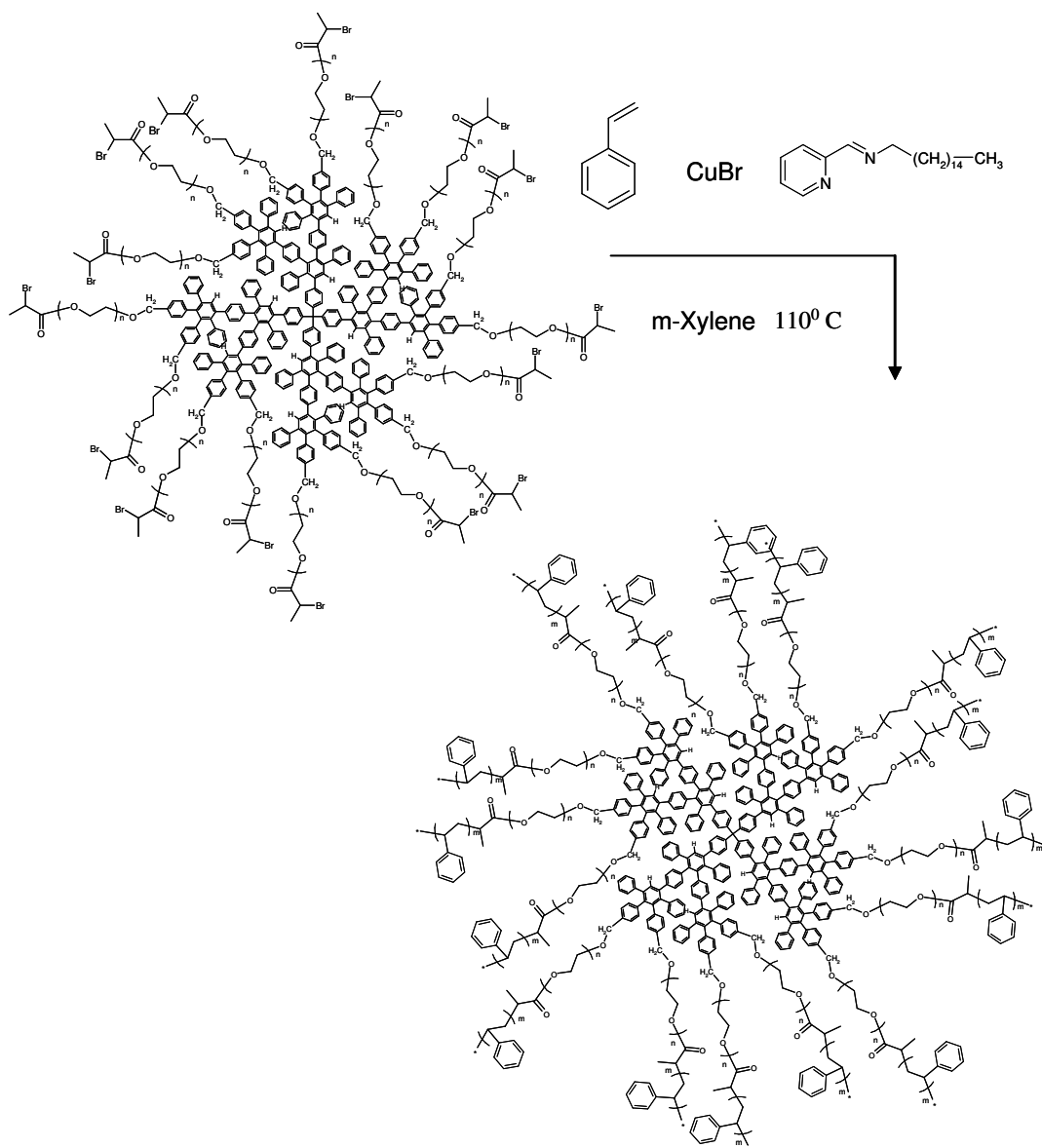
A relatively high polydispersity was observed and already contributed to the restricted solubility of the dendritic multi-anion initiator (see end of the section I.3.2). Additionally, the end-capping reaction with 2-bromopropionyl bromide can be accompanied by side reactions between both the ester group (A_N) and alkyl bromide and PEO living anionic ends. These side reactions can take place either as intra- or as intermolecular interaction, leading to products (oligomers or even networks of core-shell) possessing a much higher molecular weight.

VI.4.3 Synthesis of core-double-shell macromolecules. ATRP of styrene initiated from core-shell macroinitiator.

Reviewing the results in the model experiments (see section VI.4.2), and succeeded by preparation the ATRP macroinitiators **D-PEO₁₄₀Br** and **D-PEO₁₃₀₀Br** (see above) we aim to prepare well-defined core-double-shell nano-particles comprising of a stiff polyphenylene dendrimer as the core, flexible and hydrophilic PEO inner-shell and PS hydrophobic outer-shell.

The reaction scheme involves **D-PEO₁₄₀Br** or **D-PEO₁₃₀₀Br** as ATRP macroinitiators, Cu(I)Br and complex forming ligand N-hexadeca-2-pyridylmethanimine, and styrene as ATRP polymerisable monomer (see Scheme VI.10).

Scheme VI.10 Synthesis of core-double-shell macromolecules *via* ATRP of styrene using ATRP core-shell macroinitiators.



Detailed description of the polymerization mechanism was given in the section VI.4.1. It consists of formation of a complex between Cu(I)Br and nitrogen containing ligand (N-hexadeca-2-pyridylmethanimine) followed by homogeneous breaking of the Br-C bond (of the core-shell macroinitiator) and creating a free macro-radical. This macro-radical is able to polymerize styrene or reversibly accept the bromine radical from the Cu-complex and to transform a “dormant” state. Thus, the probability for termination reaction (chain-transfer or recombination) is kept low.

All attempts to polymerize styrene using such core-shell multi ATRP initiators failed. The products obtained by these initiator systems possessed multimodal molecular weight distribution proved by GPC and neglectable amounts of oligostyrenes determined by the corresponding signals in the $^1\text{H-NMR}$ spectra. Therefore, one could try to modify the initiator system in respect to both ligands and metal halide. A unique combination of initiator, metal, ligands, deactivator, temperature, reaction time, and solvent must be employed for the ATRP of each particular monomer. Therefore, understanding the role of each component of ATRP is crucial for obtaining well-defined polymers.

Summary and conclusions

A series of new core-*double*-shell macromolecules, consisting rigid, hydrophobic polyphenylene dendrimer as the core, soft and hydrophilic PEO inner shell and hydrophobic, rigid PS or flexible PI outer shell have been synthesized by deactivation of an anionic living block copolymers with a multifunctional dendrimeric electrophile. The molecular weights of the core-*double*-shell macromolecules and diblock copolymers were determined by $^1\text{H-NMR}$ spectroscopy, GPC and MALDI-TOF mass-spectrometry. The number of the diblock arms attached to the dendrimer molecule was found to increase with an increasing number of dendrimer functional groups and decrease with the length of the copolymer chains. Such dependences can be explained by steric hindrance between the attacking copolymer chains and the already grafted arms.

This is the disadvantage of the “*grafting-onto*” method. However, the problem was overcome within the “*grafting-from*” approach. On account of the fact, that sequential anionic polymerization of EO followed by styrene is infeasible due to the weakness of the alkoxyl anion, the use of a combination between anionic polymerization of PEO (by grafting from the dendrimer surface), and ATRP of styrene (utilizing the core-shell multi ATRP initiator) was required.

The hydrodynamic radii of the core-*double*-shell nano-particles were measured by Dynamic Light Scattering to be in the range of 4 to 7 nm. The influence of both the length and the number of arms (PPDs with different average number of

functionality were used - $\text{TdG}_2(\text{CH}_2\text{Cl})_{-12}$ and $\text{TdG}_2(\text{CH}_2\text{Cl})_{-8}$) on the hydrodynamic radius was investigated. Increasing either the length or the number of the arms and hence molecular weight of the core-*double*-shell system increases the R_h of the particles. Since DLS suffer from the even neglectable amounts of aggregates present in the system (see discussion in section IV.5.2), the investigations over the influence the media polarity over the conformational changes of the core-*double*-shell system were performed using a combination of surface topography characteristic method (AFM) and surface polarity characteristic method (contact angle) over thin layers of **D(PEO-PS)12**. Initially, the dense enough layers were prepared varying the concentration of **D(PEO-PS)12** from 0.001 to 1.0 g/L and observing the topographic smoothness of the surface by measuring root-mean-square roughness values. Additionally, the size of a single particle was found to be 15 nm, which is in a very good agreement with $R_h=7.3$ nm found by DLS.

The use of contact angle measurements over the thin layers of **D(PEO-PS)12** prepared by spin-coating of solutions differ in the solvent polarity, result in increase the contact angle with decrease the solvent polarity. The effect is attributed to the conformational change of the amphiphilic block copolymers with respect to the media polarity. It is supposed that in the case of more polar solvents the PEO block is better solved by the solvent and therefore dominate in the outer shell of the core-*double*-shell molecules, whereas polystyrene aggregates either by inter- or by intra-molecular manner.

Remarkably, a “*sandwich*” structure with a polar (hydrophilic) layer between two hydrophobic layers was obtained upon the polyphenylene dendrimers. Such materials may serve for example as dendritic box allowing for a selective loading of either polar compounds in the hydrophilic PEO-shell or non-polar – in both PS-shell and dendritic core. Additionally, a material with such a behavior can be useful as a drug delivery system, where the deliver should be soluble in both water and lipids (amphiphilics consist of non- or branched aliphatic chain(s) and phosphoholine-glycerol hydrophilic part, building a bilayer lipid membrane of the living cells), which allows the penetration across the cells membrane.

References.

1. Advincula, R. C., *J. Disp. Sci. Techn.*, **2003**, 24, 343.
2. Voit, B., *J. Polym. Sci., Polym. Chem.*, **2000**, 38, 2505.
3. Matthews, O. A.; Shipway, A. N.; Stoddart, J. F. *Prog. Polym. Sci.* **1998**, 23, 1
4. Roovers, J. Comanita, B. *Adv. Polym. Sci.* **1999**, 142, 179.
5. Tomalia, D. A.; Huang, B.; Swanson, D. R.; Brothers II, H. M.; Klimash, J. W. *Tetrahedron*, **2003**, 59, 3799.
6. Hedrick, J. L.; Trollsås, M.; Hawker, C. J.; Atthoff, B.; Claesson, H.; Heise, A.; Miller, R. D.; Mecerreyes, D.; Jérôme, R.; Dubois, Ph. *Macromolecules* **1998**, 31, 8691.
7. Avgeropoulos, A.; Poulos, Y.; Hadjichristidis, N. *Macromolecules* **1996**, 29, 6076.
8. Roovers, J. *Macromolecules* **1994**, 27, 5359.
9. Xu, H.; Erhardt, R.; Abetz, V.; Müller A.H.E.; Goedel W.A. *Langmuir*. **2001**, 17, 6787
10. Webster, O.W. *Science* **1991**, 251, 887.
11. Riess, G.; Hurtez, G.; Bahadur, P. in *Encyclopedia of Polymer Science and Engineering*, 2nd ed.; Kroschwitz, J. I., Ed.; Wiley Interscience: New York, **1985**; 2, 324.
12. Tuzar, Z.; Kratochvil, P. *Adv. Colloid Interface Sci.* **1976**, 6, 201.
13. Riess, G.; Rogez, D. *Am. Chem. Soc. Polym. Prepr.* **1982**, 23, 19.
14. Barker, M.C.; Vincent, B. *Colloids Surf.* **1984**, 8, 297.
15. Zhao, C.L.; Winnik, M.A.; Riess, G.; Croucher, M.D. *Langmuir* **1990**, 6, 514.
16. Xu, R.; Winnik, M.A.; Hallet, F.R.; Riess, G.; Croucher, M.D. *Macromolecules* **1991**, 24, 87.
17. Wilhem, M.; Zhao, C.L.; Wang, Y.; Xu, R.; Winnik, M.A.; Mura, J.L.; Riess, G.; Croucher, M.D. *Macromolecules* **1991**, 24, 1033.
18. Kahn, T.N.; Mobbs, R.H.; Price, C.; Quintana, J.R.; Stubbsfield, R.B. *Eur. Polym. J.* **1987**, 23, 191.
19. Kazanskii, K.S.; Solovyanov, A.A.; Eutelis, S.G. *Eur. Polym. J.* **1971**, 7, 1421.
20. Esswein, B.; Moeller, M. *Angew. Chem., Int. Ed. Engl.* **1996**, 35, 623
21. Eßwein, B.; Molenberg, A.; Moeller, M. *Macromol. Symp.* **1996**, 107, 331.

22. Quirk, R.P.; Kim, J.; Kausch, Ch.; Chun, M. *Polym. Int.* **1996**, 39, 3.
23. Nielen, M. W. F. *Mass Spectr. Rev.* **1999**, 18, 309.
24. Przybilla, L.; Francke, V.; Raeder, H. J.; Muellen, K. *Macromolecules*, **2001**, 34, 4401.
25. Berlinova, I.V.; Vladimirov, N.G.; Panayotov, I.M. *Macromol. Chem., Rapid Commun.* **1989**, 10, 163.
26. Räder, H.J.; Schrepp, W. *Acta Polym.* **1998**, 49,272.
27. Fetters J.E. Chapter "Synthesis and Characterization of Block Polymers via Anionic Polymerization" Meier, D. J., editor "Block Copolymers: Science and Technology" *MMI Press Symposium Series* **1979**, 3, 17.
28. Worsfold, D.J. *J. Polym. Sci., Part A: Polym. Chem.* **1983**, 21, 2237.
29. Hadjichristidis, N.; Pispas, S.; Pitsikalis, M. *Prog. Polym. Sci.* **1999**, 24, 875.
30. Hillmyer, M. A.; Bates, F. S. *Macromolecules* **1996**, 29, 6994.
31. Allgaier, J.; Poppe, A.; Willner, L.; Richter, D. *Macromolecules* **1997**, 30, 1582.
32. Boileau, A. *C. S. Symp. Ser.* **1981**, 166.
33. Foester, S; Kraemer, E. *Macromolecules* 1999, **32**, 2783.
34. Worsfold, D.J.; Bywater, S. *Can. J. Chem.* **1960**, 38, 1891.
35. Atanasov, V; Sinigersky V.; Klapper M.; Muellen K. *Macromolecules* **2005**, 38, 1672.
36. Klapper, M.;Wehrmeister, T.; Mullen, K. *Macromolecules*, **1996**, 29, 5805.
37. Räder, H.J.; Schrepp, W. *Acta Polym.* **1998**, 49,272.
38. Wiesler, U.-M. *Ph.D. Thesis*, Johannes Gutenberg University – Mainz, Germany **2000**.
39. Marek, T.; Suvegh, K.; Vertes, A.; Ernst, A.; Bauer, R.; Weil, T.; Wiesler, U.-M.; Klapper, M.; Muellen K. *Radiation Physics & Chemistry.* **2003**, 67, 325.
40. T. Song, S. Dai, K. C. Tam, S. Y. Lee, S. H. Goh *Langmuir* **2003**, 19, 4798.
41. Jankova, K.; Chen, X.; Kops, J.; Batsberg, W. *Macromolecules* **1998**, 31, 538.
42. Wang, J.-S.; Matyjaszewski, K. *J. Am. Chem. Soc.* **1995**, 117, 5614.
43. Kata, M.; Kamigaito, M.; Sawamoto, M.; Higashimura, T. *Macromolecules* **1995**, 28, 1721.

Chapter VII

APPLICATIONS OF CORE-SHELL SYSTEMS

VII.1 Core-Shell Systems - applications as metallocene supports in heterogeneous olefin polymerization

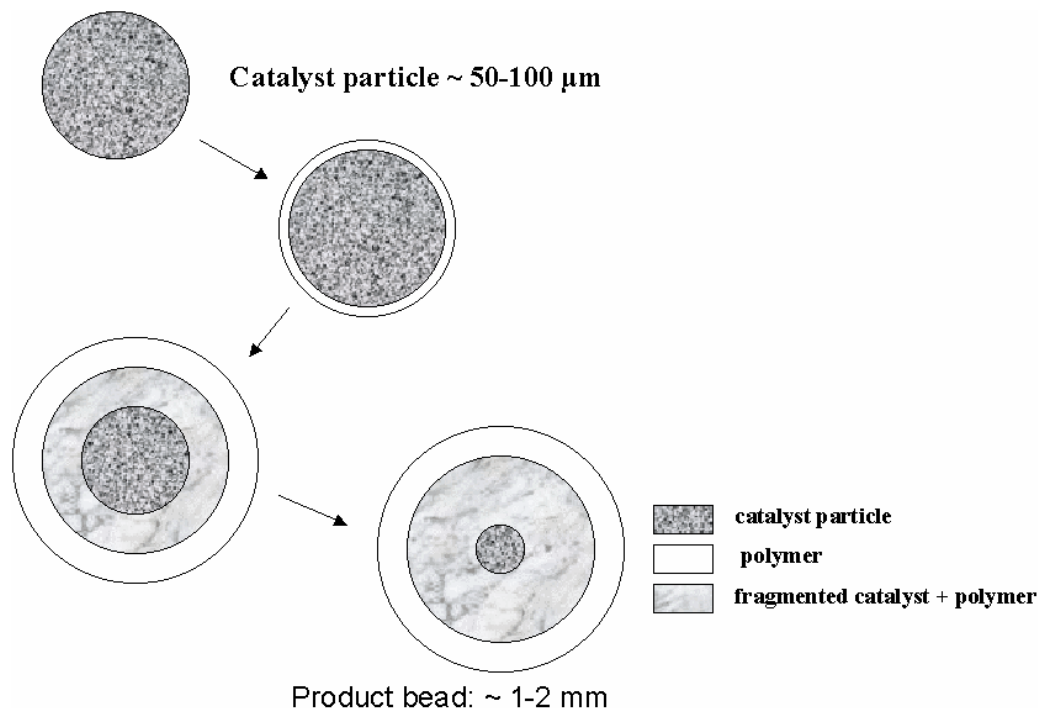
Core-shell nanoparticles consisting of shape-persistent polyphenylene dendrimers as a core and PEO chains as a shell, were used as supports for metallocene based catalysts in heterogeneous polymerizations of ethene and co-polymerizations of ethene with 1-hexene. The investigation of catalyst fragmentation in olefin polymerization was done by Dr. N. Nenov. [1]

VII.1.1 Introduction

In heterogeneous olefin polymerization using supported „single-site“ metallocene catalysts, the fragmentation process of the used catalyst support is of utmost significance for the quality of the polyolefins obtained[2][3]. The fragmentation represents the distribution of the catalyst within the formed polymer during olefin polymerization down to the size of the primary particles of the support. The good support distribution in the polymerization process, makes even the most inner active sites of the catalyst particle easy reachable for fresh monomer. The reaction starts from the most outer parts of the catalyst unit, and their smooth and fast fragmentation lead to easier further diffusion of the monomer gas to the inner active sites. In this way all active species of the catalyst are involved in the polymerization process. The support particles will be homogeneously distributed into the obtained polyolefin beads, not influencing the qualities of the product obtained (for example big scattering centers in a polyolefin film). A huge number of investigations, mainly on inorganic carriers, have been performed in this field in order to better understand the catalyst behavior under different polymerization conditions and therefore to improve the fragmentation reactions[4].

The model of fragmentation for silica-supported catalysts proposed by Fink et al. [4] and illustrated in scheme VII.1 clearly shows the process of catalyst distribution.

Scheme VII.1. Model of fragmentation for silica supported catalyst.



In order to achieve uniform distribution of the catalyst into the polyolefin, resulting in excellent morphology of the obtained products, the carrier particles size as well as their size distribution should be as small as possible. Control of the secondary particles (after loading of the carrier) is also necessary. As the zirconocene/methylalumoxane (MAO) complexes, used as initiators in olefin polymerization exhibit cationic character, it is appropriate to immobilize them noncovalently on organic supports, which carry nucleophilic groups containing oxygen. Recently carrier materials have been developed based on polystyrenes nanoparticles, crosslinked with divinylbenzene and either functionalized covalently by PEO-chains [5], or simply prepared without any functionalization by using polystyrene-polyethylene oxide block co-polymers as surfactants [6].

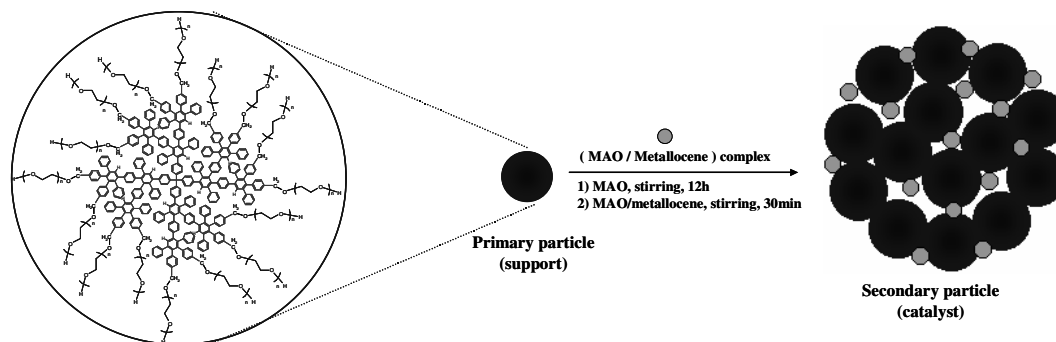
From the scientific point of view, it was tempting to study the quality of the polyolefins prepared with catalyst systems, based on carriers that have a size of one order of magnitude smaller than the previously used organic supports from the above mentioned nanoparticles. The best possible way for realizing such a concept would be the use of functionalized shape-persistent polyphenylene dendrimers.

VII.1.2 Applications of the core-shell systems as carriers for metallocene based catalysts and their use as model compounds for heterogeneous olefin polymerization.

In light of the above, it can be seen that the core-shell systems based on functionalized dendrimers (rigid core) and soft PEO shell, behave as perfect organic carriers for non-covalent immobilization of metallocene/MAO complexes. The core-shells **4.17** and **4.18** (prepared by the “grafting-from” method – see section IV.5.2), exhibit well-defined PPD as the core and PEO as the shell, were used.

In order to prepare catalyst utilizing those core-shell systems as support, the core-shells were firstly reversibly crosslinked by the interactions of MAO with the nucleophilic PEO chains, then loaded with the metallocene/MAO complexes and directly used in the olefin polymerization (scheme VII.2).

Scheme VII.2. Immobilization of the metallocene/MAO complexes on the carrier:



By this method, it was proposed (bearing in mind the investigations on fragmentation of functionalized nanoparticles supported catalyst) the desired homogeneous catalyst fragmentation during the polymerization process could be achieved, resulting in polymer products with better morphology.

VII.1.2.1 Polymerization of ethene.

Two series of experiments have been performed. Activated catalytic systems based on core-shells **4.17** and **4.18** (see Chapter IV) were used for this purpose. All catalysts were prepared using $\text{Me}_2\text{Si}(\text{2MeBenzInd})_2\text{ZrCl}_2$ (Dimethylsilyl-2-

Methylbenzylindenyl Zirconocene) as zirconocene and methylalumoxane (MAO) as co-catalyst in different ratios.

The results from the experiments of polymerization of ethene using different activated catalytical systems based on core-shell systems are presented in Tables VII.1 and VII.2.

Table VII.1. Characteristics of the prepared catalyst systems using core-shell system **4.17** and **4.18** as supports.

Exp No	[Zr] ($\mu\text{mol/g}$)	MAO / Zr	Activity (kg PE/mol Zr h)	Productivity (g PE/g cat h)	Bulk Density (g / L)
4.18 (1)	54	300	37 000	1500	400
4.18 (2)	48	300	36 000	1500	380
4.18 (3)	37	400	36 000	1300	300
4.18 (4)	25	600	30 000	800	250
4.17 (1)	54	300	40 000	1700	370
4.17 (2)	37	400	38 000	1500	300

Polymerization conditions: 400ml isobutene; 37 bar ethene pressure, 60 min.; 70°C; TIBA (scavenger) = 5ml

Table VII.2. Characteristics of the obtained polyethylene products using catalytic system based on core-shell systems **4.17** and **4.18**:

Exp No	T_m (°C)	M_n	M_w	PDI
4.18 (1)	133.4	580 000	1 380 000	2.5
4.18 (2)	133.6	550 000	1 480 000	2.7
4.18 (3)	132.3	400 000	1 200 000	2.9
4.18 (4)	132.2	520 000	1 350 000	2.6
4.17 (1)	133.2	540 000	1 200 000	2.5
4.17 (2)	133.6	510 000	1 120 000	2.7

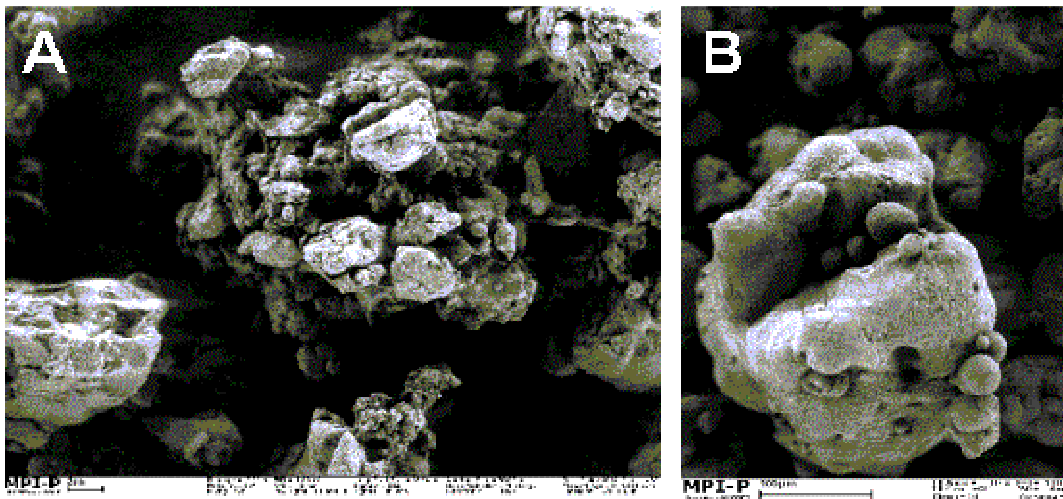
The two core-shell systems used differ only in the length of the PEO arms (see Chapter IV). The PEO chains act as „anchors“ in the supporting process of metallocene/MAO species, immobilizing those active sites non-covalently by their

nucleophilic groups. In all polymerizations performed with the so obtained catalysts, no reactor fouling was observed. Bearing this in mind it was proposed that the metallocene/MAO complexes are completely immobilized on the carrier. No leaching of the active catalyst sites from the carrier occurred, therefore no homogeneous polymerization was observed. The PEO chains of **4.18** are about 3 times longer than those of **4.17** (calculated from the $^1\text{H-NMR}$ data). That however has a very minor influence on the activity and productivity of the catalysts. Even the shorter PEO arms are nucleophilic enough to completely immobilize the active catalyst species.

The activities and productivities of the catalyst systems used are roughly similar to the nanoparticles supports described in the literature[5]. On the other hand, comparing the catalyst characteristics of catalyst systems based on simple PEO functionalized polystyrene as carriers [7], or catalysts supported on SiO_2 [8] the parameters of the systems presented here are better. This mostly due to the relatively small size and narrow size distribution of the particles, guaranties the larger surface area, more homogeneous catalyst distribution and better permeability of the incoming monomer through the primary particle support. All these factors play a crucial role over the activities and productivities of the catalyst system.[6] Moreover, the molecular weights and melting points of the products retain in the same range or are even higher than those obtained by systems supported on PEO-functionalized nanoparticles or polystyrene resins [9,10]. Thus, the obtained polymer does not lose its characteristics because of the increased catalyst activity and leads to higher productivity.

In all experiments performed, using both support systems in homopolymerization of ethene, the polyethylene products were obtained as defined uniform beads with diameters about 0.2 mm. Scanning electronic microscopy pictures of the catalyst particles and obtained polyethene beads are shown on Figure VII.1

Figure VII.1. SEM images of: (A) catalyst particle (see Exp 4.18 (1), Table VII.1); (B) single polyethene particle (Exp 4.17 (1), Table VII.1).



From the SEM pictures it can be seen that the shape of the polyethene beads corresponds exactly to the shape of the starting catalytic particle, its size being reproduced on a several orders of magnitude larger scale. It was supposed, that the fragmentation process of the catalyst into the polymer products will follow the already established „shell by shell“ process of fragmentation considered for silica supports (Scheme VII.1) [4]. Following the investigations over the catalyst kinetics and the fragmentation studies of the nanoparticles supported metallocene catalysts [11], this model was considered for the here presented catalyst systems also as the most appropriate one.

It was demonstrated that the catalyst systems prepared using the core-shell particles as supports for metallocene catalysts in heterogeneous olefin polymerization, polymerize ethene with activities and productivities exceed those of catalysts supported on SiO₂, [8] and that the polyethene products obtained possess high molecular weights, low polydispersities and high bulk densities. This proves the excellent properties of the core-shell systems as supports for metallocene catalysts and their use for further investigations of catalyst fragmentation and their influence on the properties of the polyolefins obtained.

VII.1.2.2 Copolymerization of ethene with 1-hexene.

Copolymers of ethene with 1-hexene have considerable industrial potential,[12] due to lower melting points and lower molecular weights than ethylene homopolymers. Catalysts used for the co-polymerization of ethene or propene with higher α -olefins, show much higher activities and productivities than in homopolymerization reactions [13]. This can be explained by the increased number of active sites during polymerization and improved diffusion due to the decrease of crystallinity [14].

In the present section catalyst systems based on core-shell particles **4.18** have been investigated as support of metallocene catalyst for the copolymerization of ethene with 1-hexene. The results obtained are presented in Tables VII.5 and VII.6.

Table VII.5. Characteristics of the used catalyst system based on core-shell particles **4.18** by using different comonomer concentrations.

Exp No	1-Hexene (ml)	Ethene consumption (L)	Activity (kg PE/mol Zr h)	Productivity (g PE/g cat h)
1	30	19.76	59 000	2090
2	40	21.33	63 000	2500
3	50	24.33	67 000	2600
4	60	46.00	61 000	2450

Polymerization conditions: Cat = 25mg; [Zr] = 54 μ mol/g ; MAO / Zr = 300 ; Ethene = 37 bar;

T = 70°C; t = 60min; TIBA (scavenger) = 5ml

Table VII.6. Characteristics of the obtained ethane-1-hexene co-polymers using the catalyst system based on core-shell particles **4.18** by using different co-monomer concentrations:

Exp No	T _m (°C)	M _n	M _w	PDI	1-Hexene ^(a) Incorporation (%)
1	102.3	250 000	690 000	2.7	3.8
2	100.2	198 000	590 000	2.9	6.4
3	98.7	205 000	590 000	2.8	6.9
4	99.3	220 000	630 000	2.8	5.8

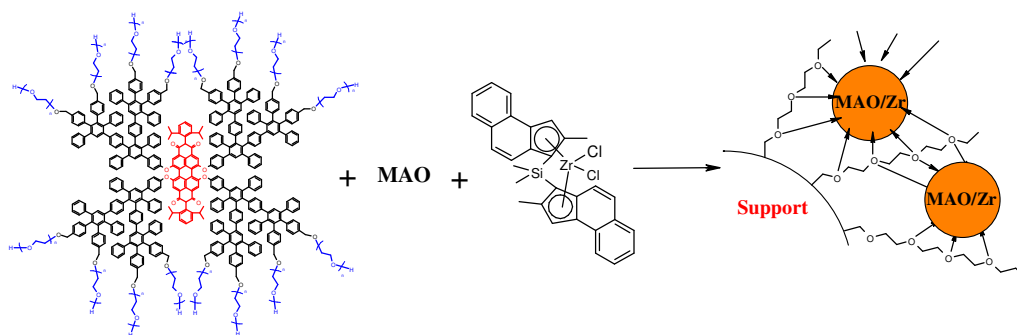
(a) 1-Hexene incorporation has been determined by ¹³C NMR spectra in C₂D₂Cl₄

Increasing the comonomer concentration in the reactor increases the activities and productivities of the catalyst, giving co-polymers with higher comonomer incorporation and lower melting points. However at very high comonomer concentrations (run 4) the activities and productivities of the catalytic systems started to decrease slowly. At such high concentrations, the local polymerization temperature in every catalyst particle during the formation of the co-polymer chains is very high which leads to melting of the support around the inner active sites. These sites are thus covered with a thick film of the melted support, which practically stops the monomer diffusion. Compared to the co-polymerizations performed by catalysts on nanoparticles or simple functionalized polystyrene carriers, the values of co-monomer incorporation are in the same range or even slightly higher [1]. The comonomer concentration increases the catalyst activity and therefore the local temperature at each forming polymer particle. As the co-polymer products obtained have lower melting points than that of ethene homopolymers, and due to their higher solubility in the polymerization medium, in all co-polymerizations the products were obtained where the polymer beads were melted together in a rubber like material. However, it was easy to locate the single product particles indicating for morphology control of the catalysts used.

VII.2. Core-shell macromolecules bearing a chromophore at the focal point - applications as metallocene supports in heterogeneous olefin polymerization. Fragmentation study.

The following study was performed by my colleague Dr. Yong-Jun Jang in order to investigate the influence the particle size of the support on the catalyst features in the olefin polymerization. The idea is to use a fluorescent labeled support, which makes it possible to investigate the fragmentation process in terms of dynamical diffusion of the support into the polymer (the related techniques are recording with high resolution CCD cameras or laser scanning confocal fluorescent microscopy). Thus, the distribution of the support molecules during the polymerization time can be recorded and analyzed. An appropriate support for the proposed investigation was the core-shell system bearing a chromophore in the focal point (see product **5.3** in Chapter V). Considering the size (up to 30 nm) of the fragmented particles, no catalyst systems based on organic carriers that can undergo such fine fragmentation and uniform distribution in olefin polymerization reactions have been used until now. After immobilization of the active zirconocene/MAO complexes on the prepared nanoparticles, the catalyst systems would be then used for heterogeneous polymerization of olefins (see Scheme VII.3).

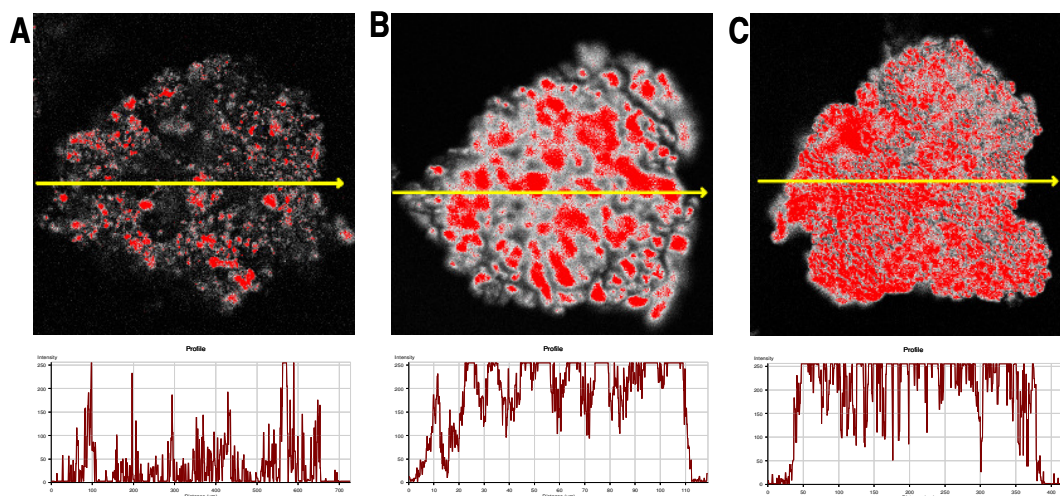
Scheme VII.3. The preparation of supported catalyst on the polyethyleneoxide (PEO) functionalized dendrimer with perylene dye (**5.3**)



The fluorescence microscopy images of the polyethylene (PE) particle obtained utilizing core-shell supported metallocene catalyst (Figure VII.5) display the dense red-colored catalyst dispersed in the whole PE particle. The profile of perylene dye explains how dense the dye is, with respect to the support molecules, in the PE

particle (slice A). The fluorescence images of the dye distribution in PE beads after 1, 10 and 30 min polymerization indicate that molecules of the support are initially aggregated (slice A), but well dispersed after relatively short time period - 10 min (slice B) and homogeneously distributed into PE beads after 30 min (slice C). The profile of the dye intensity in PE represents the concentration of dye in the polymer beads, decreasing in time – proving the catalyst is homogeneously spread into the PE particle.

Figure VII.5. Laser scanning confocal fluorescence image of PE: (A) 1 min, (B) 10 min and (C) 30 min polymerization time.



It had been shown that the organic supports based on latex particles undergo a fragmentation according to the multi-grain model [15] which is established for Ziegler-type catalysts supported on $MgCl_2$. [16] Also according to the confocal fluorescence measurements of PPD based dendrimers which are half of a magnitude smaller than the latex-particles a similar model for the fragmentation can be assumed.

The investigation of the fluorescence distribution of a catalyst based on dendrimer **5.3** led to a very homogeneous distribution of the catalyst particles already at a very early stage of the polymerization. Comparing these results with the fragmentation process of the aggregated latex particles, where one observes still unfragmented parts after 15 min of polymerization [17], the fragmentation of the dendrimers seems to be much more homogeneous. In parallel both, the activity and the bulk density using the supports **4.17** and **4.18** (see section VII.1.2.1) are very high. This is very unusual as from previous work it is known that with increasing activity

the bulk density drops drastically.[18] This was attributed to a too weak cross-linking resulting in a too fast fragmentation of the supports and as a result in fluffy polyolefin powders. It seems that in the case of PEO functionalized dendrimers an optimized ratio between activity and reversibility of the cross-linking has been found. Therefore one may conclude that dendrimers due to their homogeneous fragmentation are very suitable supports for metallocene catalysts. However due to their high costs they can serve only as model compounds for the latex based systems.

VII.3. Application of core-shell macromolecules bearing chromophore as drug delivery assays targeting the Blood Brain Barrier

My colleague Dr. Georgy Mihov tested a number of dendritic molecules for drug delivery and for transfer through the Blood Brain Barrier (BBB). The dendrimer-polymer core-shell molecules possessing PEO as a shell (ensures water solubility as well as bio-compatibility) and dendrimer as a core (hydrophobic reservoir) with covalently attached chromophore dye which enables direct monitoring of the delivery process.

In general dendrimers are promising drug delivery systems because of their nanometer size range their ability to bear multiple copies of surface groups for biological recognition processes and loading with drug molecules in the interior of the dendrimers as well as attached to surface groups. All that makes dendrimers attractive candidates for the transfer of small molecules through the BBB since they combine structural perfection with the ease of introducing a wide range of surface functionalities as well as the presence of large cavities in their interior which are accessible to guest molecules. Since *in vivo* applications require a high metabolic stability of the host molecule as well as low toxicity of the latter, the inert polyphenylene dendrimers should be particularly suited for such applications. Furthermore, *in vivo* studies have shown that polyphenylene dendrimers display no toxicity.

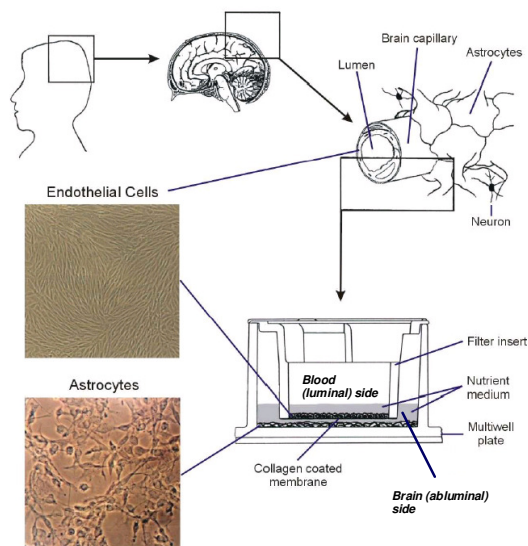
The reasons for selecting core-shell molecules bearing dye in a focal point are presented in Table VII.8.

Table VII.8. Core-shell used for drug delivery assays

Description	Remarks
PDIG ₂ (PEO ₁₇₀) ₁₆ product 5.3	<ul style="list-style-type: none"> • Chromophores for UV and Fluorescence - easy detection • Water soluble, thanks to PEO chains • PEO is immunologically scilent and biocompatible • Size (DLS and FCS) about 17 nm • Core-shell structure – expected to solubilize drugs

The principle of operation of the transport cell used for these experiments is present at Figure VII.6. It was designed by Merz Parmaceuticals who also did the transport experiments. The detection of the transport across the BBB was done in MPI employing analytical HPLC. Figure VII.6 demonstrates the integrity of the BBB. Transport studies are performed using the *in vitro* standard drugs insulin and sucrose which do not pass the BBB *in vivo*.

Figure VII.6 Schematic representation of the *in-vivo* BBB and it *in-vitro* model provided by Merz Parmaceuticals.



The registration and detection of the compounds that have passed across the model BBB (*in vitro* BBB) was performed by means of analytical HPLC. Controlled amounts of the compound of interest were dissolved in 0.5 ml ultra pure water and passed through a RP-HPLC column (Resource RPC with a volume of 3 mL). The core-*mono*-shell system (**5.3**) was eluted with a mixture of 50% acetonitrile and 50% 2-propanol. The flow rate was 1.5 mL/min. The area of the detected peak was calculated for each concentration. For the detection of the core-shell, one relies on the UV-VIS absorption of the core (absorption maximum at 520 nm).

In the particular case under these experimental conditions the selected core-shell macromolecules did not cross the BBB. This compound cannot be detected on the abluminal side on the model BBB. One possible reason is the relatively large size of the compound. However, similar core-shell systems based on PPD possessing pentylsine and cholesterol in external shell succeed and gave the hope for realization of core-shell architectures based on PPD. [19]

Summary and conclusions

For the first time, a supporting system based on core-shell nanoparticles comprising a stiff core, forms stable dendritic polyphenylene core and soft PEO shell has been developed. The catalyst systems prepared with this support exhibit high activities and productivities in producing polymers with high molecular weights, high bulk densities and low dispersities. The small size of the particles (~40 nm) and the narrow size distribution lead to completely homogeneous fragmentation of the catalyst back to the nanometer size of the carrier giving polyolefins with excellent qualities. The results indicate that such catalyst systems could be very useful as model compounds for further investigations on the catalyst fragmentation and its influence on the product parameters.

The investigation over the fragmentation process was done by utilizing a fluorescent-labeled core-shell support. The fluorescence activity of the support allowed monitoring its distribution with the time by confocal fluorescence microscopy and thus defining the mechanism of the fragmentation. Additionally, the most appropriate polymerization conditions were explored in order to achieve a catalyst

system possessing much higher activity and productivity than those used up to now (organic (latexes, PS beads) and inorganic (SiO_2) carriers) producing polymers with excellent characteristics (high bulk densities).

Finally, the core-shell molecules were tested for drug deliveries. Either, the results were negative, it is extremely important to investigate the influence between the structure (in a chemical and physical means) and biological recognition processes.

References

1. N. Nenov, Ph.D. Thesis, **2003**, Johannes Gutenberg University – Mainz, Germany
2. Fink G, Tesche B, Korber F, Knoke S, *Macromol. Symp.*, **2001**, 173, 77.
3. Fink G, Steinmetz B, Zechlin J, Przybyla C, Tesche B, *Chem Rev*, **2000**, 100, 1377.
4. B. Steinmetz, B. Tesche, C. Przybyla, J. Zechlin, G. Fink, *Acta Polymer.*, **1997**, 48, 392.
5. M. Klapper, M Koch, M. Stork, N. Nenov, K. Müllen, „Organometallic catalysts and Olefin Polymerization“, Blom R et al ed., **2001**, 387.
6. Nenov N, Klapper M, Muellen K, Fink G, „ Kinetic studies on heterogeneous polymer supported metallocene catalysts for olefin polymerisation“, *in preparation*
7. A. Heise, C. Nguyen, R. Malek, J. L. Hedrick, C. W. Frank, R. D. Miller, *Macromolecules*, **2000**, 33, 2346.
8. T. Nemnich, Diploma Thesis, Fach Hochschule „Fresenius“ – Wiesbaden, Germany, **2000**
9. M. Koch, M. Stork, M. Klapper, K. Müllen, *Macromolecules*, **2000**, 33, 7713.
10. N. Nenov, M. Koch, M. Klapper, K. Müllen, *Pol. Bull.*, **2002**, 47, 391.
11. M. Koch, A. Falcou., N. Nenov, M. Klapper, K. Müllen, *Macromol Rapid Comm*, **2001**, 22 (17), 1455.
12. Ray G., Spanswick J, Knox J, Serres C, *Macromol*, **1981**, 14, 13223.
13. Koivumaki J, Seppala J, *Macromol*, **1993**, 26, 21.
14. N. Herfert, P. Montag, G. Fink, *Makromol. Chem.*, **1993**, 194, 3167
15. Yong-Jun Jang, Corinna Naundorf, Markus Klapper *, Klaus Müllen, *Macromolecular Chemistry and Physics*, Volume 206, Issue 20 , 2027.
16. Y. I. Yermkov, V. Zakharov, *Adv. Catal.* **1975**, 24, 173.
17. M. Klapper, C. Naundorf, Y. J. Jang, G. Fink, K. Müllen, *e-Polymers* **2005**, 13
18. M. Klapper, Y. J. Jang, N. Nenov, K. Bieber, T. Nemnich, K. Müllen, *Macromol. Sym.* **2004**, 213, 131.
19. G. Mihov, Ph.D. Thesis, **2004**, Johannes Gutenberg University – Mainz, Germany

Chapter VIII

NEW APPROACHES IN THE SYNTHESIS OF BLOCK COPOLYMERS

The block copolymers described in the present chapter, being apart from the main topic of the current work, were exclusively new investigation concerning synthetic conditions (see first section – polymerization in magnetic field) and molecular content (see section VIII.3 - block copolymers bearing dye in the junction point).

VIII.1. Polymerization in a magnetic field. Theoretical background.

Most organic and inorganic polymeric materials are diamagnetic. The intensity of the response (induced magnetization) is more than six orders of magnitude smaller than the magnetization developed in ferromagnetic materials. The most important magnetic field effects on purely diamagnetic molecules are magnetic orientation and concentration. This is a result of the anisotropic diamagnetic susceptibility of the molecules in general. Uniform magnetic fields tend to align molecules, and the degree of orientation is determined by the Boltzmann factor: $\exp(-\Delta\chi_m H^2/2RT)$; where $\Delta\chi$ is the diamagnetic anisotropy and H is the magnetic field.

It is known that reaction rates and efficiencies depend not only on energetic factors but also on entropic factors. The rate is given by $k = Ae^{-\Delta E/RT}$ according to the Arrhenius formulation. Magnetic effects upon the A factor can be observed if states that possess different magnetic properties (i.e. triplet states and singlet states) are involved in a rate determining step whose rate constant is given by k [1].

Concerning magnetic effects on the chemistry of radical pairs, there are some fundamental postulates that must be taken into account, namely [1]:

1. when the bond connecting two groups (R1–R2) undergoes homolytic cleavage, the primary radical pair R1 R2 is produced with complete conservation of spin;
2. singlet radical pairs can undergo “cage” reactions such as recombination and disproportionation, but triplet radical pairs cannot undergo cage reactions directly. They must first intersystem cross to singlet radical pairs;

3. the chemical reactivity of a radical pair depends on the hyperfine interactions of the orbitally uncoupled electrons of the radical pair with nuclear spins or an external magnetic field.

The strength of a continuous external magnetic field can lead to magnetic-field-dependent chemical yields and kinetics for the processes. The application of a strong external magnetic field to a radical pair determines the “splitting” of T_+ and T_- from T_0 , however T_0 and S remain degenerate. The interconversions of $T_{\pm} \leftrightarrow S$ are slowed down and only $T_0 \leftrightarrow S$ transitions remain probable. In this way, because the lifetime of correlated pairs is dependent on the magnetic field, the kinetics and conversion of the chemical process rely on the field intensity.

The fundamental articles of Steiner specify the main requirement for magnetically sensitive reactions, namely the existence of intermediates with one unpaired electron spin [2].

Reactions involving carbon radical pairs, including polymerization reactions, are a category for which electron and nuclear spins are not conserved. This leads to some unusual phenomena including chemically induced nuclear polarization (CIDNP), magnetic spin isotope effects and magnetic field effects on chemical reactions [1]. The radical species determine the subsequent evolution of the polymerization processes. Consequently, the reactions are influenced by the existence of an external continuous magnetic field and therefore magneto-kinetic effects are exhibited.

VIII.2. Effect of high magnetic field upon the decomposition reaction of a radical macroinitiator

VIII.2.1. Introduction

Grafting reactions and block copolymerizations provide the potential for significant modifications of the macromolecular and organo-chemical properties of the substrate material. In this section, stress is generally laid on improving the chemical, hydrophobic, hydrophilic, thermoplastic properties without significantly altering others. The difficulties that appear during the grafting reactions or block copolymerization are

due to the monomer sensitivity, which leads to homo-polymerization and irreproducibility.

An increased efficiency of the polymerization process from the viewpoint of the minimizing of concurrent homo-polymer formation can be achieved through the performance of the reactions in a continuous magnetic field (MF).[3-5]

In the presence of a MF of 12-kG the graft copolymerization of isoprene onto tetrafluoro-ethylene-propylene copolymer, was realized. The grafting reaction of methylmethacrylate onto polyvinylalcohol in a continuous MF was also performed using UV-radiation and benzophenone as catalyst.[6] At the same time, the grafted copolymers obtained under MF showed improved moisture and heat resistance. This has been attributed to the increased graft ratio and greater stereoregularity of the copolymers obtained under the field.

In order to obtain supplementary evidences regarding to influence of the MF in the reactions of polymerization, the behavior of poly(styrene) macro-initiator (PSt*) in a high field of 7 T was studied in the present study. In this context the copolymerization of MMA onto poly(styrene) anionic pre-formed and functionalized as macro-initiator with 4,4'-azobis (4-cyanopentanoyl chloride) have been studied.

It was expected that the MF effect would be shown by an increase the efficiency of the PSt* as an initiator, by increasing the lifetime of the radicals and the copolymerization reactions to become more efficient in the nonconventional conditions owing to the catalytic effect of the field.

VIII.2.2. Radical macroinitiators. Introduction.

Living anionic polymerization is the most suitable method for preparation of block copolymers.[7] This method, which leads to well defined copolymers of low polydispersity, is however restricted to monomers of low polarity like isoprene, butadiene or styrene.

More polar monomers, for instance vinyl chloride or maleic anhydride, cannot be polymerized by this technique. Thus, in order to obtain block copolymers containing a

sequence of such polar monomer units, it is necessary to use free or controlled radical polymerization step. The initiation of this type of polymerization can be achieved with a polymeric initiator, *e.g.* a polymer containing peroxide or azo-groups. As the different types of synthesis, which have been described for the preparation of such polymeric initiators, generally have the disadvantage of requiring several reaction steps,[8,9] it is more desirable to prepare these initiators in a one step reaction, thus keeping the advantages of the anionic polymerization.

Polymeric peroxides have been obtained by deactivation of a living anionic polymer either with functionalized peroxide or directly with oxygen.[10] This type of polymers was also prepared via reaction of poly(ethylene oxide) with a diisocyanate to form an isocyanate-capped polymer. The NCO group was then reacted with dihydroperoxides to form a peroxy carbamate, which then initiated the radical polymerization of styrene.[11]

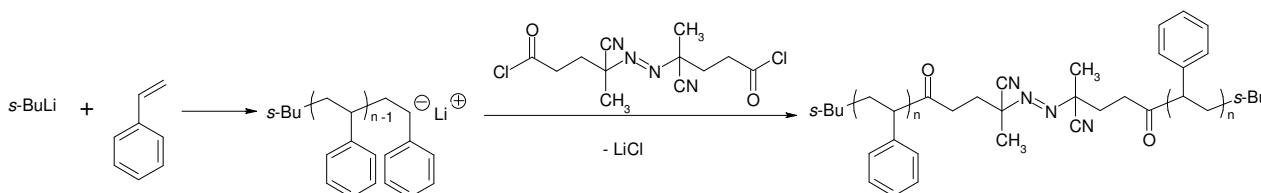
In a similar way, polymeric azo initiators have been prepared by deactivation of living anionic polymers with functionalized azo-derivatives such as azobisisobutyronitrile (AIBN).[12] In the work of *Riess et al*[13] concerning reactions between monofunctional living polystyrene and AIBN, it has been shown that a coupling reaction occurs leading to the incorporation of azo-groups either in the middle of the chain or at the end. The mechanism and the influence of temperature, the type of end-group carbanion and the counter ion aspects, were later described by the same authors,[14] who proved that the reaction between the living anionic polystyrene with AIBN involves chain coupling with elimination of CN^- groups.

An analogous strategy for preparation of azo-group containing poly(ethylene oxide) macroradical initiator has been reported by *Ueda and Nagai*. [15] They prepared the macroinitiator using an esterification reaction between the hydroxyl end-groups of poly(ethylene oxide) and azobiscyanopentanoyl chloride and further applied this initiator for free radical polymerization of styrene to yield poly(ethylene oxide-*block*-styrene) copolymers.

VIII.2.3. Synthesis and characterization of 4,4'-azobis(4-cyanopentanoyl) polystyrene radical macroinitiator.

For the synthesis of radical macroinitiator molecules, living anionic polymerization of styrene was applied in order to prepare well-defined polystyrenes, end-coupled with 4,4'-azobis(4-cyanopentanoyl chloride) (ABCPC).

Scheme VIII.1. Synthesis of 4,4'-azobis(4-cyanopentanoyl)polystyrene radical macroinitiator



ABCPC was previously synthesized according to the procedure described by *Smith*,^[16] involving chlorination of azobiscyanopentanoic acid with PCl_5 . In order to avoid side reactions (A_N of PS^- to CN groups and PS-C(O)-azo) the coupling reaction between polystyryllithium and ABCPC was performed at $0\text{ }^\circ\text{C}$ overnight. Addition of strictly stoichiometric amounts of ABCPC to the polystyryllithium solution plays a crucial role as well, because of only a strictly fixed ratio of 2/1 between PS^- and ABCPC, guarantees the total reaction of both the reactants. A slight excess of ABCPC will lead to a mono-substituted product, which will efficiently initiate radical polymerization of second monomer as well. On the other hand, an excess of polystyryllithium will produce a further nucleophilic addition reaction with the di-substituted product, yielding tri- and four-substituted compounds.

The molecular weights of the obtained products are summarized at Table VIII.1. A doubling of molecular weight of PS-azo-PS comparing to the corresponding polystyrene aliquots, was observed by GPC (in $^1\text{H-NMR}$ spectroscopy the signals of the azo-compound overlap with the signals of polystyrene), confirming the appearance of a

disubstituted PS-azo-PS compound. A polydispersity increase with decreasing molecular weight of the polymer, was observed in the present case (products with lower molecular weight (**8.1** and **8.2**) possess PDI 1.42-1.71, and 1.1-1.38 for the higher molecular weight products (**8.3-8.5**)).

Table VIII.2. Molecular weights of polystyrene aliquots and PS-azo-PS target products.

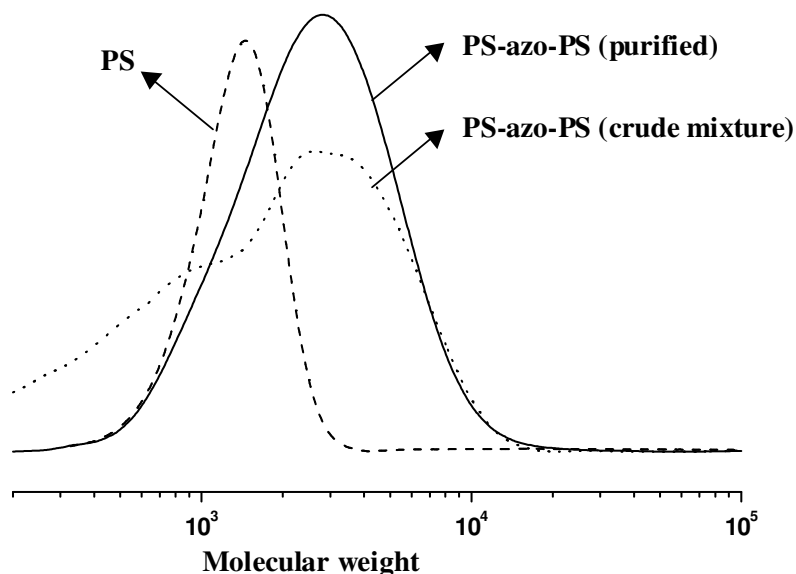
No	Polystyrene before reaction with ABCPC				PS-azo-PS		
	Theoret.	GPC		¹ H-NMR	Theoret.	GPC	
	M _n *	M _n	PDI	M _n	M _n **	M _n	PDI
8.1	1 000	1 080	1.42	1 000	2 000	1 900	1.66
8.2	1 000	940	1.71	1 200	2 000	2 000	1.55
8.3	5 000	3 400	1.41	3 600	10 000	6 900	1.54
8.4	5 000	4 400	1.16	4 400	10 000	9 300	1.38
8.5	5 000	8 300	1.11	8 200	10 000	12 600	1.39

* M_n (PS) = gr Styrene / mol *s*-BuLi

** M_n (PS-azo-PS) = 2 x M_n (PS)

The polydispersity of the polystyrene aliquots was found to be lower than that of the final products (except for **8.2**), which could be explained by the presence of single polystyrene chains, or monosubstituted azo-compound in the obtained products. The presence of these side products was confirmed by the appearance of low-molecular weight shoulders in the GPC elugrams. (see Figure VIII.1) Purification of such mixtures of polymers with two different chain-lengths was achieved by fractionation of the products using precipitation of the crude product in an appropriate mixture of solvents (THF and methanol). Thus, products with the highest molecular weight precipitated first and with the increasing contents of nonsolvent, further precipitation of the products with lower molecular weight was possible.

Figure VIII.4. GPC (THF – eluent, PS – standard) of 8.2.



In general, the main drawback of radical macroinitiators is their relatively fast recombination because of their moderate mobility and close proximity in the moment of their formation. It was found that an external magnetic field can separate both radicals immediately after their formation, and thus increase their life time.[17] The products **8.1** and **8.4** were selected among the all radical macroinitiators as the most appropriated macroinitiators (possessing two different molecular weights and the lowest polydispersity) for free-radical polymerisation of methylmethacrylate in a continuous magnetic field of 7 T (see next section).

VIII.2.4. Synthesis of diblock copolymers utilizing polymerization in a magnetic field.

Kinetic data

Some of the most important factors in polymerization reactions of different monomers initiated by macro-radicals are as follows:

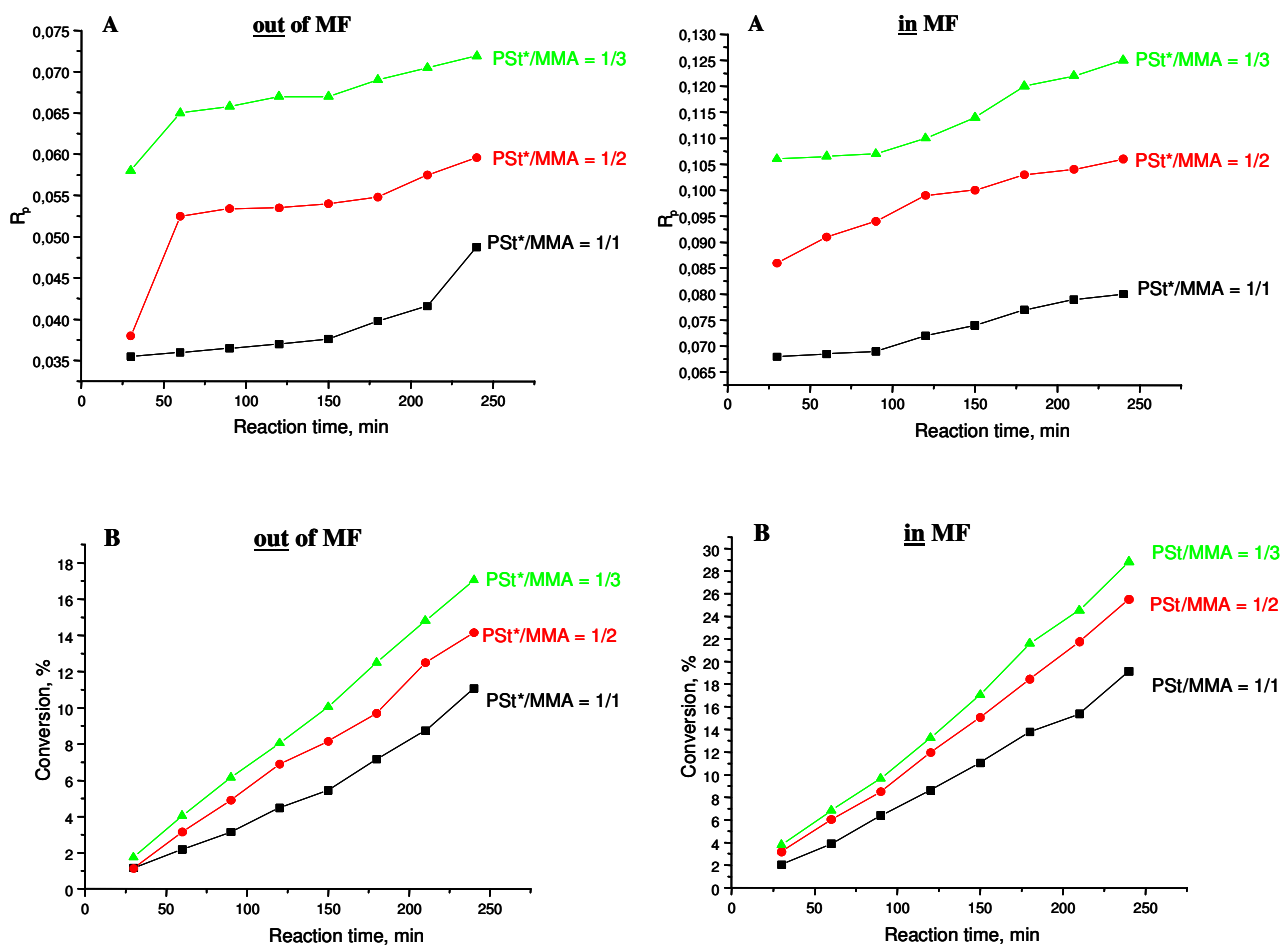
- the lifetime of the macro-radicals;
- the accessibility of the monomers to the radicals;

- accelerating effects of the solutions of the monomers on the rate and extent of polymerization reactions;

- the effects of the solution of the monomers on molecular orientation and morphology of the macro-radicals.

It is already known that the magnetic field has a double effect exerted on the one hand on the dynamics of molecular movement and on the other hand on the dynamics of radical spins. In this context it is envisaged that a presence of a MF would have a beneficial effect on the following processes. Polystyrene formed by anionic polymerization has been deactivated with 4,4'-azobis (4-cyanopentanoyl chloride) (for more details concerning synthesis of the polystyryl macroinitiator see section VIII.2.3.). The resulting macroinitiator has been used for the formation of a second block by radical polymerization of methylmethacrylate. The evolution of the copolymerization processes under various reaction conditions is illustrated in Figure VIII.2 (A and B) and Table VIII.2.

Figure VIII.2. Evolution of the momentary polymerization rate [$R_p = \frac{C_T}{T_{\min}}$] (C_T – conversion) in THF (A) and conversion in dioxane (B) of polymerization of MMA initiated by PSt* (see section VIII.2.3 product **8.1**) **out** and **in** magnetic field.



The experimental data confirm our assumptions regarding the beneficial effect of the field for the development of the polymerization processes. The magneto-kinetic changes are attributed to the catalytic effect of the field, which determines the orientation and the mobility of the macro-initiator as well of the monomer, and also to an increase the lifetime of the radicals.

Polarity and viscosity of solvents are very important parameters in controlling the magneto-kinetic effects, which is explainable by involving a radical pairs mechanism. In solvents with high viscosity, the radicals' lifetime grows due to slower diffusion of charge carriers, the recombination reactions among radicals are limited, and it is possible the spin evolves to the triplet state as a result of the magnetic field presence.

Comparing the block polymerization processes in a MF in THF with those in dioxane, a solvent with higher viscosity, present more evidence of magnetic-changes. Thus in comparing the conversion the increase in a MF ranges between 89.9 % (in case PSt*(**8.1**) /MMA = 1/1) to 63 % (for PSt*(**8.1**) /MMA = 1/3). The comparison between the conversion values for variants of syntheses (PSt*(**8.1**) /MMA = 1/2) realized in MF in THF versus dioxan are between 78.32 % and 86.62 % higher than those without a MF (see Table VIII.2).

Table VIII.2. Conversions and molecular weights of block copolymers obtained in and out of a magnetic field of 7 T.

PSt*(8.4) / MMA	Solvent	Conversion, %*		\overline{M}_w	
		Without MF	In MF	Without MF	In MF
1 / 1	THF	9.15	10.85	12 450	14 670
	Dioxan	8.90	11.45	12 327	14 588
1 / 2	THF	11.30	13.95	12 620	16 050
	Dioxan	10.05	14.55	12 401	15 191
1 / 3	THF	14.50	16.15	14 505	15 650
	Dioxan	12.30	16.85	14 703	15 545

reaction time - 240 min

Thus the effects of the MF are to reduce the induction period (I_p) of the reactions

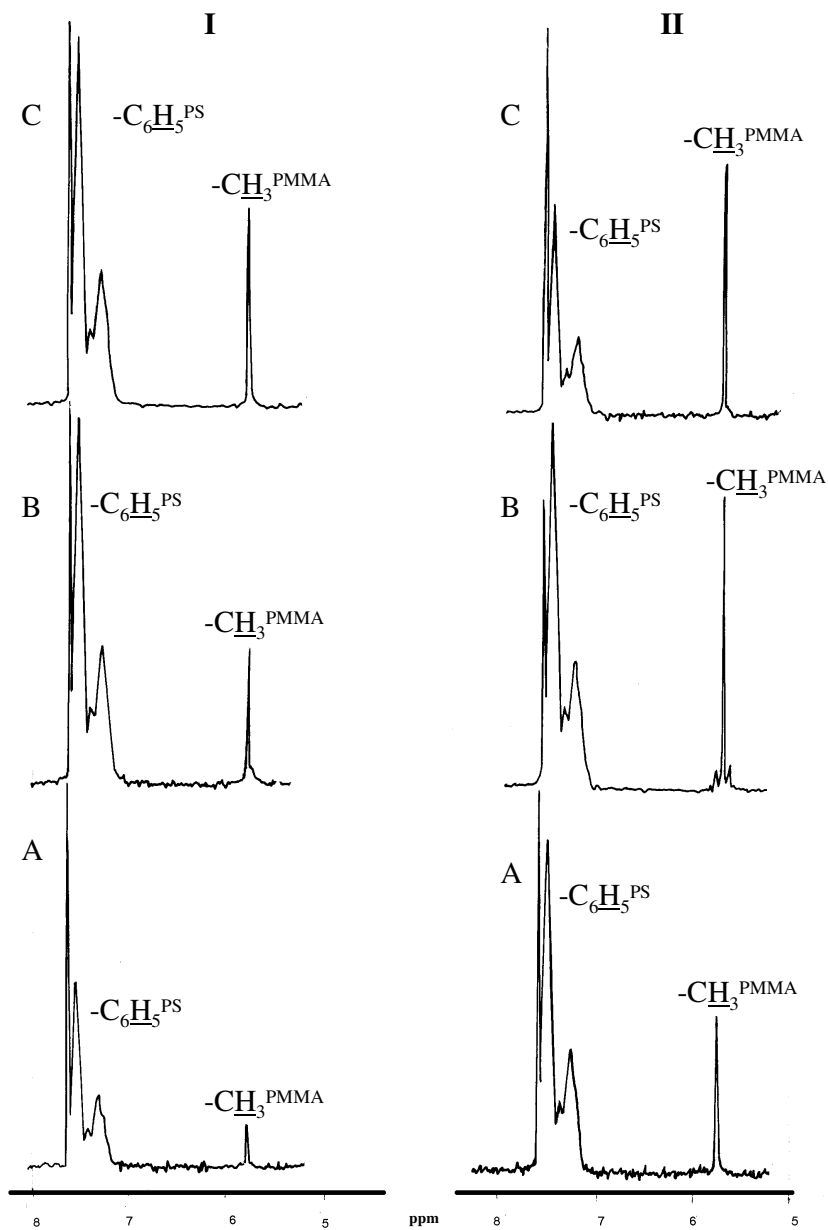
$$(I_p = \frac{\sum R_p^n / n}{T}, \text{ where } R_p^n = \text{momentary polymerization rate, } n = 8 - \text{number of the rate}$$

determination and T = reaction time, respectively 240 minutes); - to raise the rate of polymerization; - superior conversions are registered, - the processes evolution according to the reaction condition is better represented in case of syntheses assisted by the MF in that order a constantly growth of conversion and rate of polymerization are registered correlated also with the reaction conditions (ratio between PSt* and MMA).

¹H-NMR data

In order to investigate the magneto-kinetic effect of the macroinitiator on the polymerization of MMA two 4,4'-azobis(4-cyanopentanoic) functionalized polystyryl macroinitiators differ in molecular weights (PSt* with M_n 9 300 (8.4) and M_n 1 900 (8.1) for more details see section IV.5.2) were used. In case of PSt* with M_n 9 300 (8.4) magneto-kinetic effects were detected but not as noticeable as for PSt* having M_n 1 900 (8.1), whose conversion values were almost 45 % higher. These magneto-kinetic effects were confirmed by the ¹H-NMR data (see Figure VIII.3 and Table VIII.3).

Figure VIII.3. $^1\text{H-NMR}$ spectra of I – made without MF and II – made in MF, performed in THF with ratio of $\text{PSt}^*(8.1) / \text{MMA} = 1/1$ (A), $1/2$ (B), and $1/3$ (C).



The block copolymer compositions determined from the $^1\text{H-NMR}$ spectra are presented in Table VIII.3.

Table VIII.3. Composition of the block copolymers obtained from $^1\text{H-NMR}$ spectra.

Initiator/monomer PSt* / MMA	Solvent	Rates in product PSt / PMMA	
		Without MF	In MF
1 / 1*	THF	72.5	10.8
	Dioxane	16.9	11.8
1 / 2*	THF	11.1	5.6
	Dioxane	9.8	4.1
1 / 3*	THF	7.5	2.4
	Dioxane	6.2	1.3
1 / 1**	THF	79.6	32.9
	Dioxane	68.5	31.8
1 / 2**	THF	13.3	6.1
	Dioxane	14.4	5.7
1 / 3**	THF	10.7	4.7
	Dioxane	10.4	3.2

* PSt*(**8.1**)

** PSt*(**8.4**)

The macroinitiator molecular weight effect on the polymerization reaction is similar to those of the polarity and viscosity of the solvent. The increase of the macroinitiator molecular weight increases the radicals' lifetime, due to slower diffusion

of charge carriers, and decreases the probability for recombination reactions among radicals.

The reaction conditions, respectively ration between PSt* and MMA, as well the beneficial effect of the magnetic field presence, are confirmed by spectra feature. The anticipated effect of the magnetic field upon the block polymerization reactions is reflected also by the composition of the copolymers comparing with classic variants. Thus, accordingly with the reaction conditions and the conversion values the proportion between the block copolymers is better represented in case of the syntheses performed in MF.

Making a comparison between the conversion values and the composition data can be considered that magnetic field effects are exerted equally on the dynamics of molecular movement and upon the dynamics of radical's spins. These conclusions are sustained also by the data obtained from the syntheses performed in dioxane comparing with those in THF.

GPC data

Because sometimes the MF influence cannot be detected only through the kinetic changes the behavior of the polymerization processes were completed by the determination of the molecular weights of the block copolymers to determine the MF effect as well the efficiency of the field (the corresponding molecular weights of the block macromolecular chains poly(styrene–b–methylmethacrylate) are presented in Figure VIII.4). The growing ratio between PSt* and the co-monomers is evidenced by the higher values of the molecular weights. Block copolymers obtained without MF with $\text{PSt}^* / \text{MMA} = 1/1$ have a molecular weight of 3 000 and for the ratio of $\text{PSt}^* / \text{MMA} = 1/3$, \overline{M}_w is about 4 000 for the syntheses performed in THF.

The magnetic field influence is shown by increased the molecular weights of the block copolymers. Thus, in case of the ratio of $\text{PSt}^*/\text{MMA} = 1/1$ the molecular weight obtained in magnetic field is about 4 000. Practically for all variants of co-polymers

obtained in MF their molecular weights are higher than those of the corresponding products synthesized in the absence of the field as can be observed from Figure VIII.4 and VIII.5. This is attributed to the action of the magnetic field on the macromolecular chains, termination by recombination being preferred to the detriment of disproportionation.

Figure VIII.4. Molecular weights of the block copolymers accordingly to the reaction conditions (PSt*(8.1)).

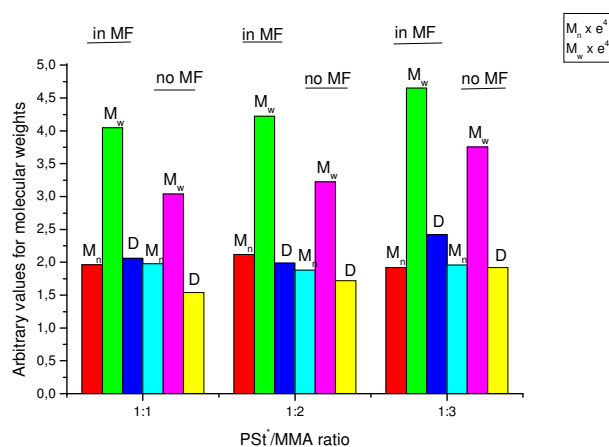
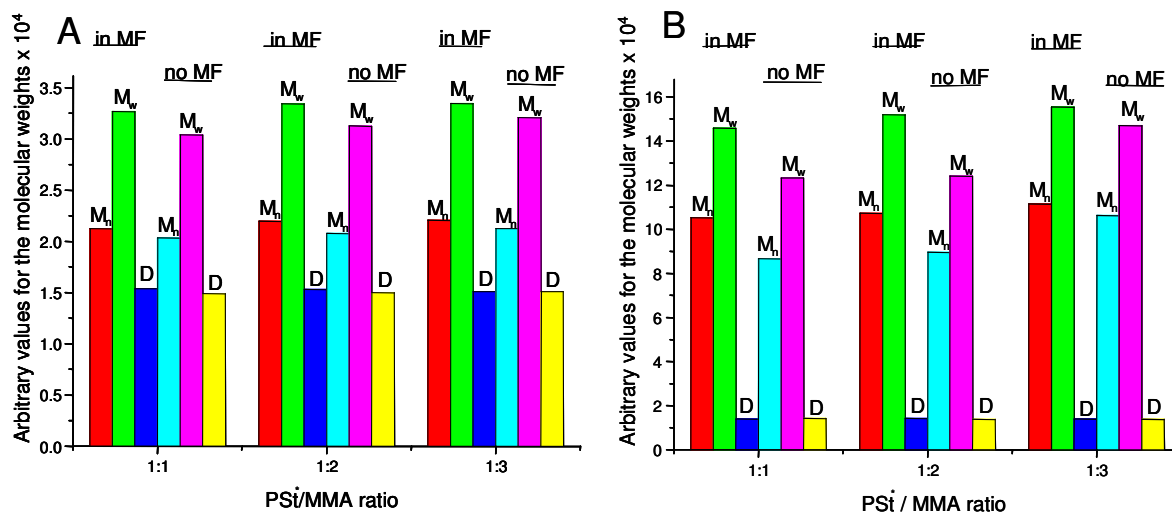


Figure VIII.5. Molecular weights of the block copolymers obtained in dioxane (A) and in THF (B) by different ratio PSt*(8.4)/MMA.



The molecular weights of the macromolecular products obtained in THF and dioxane in the absence of the magnetic field are in the same range. The MF contribution is not so obvious in obtaining higher molecular weights of the products for syntheses performed in dioxane.

In case of reactions in THF using PSt*(**8.1**) as macro-initiator the magnetic field influence produces an increase of the molecular weights of the block copolymers of up to 33%, while for the same reactions performed in dioxane the molecular weights of the block copolymers are only up to 7% higher. The molecular weights of poly(styrene-*b*-methylmethacrylate) obtained in THF using PSt*(**8.4**) are presented in Figure VIII.5. For these syntheses as well for the processes in dioxane the molecular weights of the synthesized block copolymers are up to 23% higher than those of the copolymers obtained in the absence of the field.

The obtained data confirm the dual character of the MF effect exerted on the one hand on the dynamics of molecular movement and on the other hand on the dynamics of radical spins. It is also evidenced the technological interest of using the magnetic effects as a new way to perform radical processes. This is because through very weak perturbations of the magnetic field, one can control chemical kinetics and thus the course and the rate of reactions that normally require much higher chemical energies.

VIII.3. Diblock copolymers bearing 3-(1-phenyl-vinyl)-perylene (dye) between the blocks

The synthesis of fluorescently labeled polymer is an important task with respect to the accelerated progress of fluorescence related analytical techniques (*e.g.* fluorescence microscopies and spectroscopies). The use of fluorescently labeled polymers ranges from fundamental aggregation research to very modern drug deliveries investigations. The dye-bearing block copolymers described in the current work were synthesized to be used as polymers in the polymer-dendrimer hybrids or by preparation of self-assembly hyperstructures.

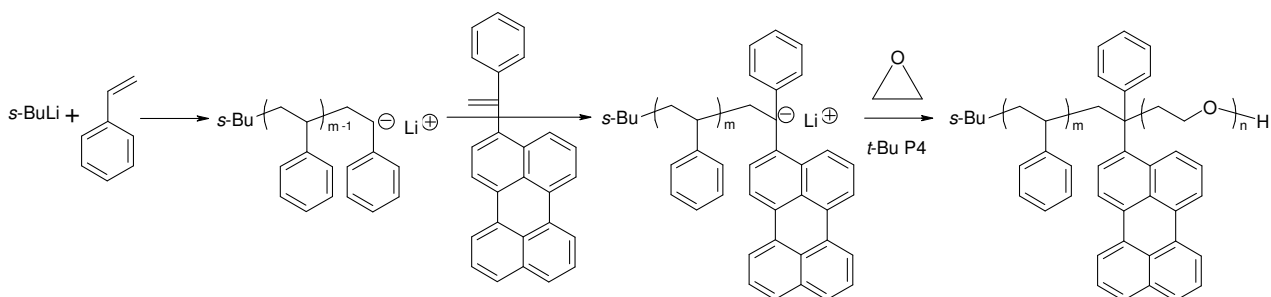
VIII.3.1. Introduction

Block copolymers labeled with suitable chromophores at strategic places along the polymer chain are becoming the important tools in the studies over the nature of the micelles interface as well as the exchange dynamics in micelle systems. *Quirk et al.* have reported the preparation of PS-*b*-PEO diblock copolymers having chromophore groups (pyrene or naphthalene) located at the block junctions or at the free ends of the PS blocks.[18,19] These authors used a nonradiative energy transfer from naphthalene (donor) to pyrene (acceptor) to monitor the micelle formation and to examine the location of the free PS ends within the copolymer micelles. Recently, a series of singly and doubly labeled PS-*b*-PMMA,[20] PS-*b*-PEO,[21] PI-*b*-PS and PS-*b*-PMMA[22] block copolymers using either sequential living anionic polymerization[23,24] and atom transfer radical polymerization[22] has been prepared by *Winnik et al.* The prepared copolymers were used in energy transfer studies in solution as well as to investigate the influence of chain length and salt concentration on block copolymer micellization.[25] Very recently, the same authors have reported the synthesis of fluorescent-dye labeled PMMA-*b*-PBA diblock copolymers utilizing a hydroxyl-protected initiator and the combination of anionic and atom transfer radical polymerization techniques.[26]

VIII.3.2. Synthesis of poly(styrene-dye-ethylene oxide) and poly(isoprene-dye-ethylene oxide).

Dye-molecules based on condensed aromatic structures as phenanthrene, pyrene, perylene etc. possessing double bond as functional group, could react with the living anionic end of polystyrene or polydienes. The synthetic scheme consisting in initially polymerization of styrene (see Scheme VIII.2) (the scheme is essentially the same in the case of poly(isoprene-dye-ethylene oxide) preparation), followed by nucleophilic addition reaction between polystyryllithium and double bond of the dye and further polymerization of ethylene oxide:

Scheme VIII.2. Synthesis of poly(styrene-dye-ethylene oxide)



As dye-molecule 3-(1-phenyl-vinyl)-perylene (named for simplicity “dye” in the present study) was synthesized by Dr. Jang Qiang Qu from the group of Prof. Müllen. It should be pointed out that this particular molecule could be inserted only between the blocks due to the fact that the dye-anion (which can be prepared by reaction of *s*-BuLi with the dye molecule) is less reactive, and cannot initiate polymerization of styrene, and on the other hand polyethylene oxide living anionic end is not able to perform nucleophilic additions to vinyl derivatives. Thus, an important role for every anionic polymerization is a gradually decreasing reactivity of the anionic end *e.g.* $s\text{-Bu}^- > \text{PS}^-$ or $\text{PI}^- > \text{PS}(\text{PI})\text{Dye}^- > \text{PS}(\text{PI})\text{DyePEO}^-$.

One important feature of this PS-dye-PEO block copolymer is that every polymer chain contains only one dye molecule between the blocks. It has been proven that 1,1-substituted vinyl derivatives cannot be polymerized, especially when they bear bulky electrophilic substitutes such as benzene and perylene.

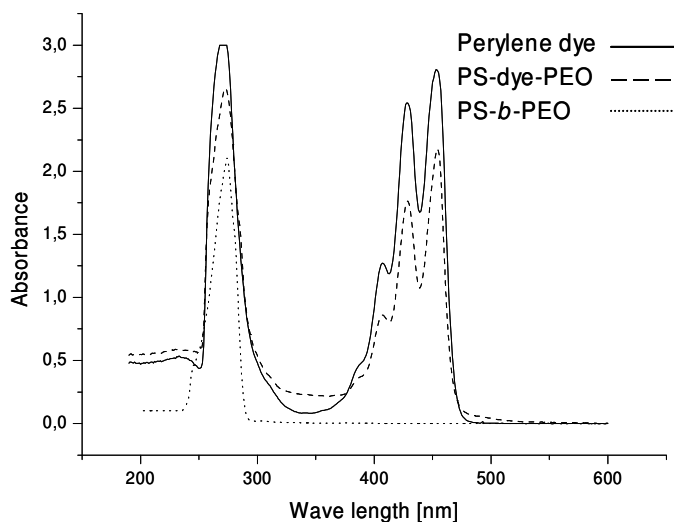
Molecular weights of the prepared PS(PI)-dye-PEO block copolymers were determined by GPC, and calculated from $^1\text{H-NMR}$ spectra (see Table VIII.4).

Table VIII.4. Molecular weights of the prepared PS-dye-PEO and PI-dye-PEO block copolymers.

No	GPC				$^1\text{H-NMR}$	
	M_n PS(I)-dye	PDI	M_n PS(I)-dye-PEO	PDI	M_n PS(I)-dye	M_n PS(I)-dye-PEO
8.6 (Styrene)	6 000	1.14	7 400	1.16	5 600	15 500
8.7 (Isoprene)	4 000	1.53	4 800	1.31	5 800	13 300

While the molecular weight of PS(I)-dye obtained by GPC was confirmed by $^1\text{H-NMR}$ calculations, the molecular weights of PS(I)-dye-PEO obtained from GPC and calculated from $^1\text{H-NMR}$ spectrum deviate considerably from each other (due to difference in retention volume of PS(I) and PEO - see more detailed explanation in section IV.5)

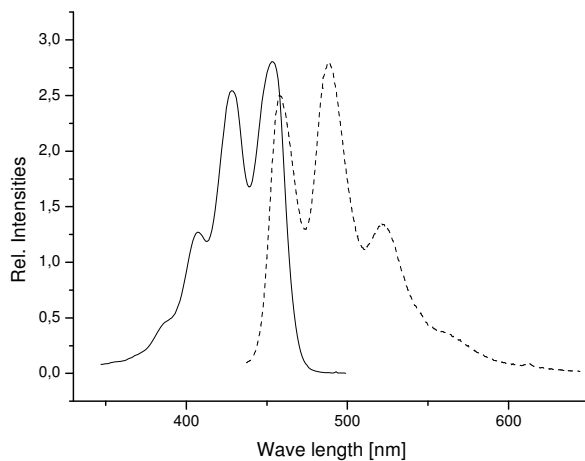
Important characteristics, in respect to their applications, are absorbance and fluorescence spectra of the dye-labeled polymers. In order to investigate the optical properties of those molecules, UV- and fluorescent-spectroscopy were applied (see Figure VIII.6).

Figure VIII.6 UV-spectra of perylene-dye, PS-dye-PEO and PS-*b*-PEO in THF.

It is seen from the spectra that both dye and block copolymer bearing the dye possess two distinct bands. The first one is in the visible region (380-480 nm) and the second one is in the UV region (260-330 nm). The absorption in the visible region is due to $S_0 \rightarrow S_1$ transition with distinct vibronic fine structure, which is the characteristic band for perylene. The characteristic absorption maximum of perylene in the PS-dye-PEO spectrum does not show any shift effect (batho- or hypsochromic shift) due to the fact that perylene π -electrons are not conjugate neither with double bond nor with the benzyl ring [27]. Thus, the polymerization reaction involving π -electrons of the double bond does not influence those of the perylene ring.

The emission spectrum of PS-dye-PEO (**8.6**) in solution (shown in Figure VIII.7) exhibits a similar spectrum to the absorption spectrum with a distinct vibronic fine structure with maxima at 457, 488 and 521nm.

Figure VIII.7 Normalized absorption (solid line) and emission (dashed line, $\lambda_{\text{ex}} = 408$) spectra of PS-dye-PEO (**8.6**) in THF.



Conclusions

This chapter presents the benefit of the magnetic field influence in the synthesis of poly(styrene-*b*-methacrylate). Magneto-kinetic field effects result in a higher reaction rate and conversion and also a diminution of the induction period. This chapter reported the influence of a high MF of 7 T on the radical polymerization of MMA initiated by a PS-azo-PS macroinitiator and confirmed the kinetic data obtained in the same sustained by the molecular weights of the reaction products synthesized in the field and by the higher MW of the polymers obtained in the MF. Additionally, the presence of MF induced a higher efficiency of the azo-initiators comparing with those in the absence of MF. The effect was attributed to changes in the state of the radicals from a singlet to triplet state through the hf mechanism, transitions that are attributed to the intensity of the external MF.

The second topic of this chapter is block copolymers bearing chromophore molecule. The amphiphilic block copolymers bearing a dye in the junction point PS(I)-dye-PEO are important for investigation over self-assembly process of the block copolymer structures, regarding the tendency for the polymer backbone to prefer a

specific orientation with respect to a local plane passing through the interface. If the backbone vector has a preferred direction at the interface, this will affect the orientation of the transition dipole of a dye attached directly to the backbone. Additionally, by attaching a dye one could apply a FRET technique to examine the orientation itself (*e.g.* perpendicular to the interface in a lamellar structure) by the observed differences in the rate and extent of energy transfer.

References

1. Turro N.J., Kraeutler B. *Acc Chem Res* **1980**,13, 369.
2. Steiner U.E., Ulrich T. *Chem Rev* **1989**, 89, 51.
3. Sugiyama, J. *Macromolecules*, **1992**, 25, 4232.
4. Chiriac, A. P.; Simionescu, C.I. *Progress in Polymer Science* **2000**, 25, 219.
5. Chiriac, A.P.; Neamtu, I.; Simionescu, C.I. *Die Angew. Makromol. Chem.* **1999**, 273, 75.
6. Junlian, H.; Wu, Q. *Chinese J. Polym. Sci.*, **1990**, 8, 108.
7. Fetters J.E. Chapter "Synthesis and Characterization of Block Polymers via Anionic Polymerization" Meier, D. J., editor "Block Copolymers: Science and Technology" *MMI Press Symposium Series* **1979**, 3, 17.
8. Vuilleminot, J.; Barbier, B.; Riess, G.; Banderet, A. *J. Polym. Sci.* **1965**, A3, 1969.
9. Vollmert, B.;Bolte, H. *Macromol. Chem.* **1960**, 36, 17.
10. Brossas, J.; Catala, J. M.; Clouet, G.; Gallot, Z. *C.R. Hebd. Seanc. Acad. Sci.* **1974**, 278, 1031.
11. Orhan, .H.; Yilgor, I.; Baysal, B.M. *Polymer* **1977**, 18, 286.
12. Echte, A.; Stein, D.; Fahrbach, G.; Adler, H.; Geberding, K. *Ger. Offen.* **21-4-1977**, 2546377.
13. Vinchon, Y.; Reeb, R.; Riess, G. *Europ. Polymer J.* **1976**, 12, 317.
14. Riess, G. and Reeb, R. Chapter "Preparation of Polymeric Free-Radical Initiators by Anionic Synthesis: Polymeric Azo Derivatives" McGrath, J.E., Editor of "Anionic Polymerization" *ACS Symposium Series* **1981**, 166, 477.
15. Ueda, A.; Nagai, S. *J. Polym. Sci. Part A: Polym. Chem.* **1986**, 24, 405.
16. Smith, D. A. *Macromol. Chem.* **1967**, 103, 301.
17. Sugiyama, J. *Macromolecules* **1992**, 25, 4232.
18. Quirk, R.P.; Kim, J.; Rodrigues, K.; Mattice, W.L. *ACS Polym. Prepr.* **1990**, 31,87.

19. Rodrigues, K.; Kausch, C.M.; Kim, J.; Quirk, R.P.; Mattice, W.L. *Polym. Bull. (Berlin)* **1991**, 26, 695.
20. Ni, S.; Juhue, D.; Moselhy, J.; Wang, Y.; Winnik, M.A. *Macromolecules* **1992**, 25, 496.
21. Calderara, F.; Hruska, Z.; Hurtrez, G.; Nugay, T.; Riess, G.; Winnik, M.A. *Macromol. Chem.* **1993**, 194, 1421.
22. Tong, J.; Ni, S.; Winnik, M.A. *Macromolecules* **2000**, 33.
23. Ni, S.; Zhang, P., Wang, Y.; Winnik, M.A. *Macromolecules* **1994**, 27, 5742.
24. Tcherkasskaya, O.; Ni, S.; Winnik, M.A. *Macromolecules* **1996**, 29, 610.
25. Rager, T.; Meyer, W.H.; Wegner, G.; Winnik, M.A. *Macromolecules* **1997**, 30, 4911.
26. Tong, J.D.; Zhou, C.; Ni, S.; Winnik, M.A. *Macromolecules* **2001**, 34, 696.
27. Schille, K.; Yekta, A.; Ni, S.; Farinha, J. P. S.; Winnik M. A. *J. Phys. Chem. B* **1999**, 103, 9090-9103.

Chapter IX

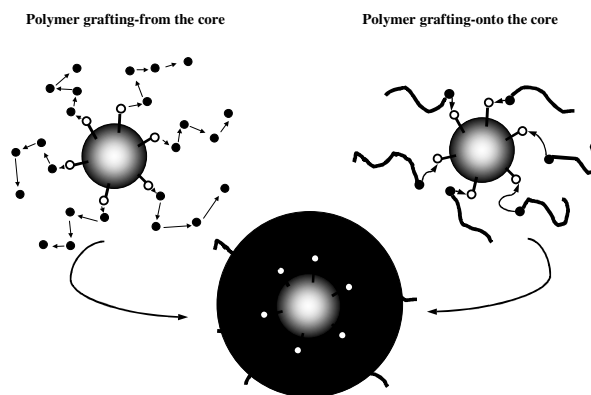
SUMMARY AND CONCLUSIONS

The aim of this study was the synthesis, characterization and further application of core-shell macromolecules possessing a hydrophobic stiff core (polyphenylene dendrimers) surrounded with a hydrophilic, soft, covalently bonded polymer shell (poly(ethylene oxide) and its copolymers). The requirements for such complex substances were that they should be well-defined in terms of molecular weight (narrow molecular weight distribution) and in molecular structure. Most of the dendrimer-polymer hybrids examined up to now possessed “soft” or “semirigid” dendrimer (*e.g.* PAMAM dendrimers), while polymers with different morphology and behavior were utilized for building a huge variety of macromolecular structures. Architectures based on rigid, stiff dendrimers are synthesized and investigated in the present study. The rigidity of the dendritic core ensures both the shape persistence of the entire system (in case of relatively stiff polymeric shell – polystyrene, polyphenylenes etc.) and fixed position of the dendrimer functionalities that guarantees their reaction ability.

Polyphenylene dendrimers exhibiting an outstanding shape-persistence and allowing the attaching of functional groups in well-defined positions on the dendrimers surface in many cases are the best candidates that fulfill the requirement for rigidity and can be used as a stiff-core-dendrimer - polymer hybrids. Core-shell structures are mainly interesting due to their possessing a combination of stiff core and a flexible shell (inorganic-organic hybrids and latexes). Core-shells based on polyphenylene dendrimers were applied for the investigation of the film formation of dispersions, as drug delivery and fragmentation processes of polymeric supports for metallocenes applied in olefin polymerizations.

The preparation of core-shell molecules containing dendrimer as a core was possible *via* two synthetic routes: (i) “grafting-onto” and (ii) “grafting-from” (see Fig. X.1)

Figure X. 1 Synthetic strategies for synthesis of core-shell molecules.



In the “grafting-onto” (*i*) approach, first a polymer with appropriate end-functionality or living polymer chains was synthesized and then reacted with the functional groups on the dendrimer. In the “grafting-from” (*ii*) approach the functional groups on the dendrimer serve as species, which can efficiently initiate the polymerization of a certain monomer, producing polymer chains covalently bonded to the dendrimer surface. Both methods were utilized for preparation of core-shell nanoparticles containing polyphenylene dendrimer as the core and poly(ethylene oxide) as the shell.

Poly(ethylene oxide) was synthesized *via* anionic polymerization of ethylene oxide with potassium *tert.*-butoxide as initiator. The living anionic chain-ends were then reacted with chloromethyl functionalized second-generation polyphenylene dendrimers in a Williamson reaction. The resulting core-shell macromolecules possessed narrow polydispersity as guaranteed by the excellent structural and functional definition of the dendrimer and the narrow polydispersity of the poly(ethylene oxide) attached to the dendrimer surface. Additional investigation of the size of the particles indicated a relation between both the length and the number of the polymer chains and the hydrodynamic radius determined by Dynamic Light Scattering. It was found that an increase both the length and the number of the polymer chains is accompanied by an increase in the hydrodynamic radius. Moreover, the change of the size of those core-shell particles can be controlled and adjusted by changing the polarity of the solvent. The study of hydrodynamic radius of the particles in water and THF proved that size increases in the solvents possessing higher

degree of solvating power for the chains (water for PEO) result form more stretched conformation of the grafted polymer chains, while less solvated polymers (PEO in THF), possess higher degrees of freedom, and tend to have more a coiled conformation, which decreases the total size of the system.

Another investigation concerning the number of the polymer chains grafted onto the dendrimer with respect to the length of the chain showed that an increase of the chain length is accompanied by a decrease the number of the attached polymer chains. This relation can be explained by the shielding effect of the attached polymer chains on the neighboring functional groups on the dendrimer. The reactive groups of the dendrimer became more sterically shielded with increasing the length of the polymer chains. Thus, the polymer with living chain-end cannot penetrate the already existing polymer shell.

In order to overcome this problem a “grafting-from” approach was applied. A second-generation polyphenylene dendrimer with tetrahedral core and 16 hydroxymethyl groups was utilized, after deprotonation of the hydroxyl groups, as a macro-multi-initiator for the polymerization of ethylene oxide. In this case, polymer chains grow up from the functional group of the dendrimer unrestricted from any steric hindrance. In order to prove that polymerization of ethylene oxide can efficiently start from all the functional groups of the dendrimer, model experiments based on ethylene oxide polymerization using 1,4-dihydroxymethyl benzene as a substance that mimic dendrimer functionality. The completeness of this reaction, involving all hydroximethyl groups (as proven by $^1\text{H-NMR}$), and the narrow polydispersity (GPC) of the products led us to apply the same method to polyphenylene dendrimers. However, a limitation of the method is the poor solubility of the dendritic multi-anion species in the reaction medium (THF). In order to increase solubility, a more polar medium (DMSO) had been applied with some success by other authors investigating multianionic systems. In the particular case of polyphenylene dendrimers, the fact that several units of ethylene oxide attached to the surface of dendrimer increased drastically the solubility of the substance was utilized for the successful preparation of core-shell macromolecules *via* the “grafting-from” method. The presence of initiators associates disturbing simultaneously starting the polymerization from all functional groups of the dendrimer, leading to increase of the polydispersity.

The obtained core-shell particles were investigated by Dynamic Light Scattering in order to characterize them in terms of hydrodynamic radius (R_h) in water and THF. It was found that R_h is in the range of 5-20 nm, and increases with increasing length of the poly(ethylene oxide) chains. A considerable increase of R_h in water was observed in comparison to that in THF, which was explained by a more stretched conformation due to the better solubility of PEO in water than in THF.

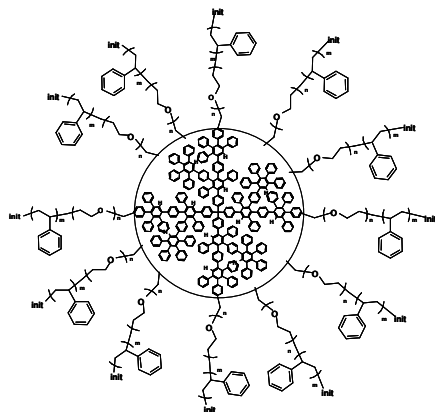
The obtained core-shell nano-particles were applied as metallocene supports in heterogeneous olefin polymerizations by my colleague Dr. Nikolay Nenov. From the scientific point of view, it was tempting to study the quality of the polyolefins prepared with catalyst systems, based on carriers, that have a size of at least one order of magnitude smaller than the used by now organic supports from the above mentioned nanoparticles. The catalyst systems prepared with this support exhibit good activities and productivities producing polymers with high molecular weights, high bulk densities and low dispersities. The small size of the particles and the narrow particle size distribution lead to completely homogeneous fragmentation of the catalyst back to the nanometer size of the carrier giving polyolefins with excellent qualities. Our results indicate that such catalyst systems could be very useful as model compounds for investigations on catalyst fragmentation and its influence on the product parameters.

Core-shell macromolecules with a perylenediimide containing polyphenylene dendrimer for the core and poly(ethylene oxide) for the shell were obtained. In this study we applied “grafting-from” approach in order to prepare core-shell structures based on polyphenylene dendrimer possessing 16 poly(ethylene oxide) outer chains chemically bonded to a perylenediimide molecule at a focal point. Therefore, combining an amphiphilicity with nano-scale and fluorescence efficiency, we suggest that such particles can serve as model compounds for all applications of fluorescence labeled organic nanoparticles where the size of the particle plays an important role for the properties. Therefore, they are currently being investigated as supports for metallocenes catalyzing the olefin polymerization (Dr. N. Nenov and Joung-Jun Jang). It is expected that the obtained results can improve the understanding of the role of the already established organic supports in the heterogeneous olefin polymerization.

The presence of a chromophore within the macromolecular structure gave us an opportunity for more detailed investigation in terms of hydrodynamic radius of these core-shell structures. Since the amphiphilicity of the PDIG₂(core)-PEO(shell) macromolecules provoked a strong tendency for aggregation in polar or nonpolar media, Dynamic Light Scattering failed to obtain R_h in the case of very short PEO chains, where they cannot serve as stabilizer shell. Therefore Fluorescence Correlation Spectroscopy was successfully applied to find R_h values of the core-shell structures. The advantage of this method is its very high sensibility allows one to use nanomolar concentrations, where the tendency for aggregation is negligible. By this means, the R_h values of these molecules were found to be in the range 10-30 nm. The obtained experimental results were confirmed by computer simulations of the structural conformations (Hyper Chem Pro 6 software program).

Multi-shell nano-particles consisting of shape-persistent second-generation tetrahedral polyphenylene dendrimers as core and poly(isoprene-*block*-ethylene oxide) (PI-*b*-PEO) or poly(styrene-*block*-ethylene oxide) (PS-*b*-PEO) arms forming the hydrophilic (PEO) and hydrophobic (PI, PS) shells, have also been synthesized and characterized (see Figure X.2).

Figure X.2. Structure of core-*double*-shell macromolecules.



PI-*b*-PEO and PS-*b*-PEO copolymers were synthesized *via* anionic polymerization of isoprene or styrene followed by ethylene oxide as a second monomer. The hydroxy end-functionalized copolymers are grafted on a dendrimer with an average number of 12 or 8 chloromethyl groups by a Williamson etherification reaction. The molecular weights of the core-shell macromolecules and diblock copolymers were determined by ¹H-NMR spectroscopy, GPC and MALDI-

TOF mass-spectrometry. The number of the diblock arms attached to the dendrimer molecule was found to increase with an increasing number of functional groups on the dendrimer and decrease with the length of the copolymer chains. Such dependence can be explained by steric hindrance between the attacking copolymer chains and the already grafted chains. Four core-shell nano-particles with molecular weights between 20 000 and 60 000 Dalton, differing in number, type and length of the copolymer chains, were synthesized and characterized. The hydrodynamic radius of the particles was determined by Dynamic Light Scattering to be in the range of 4 to 7 nm, depending on the length of the diblock copolymer chains attached to the dendrimer surface.

As an outlook one could propose a synthesis of core-shell molecules based on polyphenylene dendrimers possessing a different type of shell. The use of poly(propylene oxide) (PPO) and its block copolymers with PEO (known as Pluronic) will give access to a core-shell system possessing a temperature dependent amphiphilicity (aqueous solutions of poly(propylene oxide), PPO, exhibit dramatic temperature dependence - below 15 °C at ambient pressure, water is a good solvent for PPO, whereas PPO at higher temperatures segregates). Poly(ethylene oxide) (PEO), on the other hand, is dominantly hydrophilic within the temperature range from 0 to 100 °C. Thus, by controlling the temperature one can control the self-association processes giving rise to a wide range of phase behavior, including the formation of micelles of various form and size, complex structured microemulsions and liquid-crystalline phases.

Another very promising project is the application of the core-shell molecules as drug deliveries and particularly in transfer process through the Blood Brain Barrier (BBB). The development of investigations may concern both the variation of length of PEO chains (the size of the deliver is an issue in the drug delivery through the BBB) and the use of biopolymers like polypeptides as the shell. First attempts to use polylysine functionalized polyphenylene dendrimers gave very positive results (described in the thesis of Dr. G. Mihov 2004, MPIP-Mainz).

The use of fluorescent labeled dendrimers in the above-mentioned applications will provide additional possibilities to use fluorescent related techniques like fluorescent correlation spectroscopy and confocal fluorescent microscopy. Thus, investigations over the diffusion coefficient, size (hydrodynamic radius) and particle

distribution can be performed in order to better understand behavior and properties of those materials.

Chapter X

EXPERIMENTAL PART

X.1. Analytical instruments:

GPC: in THF

Waters[®] pump model 515, detectors: RI 101 ERC and UV-VIS S-3702 Soma (255 nm), temperature: 30 °C, standards: PS or PI, concentration: 1.000 g/l, flow rate: 1.0 ml/min, columns: “MZ-Gel” Sdplus 500, 10⁴, 10⁶ Å, particle size 10 µm;

in water

Waters[®] pump model 590, detectors: RI ERC-7510 and UV-VIS Soma S-3702 (255 nm), temperature: 25 °C, standard: PEO, concentration: 1.000 g/l, flow rate: 0.8 ml/min, columns: “TSK-Gel” G3000PW_{XL} 500, 10⁴, 10⁶ Å, particle size 13 µm;

in DMF

Waters[®] pump model 590, detectors: RI ERC-7512 and UV-VIS Soma S-3702 (255 nm), temperature: 60 °C, standards: PEO or PS, concentration: 1.000 g/l, flow rate: 1.0 ml/min, columns: “MZ-Gel” Sdplus 500, 10⁴, 10⁶ Å, particle size 10 µm.

¹H- and ¹³C-NMR spectroscopy:

“Bruker DXP” 250 MHz, “Bruker AMX 300” 300 MHz, “Bruker ASX 500 Widebore-Magnet” 500 MHz and “Ultrashield” 700 MHz spectrometers.

UV/VIS/NIR spectroscopy :

Lambda 900 “Perkin-Elmer” with 60 mm integrating sphere, deuterium source (UV) and tungsten-halogen source (VIS).

Dynamic Light Scattering:

ALV 5000 – Korrelator, ALV-SP81-Goniometer, Avalanche Photodiode Laser: Krypton-Ion-Laser 647.1 nm (Spectra Physics model Kr 2025);

Malvern-Zetasizer 3000 HS_A.

Mass spectroscopy:

VG ZAB2-SE-FPD Spectrofield, Bruker Reflex I (MALDI-TOF) and Bruker Reflex II (MALDI-TOF) mass spectrometers.

Fluorescent Spectroscopy (FS):

Fluorescent spectrometer “Spex Fluorolog2” type F 212 equipped with 450 W “Xenone-Bogen” source of light XBO “Osram” and Hamamatsu Photomultiplier “PMT R 508” and “PMT R 928” detectors.

Fluorescent Correlation Spectroscopy (FCS):

Commercial FCS setup manufactured by Carl Zeiss (Jena, Germany) consists of the module ConfoCor 2 and the inverted microscope model AXovert 200. He/Ne green laser with wavelength 543.5 nm. Output power 1 mW and max. power 0.23. Microscope water immersion objective ZEISS C-Apochromat (40x/1.2 W Corr. 40), numerical aperture 1.2, working distance 0.29 mm.

DSC: Mettler Digital Scanning Calorimeter 300, with a heating rate of 10 K/min.

TGA: Mettler 300 Thermogravimetric analyser.

IR: Nicolet 320 FT-IR

AFM measurements:

The samples were scanned with a Dimension 3100 model (Veeco, Santa Barbara, CA) at room temperature under ambient conditions. Single beam silicon cantilevers (Olympus OMCL-AC160TS-W2 TappingMode) with spring constants of ~45 N/m and resonant frequencies of ~300 kHz were used. All topographs were recorded in tapping mode. The resulting images have been flattened and plane fitted, some have been median and low-pass filtered.

Ellipsometry:

The measurements were performed on a null-ellipsometer with external reflection mode. The laser for ellipsometry measurements had a wavelength of 632.8 nm (Uniphase, 5 mW).

Contact angle goniometry:

The measurements were carried out on DSA10-MK2 model (Krüss GmbH, Hamburg, Germany) contact angle measuring system with full computer control and automated image analysis system. Drops of liquid of known volume (1 μL) were applied from a microsyringe to the surface of the test material. The reported values are the average of at least 8 drops placed and measured on different parts of the sample surface. The precision of measurements was below $\pm 1^\circ$.

X.2. High Vacuum Techniques

X.2.1. High-Vacuum Line

For the synthesis of polymers by anionic polymerization, special care should be taken in the purification of the reagents used. All impurities capable of affecting the polymerization (moisture, oxygen, etc) must be removed from the polymerization mixture if a full use of the living character of the anionic system is desired. For this purpose, the use of a high-vacuum line is usual (Scheme X. 1).

Figure X. 1 Oil and diffusion pump and high-vacuum line

A – oil pump; B – diffusion pump; C – vacuum tube; D – argon tube; E – reactor; F – short-path distillation glassware (a – flask containing liquid, b – port for liquid, c – calibrated ampoule); G – distillation glassware (a – U-shaped tube); H – dilution or mixing solution glassware; I – ports; J – vacuum detector device; K – vertically attached ampoule to reactor; L – horizontally attached ampoule to reactor; M – reservoirs for dry solvents;



The main parts of the high-vacuum line used were the oil pump (A) (Alcatel[®] Type 2005C), the diffusion pump (B) (Alcatel[®] Crystal 62), the liquid nitrogen trap, the vacuum (C) and argon (D) borosilicate glass tube lines, and the teflon valves (Rotaflo[®]). The oil pump was used in order to reduce the pressure in the diffusion pump to a level where polysiloxane vaporization by heating through a mantle was possible. After polysiloxane distillation was achieved, the diffusion pump reduced the pressure to a value around 10^{-5} mbar. A liquid nitrogen trap was used to condense any volatile substances incorporated in the system and protect in this way the oil and the diffusion pumps from contamination. The vacuum line is separated from the argon one by high vacuum teflon valves, which gives the possibility to use every port (I) separately and perform different procedures (*e.g.*, distillations, degassing) simultaneously. Reactors (E) and other glassware (E-H) are connected to the vacuum line through the ports. The vacuum detector (J) (VAP 5 Vacuubrand[®]) was connected to the vacuum line, detecting the vacuum value when the vacuum line was properly evacuated.

X.3. Glassware

Polymerization reactors (E), dilution apparatus (H), and ampoules were constructed from Pyrex glass flasks and tubing. The clean glassware was rinsed with deionized water several times and dried on the vacuum line under dynamic vacuum at 600 °C using a hot air-gun (Atlas Copco[®] HABE2000). In this way volatile contaminants present on the inner surface of the glass were removed. For the introduction of reagents under vacuum conditions into the main reactor, ampoules equipped with Teflon valve were used. They were attached to the reactor either vertically (to pour the substance into the reactor) or horizontally (to distill the substance into the reactor). The first variant was mainly using for substances that could not be distilled into the reactor (solid substances or solutions), substances which could be distilled were added into the reactor by the second variant.

X.4. Simple High Vacuum Procedures

X.4.1. Degassing

In order to remove oxygen and other gasses from a liquid system, a simple procedure of degassing was employed. The flask containing the liquid was connected to the vacuum line through a port. The Teflon valve was opened two or three times for a short period of time

(seconds) until bubbles were produced in its bulk. The liquid was then frozen, using liquid nitrogen and then the valve was opened and sufficient time was allowed for the whole system to be pumped down. After high vacuum was attained, the valve was closed and the liquid was thawed. The freeze-thaw cycle was repeated two or three times. In this way during every cycle a new equilibrium was attained between the gasses dissolved in the liquid and the part of the flask above the liquid. The gasses occupying the free space were driven out of the liquid into the vacuum, line while the liquid was maintained in the solid state.

X.4.2. Distillation

Since a high-vacuum level was attained in the vacuum line, distillation of liquids (solvents, monomers, etc.) were accomplished simply by heating the round bottom flask containing the liquid and freezing the receiving flask. Both flasks were usually connected to one of the ports using a short U-shaped tube (see Figure X. 1 G, a) as the distillation pathway. Before the beginning of the distillation, the liquid was degassed. While the liquid was thawed, the receiving flask was evacuated thoroughly and cooled to liquid nitrogen temperature. The port was closed to the high vacuum and distillation begins. After the whole volume of the liquid had been collected in the receiving flask, the flask was connected to the vacuum by opening the appropriate valve and the frozen liquid was degassed.

X.4.3. Short Path Distillation

In the case of very high boiling liquids (usually monomers), a special glass rig for distillation was constructed (Figure X. 1 F). The apparatus was connected to the vacuum line and evacuated. Then the liquid to be distilled was transferred into the flask (a), through port (b) under flushed argon, degassed on the vacuum line and then distilled into a calibrated ampoule (c).

X.5. Purification of Reagents

X.5.1. Solvents

Cyclohexane (Acros) was purified by stirring over concentrated sulfuric acid for a week in a conical flask. This procedure removes the thiophenes, substituted phenyl-compounds like toluene and vinyl compounds that may alter the microstructure of polydienes, or influence the polymerization. Then it was washed with an aqueous solution of NaOH, followed by washing

with water until it was neutral and finally was dried with CaCl_2 . Afterwards, it was transferred into a round bottom flask containing fresh finely ground CaH_2 and stirred overnight. Then it was distilled into storage glass-containers (Figure X. 1 M) connected to the vacuum line, containing $n\text{-BuLi}$ and 1,1-diphenylethylene (DPE). The persistence of a deep red color indicated the presence of 1,1-diphenylhexyllithium (DPHLi). Depending on the moisture levels of the solvent, an intermediate drying step over sodium or sodium dispersion, before distillation onto DPHLi was sometimes necessary.

Tetrahydrofuran (Acros) was refluxed over CaH_2 followed by distillation and reflux over LiAlH_4 . Then THF was distilled over K/Na alloy and refluxed under inert atmosphere in the presence of benzophenone, until a bright blue color was observed. Then it was distilled in storage glass-containers (Figure X. 1 M) attached to the vacuum line, containing $n\text{-BuLi}$ and DPE. Again the persistence of the deep red color indicated the presence of DPHLi.

Others. All others solvents were HPLC grade (Aldrich, Fluka, Fischer, Stream, and Acros) and were used as received.

X.5.2. Monomers

Styrene (Acros) This high boiling monomer (bp: 145 °C) was distilled in large volume (100 ml), on the vacuum line in a short path distillation apparatus in the ampoule containing CaH_2 and stored at $-30\text{ }^\circ\text{C}$. The styrene was distilled into a flask containing fluorenyllithium (obtained by miXng over night fluorene with $n\text{-BuLi}$) followed by short path distillation into a calibrated ampoule, prior to use.

α -Methylstyrene (Aldrich) (bp: 167 °C) was purified in the same way as styrene. A short path distillation apparatus was used and $n\text{-BuLi}$ instead of fluorenyllithium was used, since this monomer has a low ceiling polymerization temperature and no polymerization occurs at room temperature. The purity of the monomer was determined from the red color of the anions formed.

Isoprene (Acros) (bp: 34 °C). This diene was dried over finely grounded CaH_2 on the vacuum line overnight. It was then distilled over $n\text{-BuLi}$ and continuous stirred for 30 min at 0 °C. The pure monomer was distilled in calibrated ampoules prior to use.

Methacrylates and Acrylates. (Aldrich) These monomers were usually purified as given in literature .[1] Commercial monomer was dried over CaH_2 overnight in a short path apparatus connected to the vacuum line (Figure X. 1 F). After 24 h, the monomer was distilled into calibrated ampoules. The inhibitor free monomer was stored at $-30\text{ }^\circ\text{C}$ for one month. It was finally purified just prior to polymerization by a short exposure to triethylaluminum (TEA) (for low boiling monomers) or trioctylaluminum (TOA) (for high boiling monomers) using a short path distillation apparatus. As soon as a yellow-greenish color persisted in the bulk of the monomer, it was considered pure enough for anionic polymerization and was distilled into a calibrated ampoule. Traces of alcohols present from the synthesis of the monomer were removed during this last exposure since they react readily with the aluminum compounds. TOA is also efficient in removing secondary or tertiary alcohols. The yellow greenish color is due to the complex formed between the aluminum compound and the carbonyl group of the monomer.

Ethylene oxide (EO) (Fluka) (bp: $10\text{ }^\circ\text{C}$). This low boiling monomer was initially condensed in a large volume (50 ml) in calibrated ampoule containing CaH_2 and was stored at $-30\text{ }^\circ\text{C}$. Distillation over *n*-BuLi was necessary before reaction. During its exposure to *n*-BuLi, EO was kept at $0\text{ }^\circ\text{C}$ with stirring for 10 min. Finally, the pure monomer was distilled into calibrated ampoules prior to use.

X.5.3. Terminating Agents.

The compounds used for deactivation of the living anions are usually alcohols or acids. Methanol and HCl were widely used as the terminating agents. These compounds were degassed on the vacuum line several times and distilled into ampoules.

X.5.4. Coupling Agents.

The solid coupling agents like bromo- or chloromethyl derivatives of benzene were sublimed under vacuum. Solid commercial products of high purity were dried on the vacuum line. They were placed in a dilution apparatus, which was left overnight under dynamic vacuum. Subsequently, they were diluted by distilling the appropriate solvent into the apparatus.

1. Tselikas, Y.; Iatrou, H.; Hadjichristidis, N.; Liang, K. S.; Mohanty, K.; Lohse, D. J. *J Chem Phys* **1996**, 105, 2456.

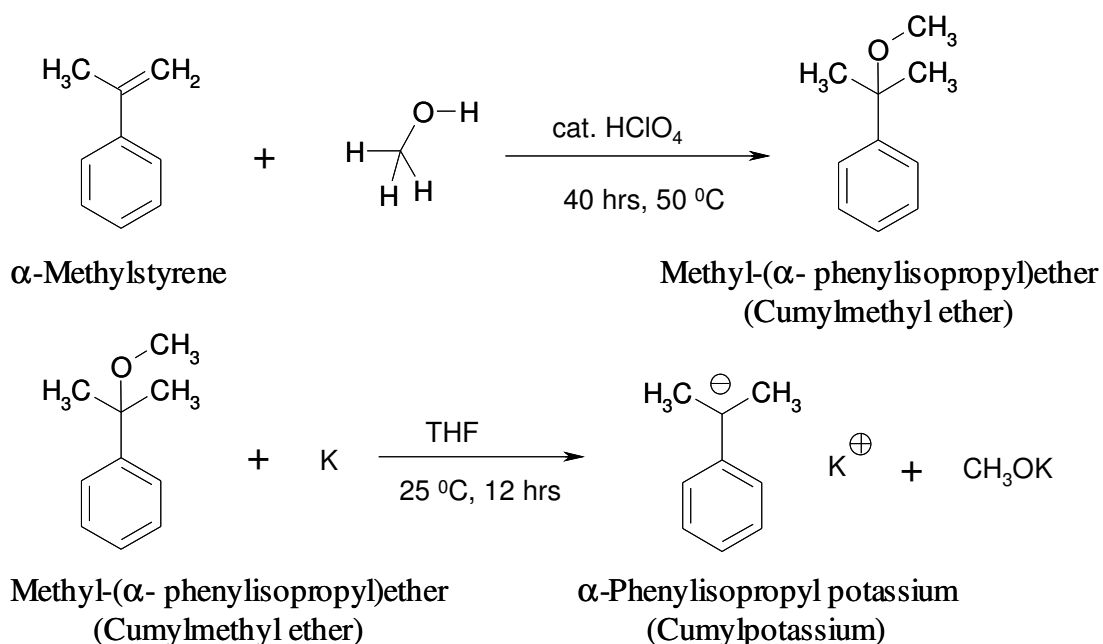
X.6. Preparation of Initiators.

X.6.1. Synthesis of Monofunctional Initiators

The most commonly used anionic initiator was *sec*-BuLi. This initiator is commercially available (Fluka, Aldrich) but it is less thermally stable than *n*-BuLi. The reported rate of decomposition is 1.4% per month at 20 °C.[2] This initiator can be synthesized by the reaction of *sec*-BuCl with Li metal[3,4] and kept in solution at low temperature. Under these conditions, the concentration does not change appreciably over a period of several months. In the current work only the commercial product was used.

Cumylpotassium was prepared according to the procedure described elsewhere[5,6] in two step reaction (Scheme X. 1)

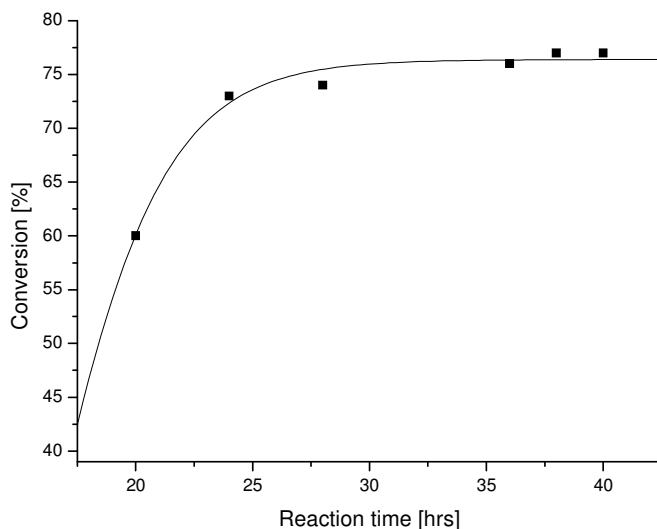
Scheme X. 1 Synthesis of cumylpotassium.



- Hsieh, H. L.; Quirk, R. P. *Anionic Polymerization: Principles and Practical Applications*; Marcel Dekker: New York, 1996.
- Ziegler, K.; Gellert, H. G. *Annales* **1950**, 567, 179.
- Urwin, J. R.; Reed, P. J. *J Organomet Chem* **1972**, 39, 1.
- Russel, G. A. *J. Am. Chem. Soc.*, **1957**, 79, 3871.
- Ziegler, K.; Dislich, H., „*Metallorganische Verbindungen*“, **1957**, 23, 1112.

At the first step α -methylstyrene (21.22 g, 180 mmol) is reacted with methanol (14.6 ml, 360 mmol) in the presence of catalytic amounts of HClO_4 (0.17 ml, 3 mmol) to form methyl(α -phenylisopropyl)ether (cumylmethyl ether). Small aliquots were taken from the reaction mixture for monitoring the yield of the target product and side products (oligomers of α -methylstyrene). The conversion of the reactants to the cumylmethyl ether was determined using the integral ratio between protons from the double bonds of α -methylstyrene and the protons of methoxy group of the cumylmethyl ether in the $^1\text{H-NMR}$ spectra:

Figure X. 2 Conversion / time dependence of the synthesis of cumylmethyl ether.



Practically, a maximum conversion of 77 % was reached after 35 h reaction time. The remaining 23% was mainly unreacted α -methylstyrene and oligomers of α -methylstyrene (less than 1%). In order to increase the conversion, the temperature was increased ($60\text{ }^\circ\text{C}$) at the end of the reaction. The conversion of cumylmethyl ether was slightly increased to 78 %, but conversion to oligo(α -methylstyrene) also increased to 1.5 %. The crude mixture was washed with aqueous NaOH (1%), and then with water to neutral pH, in order to remove the catalyst (HClO_4) and the majority of the methanol. After drying over CaCl_2 overnight, the rest of the methanol, unreacted α -methylstyrene and oligomers were separated from cumylmethyl ether by vacuum-distillation,

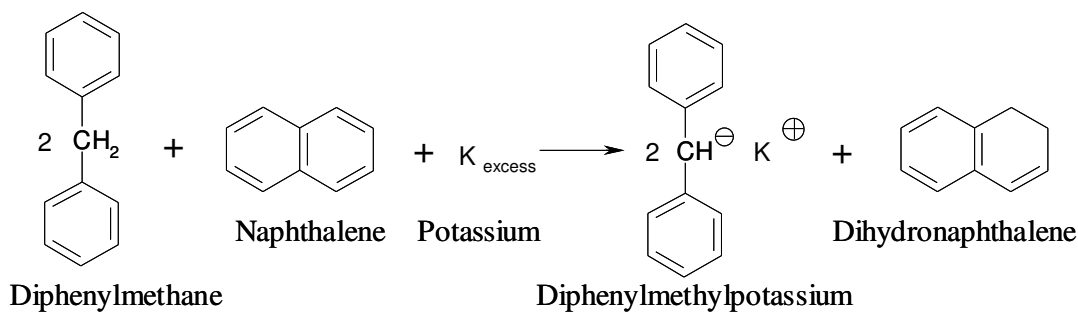
collecting the fraction at 23.0-23.5 °C by 0.6 mbar. The purity of the product was proven by $^1\text{H-NMR}$ spectroscopy to be 97% (3% α -methylstyrene). Yield 10.9 g (40%).

As a second step high vacuum technique was used to perform a reaction between cumylmethyl ether (10.9 g, 73 mmol) and potassium (7.1 g, 182 mmol) in THF (see Scheme X. 1). Initially, potassium mirror was made on the bottom of the flask followed by cryodistillation of the solvent. Cumylmethyl ether was added under high vacuum, turned the color to dark red and the mixture was shaken for 24 h at RT. Then, the mixture was cooled (-20 °C) and filtered under vacuum from the precipitated methoxypotassium (coproduct of cumylpotassium) and small potassium pieces and separated into different ampoules. One of the ampoules was used for determination the active concentration of the initiator by a titration method (see “Analysis of the initiators” below).

$C = 0.1479$ mol/l; Yield 67%.

Diphenylmethylpotassium was synthesized by an indirect metallation method as described in literature [7,8] (Scheme X. 2)

Scheme X. 2 Synthesis of diphenylmethylpotassium.



Initially, a potassium mirror (9.39 g, 240 mmol) was made on the bottom of the flask followed by addition a solution of naphthalene (10.25 g, 80 mmol) in THF (100 ml), which turned dark green in color. Then, diphenylmethane (26.8 ml, 160 mmol) dissolved in THF (50 ml) was added and the mixture was shaken for 48 h at RT. Finally, the reaction mixture was filtered under vacuum from the residual small potassium pieces and separated into ampoules. One

7. Candau, F.; Afchar-Taromi, F.; Rempp, P. *Polymer* **1977**, 18, 1253.

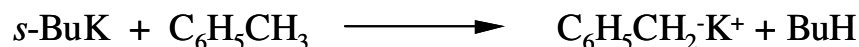
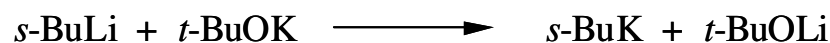
8. Normant, M.; Angelo, B. *Bull. Soc. Chim. Fr.* **1960**, 354

of the ampoules was used for determination the active concentration of the initiator by a titration method (see “Analysis of the initiators” below).

C = 0.7893 mol/l; Yield 74%.

Benzylpotassium was obtained by the reaction between toluene and “super base”. The “super base” was produced by the metal-exchange reaction between *s*-BuLi and *t*-BuOK:[9-11]

Scheme X. 3 Synthesis of benzylpotassium



“Super base” was prepared by mixing *t*-BuOK (2.95 g, 25 mmol) and *s*-BuLi (1.60 g, 25 mmol) in toluene (25 ml) which was used both as metallation reagent and as reaction solvent. The reaction was performed for 4 h at RT, which turned dark red. Then the rest of the toluene was evaporated and dry THF (150 ml) was cryodistilled. Finally, the reaction mixture was filtered under vacuum and separated into ampoules. One of the ampoules was used for determination the active concentration of the initiator by the “polymerization of styrene” method (see “Analysis of the initiators” below). C = 0.1367 mol/l; Yield 82%.

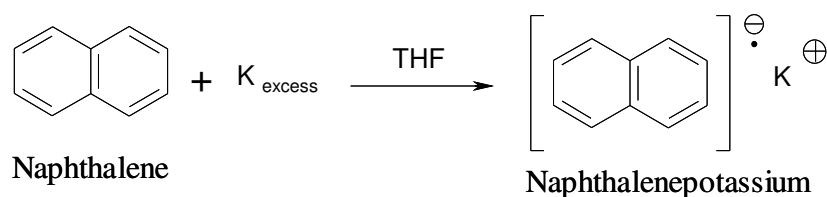
X.6.2. Preparation of Bifunctional Initiators

Naphthalene potassium is a common initiator for polymerization of styrene and butadiene leading to polymers with two living chain ends. The mechanism of initiation has been proven to be a reaction between naphthalene potassium anion radical and monomer molecule resulting in a styryl or butadienyl anion radical, which after recombination gives a dianion initiator. This initiator possessing two active sides can initiate further polymerization of monomer which propagation takes place at both ends of the polymer chain. Thus, naphthalene potassium is an

-
9. Ekizoglou, N.; Hadjichristidis, N.; *J. Polym. Sci. A: Polym. Chem.* **2001**, 39, 1198.
 10. Bucca, D.; Gordon, B.; *III Polym Prepr (Am Chem Soc Div Polym Chem)* **1990**, 31, 509.
 11. Lochmann, L.; Petranek, J. *Tetrahedron Letters*, **1991**, 32, 1483.

indirect initiator, which creates the dianion initiator after reaction with monomer molecule. Naphthalene potassium is very common deprotonation agent as well, and can create di- or multi anion initiators by deprotonation of di- or multi-hydroxyfunctionalized substances, that can serve as initiators for polymerization of oxirane derivatives. The reaction used for the preparation of naphthalene potassium is shown at Scheme X. 4. [12]

Scheme X. 4 Synthesis of naphthalene potassium



Potassium mirror (0.40 g, 10 mmol) was made on the bottom of the flask followed by addition of THF solution (80 ml) of naphthalene (0.385 g, 3 mmol) which turned dark green. The reaction mixture was shaken for 16 h at RT. Finally, the reaction mixture was filtered under vacuum from the small potassium pieces and separated into ampoules. One of the ampoules was used for determination of the active concentration of the initiator by a titration method (see “Analysis of the initiators” below). $C = 0.0312 \text{ mol/l}$; Yield 83%.

X.6.3. Analysis of the Initiators

The active concentration of the initiator could be determined by several methods. The simplest and most accurate methods are the following:

Titration Method

A known amount of the initiator solution was hydrolyzed, by pouring the ampoule contents into excess water. The resulting KOH was titrated with aqueous HCl solution to a phenolphthalein end point. Alternatively, the double titration method of Gilman and Haubein

12. Jerome, R.; Teyssie, Ph.; Huynh-Ba, G., “Anionic Polymerization. Kinetics, Mechanisms, and Synthesis”; Chapter 15 “Original anionic pathway to new PA(PO)₂ star-shaped block polymers based on polyvinyl or polydiene hydrocarbons and polyoxirane”, ACS Symposia series 166, **1981**.

[13,14] were used. According to this method a sample of the initiator solution was directly hydrolyzed and titrated and another sample of the same solution was reacted with benzylchloride in dichloromethane, followed by acid titration as well. With the second titration the residual alkalinity was determined due to any materials initially present in the solution, which do not contain C-O-K bonds.

Polymerization of Styrene

A known amount of styrene, purified according to the standards of anionic polymerization was polymerized by a known amount of initiator solution. The active concentration was calculated by means of the equation:

$$\text{Moles initiator} = \text{g monomer}/M_n$$

where M_n = the number-average molecular weight of the polystyrene formed, as determined by GPC.

X.7. Polymerization Procedures

The basic reactor and glassware used for the synthesis of linear homopolymers, block copolymers, star-shaped macromolecules, and core-shell structures are shown in Figure X. 1. The ampoules containing all necessary reagents: initiator and purified monomers were connected to the main reactor. The reactor was connected to the vacuum line through one of the ports (I), and alternatively evacuated and flushed with argon for 1 h in order to remove the volatile species such as air and moisture. Then the reactor was cooled down with liquid nitrogen, the valve connecting vacuum line and pump was closed and the valve to the solvent reservoir opened. Due to the vacuum in the system and the temperature gradient, the solvent was cryodistilled into the reactor (E). After distillation of a desired amount of solvent, the valve of the reactor port and the solvent reservoir were closed and the monomer was distilled followed by addition of the initiator and the ampoule was rinsed with solvent. Termination was accomplished by addition of several drops of a well-degassed termination agent enclosed in a separate ampoule.

13. Gilman, H.; Haubein, A. H. *J Am Chem Soc* **1944**, 66, 1515.

14. Gilman, H.; Cartlidge, K. F. *J Organomet Chem* **1964**, 2, 447.

X.7.1. Synthesis of Homopolymers

Poly(ethylene oxide):

Ethylene oxide (see Table X.1) and THF (100 ml) were consecutively cryodistilled into the reactor. Initiator was added (through glass filter G3 in **4.8**) and polymerization was performed at 40 °C for 3 days. An excess of HCl was added in order to terminate the reaction. The product was precipitated from hexane, filtered and dried at 30 °C under dynamic vacuum.

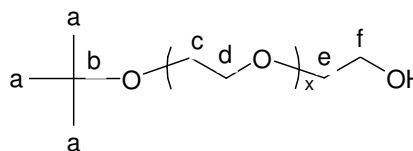


Table X. 1 Type and amounts of initiators and ethylene oxide. Yield of the homopoly(ethylene oxide).

No	Initiator			Ethylene oxide ml, mmol	Yield g, [%]
	Type*	C mol/l	ml, mmol		
4.1	CP	0.150	0.50, 0.08	8.50, 170	4.23, 55
4.2	BOK	0.031	10.0, 0.31	3.50, 71	0.70, 22
4.3	BuOK	1.000	2.20, 2.20	20.0, 400	17.46, 99
4.4	BuOK	1.000	0.51, 0.51	0.38, 7.7	0.31, 92
4.5	BuOK	1.000	0.16, 0.16	0.13, 2.5	0.08, 73
4.6	BuOK	1.000	2.70, 2.70	2.00, 40	1.25, 71
4.7	BuOK	1.000	3.30, 3.30	2.50, 50	0.97, 44
4.8	NP	0.060	10.0, 0.60	3.50, 70	2.84, 92

* CP-cumylpotassium; BOH-benzylalcohol; NP-naphthalene potassium; BuOK-potassium-*tert.*-butoxide.

¹H-NMR (250 MHz, CD₂Cl₂, RT) δ, ppm: 3.6 (s, H_{cd}), 1.1 (s, H_a);

¹³C-NMR (75 MHz, CD₂Cl₂, RT) δ, ppm: 70 (C_{d,f}), 69 (C_c), 65 (C_f), 30 (C_a);

MALDI-TOF (matrix dithranol, THF, without salt) m/z (**4.3**): M_n 7 640 and PDI 1.02.

GPC (water – eluent, PEO – standard):

No	M _n	PDI
4.1	74 000	1.21
4.2	4 000	1.23

4.3	7 300	1.06
4.4	1 700	1.23
4.5	1 100	1.18
4.6	650	1.11
4.7	340	1.33
4.8	13 700	1.09

TGA/DSC (4.3): Decomposition interval 115 - 540 °C (101.6%) with maximum rate of degradation at 374.8 °C. $T_g = 62.29$ °C;

Elemental analysis (4.3): Calculated: C 54.54% H 9.09%

Obtained: C 53.86%, H 8.72%

End-hydroxyfunctionalized polystyrene (PS-OH).

Styrene (see Table X.2) and solvent THF (Cyclohexane in **4.6**) (100 ml) were consecutively cryodistilled into reactor, *sec*-butyllithium was added and polymerization was performed for 1 h at -77 °C in THF (increasing the temperature from -77 to 50 °C for 3 h in cyclohexane). The color of the reaction mixture turned to orange-red. Ethylene oxide was distilled into the reactor and the mixture was heated at 50 °C for 1 h. An excess of HCl was added, in order to terminate the reaction. The product was precipitated from methanol, filtered, and dried at 40 °C under dynamic vacuum for 48 h.

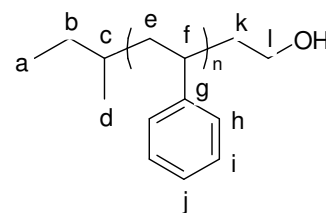


Table X. 2 Amounts of initiator and monomers, yield of the obtained homopolystyrene.

Exp No	<i>s</i> -BuLi (1.3M) ml, mmol	Styrene ml, mmol	Ethylene oxide ml, mmol	Yield g, [%]
6.1	1.0, 1.27	7.0, 61	0.3, 6.35	1.27, 19
6.2	4.0, 5.2	5.7, 50	2.6, 52	2.18, 42
6.3	7.0, 9.1	10.0, 87	4.5, 91	3.00, 33
6.4	7.0, 9.1	10.0, 87	4.5, 91	7.82, 86
6.5	7.0, 9.1	10.0, 87	4.5, 91	7.55, 83
6.6	7.0, 9.1	10.0, 87	4.5, 91	8.64, 95

$^1\text{H-NMR}$ (250 MHz, CD_2Cl_2 , RT) δ , ppm: 7.3-6.3 (obp, H_{high}), 3.6 (s, H_l), 2.1-1.7 (m, H_f), 1.7-1.2 (m, H_e), 0.8 (m, H_{bc}), 0.7 (m, H_{ad});

$^{13}\text{C-NMR}$ (75 MHz, CD_2Cl_2 , RT) δ , ppm: 146 (C_g), 128 (C_{hi}), 126 (C_j), 60 (C_l), 44 (C_e), 40 (C_f), 31 (C_c), 30 (C_b), 16 (C_d), 11 (C_a);

MALDI-TOF (6.6) (matrix dithranol, THF, Li^+) m/z : homologous series with repetitions $m/z_{\text{calc.}} = 104$, $m/z_{\text{found}} = 104 \pm 2$, and maximum at $m/z = 2\ 312$ with M_n 2 434 and PDI 1.08.

GPC (THF – eluent, PS – standard):

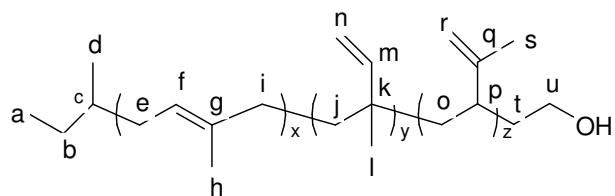
No	M_n	PDI
6.1	4 000	1.7
6.2	3 200	1.30
6.3	4 200	1.35
6.4	3 800	1.18
6.5	3 300	1.23
6.6	2 200	1.08

TGA/DSC (6.6): Decomposition interval 180 – 525 $^{\circ}\text{C}$ (99.7%) with maximum rate of degradation at 437.5 $^{\circ}\text{C}$. $T_g = 69.17$ $^{\circ}\text{C}$;

Elemental analysis (6.6):
 Calculated: C 91.33% H 7.95%
 Obtained: C 90.82%, H 7.89%

End-hydroxyfunctionalized polyisoprene (PI-OH).

Isoprene (10.0 ml, 100 mmol) and THF (100 ml) were consecutively cryodistilled into reactor. *sec*-Butyllithium (10.5 ml, 1.3 M, 6.8 mmol) was added and polymerization was performed for 3 h while increasing the temperature from -77 to 0 $^{\circ}\text{C}$. The color of the reaction mixture changed to yellow. Ethylene oxide (4.5 ml, 91 mmol) was distilled into the reactor and the mixture was heated at 50 $^{\circ}\text{C}$ for 30 minutes. An excess of



HCl was added in order to terminate the reaction. The product was precipitated from water and extracted with diethylether. The organic layers were collected and dried over magnesium sulfate. The solvent was evaporated and the residue was dried at 40 °C under dynamic vacuum for 48 h. Yield: 6.23 g (91%).

¹H-NMR (250 MHz, CD₂Cl₂, RT) δ, ppm: 5.8 (s, H_m), 5.1-4.8 (m, H_{fn}), 4.6 (d, H_r), 3.7-3.4 (m, H_{zu}), 2.3-1.8 (m, H_{pei}), 1.6 (s, H_{sh}), 1.5-1.1 (m, H_o), 1.1-0.9 (m, H_j), 0.8 (m, H_l), 0.7 (m, H_{ad}).

¹³C-NMR (75 MHz, CDCl₃, RT) δ, ppm: 152 (C_q), 148 (C_m), 136 (C_g), 124 (C_f), 111 (C_n), 109 (C_r), 63 (C_u), 42 (C_j), 40 (C_{ip}), 37 (C_t), 35 (C_c), 32 (C_o), 31 (C_b), 28 (C_l), 23 (C_e), 21 (C_d), 18 (C_s), 16 (C_h), 11 (C_a).

MALDI-TOF (matrix dithranol, THF, Ag⁺) m/z: homologous series with repetitions m/z_{calc.} = 68, m/z_{found} = 68±2, and maximum at m/z = 687 with M_n 894 and PDI 1.09.

GPC (THF – eluent, PI – standard): M_n 700 and PDI 1.11.

TGA/DSC (6.21): Decomposition interval 90 – 530 °C (98.9%) with maximum rate of degradation at 433.0 °C. T_g = -33.56 °C;

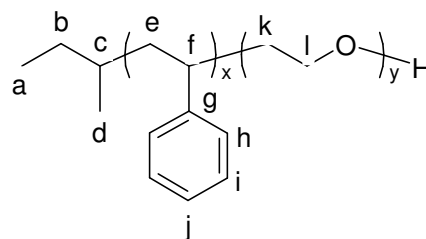
Elemental analysis (6.21): Calculated: C 85.71% H 12.04%
 Obtained: C 84.87%, H 11.95%

X.7.2. Synthesis of diblock copolymers

Poly(styrene-b-ethylene oxide) (PS-b-PEO):

General procedure (6.7-6.19):

Styrene (see **Table X. 3**) and THF (100 ml) were consecutively cryodistilled into the reactor. Initiator was added and polymerization of styrene was performed at - 77 °C for 1 h. An aliquot was taken for determination of M_n of the polystyrene block. Then, ethylene oxide was distilled into the reactor and temperature increased to 40 °C. The mixture was stirred at this temperature for 3-7 days, depending on the desired length of the PEO chains. An excess of HCl was added in order to terminate the reaction. The product was precipitated from hexane, collected by filtration, and dried at 40 °C under dynamic vacuum for 48 h.



Synthesis of PS-b-PEO using end-hydroxyfunctionalized polystyrene (PS-OH) (6.6) as anionic macroinitiator:

PS-OH (3.0 g, 1.4 mmol) (product **6.6** see Table X.2) was introduced into reactor and dried at 40 °C overnight. THF (100 ml) was cryodistilled and the solution was titrated with a THF solution of naphthalene potassium (~0.1M) at 0 °C until the slight green color persisted for more than 2 min. After 30 minutes ethylene oxide (4.0 ml, 80 mmol) was distilled into the reactor and the mixture was kept at 22 °C for 3 h. Then the reaction mixture was heated at 50 °C for 6 days. An excess of HCl was added in order to terminate the polymerization. The product was precipitated in diethylether at -77 °C, collected by filtration and dried under dynamic vacuum for 48 h.

Table X. 3 Type and amounts of initiator and monomers. Yield of the obtained polymers.

No	Initiator			Styrene ml, mmol	EO ml, mmol	Yield g, [%]
	Type	C mol/l	ml, mmol			
6.7	CP	0.410	4.00, 1.64	5.40, 47	11.50, 230	7.87, 52
6.8	CP	0.410	3.40, 1.4	6.00, 53	6.20, 124	8.47, 77
6.9	CP	0.410	3.40, 1.4	6.00, 53	6.20, 124	8.25, 73
6.10	CP	0.410	3.40, 1.4	7.70, 67	7.9, 159	7.75, 55
6.11	CP	0.410	2.00, 0.82	5.40, 47	9.00, 180	4.20, 30
6.12	CP	0.465	1.95, 0.91	1.00, 8.7	3.08, 62	3.63, 97
6.13	CP	1.250	1.00, 1.25	3.40, 36	4.30, 85	5.80, 77
6.14	CP	1.250	1.00, 1.25	2.70, 24	2.80, 57	2.22, 45
6.15	DPMP	0.630	1.07, 0.68	1.50, 13	2.45, 49	2.30, 65
6.16	BP	0.012	1.70, 2x10 ⁻⁵	9.46, 82.6	14.6, 293	7.60, 35
6.17	BuLi/BuP ₄	1.300	0.54, 0.70/0.72	8.00, 70	11.00, 220	11.88, 70
6.18	BuLi/BuP ₄	1.300	0.70, 0.91/1.36	1.00, 8.7	3.10, 61.9	3.60, 99
6.19	BuLi/BuP ₄	1.300	0.30, 0.39/0.78	2.2, 18.7	3.30, 66.4	4.84, 99
6.20	PS-OH/NP*	M _n 2 200	3 g, 1.36	-	4.00, 80	6.03, 92

CP-cumylpotassium; DPMP-diphenylmethyl potassium; BP-benzyl potassium; BuP₄-phosphazene-base; NP-naphthalene potassium.

Experimental part

* PS-OH – hydroxyl end-functionalized polystyrene (**6.6**) as anionic macroinitiator.

¹H-NMR (250 MHz, CD₂Cl₂, RT) δ, ppm: 7.3-6.3 (obp, H_{hij}), 3.6 (s, H_{kl}), 2.1-1.7 (m, H_f), 1.7-1.2 (m, H_e), 0.8 (m, H_b), 0.7 (m, H_{ad});

¹³C-NMR (75 MHz, CDCl₃, RT) δ, ppm: 145 (C_g), 128 (C_{hi}), 126 (C_j), 73 (C_k next to PS), 70 (C_{kl}), 62 (C_l nex to OH), 44 (C_e), 40 (C_f), 31 (C_c), 30 (C_b), 18 (C_d), 11 (C_a);

MALDI-TOF (matrix dithranol, K⁺) m/z (**6.20**): homologous series with maximum at m/z = 5 817 with M_n 5 684 and PDI 1.03.

GPC (THF – eluent, PS – standard):

No	M _n PS	PDI	M _n PS-b-PEO	PDI
6.7	58 000	1.28	65 000	1.19
6.8	12 500	1.25	30 800	1.05
6.9	37 000	2.43	41 000	1.18
6.10	25 000	1.56	36 000	1.12
6.11	32 000	1.50	36 500	1.07
6.12	8 600	1.13	14 700	1.18
6.13	4 100	1.53	8 500	1.07
6.14	3 000	1.70	6 000	1.11
6.15	36 600	1.25	45 000	1.06
6.16	670 000	1.23	790 000	1.21
6.17	700 000	1.43	800 000	1.44
6.18	2 000	2.37	12 000	1.18
6.19	3 500	1.07	15 000	1.23
6.20	2 200	1.08	6 000	1.07

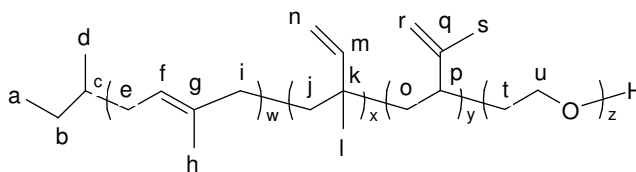
TGA/DSC (**6.20**): Decomposition interval 70 - 520 °C (100.7%) with maximum rate of degradation at 295.5 °C. T_g = 49.86 °C;

Elemental analysis (**6.20**): Calculated: C 70.51%, H 8.50%
 Obtained: C 71.30%, H 8.36%

*Poly(isoprene-*b*-ethylene oxide) (PI-*b*-PEO):*

General procedure (exp 6.22 – 6.26):

Isoprene (see Table X.4) and THF (100ml) were consecutively cryodistilled into the reactor. Initiator was added (in case of



BuLi/BuP₄, BuP₄ was previously dried in the reactor) and polymerization of isoprene was performed at -77 °C with the temperature increases slowly to 22 °C for 3 h. An aliquot was taken for determination of M_n of the polyisoprene block. Then ethylene oxide was distilled into the reactor and the temperature increased to 40 °C. The mixture was stirred at this temperature for 3-7 days, depending on the desired length of the PEO block. An excess of HCl was added in order to terminate polymerization. The product was precipitated in hexane, filtered, and dried at 30 °C under dynamic vacuum for 48 h.

*Synthesis of PI-*b*-PEO using end-hydroxyfunctionalized polyisoprene (PI-OH) as anionic macroinitiator (6.21):*

PI-OH (2.1 g, 2.8 mmol) was introduced into reactor and dried at 30 °C overnight. THF (60 ml) was cryodistilled and the solution was titrated by THF solution of naphthalene potassium (~0.1M) at 0 °C until the slight green color persisted for more than 2 min. After 30 minutes ethylene oxide (4.0 ml, 80 mmol) was distilled into the reactor and the mixture was kept at 22 °C for 3 h. Then, the reaction mixture was heated at 50 °C for 4 days. An excess of HCl was added in order to terminate polymerization. The product was precipitated in hexane at -30 °C, collected by filtration and dried under dynamic vacuum for 48 h. Yield: 5.0 g (90%).

Table X. 4 Type and amounts of initiator and monomers. Yield of the obtained polymers.

No	Initiator			Isoprene ml, mmol	EO ml, mmol	Yield g, [%]
	Type	C mol/l	ml, mmol			
6.22	DPMP	0.63	2.15, 1.35	2.0, 20	3.1, 60	1.08, 27
6.23	DPMP	0.63	4.30, 2.7	4.0, 40	3.8, 77	2.70, 44
6.24	BuLi/BuP ₄	1.30	0.77, 1/1.1	4.4, 44	2.6, 51	2.44, 46
6.25	BuLi/BuP ₄	1.30	0.77, 1/1.6	2.9, 29	5.7, 114	5.61, 80
6.26	BuLi/BuP ₄	1.30	0.83, 1.1/1.5	4.8, 48	5.9, 118	5.74, 68
6.27	PI-OH/NP*	M _n 700	2.08 g, 2.78	-	4.0, 80	5.00, 90

DPMP-diphenylmethyl potassium; BuP₄-phosphazene-base; NP – naphthalene potassium

* PI-OH – hydroxyl end-functionalized polyisoprene (**6.21**) as anionic macroinitiator.

¹H-NMR (250 MHz, CD₂Cl₂, RT) δ, ppm: 5.8 (s, H_m), 5.1-4.8 (m, H_{fn}), 4.6 (s, H_r), 3.6 (s, H_{tw}), 2.3-1.8 (m, H_{pei}), 1.6 (s, H_{sh}), 1.5-1.1 (m, H_o), 1.1-0.9 (m, H_j), 0.8 (m, H_l), 0.7 (m, H_{a,d}).

¹³C-NMR (75 MHz, CDCl₃, RT) δ, ppm: 151 (C_q), 147 (C_m), 139 (C_g), 123 (C_f), 111 (C_{nr}), 73 (C_t next to PI), 70 (C_{tu}), 62 (C_u next to OH), 45 (C_p), 42 (C_j), 40 (C_i), 32 (C_o), 30 (C_b), 28 (C_l), 23 (C_e), 20 (C_{dh}), 18 (C_s), 11 (C_a);

MALDI-TOF of **6.27** (matrix dithranol, without salt): maximum at m/z = 1 362 with M_n 1 395 and PDI 1.15.

GPC (THF – eluent, PI – standard):

No	M _n PI	PDI	M _n PI-b-PEO	PDI
6.22	20 000	1.32	23 000	1.22
6.23	27 000	1.60	34 000	1.32
6.24	3 300	1.36	5 000	1.08
6.25	3 400	1.33	5 200	1.24
6.26	2 500	1.36	5 700	1.21
6.27	700	1.11	1 400	1.12

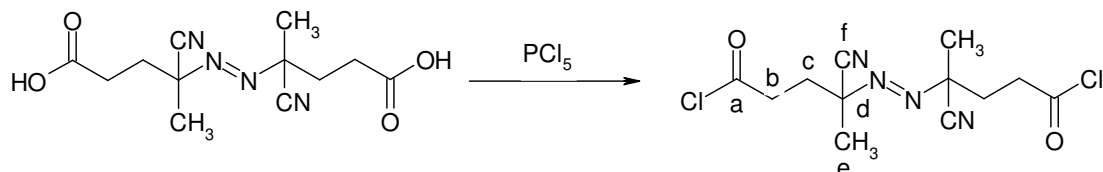
TGA/DSC (**6.27**): Decomposition interval 150 - 550 °C (98.5%) with maximum rate of degradation at 332 °C. T_g = 39.6 °C;

Elemental analysis (6.27): Calculated: C 70.74% H 10.63%
 Obtained: C 64.78%, H 9.63%

X.7.3. Synthesis of macroinitiators for radical polymerization.

1. 4,4'-azobis(4-cyanopentanoyl chloride) (ABCPC).

4,4'-Azobis(4-cyanopentanoyl chloride) was prepared according to the procedure previously published.[15]



A mixture of 4,4'-azobis(4-cyanopentanoic acid) (0.50 g, 1.8 mmol) in methylene chloride (5 ml) was chilled in an ice bath and treated with PCl_5 (1.87 g, 9 mmol). Stirring was continued for 3 h at 0°C , then the reaction was continued at RT overnight. The solution was filtered (removing unreacted PCl_5) and concentrated to a pasty solid. The phosphorus oxychloride was removed by leaching with 3x3 ml portions of ether/hexane (1:3). The product was precipitated from methylenechloride with cool hexane. Yield: 0.38 g (66%).

m.p. 77.1-78.5 $^\circ\text{C}$;

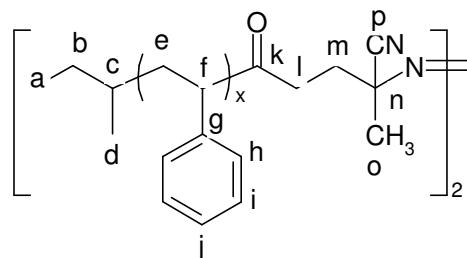
$^1\text{H-NMR}$ spectroscopy (250 MHz, $\text{C}_2\text{D}_2\text{Cl}_4$, RT) δ , ppm: 3.2-2.9 (m, H_b), 2.5-2.2 (m, H_c), 1.6 (s, H_e);

$^{13}\text{C-NMR}$ spectroscopy (75 MHz, $\text{C}_2\text{D}_2\text{Cl}_4$, RT) δ , ppm: 174 (C_a), 117 (C_f), 72 (C_d), 42 (C_b), 33 (C_c), 24 (C_e);

FD-mass-spectrum: 144 (M^+);

Elemental analysis: Calculated: C 45,44% H 4.45% N 17.66%
 Obtained: C 45,36%, H 4.49% N 17.65%

15. Smith, D. A., *Macromol. Chem.* **1967**, 103, 301.



2. *Synthesis of polystyrene macroinitiator*: Styrene (see Table X.5) and THF (100 ml) were consecutively cryodistilled into reactor. *sec*-Butyllithium was added and polymerization of styrene was performed at $-77\text{ }^{\circ}\text{C}$ for 1 h. The color of the reaction mixture turned to orange-red. An aliquot of 20 ml was taken for determination molecular weight of polystyrene. THF (20 ml) solution of ABCPC was added dropwise into the reactor (the temperature of the reaction mixture did not exceed $5\text{ }^{\circ}\text{C}$), and the mixture was stirred at $0\text{ }^{\circ}\text{C}$ over night. The product was precipitated from methanol, collected and dried at RT under dynamic vacuum for 24 h.

Table X. 5 Amounts of initiator, styrene and ABCPC, yield of the obtained macroinitiator.

No	<i>s</i> -BuLi (1.3M) ml, mmol	Styrene ml, mmol	ABCPC g, mmol	Yield g, [%]
8.1	3.12, 2.4	2.6, 23	0.30, 0.95	1.15, 48
8.2	3.12, 2.4	2.6, 23	0.30, 0.95	0.89, 37
8.3	3.12, 2.4	13.2, 115	0.30, 0.95	11.50, 96
8.4	3.12, 2.4	13.2, 115	0.30, 0.95	10.66, 89
8.5	3.12, 2.4	13.2, 115	0.30, 0.95	10.90, 91

$^1\text{H-NMR}$ (250 MHz, $\text{C}_2\text{D}_2\text{Cl}_4$, RT) δ , ppm: 7.3-6.3 (obp, H_{hij}), 2.5-2.3 (m, H_{lm}), 2.1-1.7 (m, H_f), 1.7-1.6 (m, H_o), 1.6-1.2 (m, H_e), 0.8 (m, H_b), 0.7 (m, H_{ad}).

$^{13}\text{C-NMR}$ (75 MHz, CDCl_3 , RT) δ , ppm: 145 (C_g), 128 (C_{hi}), 126 (C_j), 117 (C_p), 126, (C_f next to $\text{C}=\text{O}$), 44 (C_f), 40 (C_e), 32 (C_c), 31 (C_b), 30 (C_i), 29 (C_m), 20 (C_d), 19 (C_o), 11 (C_a);

GPC (THF – eluent, PS - standard):

No	Polystyrene before reaction with ABCPC		PS-azo-PS	
	M_n	PDI	M_n	PDI
8.1	1 080	1.42	1 900	1.66
8.2	940	1.71	2 000	1.55
8.3	3 400	1.41	6 900	1.54
8.4	4 400	1.16	9 300	1.38
8.5	8 300	1.11	12 600	1.39

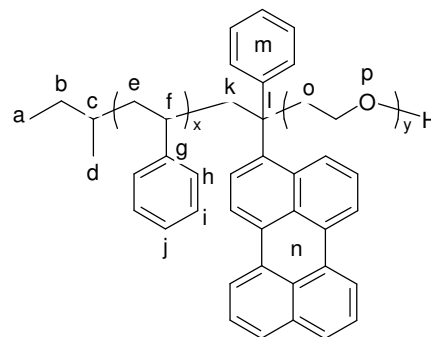
Elemental analysis (8.4):	Calculated:	C 91.32%	H 7.74%	N 0.60%
	Obtained:	C 90.50%,	H 7.93%	N 0.26%

X.7.4. Synthesis of diblock copolymers bearing 3-(1-phenyl-vinyl)-perylene (dye)

molecule between the blocks

Poly(styrene-dye-ethylene oxide):

Styrene (2.00 g, 17.3 mmol) and THF (100 ml) were consecutively cryodistilled into the reactor. *sec*-Butyllithium (0.46 ml, 1.3M, 0.60 mmol) was added (BuP₄ (1.0 ml, 1M, 1.0 mmol) was previously dried into reactor overnight) and polymerization of styrene was performed at -77 °C for 1h. A solution of dye 0.2124 g (0.60 mmol) in THF (20 ml) was poured into the reaction mixture and stirred for 30 min while increasing the temperature from -77 to 20 °C. An aliquot was taken for determination of M_n of the polystyrene block and presence of dye. Then ethylene oxide 3.26 ml (65 mmol) was distilled into the reactor at 0 °C, the temperature was increased to 40 °C, and the mixture was stirred at this temperature for 3 days. An excess of HCl was added in order to terminate polymerization. The product was twice precipitated from diethyl ether, collected on a filter, and washed with diethyl ether in order to remove unreacted dye. The product was dried at 40 °C under dynamic vacuum for 48 h. Yield: 4.438 g (90%).



¹H-NMR (250 MHz, C₂D₂Cl₄, RT) δ, ppm: 8.1 (m, H_n), 7.6-7.4 (m, H_m), 7.3-6.3 (obp, H_{hij}), 3.6 (s, H_{op}), 2.1-1.7 (m, H_f), 1.7-1.2 (m, H_e), 0.8 (m, H_b), 0.7 (m, H_{ad}).

¹³C-NMR (75 MHz, CDCl₃, RT) δ, ppm: 145 (C_g), 141 (C_m), 139 (C_{mn}), 133 (C_{mn}), 128 (C_{hi}), 126 (C_j), 70 (C_{op}), 61 (C_p next to dye), 50 (C_{kp} next to dye), 40 (C_f), 37 (C_e), 33 (C_c), 32 (C_b), 20 (C_d), 12 (C_a);

GPC (THF – eluent, PS – standard): PS-dye M_n 6 000 (PDI 1.14), PS-dye-PEO M_n 7 400 (PDI 1.16).

MALDI-TOF (matrix dithranol, THF, without salt): M_n 8 620 and PDI 1.02.

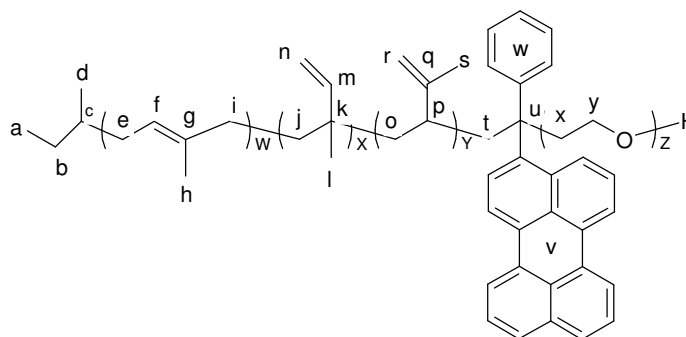
UV-VIS spectroscopy (in THF) λ_{max} = 454 nm, quartet of maximums characteristic for perylene

λ_{max} = 454, 429, 407, 390 nm.

TGA/DSC (5.24): Decomposition interval 120 - 580 °C (92.3%) with maximum rate of degradation at 405.5 °C. $T_g = 54.35$ °C;

Elemental analysis (5.24): Calculated: C 68.85% H 8.50%
 Obtained: C 63.44%, H 8.64%

Poly(isoprene-dye-ethylene oxide):



Isoprene (2.64 ml, 26 mmol) and THF (100 ml) were consecutively cryodistilled into the reactor containing dry phosphazene-base t-Bu-P4 (1 ml (1M), 1 mmol) (BuP₄). *sec*-Butyllithium (0.46 ml (1.3M), 0.6 mmol) was added and polymerization of isoprene was performed at -77 °C for 3 h. THF (25 ml) solution of dye (0.21 g, 0.6 mmol) was poured into reaction mixture and stirred for 40 min while increasing the temperature from -77 to 20 °C. An aliquot was taken for determination of M_n of the polystyrene block and presence of dye. Then ethylene oxide (3.26 ml, 65 mmol) was distilled into the reactor at 0 °C, the temperature was increased to 40 °C, and the mixture was stirred at this temperature for 3 days. An excess of HCl was added in order to terminate polymerization. The product was twice precipitated from diethylether, collected on a filter, and washed with diethylether in order to remove unreacted dye. The product was dried at 30 °C under dynamic vacuum for 48 h. Yield: 3.73 g (76%).

¹H-NMR (250 MHz, C₂D₂Cl₄, RT) δ , ppm: 8.1 (m, H_v), 7.6-7.4 (m, H_w), 5.7 (s, H_m), 5.1-4.8 (m, H_{nf}), 4.8-4.5 (d, H_r), 3.6 (s, H_{xy}), 2.3-1.8 (m, H_{pei}), 1.6 (s, H_{sh}), 1.5-1.1 (m, H_o), 1.1-0.9 (m, H_{sh}), 0.8 (m, H_j), 0.7 (m, H_{ad}).

¹³C-NMR (75 MHz, CDCl₃, RT) δ , ppm: 151 (C_q), 147 (C_m), 143 (C_w), 134 (C_g), 132 (C_v), 127 (C_{fwv}), 112 (C_n), 108 (C_r), 70 (C_{xy}), 62 (C_y next to dye), 48 (C_x next to dye), 42 (C_j), 40 (C_{ip}), 35 (C_c), 32 (C_b), 30 (C_{eo}), 22 (C_l), 18 (C_{shd}), 11 (C_a);

GPC (THF – eluent, PI – standard): PI M_n 4 000 (PDI 1.53), PI-b-PEO M_n 4 800 (PDI 1.31).

MALDI-TOF (matrix dithranol, THF, K⁺): M_n 6 560 and PDI 1.02.

UV-VIS spectroscopy (in THF) $\lambda_{\text{max}} = 454$ nm, characteristic quartet for perylene $\lambda = 454, 429, 407, 390$ nm.

TGA/DSC (5.25): Decomposition interval 90 - 590 °C (96.6%) with maximum rate of degradation at 426.8 °C. $T_g = 58.47$ °C;

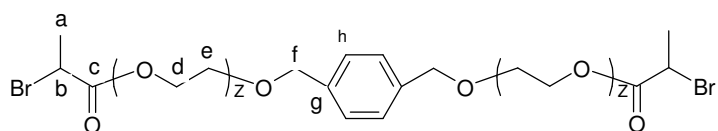
Elemental analysis (5.25): Calculated: C 64.48% H 9.66%
 Obtained: C 67.45%, H 9.49%

X.7.5. Synthesis of triblock copolymers (model reaction for preparation of core-double-shell macromolecules by grafting-from method)

Poly(styrene-b-ethylene oxide-b-styrene) (PS-b-PEO-b-PS).

1. *Synthesis of PEO bifunctional ATRP macroinitiator:*

4-(Hydroxymethyl)-benzylalcohol (0.081 g, 0.6 mmol – 1.2 mmol OH-groups) was introduced into the reactor



followed by cryodistillation of THF (100 ml). The alcohol was titrated with a THF solution (25 ml) of naphthalene potassium (5.8 mmol) at 0 °C until the slight green color persisted for more than 2 min. After 30 minutes ethylene oxide (4.0 ml, 81 mmol) was distilled into the reactor and the mixture was heated at 40 °C for 64 h. 2-Bromopropionyl bromide (0.19 ml, 1.75 mmol) dissolved in THF (20 ml) was added in order to end-bromofunctionalize the PEO and terminate the polymerization reaction. The product was precipitated from diethyl ether, collected on a filter and dried under dynamic vacuum for 48 h. Yield: 3.55g (98%).

¹H-NMR (250 MHz, CD₂Cl₂, RT) δ , ppm: 7.3 (s, H_h), 4.5 (s, H_f), 4.4 (q, H_b), 4.3 (t, H_d), 3.6 (s, H_{de}), 1.8 (d, H_a).

¹³C-NMR (62.5 MHz, CD₂Cl₂, RT) δ , ppm: 171 (C_c), 138 (C_g), 128 (C_h), 72 (C_f), 70 (C_{de}), 61 (C_d to C=O gr), 40 (C_b), 22 (C_a);

GPC (DMF – eluent, PEO – standard): M_n 4 700, PDI 1.31.

MALDI-TOF (matrix dithranol, THF, K⁺): M_n 2 470 and PDI 1.08.

TGA/DSC (6.28): Decomposition interval 120 - 550 °C (96.5%) with maximum rate of degradation at 258.2 °C. $T_g = 54.59$ °C;

Elemental analysis (6.28): Calculated: C 51.22% H 8.36%

Obtained: C 51.38%, H 8.33%

2. Synthesis of poly(styrene-*b*-ethylene oxide-*b*-styrene) (PS-*b*-PEO-*b*-PS).

PEO bifunctional ATRP macroinitiator, Cu^IBr, *N*-hexadeca-2-pyridylmethanimine (ligand) in molar ratio 1/2/4 and styrene (see Table X. 6) were dissolved in *m*-xylene (25 ml). The mixture was degassed and heated at 110 °C for 24 h. The product was precipitated from hexane, collected by filtration, and dried at 40 °C under dynamic vacuum for 48 h.

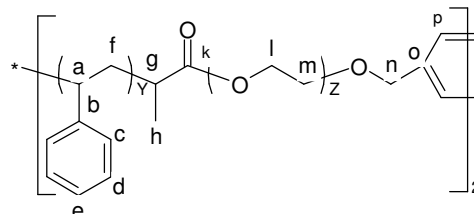


Table X. 6 Amounts of initiator, Cu^IBr, ligand. Yield of the obtained polymers.

No	Initiator g, mmol	Cu ^I Br g, mmol	Ligand g, mmol	Styrene ml, mmol	Yield g, [%]
6.29	0.5, 0.1	0.03, 0.2	0.14, 0.4	0.23, 2	0.48, 67
6.30	0.5, 0.1	0.03, 0.2	0.14, 0.4	0.23, 2	0.58, 83
6.31	1.0, 0.2	0.06, 0.4	0.28, 0.8	0.46, 4	1.19, 81

¹H-NMR (250 MHz, CD₂Cl₂, RT) δ, ppm: 7.3 (s, H_p), 7.3-6.3 (obp, H_{cde}), 4.5 (s, H_n), 3.6 (s, H_{lm}), 1.8-1.2 (obp, H_{fagh}).

¹³C-NMR (62.5 MHz, CD₂Cl₂, RT) δ, ppm: 137 (C_b), 127 (C_{cd}), 126 (C_e), 73 (C_n), 70 (C_{lm}), 48 (C_f), 32 (C_a), 14 (C_h);

GPC (DMF – eluent, PEO – standard):

No	Mn PS-PEO-PS	PDI
6.29	7 800	1.39
6.30	7 000	1.44
6.31	8 800	1.35

MALDI-TOF (matrix dithranol, THF, without salt): **(6.29)** M_n 7 340 and PDI 1.03; **(6.30)** M_n 8 160 and PDI 1.04; **(6.31)** M_n 4 960 and PDI 1.04;

TGA/DSC: **(6.29)** Decomposition interval 100 - 585 °C (89.9%) with maximum rate of degradation at 407.2 °C, T_g = 48.50 °C; **(6.30)** Decomposition interval 170 - 590 °C (91.1%) with maximum rate of degradation at 398.8 °C, T_g = 48.82 °C; **(6.31)** Decomposition interval 80 - 590 °C (91.1%) with maximum rate of degradation at 383.3 °C, T_g = 48.97 °C;

Elemental analysis (6.31): Calculated: C 56.14% H 9.03%
 Obtained: C 55.95%, H 8.37%

X.8. Synthesis of core-*mono*-shell macromolecules

X.8.1. PEO grafting-onto TdG₂(CH₂Cl)₋₁₂.

Variable amounts of ethylene oxide (see Table X.7) were added to THF solution of potassium *tert*-butoxide (100 ml) and polymerization was carried out at 40 °C for 6, 16 or 69 h respectively (**4.9**, **4.10**, **4.11**). Aliquots (50 ml) were taken from each reaction mixture to determine M_n of the single PEO chains prior to addition of TdG₂(CH₂Cl)₋₁₂. Then THF solution (20 ml) of TdG₂(CH₂Cl)₋₁₂ was added and the reaction was continued at 40 °C for 48, 69 or 96 h respectively (**4.9**, **4.10**, **4.11**). The reaction mixtures as well as the samples taken were precipitated in a 15-fold excess of hexane. The excess of PEO chains were removed by dialysis in a Stirred Ultrafiltration Cell “Millipore” model 8050 equipped with polyethersulfone membrane cut-off 50 kDa (**4.9**) and 100 kDa (**4.10**, **4.11**). The substances were freeze-dried over night and then dried for 2 days under dynamic vacuum.

Table X. 7 The starting amounts of initiator, EO and dendrimer.

Exp. No	<i>t</i> -BuOK [mol]x10 ⁻³	Ethylene oxide [mol]x10 ⁻²	TdG ₂ (CH ₂ Cl) ₋₁₂ [mol]x10 ⁻⁶	Ph-CH ₂ -Cl [mol]x10 ⁻⁵	Yield [g; %]
4.9	2.2	5	9.1	10.9	1.9; 84
4.10	1.3	29	5.5	6.5	12.6; 99
4.11	1.3	44	5.5	6.5	17.8; 92

¹H-NMR (250 MHz, CD₂Cl₂, RT) δ, ppm: 7.6-6.4 (obp, H_{Dendr}^{arom}), 4.6-4.1 (m, Dendr-CH₂O-PEO), 3.6 (s, -CH₂CH₂O-), 1.1(s, (CH₃)CO-);

¹³C-NMR (75 MHz, CDCl₃, RT) δ_C, ppm: 137.5, 135.1, 130.0, 127.7, 113.0, 109.5, 72.8, 72.3, 70.4, 69.9, 69.2, 61.3, 40.5;

GPC (standard: PEO, eluent: DMF):

No	PEO arms		Core-shell nanoparticles	
	M _n	PDI	M _n	PDI
4.9	340	1.33	9 400	1.69
4.10	7 300	1.06	110 000	1.08
4.11	13 700	1.09	200 000	1.34

UV Spectroscopy (in THF) λ_{max} = 293 nm

 Table X. 8 UV absorptions at 330 nm, volume of the THF solution and amount of TdG₂(CH₂O-PEO)₁₆ used for preparation of the solutions.

Exp. No	UV absorption at 330 nm	Volume [ml]	Weight [mg]
4.9	0.0775	25	1.44
4.10	0.0805	25	12.50
4.11	0.1097	10	10.78

extinction coefficient of TdG₂(CH₃)₁₆ in THF at 330 nm is 13 600 L mol⁻¹ cm⁻¹

Dynamic Light Scattering in THF: **4.9** R_h 4.0nm; **4.10** R_h 10.4nm; **4.11** R_h 12.0nm

TGA/DSC Decomposition starts at 150 °C with maximum rate of degradation at 380 °C and

ended at 550 °C. T_g (**4.9**) = 46.5 °C, T_g (**4.10**) = 54.8 °C, T_g (**4.11**) = 57.6 °C

Elemental analysis

Exp. No	%C		%H	
	Calculated	Found	Calculated	Found
4.9	73.9	62.9	7.5	8.1
4.10	56.6	58.4	8.9	8.9
4.11	56.0	58.4	9.0	8.7

X.8.2. PEO grafting-from TdG₂(CH₂OH)₁₆
X.8.2.1. Polymerization of EO on 1,4-dihydroxymethyl benzene (model reaction)

A variable amount of 1,4-dihydroxymethyl benzene (see **Table X. 9**) was titrated with THF solution of naphthalene potassium for 2 h at 25 °C. The calculated amounts of EO were added and the temperature was increased to 40 °C for 20, 24 and 64 h, respectively (**4.12**, **4.13**, **4.14**). The reaction was terminated with an excess of degassed acetic acid. The product was precipitated from hexane, collected by filtration, and dried under dynamic vacuum for two days.

Table X. 9 The starting amounts and yields of the polymerization of EO on 1,4-dihydroxymethyl benzene (model reaction).

Exp No	1,4-dihydroxymethyl benzene [mmol]	Ph- <u>CH₂-OH</u> [mmol]	Ethylene oxide [mmol]	Yield [%]
4.12	0.850	1.7	19.3	99
4.13	0.585	1.17	80.1	98
4.14	0.175	0.35	80.1	96

$^1\text{H-NMR}$ (250 MHz, CD_2Cl_2 , RT) δ , ppm: 7.31 (s, H^{arom}), 4.52 (s, PhCH_2O), 3.6 (s, $-\text{CH}_2\text{CH}_2\text{O}-$); [for comparison $^1\text{H-NMR}$ of 1,4-dihydroxymethyl benzene (250 MHz, CD_2Cl_2 , RT) δ , ppm: 7.34 (s, H^{arom}), 4.65 (s, PhCH_2OH)];

GPC (standard: PEO, eluent: THF):

Exp. No	M_n	PDI
4.12	1 100	1.13
4.13	4 800	1.27
4.14	19 000	1.07

X.8.2.2. PEO grafting-from $\text{TdG}_2(\text{CH}_2\text{OH})_{16}$

Naphthalene potassium (20 mM in THF) was used for titration of $\text{TdG}_2(\text{CH}_2\text{OH})_{16}$ (see **Table X. 10**) in dry THF (100 ml). The titration was carried out at 25 $^\circ\text{C}$ until the green color slowly disappeared (approximately 2 min). When the titration was complete, the reaction mixture was cooled to 5 $^\circ\text{C}$ and calculated amounts of ethylene oxide were added. The temperature was slowly increased to 40 $^\circ\text{C}$ and the polymerization was carried out at this temperature for 48 h. The reaction was terminated with an excess of degassed HCl. The obtained products were precipitated from hexane, collected by filtration and dried *in vacuo* for two days.

Table X. 10 The starting amounts of dendrimer and EO, yields of the products obtained by “grafting-from” procedure.

Exp No	$\text{TdG}_2(\text{CH}_2\text{OH})_{16}$ [mol] $\times 10^{-6}$	$\text{Ph-CH}_2\text{-OH}$ [mol] $\times 10^{-5}$	Ethylene oxide [mol] $\times 10^{-2}$	Yield [g; %]
4.15	9.3	15	0.34	0.12; 60
4.16	9.3	15	1.7	0.64; 80
4.17	4.7	7.5	3.4	1.28; 84
4.18	4.7	7.5	8.5	2.82; 75

$^1\text{H-NMR}$ (250 MHz, CD_2Cl_2 , RT) δ , ppm: 7.6-6.2 (overlapping broad peak, H^{arom}), 4.8-4.0 (m, CH_2Cl), 3.6 (s, $-\text{CH}_2\text{CH}_2\text{O}-$);

$^{13}\text{C-NMR}$ (75 MHz, CDCl_3 , RT) δ_{C} , ppm: 137.8, 134.6, 126.4, 123.6, 121.5, 120.9, 110.6, 109.2, 108.0, 73.6, 72.8, 70.5;

GPC (standard: PEO, eluent: THF):

Exp No	M_n	PDI
4.15	4 100	2.17
4.16	17 000	1.24
4.17	75 700	1.34
4.18	120 000	1.58

UV Spectroscopy (in THF) $\lambda_{\text{max}} = 294 \text{ nm}$

Table X. 11 UV absorbance at 330 nm, volume of the THF solution and amount of $\text{TdG}_2(\text{CH}_2\text{O-PEO})_{16}$ used for preparation of the solutions.

Exp No.	UV absorption at 330 nm	Volume [ml]	Weight [mg]
4.15	0.6682	2.5	0.825
4.16	1.0217	2.5	12.36
4.17	0.1608	5	15.04
4.18	0.3022	2.5	53.07

extinction coefficient of $\text{TdG}_2(\text{CH}_3)_{16}$ in THF at 330 nm is $13\,600 \text{ L mol}^{-1} \text{ cm}^{-1}$

Dynamic Light Scattering in THF: **4.15** aggregates (water and THF); **4.16** $R_h = 5.5 \text{ nm}$ (water); **4.17** $R_h = 8.6 \text{ nm}$ (THF), 15.8 nm (water); **4.18** $R_h = 28.8 \text{ nm}$ (THF), 10.0 nm (water).

TGA/DSC Decomposition starts at $200 \text{ }^\circ\text{C}$ with maximum rate of degradation at $400 \text{ }^\circ\text{C}$ and ended at $500 \text{ }^\circ\text{C}$. $T_g = 61 \text{ }^\circ\text{C}$;

Elemental analysis

Exp. No	%C		%H	
	Calculated	Found	Calculated	Found
4.15	76.2	57.3	6.9	7.5
4.16	58.3	56.1	8.7	4.7
4.17	55.1	55.0	9.0	9.9
4.18	54.7	56.0	9.1	8.8

X.9. Preparation of core-shell macromolecules bearing covalently bonded chromophore molecule

PEO grafting-from PDIG₂(CH₂OH)₁₆

THF (30 ml) solution of naphthalene potassium was added dropwise to PDIG₂(CH₂OH)₁₆ (previously dried into the reactor at 40 °C over night) solution in THF (100 ml) at 0 °C in order to deprotonate hydroxyl groups on the dendrimer surface. Calculated amount of ethylene oxide (see **Table X. 12**) was distilled into the reactor. The temperature was slowly increased to 50 °C and the polymerization was carried out at this temperature for 7 days. The reaction was terminated with an excess of hydrochloric acid. The obtained products were precipitated in hexane, collected by filtration and dried *in vacuo* for two days.

The crude products were purified from low molecular weights substances (PEG, KCl and naphthalene) by filtration of an aqueous solution in a Stirred Ultrafiltration Cell “Millipore” model 8050 equipped with polyethersulfone membrane cut-off 50 kDa (**5.1**) and 100 kDa (**5.2**, **5.3**). Then the substances were freeze-dried overnight and then dried for 2 days under dynamic vacuum.

Table X. 12 The starting amounts and yields of the products obtained by “grafting-from” procedure.

Exp No	Naphthalene potassium [mol x10 ⁻⁵]	*PDIG ₂ (CH ₂ OH) ₁₆ [mg, mol x10 ⁻⁶]	PDIG ₂ - <u>CH₂-OH</u> [mol x10 ⁻⁵]	Ethylene oxide [ml, mol x10 ⁻²]	Yield [g, %]
5.1	14	60, 9.8	16	1.1, 2.2	0.9, 79
5.2	7.1	30, 4.9	7.8	0.7, 1.7	0.7, 88
5.3	4.7	20, 3.3	5.2	1.8, 3.5	1.5; 84

*M_n of PDIG₂(CH₂OH)₁₆ is 6 126.

¹H-NMR (700 MHz, C₂D₂Cl₄, 373 K) δ, ppm: 8.10 (s, H_{Peryl}^{Arom}), 7.50-6.45 (obp, H_{Dendr}^{Arom}), 4.26 (d, Dendr-CH₂O-PEO), 3.59 (s, -CH₂CH₂O-), 1.25 (s, CH₃ Peryl);

GPC (standard: PEO, eluent: THF):

Experiment No	M _n	PDI
5.1	33 000	1.57
5.2	74 000	1.67
5.3	160 000	1.97

UV Spectroscopy (see Table 1 and 4) λ_{max} = 572 nm

 Table X. 13 UV absorption at λ_{max}, volume of the methanol solution and amount of PDIG₂(CH₂O-PEO)₁₆ used for preparation of the solutions.

Exp No.	UV absorption at 572 nm	Volume [ml]	Weight [mg]
5.1	0.0263	100	5.84
5.2	0.0266	25	3.55
5.3	0.0235	25	11.80

Extinction coefficient of PDIG₂(CH₂OH)₁₆ in methanol at 572 nm (λ_{max}) was found to be 33 300 L mol⁻¹ cm⁻¹.

Fluorescent Spectroscopy (in methanol) $\lambda_{exc} = 607 \text{ nm}$;

Fluorescent Correlation Spectroscopy (FCS):

Sample	Conc. nmol/L	Temp. ° C	Viscosity cp	Diff.time μs	Diff. Coef.x10 ⁻¹⁰ m ² /s	d_s nm
PDI(OPh) ₄	50	22.7	*0.56707	28.1	3.30	0
PDIG ₂ (CH ₂ OH) ₁₆	70	22.6	*0.56789	27.2	1.28	2.7
5.1	19	23.3	**0.92910	466.3	21.4	7.9
5.2	41	23.6	**0.92255	712.1	14.0	13.8
5.3	29	24.6	**0.90137	1209.3	85.6	25.3

Dynamic Light Scattering (DLS) in THF: **5.1** $R_h = 10.9\text{nm}$; **5.2** $R_h = 16.8\text{nm}$; **5.3** $R_h = 28.3\text{nm}$

Elemental analysis

Exp. No	%C		%H	
	Calculated	Found	Calculated	Found
5.1	56.6	56.8	8.8	8.9
5.2	56.1	56.0	8.9	8.8
5.3	55.0	56.0	9.1	8.6

X.10. Preparation of core-double-shell macromolecules by “grafting-onto” method

Variable amounts of PS-*b*-PEO or PI-*b*-PEO diblock copolymers (see Table X.14) were introduced into the reactor and dried at 40 °C overnight. THF (100 ml) was cryodistilled and the solution was titrated by THF solution (30 ml) of naphthalene potassium (~50 mM) at 0 °C until the slight green color persisted for more than 2 minutes. After 30 minutes (time needed for full deprotonation of end-hydroxyfunctionalized diblock copolymers) THF (30 ml) solution of appropriate dendrimer (TdG₂(CH₂Cl)₋₁₂ or TdG₂(CH₂Cl)₋₈) (see Table X.14) was added into the reactor and the mixture was stirred at 50 °C for 7 days. Hydrochloric acid was added in order to deactivate the living diblock chains. The products were precipitated in hexane at 0 °C, filtered and dried under dynamic vacuum for 48 h. Part of the crude products was purified from the single diblock chains by preparative GPC.

Table X. 14 Amounts of the diblock copolymers and dendrimers.

Product name	Diblock copolymers		Dendrimers	
	PI- <i>b</i> -PEO [g, mmol]	PS- <i>b</i> -PEO [g, mmol]	TdG ₂ (CH ₂ Cl) ₋₁₂ [g, mmol, mmol -CH ₂ Cl groups]	TdG ₂ (CH ₂ Cl) ₋₈ [g, mmol, mmol -CH ₂ Cl groups]
D(PEO-PI)12	0.605, 0.43	-	0.036, 6.4x10 ⁻³ , 7.7x10 ⁻²	-
D(PEO-PS)12	-	2.549, 0.43	0.04, 7.2x10 ⁻³ , 8.6x10 ⁻²	-
D(PEO-PI)8	0.403, 0.29	-	-	0.032, 6.0x10 ⁻³ , 4.8x10 ⁻²
D(PEO-PS)8	-	1.77, 0.30	-	0.029, 5.5x10 ⁻³ , 4.4x10 ⁻²

¹H-NMR spectroscopy (**D(PEO-PI)12** and **D(PEO-PI)8**) (500 MHz, C₂D₂Cl₄, 373 K) δ, ppm: (see Figure 6) 7.5-6.3 (obp, H_{Dendr}^{arom}), 5.2 (s, CH₂=CH- 1,2-structure), 4.9-4.6 (obp, CH₂=CH- 1,2-structure, CH₂=C(CH₃)- 3,4-structure) 4.3-4.0 (m, Dendr-CH₂O-PEO-PI), 3.6 (s, -CH₂CH₂O-), 2.3-1.8 (m, -CH- backbone 3,4-structure), 1.6 (s, CH₂=C(CH₃)- 3,4-structure), 1.5-1.1 (m, -

CH₂- backbone 3,4-structure), 1.1-0.9 (m, -CH₂- backbone 3,4-structure and CH₃-backbone of 1,2-structure), 0.8 (m, initiator - CH₃CH₂(CH₃)CH-), 0.7 (m, initiator - CH₃CH₂(CH₃)CH-);

¹H-NMR spectroscopy (D(PEO-PS)12 and D(PEO-PS)8) (500 MHz, C₂D₂Cl₄, 373 K) δ, ppm: (see Figure 7) 7.5-6.3 (obp, H_{PS+dendr}^{Arom}), 4.3-4.0 (q, Dendr-CH₂O-PEO-PS), 3.6 (s, -CH₂CH₂O-), 2.1-1.7 (m, CH_{PS}^{aliph}), 1.7-1.2 (m, CH₂ PS^{aliph}), 0.8 (m, initiator - CH₃CH₂(CH₃)CH-), 0.7 (m, initiator - CH₃CH₂(CH₃)CH-).

GPC (D(PEO-PI)12, D(PEO-PI)8, D(PEO-PS)12 and D(PEO-PS)8) (THF – eluent, PI or PS – standard):

Product name	M _n	PDI
D(PEO-PI)8	12 600	1.13
D(PEO-PS)8	28 500	1.05
D(PEO-PI)12	17 100	1.07
D(PEO-PS)12	26 000	1.05

MALDI-ToF-MS (matrix dithranol, Na⁺) of **D(PEO-PI)8**: maximum at m/z = 14 807 with M_n 14 680 and PDI 1.05.

Dynamic Light Scattering in THF: **D(PEO-PS)12** R_h = 7.3nm; **D(PEO-PS)8** R_h = 5.8nm;

D(PEO-PI)12 R_h = 5.1nm; **D(PEO-PI)8** R_h = 4nm

UV spectroscopy λ_{max} = 294 nm in THF;

Table X. 15 UV absorption, volume of solutions and weight of the dishell-core macromolecules. Solvent: THF

Product name	UV absorption at 330 nm	Volume [ml]	Weight [mg]
D(PEO-PI)12	0.1033	5	0.66
D(PEO-PS)12	0.2362	2,5	1.75
D(PEO-PI)8	0.0899	10	1.45
D(PEO-PS)8	0.2701	2.5	1.60

extinction coefficient of **TdG₂(CH₃)₁₆** in THF at 330 nm is 13 600 L mol⁻¹ cm⁻¹

Elemental analysis

Exp. No	%C		%H	
	Calculated	Found	Calculated	Found
D(PEO-PI)12	76.9	60.6	10.3	8.6
D(PEO-PS)12	69.6	76.3	8.9	8.7
D(PEO-PI)8	77.9	63.1	10.0	8.9
D(PEO-PS)8	70.1	70.1	8.8	8.6

X.11. Preparation of core-double-shell macromolecules by “grafting-from” method

Synthesis of core-shell ATRP macroinitiator:

Naphthalene potassium (20 mM in THF) was used for titration of TdG₂(CH₂OH)₁₆ (see Table X. 16) in dry THF (100 ml). The titration was carried out at 25 °C until the green color slowly disappeared (approximately 2 min). When the titration was complete, the reaction mixture was cooled to 5 °C and calculated amounts of ethylene oxide were added. The temperature was slowly increased to 40 °C and the polymerization was carried out at this temperature for 68 h. 2-Bromopropionyl bromide (see Table X.16) dissolved in THF (20 ml) was added in order to end-bromofunctionalize the PEO and terminate the polymerization reaction. The crude products were purified by sequential precipitation in hexane, cold acetone and cold methanol in order to remove the excess of 2-bromopropionyl bromide (BPB), collected on a filter and dried under dynamic vacuum for 48 h.

Table X.16 The amounts of TdG₂(CH₂OH)₁₆, EO and BPB; yields of the products.

Exp No	TdG ₂ (CH ₂ OH) ₁₆ [mol]x10 ⁻⁶	Ph-CH ₂ -OH [mol]x10 ⁻⁵	Ethylene oxide [mol]x10 ⁻²	BPB [mol]x10 ⁻⁴	Yield [g; %]
D-PEO₁₄₀Br	4.6	7.4	1.7	9.5	0.46; 60
D-PEO₁₃₀₀Br	9.3	15	1.7	8	0.14; 18

¹H-NMR (250 MHz, CD₂Cl₂, RT) δ, ppm: 7.31 (overlapping signals, H^{arom}), 4.52 (s, ArCH₂O), 4.39 (m, -CH(CH₃)Br), 3.6 (s, -CH₂CH₂O), 1.77ppm (d, -CH(CH₃)Br)

GPC (standard: PEO, eluent: DMF):

Exp No	M _n	PDI
D-PEO₁₄₀Br	7 100	2.0
D-PEO₁₃₀₀Br	11 600	1.8

Acknowledgements

First of all, I would like to thank my wife *Petia* supporting me in everything and forgiving me every time she was disregarded because of my work. Next to her I would like to thank my daughter *Andrea* for the time I relaxed – she managed every time to keep me smiling.

My mother *Anka* and my father *Milan Atanasovi*, my sister *Tsvetanka* and my parents in law – *Ganka* and *Pavlin Mihailovi* for encourage me and making me filling better at home.

I am deeply indebted to the following people who, without their support, this work would have not been possible:

Prof. Klaus Müllen and *Dr. Markus Klapper* for giving me the great opportunity to make my Ph.D. in one of the world most famous institutes for chemical research, in Germany. For the countless discussions, advises (not only in the scientific area), ideas, patience, and for the always warm and correct approach. Thank you!

Prof. Christo Tsvetanov for giving me the opportunity to come here in Germany.

All my bulgarian collegues – *Nikolay Nenov*, *Kaloyan Koynov*, *George Mihov*, *Vesko Synigerski*, *Petko Petkov*, *Sirma Koynova*, *Anela Ivanova*, *Krassimir Vassilev*, *Tanja Dimitrova*, *Stanislav Balouchev* for the endless discussions mainly on non-scientific topics, for all the parties, bbq's, dinners, lunches, coffee breaks and trips all over Germany and abroad. Thank you very much!

My hard-working colleagues: *Maxim Peretolchin*, *Thorsten Brand*, *Nawel Khelfalla*, *Emma Caputo*, *Victor Khrenov*, *Yong-Jun Jang*, *Kirsten Bieber*, *Tanja Nemnich*, *Roland Bauer*, *Christofer Clark*, *Dörthe Grebel-Köhler*, *Natalya Tchebotareva*, *Guido Vandermuellen*, *Eric Reuther*, *Christopher Kohl*, *Christophe Eg,o Neil Pschirer*, *Fabian Nolde*, *Josemon Jacob*, *Jelko Tomovich*, *Weicheng Wu*, *Jishan Wu*, *Karl Wang*, *Jiang-Jang Qu* etc. for the support and the nice company especially during my first months in Mainz, and the knowledges I have got from their topics. For the funny and relaxing parties and „coffee and cakes” breaks.

Acknowledgements

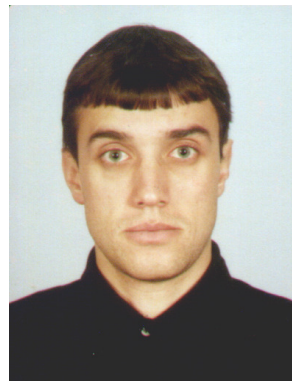
All the project leaders of AK Müllen – *Andrew Grimsdale* (especially for the beautiful work that he did correcting the English of this dissertation), *Hans-Joachim Räder*, *Harm-Anton Klok*, *Martin Baumgarten* and *Manfred Wagner* (especially for the 500 MHz – NMR measurements).

All the technicians, without whose help, this dissertation could not be realized. *Eva Sebold* - DSC and TGA, *Sandra Seywald* – GPC, *Walter Scholdei* IR, *Petra Kindervater* – NMR, the people from the electronic workshop, from the storehouse, from the EDV-team, *Mister Pilz* and his team, for helping me to dissolve the so many little problems seeming to be insignificant but very often causing great troubles. The secretary of Professor Muellen – *Frau Stiep* and especially *Frau Muensch* for always being for me there and for writing me excellent recommendation letters, helping me to get extending of my residence permission without any problem.

And of course BASF AG, Basell, Max-Planck Association and Max-Planck Research School for Polymer Material Science for the financial support.

Thank you very much to all of you! I really had incredibly nice and exciting time in MPI-P!

Curriculum Vitae



Vladimir Milanov Atanasov

Personal

Family: Atanasov

Name: Vladimir

Surname: Milanov

Sex: Male

Marital status: Married

Nationality: Bulgarian

Date of birth : 19 February 1974

Place of birth: Blagoevgrad, Bulgaria

Adress: Ilinden str., bl. 2A, app. 10

Post code: 1700 - Blagoevgrad

Country: Bulgaria

Tel: +359(73) 37897

Present address: Am Sandbruch str. 2

Post code: D-55122

City: Mainz

Country: Germany

Tel: +49(6131) 786 125

Education

09/2000 - Ph.D. student, **Max-Planck Institute f0r Polymer Research**, Mainz/Germany

PhD Thesis

Core-Shell Macromolecules with Dendritic Polyphenylene Core and Polymer Shells

Supervisors: Prof. Dr. Klaus Müllen, Dr. Markus Klapper

09/2002 – 08/2003 – **Max-Planck Research School for Polymer Material Science**

Certificate of Participation

03/1997 – 11/1997 **University of Sofia „St. Kliment Ohridsky“**

Diploma Thesis

Synthesis of N-(2-pyridyl)urea and N-(2-pyridyl)thiourea derivatives. Novel synthetic route for preparation of N-(2-pyridyl)thiourea derivatives.

Grade – excellent 5.50

10/1992 – 02/1997 **University of Sofia „St. Kliment Ohridsky“**

Master of Science degree in Organic Chemistry

Grade – very good 5.27

09/1981 – 06/1992 **National High School “St., St. Kiril i Metodii”** for general education with extended study on natural sciences

High School Diploma

Grade – very good 5.11

Options: Chemistry

Command of languages

Bulgarian – mother tongue

English – very good

German – good

Russian - good

Publications

1. O. Angelova, R. Petrova and V. Atanasov “2-(Nitroamino)pyridine” *Acta Cryst.* **1998**, C54, 441.
2. O. Angelova, K. Kossev, V. Atanasov “1-(*tert*-Butyl)-3-(2-pyridyl) thiourea” *Acta Cryst.*, **1999**, C55, 220.
3. V. Atanasov, V. Sinigersky, M. Klapper, K. Müllen “Core-Shell macromolecules with rigid Dendritic Polyphenylene Cores and Polymer Shells” *Macromolecules* **2005**, 38, 1672.
4. V. Atanasov, N. Knorr, R. S. Duran, S. Ingebrandt, A. Offenhäusser, W. Knoll, I. Köper “Membrane on a Chip: A Functional Tethered Lipid Bilayer Membrane on Silicon Oxide Surfaces” *Biophysical Journal* **2005**, 89, 1780.

**Professional
experience**

1. Institution: Max-Planck-Gesellschaft, Institut für Polymerforschung
(Mainz, Germany)
Area: Research
Since: 09/2000 -
Function: Ph.D. student
Experience : organic synthesis, polymer synthesis, anionic
polymerization, monomer and polymer characterizations,
purification techniques.

Working in team: many co-laborations and joint projects with
different institutes in Germany and abroad.

Several oral presentations, talks and posters in English.

Excellent adaptation to the life in foreign country, international
environment in the working place. Position where communication skills
are important and situations where teamwork is essential.

2. Institution: Bulgarian Academy of Sciences, Institute of Polymers
(Sofia, Bulgaria)

Area: Research

Since: 01/1998 – 08/2000

Function: Senior chemist

Experience: organic synthesis, polymer synthesis *via* anionic
polymerization, methods of characterization.

Working in team: working on project financially supported from foreign
foundation

Others

Extended experience in use of Windows, Microsoft Office, Internet.

Hobbies: Mountain climbing , Biology, Sport

Favorite sports: football, table-tennis, jogging

References

Prof. Dr. Klaus Müllen, Dr. Markus
Klapper (MPI-P, Mainz)

Max-Planck Institut für
Polymerforschung

Ackermannweg 10

55128 Mainz

Germany

tel + 49 6131 379 150/151

fax + 49 6131 379 100

e-mail : muellen@mpip-mainz.mpg.de

klapper@mpip-mainz.mpg.de